

UNIVERSITAT POLITÈCNICA DE VALÈNCIA

**CENTRO DE RECONOCIMIENTO MOLECULAR
Y DESARROLLO TECNOLÓGICO**



**Transition metal complexes for
chromo-fluorogenic detection of
carbon monoxide in environmental
and biomedical applications**

PhD. THESIS

Submitted by

María Esperanza Moragues Pons

PhD. Supervisors:

**Prof. Ramón Martínez Máñez
Dr. Félix Sancenón Galarza**

Valencia, November 2014



UNIVERSITAT
POLITÈCNICA
DE VALÈNCIA

RAMÓN MARTÍNEZ MÁÑEZ, PhD in Chemistry and Professor at the *Universitat Politècnica de València*, and FÉLIX SANCENÓN GALARZA, PhD in Chemistry and Lecturer at the *Universitat Politècnica de València*.

CERTIFY:

That the work ***“Transition metal complexes for chromo-fluorogenic detection of carbon monoxide in environmental and biomedical applications”*** has been developed by María Esperanza Moragues Pons under their supervision in the Centro de Reconocimiento Molecular y Desarrollo Tecnológico (IDM) of the *Universitat Politècnica de València*, as a Thesis Project in order to obtain the degree of PhD in Chemistry at the *Universitat Politècnica de València*.

Valencia, November 2014.

Prof. Ramón Martínez Máñez

Dr. Félix Sancenón Galarza

*A mis padres y mi hermano,
por su amor y apoyo incondicional.*

*“Como no sabia que era imposible
... lo hizo”*

*“Le pedi fuerzas a Dios para llegar más lejos,
y me hizo débil para que aprendiera la humilde obediencia.*

*Le pedi salud para hacer cosas grandiosas,
y me hizo frágil para que hiciera cosas mejores.*

*Le pedi riquezas para ser feliz,
y me dio la pobreza para que fuera sabio.*

*Le pedi poder para ser admirado por los hombres,
y me dio debilidad para que sintiera la necesidad de Dios.*

*Le pedi todas las cosas para disfrutar de la vida,
y me dio la vida para disfrutar todas las cosas”*

“No sueñes con el mañana, vive el hoy.

Atesora cada momento de tu vida.

Trabaja como si no necesitaras dinero.

Ama como si nunca te hubiesen herido.

Baila como si nadie te estuviese viendo”

Acknowledgements

Agradecimientos

Es una realidad que las personas pasamos casi más tiempo en el lugar de trabajo que en nuestra casa. De ahí que estar a gusto con tus compañeros sea un regalo impagable. Recibí mi regalo en Marzo de 2009, cuando entré a formar parte del IQMA. Gracias Ramón por darme la oportunidad de formar parte del mundo de la investigación. Gracias J.V., Loles, Juan, Jose Luis y Luis Villa por vuestra ayuda y sabios consejos. Gracias Félix por tu guía y tu apoyo.

Gracias Elena, Carmen, Rosa, Handi, Tati, Santi, Andrea, Estela, Cris, Campos, Inma y Yoli por lo bien que me acogisteis, cuando empezábamos a estar faltos de espacio.

Gracias Elena porque siempre has estado ahí, desde el primer tour que me hiciste por el departamento, pasando por cada consejo y cada confesión y por ayudarme a respirar cuando tanto lo necesitaba. Gracias Carmen y Rosa por todo lo vivido. Gracias Tati por compartir tu mundo conmigo. Gracias Santi por dejarme en herencia la mejor mesa del lab. Gracias Andrea y Estela por vuestra sincera amistad, por ser el pegamento del grupo y por convertir el peor verano de mi vida, en un viaje inolvidable. Gracias Campos porque he aprendido a quererte por encima de tu mala uva. Gracias Cris por enseñarme a relativizar las cosas, por nuestras charlas intensas sobre el futuro, por todas las palabras que has introducido en mi vocabulario y que me hacen acordarme de ti (cansas, pequeñón, molón...) y por estar ahí. Gracias Yoli "guapa", por demostrarme que se puede ir sonriendo a la vida sin cansarse, porque sabes ver las cosas en positivo, porque eres sencillamente estupenda y porque tengo mucha suerte de tenerte en mi vida. Gracias Inma porque tengo la suerte de compartir contigo mucho más que mi primer trabajo, compartimos la confianza en que no caminamos solas. Gracias por caminar conmigo amiga.

Gracias Andrea, mi fiel compi de máster, ¿qué habría hecho yo sin ti? Desde luego no me lo habría pasado tan bien quejándome, ni preparando

Acknowledgements

nuestras propias prácticas. Gracias Sara mi contemporánea de beca mi pareja de gym, mi inseparable compi en los 1000 viajes a la escuela, en las expediciones a alumnado... por todo, 1000 gracias. Gràcies Patri per tot, per ser la meua amiga, per escoltar-me encara sense entendre'm. Per tot el que m'ensenyes de la nostra llengua, per romandre al meu costat quan va coincidir que motls volaven cap a etapes noves.

Gracias chicas por todo lo que hemos vivido y compartido.

A día de hoy el IDM es una familia enorme. He coincidido con mucha gente estupenda y estoy enormemente agradecida. Edgar (por ser tan especial, por alegrarme en cada momento compartido), Laura (por tu locura), Alessandro, Diana, Nuria (por tu sensibilidad), María S., María R., Almu (por tus super abrazos), Luis Enrique (por tu amistad y tu apoyo, y por enriquecer mucho más que mi lenguaje), Cris G. (por tu buena voluntad y tus ganas por mantener el lab limpio), Marian, Sameh (por nuestras interesantes reflexiones, porque todos tenemos tanto que aprender de los demás), Cris T. (por tu sonrisa), Lluís (por tu lucha), Mar (por tu simpatía), Alberto (por las felicitaciones que guardo con tanto cariño y por todo lo que hemos compartido), Carol, Rafa, María R., Román, (por mediar cuando ha hecho falta), Krishanu (solo jai, sole jai, dur buhu dur), Cristian, Roberto (por tus diseños, tu tiempo y tu amistad), Cris M. (por tu dulzura), Angela (por ser tan apañada), Ana, Ravi (for asking me a smile when it was hard for me to find the strength), Toni (por tu sinceridad), Irene, Amelia, Lorena, Mónica, Isabel, Kim, Erick, Miguel, y tantos otros nombres.

Gracias a tantos científicos y científicas, en especial a Julio Esteban, cuyos trabajos han inspirado al desarrollo de una tesis preciosa.

During my PhD stay abroad, I realized that there is great people all over the world that can make you feel home. Thanks James for the opportunity to join your group at Imperial College London. I learnt a lot of things and regain the passion for chemistry. Thanks to Ven, Martin, Ferran, Vivi, John, Nacho, Mat, Tom, Neil, Shishir, Siva and Shuoren.

And of course, thank you Ani for your love and wisdom. My stay would have not been the same without you, my Italian sister.

He oído que las personas pasan por nuestras vidas por alguna razón, dejándonos algo que debemos aprender. Quisiera dedicar esta tesis a todas las personas que me he ido encontrando en el camino y que me han ayudado a ser quien soy. A los que viajaron a mi lado durante casi diez años y con su amor me dieron la confianza para enfrentarme a cualquier reto. Fui muy feliz compartiendo el vagón donde aprendí a soñar y a amar sin límites. A mis mejores amigas, Belen, Elena y Marga. Porque dentro de lo diferentes que somos formamos un gran equipo y eso nos hace tan especiales. Soy muy afortunada de tenerlos en mi vida y os quiero mucho. Gracias Josep porque tu amistad siempre me ha ayudado a querer mejorar y por estar ahí, dando igual dónde. Gracias Ruben, Tote y Jordi por cuidar de mis flores y por vuestra amistad. Gracias Noel y Lucía por ser unos amigos estupendos, que sigamos compartiendo momentos inolvidables. Gracias Oscar, Rafa, Marta, Fran, Edu, Celia, Javi, Blanca, Santi, Carlos, Lola por los momentos compartidos. Gracias Alejandro, Laura y Arturo porque nos encontramos en el camino. Gracias a mi familia de Juvenes. Gracias Gonzalo por ser un amigo diez.

Finalmente, gracias a mi familia. Cada uno de vosotros sois un pilar en mi vida que me ayuda a mantenerme en pie. Gracias a mis iaios, mis tíos y tías, a mi Teresita y a los amores de mi vida, mis primos: Jorge, Elisa, Nacho, Alba, Pablo, David y Martina. Gracias Jere, por creer en mí y por ser el mejor hermano que podría tener. Gracias mamá y papá, sin duda sois mi modelo de trabajo, esfuerzo y determinación; pero aún más importante, sois mi ejemplo de respeto, generosidad y amor. Gracias por habérmelo dado todo y hacerme sentir tan orgullosa de teneros como padres.

Gracias a todos por formar parte de mi vida.
¡Sigamos viajando!

Acknowledgements

Resum

La present tesi doctoral titulada “Complexos metàl·lics de transició per a la detecció cromofluorogènica de monòxid de carboni en aplicacions mediambientals i biomèdiques” es basa en la utilització dels principis de la Química de la Coordinació per al disseny i desenvolupament de nous compostos químics capaços de detectar monòxid de carboni en aire mitjançant canvis de color i/o de fluorescència.

La primera família de sondes colorimètriques que es presenta en el capítol 3 es tracta d'uns complexos binuclears de rodi hexacoordinats amb lligands triphenilphosphina i diferents àcids carboxílics. Primerament, s'exposa el treball desenvolupat amb el complex **A** de fórmula $[\text{Rh}_2(\text{C}_6\text{H}_4\text{PPh}_2)_2(\text{O}_2\text{CCH}_3)_2] \cdot (\text{HO}_2\text{CCH}_3)_2$ capaç de detectar selectivament i amb alta sensibilitat CO tant en dissolució com en aire. En presència de CO es produeix un canvi de color de morat a groc, degut a la coordinació del CO en les posicions axials del complex.

A continuació s'amplia el treball amb una col·lecció de cinc complexos de rodi (II) **B-F** adsorbits en gel de sílice i s'estudia el seu ús com a sondes per a la detecció de CO en aire mitjançant canvis de color visibles a simple vista.

En tercer lloc, es procedeix a depositar els complexos en paper de cel·lulosa per facilitar la seua aplicació a la detecció pràctica de CO. S'elegeix el complex **D** $[\text{Rh}_2[(\text{C}_6\text{H}_4)\text{P}(\text{C}_6\text{H}_5)_2]_2(\text{O}_2\text{CCF}_3)_2] \cdot (\text{CF}_3\text{CO}_2\text{H})_2$ com el més sensible a CO en aquest nou suport i s'insereix dins d'un sistema opto-electrònic capaç de quantificar el CO present en l'aire; mitjançant la transducció del canvi de color del complex en un senyal elèctric, i aquest senyal en un valor de concentració de CO determinat.

Finalment, tenint en compte el paper del CO com a agent terapèutic i donat el fet que la coordinació del CO en els complexos de rodi presentats és reversible; es seleccionen els dos complexos dicarbonílics amb cinètiques d'alliberament de CO més lentes **A·(CO)₂** i **F·(CO)₂** amb fórmules $([\text{Rh}_2[(\text{C}_6\text{H}_4)\text{P}(\text{C}_6\text{H}_5)_2]_2(\text{O}_2\text{CCH}_3)_2] \cdot (\text{CO})_2$ i $[\text{Rh}_2[(m\text{-CH}_3\text{C}_6\text{H}_3)\text{P}(m\text{-CH}_3\text{C}_6\text{H}_4)_2]_2(\text{O}_2\text{CCH}_3)_2] \cdot (\text{CO})_2$) com a possibles molècules

alliberadores de CO (CO-RMs) a emprar en estudis sobre inhibició d'agents indicadors d'inflamació cel·lular (veure capítol 4).

En la segona part d'aquesta tesi doctoral s'ha preparat una col·lecció de vinil complexos de ruteni i osmi **G-K** funcionalitzats en grups donadors d'electrons (pirè, toluè i benzè) i en un grup acceptor d'electrons (2,1,3-benzotiadiazol (BTD)). Aquests complexos són acolorits, ja que presenten una banda de transferència de càrrega. En presència de CO es produeix el desplaçament del BTD amb el consegüent canvi de color (veure capítol 5).

Primerament, per a possibilitar la detecció fluorogènica de CO, s'ha procedit a l'ancoratge del fluoròfor pirenilvinil com a ligand del complex de ruteni (II). En presència de CO i mitjançant el desplaçament del BTD s'aconsegueix un augment de fluorescència fins i tot observable a simple vista.

Per concluir la segona part de la tesi s'han sintetitzat quatre complexos més, **H-K**, dos de ruteni i dos d'osmi; que també han estat emprats en la detecció de CO en aire. Per a la preparació d'aquestes sondes també s'ha utilitzat gel de sílice com a suport. En presència de monòxid de carboni es produeix el desplaçament del BTD (colorant) i els complexos metàl·lics canvien de color, permetent així la semiquantificació del CO als rangs de concentració en què el CO és altament tòxic fins i tot per a exposicions curtes.

Resumen

La presente tesis doctoral titulada “Complejos metálicos de transición para la detección cromo-fluorogénica de monóxido de carbono en aplicaciones medioambientales y biomédicas” se basa en la utilización de los principios de la Química de la Coordinación para el diseño y desarrollo de nuevos compuestos químicos capaces de detectar monóxido de carbono en aire mediante cambios de color y/o de fluorescencia.

La primera familia de sondas colorimétricas que se presenta en el capítulo 3 está basada en unos complejos dinucleares de rodio hexacoordinados con ligandos trifenilfosfina y distintos ácidos carboxílicos. Primeramente, se expone el trabajo desarrollado con el complejo **A** de fórmula $[\text{Rh}_2(\text{C}_6\text{H}_4\text{PPh}_2)_2(\text{O}_2\text{CCH}_3)_2] \cdot (\text{HO}_2\text{CCH}_3)_2$ capaz de detectar selectivamente y con alta sensibilidad CO tanto en disolución como en aire. En presencia de CO se produce un cambio de color de morado a amarillo, debido a la coordinación del CO en las posiciones axiales del complejo.

A continuación se amplía el trabajo con una colección de cinco complejos de rodio (II) **B-F** adsorbidos en gel de sílice y se estudia su uso como sondas para la detección de CO en aire mediante cambios de color visibles a simple vista.

En tercer lugar, se procede a depositar los complejos en papel de celulosa para facilitar su aplicación en la detección práctica de CO. Se elige el complejo **D** $[\text{Rh}_2[(\text{C}_6\text{H}_4)\text{P}(\text{C}_6\text{H}_5)_2]_2(\text{O}_2\text{CCF}_3)_2] \cdot (\text{CF}_3\text{CO}_2\text{H})_2$ como el más sensible a CO en este nuevo soporte y se inserta dentro de un sistema opto-electrónico capaz de cuantificar el CO presente en el aire; mediante la transducción del cambio de color del complejo en una señal eléctrica, y esta señal en un valor de concentración de CO determinado.

Finalmente, teniendo en cuenta el papel del CO como agente terapéutico y aprovechando que la coordinación de CO en los complejos de rodio presentados es reversible; se seleccionan los dos complejos dicarbonílicos con cinéticas de liberación de CO en disolución más lentas **A·(CO)₂** y **F·(CO)₂** de fórmulas

$[\text{Rh}_2[(\text{C}_6\text{H}_4)\text{P}(\text{C}_6\text{H}_5)_2]_2(\text{O}_2\text{CCH}_3)_2] \cdot (\text{CO})_2$ y $[\text{Rh}_2[(m\text{-CH}_3\text{C}_6\text{H}_3)\text{P}(m\text{-CH}_3\text{C}_6\text{H}_4)_2]_2(\text{O}_2\text{CCH}_3)_2] \cdot (\text{CO})_2$ como posibles moléculas liberadoras de CO (CO-RMs) a utilizar en estudios sobre inhibición de agentes indicadores de inflamación celular (ver capítulo 4).

En la segunda parte de esta tesis doctoral se ha preparado una colección de vinil complejos de rutenio y de osmio **G-K** funcionalizados con grupos dadores de electrones (pireno, tolueno y benceno) y con un grupo aceptor de electrones (2,1,3-benzotiadiazol (BTD)). Estos complejos son coloreados, ya que presentan una banda de transferencia de carga. En presencia de CO se produce el desplazamiento del BTD con el consiguiente cambio de color (ver capítulo 5).

En primer lugar, para posibilitar la detección fluorogénica de CO, se ha preparado el complejo **G** mediante el anclaje del fluoróforo pirenilvinilo como ligando dador de electrones del complejo de rutenio (II). En presencia de CO y mediante el desplazamiento del BTD se consigue un aumento de fluorescencia observable incluso a simple vista.

Para concluir la segunda parte de la tesis se han sintetizado cuatro complejos más, **H-K**, dos de rutenio y dos de osmio; que han sido utilizados también para detectar CO en aire. Para la preparación de estas sondas también se ha utilizado gel de sílice como soporte. En presencia de CO se produce el desplazamiento del BTD (colorante) y los complejos metálicos cambian de color, permitiendo así la semicuantificación del CO en los rangos de concentración en que el CO es altamente tóxico incluso para exposiciones cortas.

Abstract

The present PhD thesis entitled “Transition metal complexes for chromo-fluorogenic detection of carbon monoxide in environmental and biomedical applications” is based on the use of Coordination Chemistry for the design and development of new chemical compounds capable of detecting carbon monoxide in air by colour and/or fluorescence changes.

The first family of colorimetric probes reported in chapter 3 is based on hexacoordinated binuclear rhodium complexes with different triphenylphosphines and carboxylic acids as ligands. Complex **A** of formula $[\text{Rh}_2(\text{C}_6\text{H}_4\text{PPh}_2)_2(\text{O}_2\text{CCH}_3)_2] \cdot (\text{HO}_2\text{CCH}_3)_2$ is presented in first place as it features selective and highly sensitive CO detection both in solution and in air. In presence of CO a colour change from purple to yellow takes place, due to the axial coordination of CO.

Throughout chapter 3, the work is extended with a collection of five rhodium (II) complexes **B-F** adsorbed on silica. The use of these as probes for CO detection is assessed through colour changes visible to the naked eye.

Thirdly, the rhodium complexes are deposited on cellulose paper to improve its applicability in practical CO detection. Complex **D** $[\text{Rh}_2[(\text{C}_6\text{H}_4)\text{P}(\text{C}_6\text{H}_5)_2]_2(\text{O}_2\text{CCF}_3)_2] \cdot (\text{CF}_3\text{CO}_2\text{H})_2$ is selected as the one with highest sensitivity to CO in this new support and it is introduced inside an opto-electronic system capable of quantifying CO present in air; through transduction of the complex colour change to an electrical signal, and this signal to a certain CO concentration value.

Finally, bearing in mind the role of CO as a therapeutic and taking advantage of the reversibility of CO coordination in these rhodium complexes; dicarbonylic complexes **A·(CO)₂** and **F·(CO)₂** ($[\text{Rh}_2[(\text{C}_6\text{H}_4)\text{P}(\text{C}_6\text{H}_5)_2]_2(\text{O}_2\text{CCH}_3)_2] \cdot (\text{CO})_2$ and $[\text{Rh}_2[(m\text{-CH}_3\text{C}_6\text{H}_3)\text{P}(m\text{-CH}_3\text{C}_6\text{H}_4)_2]_2(\text{O}_2\text{CCH}_3)_2] \cdot (\text{CO})_2$), this is, the two complexes with slower CO releasing kinetics were selected as carbon monoxide releasing molecules (CO-

RMs) to be used as inhibitors of indicators of cellular inflammation (see chapter 4).

The second part of this PhD thesis deals with the synthesis of a collection of vinyl ruthenium and osmium complexes **G-K** functionalized with electron donor groups (pyrene, toluene and benzene) and an electron acceptor group (2,1,3-benzothiadiazole (BTD)). These are coloured complexes, as they feature one charge transfer band. In presence of CO, the BTD is displaced and a concomitant colour change is observed (see chapter 5).

In a first step, fluorogenic detection of CO is enabled by the anchoring of pyrenylvinyl fluorophore as an electron donor ligand in ruthenium (II) complex **G**. In presence of CO and due to BTD displacement a fluorescence turn-on is achieved, being even visible to the naked eye.

To conclude the second part of the thesis, four more complexes **H-K** (two of ruthenium and two of osmium) have been synthesized and used also for CO detection in air. Silica gel has also been used as support for the preparation of these probes. In the presence of CO displacement of the BTD (dye) occurs and the metallic probes display a colour change, enabling semiquantitative sensing of CO in air at different concentration ranges at which CO is highly toxic even for short exposures.

Publications

Results of this PhD Thesis and other contributions have resulted in the following scientific publications:

- María Esperanza Moragues, Anita Toscani, Félix Sancenón, Paul Dingwall, Neil Brown, Ramón Martínez-Máñez, Andrew J. P. White, James D. E. T. Wilton-Ely, *Ruthenium(II) and Osmium(II) Alkenyl Complexes as Highly Sensitive and Selective Chromogenic Probes for the Sensing of Carbon Monoxide in air*, Chem. Sci., **2014**, submitted.
- María Esperanza Moragues, Anita Toscani, Félix Sancenón, Ramón Martínez-Máñez, Andrew J. P. White, James D. E. T. Wilton-Ely, *A Chromo-Fluorogenic Synthetic “Canary” for CO Detection Based on a Pyrenylvinyl Ruthenium(II) Complex*, J. Am. Chem. Soc., **2014**, 136, 11930-11933.
- María Esperanza Moragues, Rita Brines, M. Carmen Terencio, Félix Sancenón, Ramón Martínez-Máñez, María José Alcaraz, *CO-Releasing Binuclear Rhodium Complexes as Inhibitors of Nitric Oxide Generation in Stimulated Macrophages*, Inorg. Chem., **2013**, 52, 13806-13808.
- María Esperanza Moragues, Roberto Montes-Robles, José Vicente Ros-Lis, Miguel Alcañiz, Javier Ibañez, Teresa Pardo, Ramón Martínez-Máñez, *An optoelectronic sensing device for CO detection in air based on a binuclear rhodium complex*, Sensors and Actuators B, **2014**, 191, 257-263.
- María Esperanza Moragues, Julio Esteban, José Vicente Ros-Lis, Ramón Martínez-Máñez, María Dolores Marcos, Manuel Martínez, Juan Soto, Félix Sancenón, *Sensitive and Selective Chromogenic Sensing of Carbon Monoxide via Reversible Axial CO Coordination in Binuclear Rhodium Complexes*, J. Am. Chem. Soc., **2011**, 133, 15762-15772.

- Julio Esteban, José Vicente Ros-Lis, Ramón Martínez-Máñez, María Dolores Marcos, María Moragues, Juan Soto, Félix Sancenón, *Sensitive and Selective Chromogenic Sensing of Carbon Monoxide by Using Binuclear Rhodium Complexes*, *Angew. Chem. Int. Ed.*, **2010**, 49, 4934-4937.
- Cristina Marín-Hernández, Luis Enrique Santos-Figueroa, María Esperanza Moragues, M. Manuela M. Raposo, Rosa M. F. Batista, Susana P. G. Costa, Teresa Pardo, Ramón Martínez-Máñez, Félix Sancenón, *Imidazo-anthraquinone derivatives for the chromo-fluorogenic sensing of basic anions and trivalent metal cations*, *J. Org. Chem.*, **2014**, accepted, DOI: jo-2014-01515e.
- Estela Climent, Alessandro Agostini, María Esperanza Moragues, Ramón Martínez-Máñez, Félix Sancenón, Teresa Pardo, María Dolores Marcos, *A Simple Probe for the Colorimetric Detection of Carbon Dioxide*, *Chem. Eur. J.*, **2013**, 19, 17301-17304.
- Luis Enrique Santos-Figueroa, María Esperanza Moragues, Estela Climent, Alessandro Agostini, Ramón Martínez-Máñez, Félix Sancenón, *Chromogenic and fluorogenic chemosensors and reagents for anions. A comprehensive review of the years 2010–2011*, *Chem. Soc. Rev.*, **2013**, 42, 3489-3613.
- Luis Enrique Santos-Figueroa, María Esperanza Moragues, M. Manuela M. Raposo, Rosa M.F. Batista, Susana P.G. Costa, R. Cristina M. Ferreira, Félix Sancenón, Ramón Martínez-Máñez, José Vicente Ros-Lis, Juan Soto, *Synthesis and evaluation of thiosemicarbazones functionalized with furyl moieties as new chemosensors for anion recognition*, *Org. Biomol. Chem.*, **2012**, 10, 7418-7428.
- María Esperanza Moragues, Luis Enrique Santos-Figueroa, Tatiana Ábalos, Félix Sancenón, Ramón Martínez-Máñez, *Synthesis of a new tripodal chemosensor based on 2,4,6-triethyl-1,3,5-trimethylbenzene scaffolding bearing thiourea*

and fluorescein for the chromo-fluorogenic detection of anions, *Tetrahedron Lett.* **2012**, 53, 5110-5113.

- Luis Enrique Santos-Figueroa, María Esperanza Moragues, M. Manuela M. Raposo, Rosa M.F. Batista, R. Cristina M. Ferreira, Susana P.G. Costa, Félix Sancenón, Ramón Martínez-Máñez, Juan Soto, José Vicente Ros-Lis, *Synthesis and evaluation of fluorimetric and colorimetric chemosensors for anions based on (oligo)thienyl-thiosemicarbazones*, *Tetrahedron*, **2012**, 68, 7179-7186.
- Tatiana Ábalos, María Moragues, Santiago Royo, Diego Jiménez, Ramón Martínez-Máñez, Juan Soto, Félix Sancenón, Salvador Gil, Joan Cano, *Dyes That Bear Thiazolylazo Groups as Chromogenic Chemosensors for Metal Cations*, *Eur. J. Inorg. Chem.* **2012**, 76-84.
- María Esperanza Moragues, Ramón Martínez-Máñez, Félix Sancenón, *Chromogenic and fluorogenic chemosensors and reagents for anions. A comprehensive review of the year 2009*, *Chem. Soc. Rev.*, **2011**, 40, 2593-2643.
- Tatiana Ábalos, Diego Jiménez, María Moragues, Santiago Royo, Ramón Martínez-Máñez, Félix Sancenón, Juan Soto, Ana María Costero, Margarita Parra, Salvador Gil, *Multi-channel receptors based on thiopyrylium functionalised with macrocyclic receptors for the recognition of transition metal cations and anions*, *Dalton Trans.*, **2010**, 39, 3449-3459.
- María Comes, Elena Aznar, María Moragues, M. Dolores Marcos, Ramón Martínez-Máñez, Félix Sancenón, Juan Soto, Luis Villaescusa, Luis Gil, Pedro Amorós, *Mesoporous Hybrid Materials Containing Nanoscopic "Binding Pockets" for Colorimetric Anion Signaling in Water by using Displacement Assays*, *Chem. Eur. J.*, **2009**, 15, 9024-9033.

Abbreviations and Acronyms

ACGIH	American Conference of Governmental Industrial Hygienists
ACN	Acetonitrile
ADC	Analogue-to-Digital Converter
ASHRAE	American Society of Heating Refrigeration and Air Conditioning Engineers
BBN	Bioingeniería, Biomateriales y Nanomedicina
BTB	2,1,3-benzothiadiazole
CCDC	Cambridge Crystallographic Data Centre
cGMP	cyclic Guanosine Monophosphate
CLP	Cecal Ligation and Puncture
CO	Carbon monoxide
COHb	Carboxyhemoglobin
CO₂	Carbon dioxide
CO-RMs	Carbon monoxide Releasing Molecules
CPCM	Conductor-like Polarizable Continuum Model
DISC	Death-Inducing Signal Complex
DFT	Density Functional Theory
DMEM	Dulbecco's Minimal Essential Medium
EA	Elemental Analysis
Egr	Early growth response
ENAC	Expanded National Agency Check
EPA	Environmental Protection Agency
FBS	Fetal Bovine Serum
FT-IR	Fourier Transform Infrared Radiation
Hb	Hemoglobin
HO	Heme oxygenase
HOMO	High Occupied Molecular Orbital
HRMS	High Resolution Mass Spectrometry
HSF-1	Heat Shock Factor 1

IDM	Centro de Reconocimiento Molecular y Desarrollo Tecnológico
IL	Interleukin
iNOS	Inducible Nitric Oxide Synthase
ISO	International Organization for Standardization
LCD	Liquid Crystal Display
LEDs	Light-Emitting Diodes
LLCT	Ligand-to-Ligand Charge Transfer
LOD	Limit Of Detection
LUMO	Low Unoccupied Molecular Orbital
MAPK	Mitogen Activated Protein Kinase
MIP₁	Macrophage Inflammatory Protein 1
MO	Molecular Orbital
MS-ES	Electrospray ionization Mass Spectrometry
MTT	3-(4,5-dimethylthiazol-2-yl)-2,5-diphenyl tetrazolium bromide
NDIR	Non-Dispersive Infrared Method
NF-κB	Nuclear Factor kappa-B
NMR	Nuclear Magnetic Resonance
NO	Nitric Oxide
ORTEP	Oak Ridge Thermal Ellipsoid Plot
OSHA	Occupational Safety & Health Administration (US)
PAI-1	Plasminogen Activator Inhibitor 1
PGE₂	Prostaglandin E2
PPAR	Peroxisome Proliferator-Activated Receptor
ppm	Parts per million
QqTOF	Quadrupole Time OF Flight
RGB	Red-Green-Blue Coordinates
ROS	Reactive Oxygen Species
sGC	Soluble Guanylate Cyclase
TD-DFT	Time-dependent Density Functional Theory
TGA	Termogravimetric Analysis
TNF	Tumor Necrosis Factor

TWA	Time-Weighted Average
TZVP	Triple Zeta Valence Plus Polarization
UART	Universal Asynchronous Receiver-Transmitter
UPV	Universitat Politècnica de València
UV-Vis	Ultraviolet – Visible
VOCs	Volatile Organic Compounds

Table of Contents

1. General introduction	3
1.1 Carbon Monoxide.....	5
1.1.1 Pollutant role.....	7
1.1.2 Therapeutic role	15
1.2 Transition metal carbonyl complexes.....	22
2. Objectives.....	27
3. Rhodium complexes for CO detection	31
3.1. Sensitive and selective chromogenic sensing of carbon monoxide by using binuclear rhodium complexes.....	35
3.2. Sensitive and selective chromogenic sensing of carbon monoxide via reversible axial CO coordination in binuclear rhodium complexes.....	57
3.3. An optoelectronic sensing device for CO detection in air based on a binuclear rhodium complex.....	97
4. Rhodium complexes as CO-RMs.....	119
4.1. CO-releasing binuclear rhodium complexes as inhibitors of nitric oxide generation in stimulated macrophages.	123
5. Ruthenium and Osmium complexes for CO detection.....	143
5.1. A chromo-fluorogenic synthetic “canary” for CO detection based on a pyrenylvinyl ruthenium(II) complex	147
5.2. Ruthenium(II) and osmium(II) alkenyl complexes as highly sensitive and selective chromogenic probes for the sensing of carbon monoxide in air	179
6. Conclusions and perspectives	231
Appendix.....	235

1. *General introduction*

1.1 Carbon Monoxide

Carbon monoxide (CO), consisting of one carbon and one oxygen atoms, has a molar mass of 28.0, which makes it slightly lighter ($\rho = 1.145 \text{ kg/m}^3$ at 25 °C, 1 atm) than air. The bond length between the carbon and the oxygen atom is 112.8 pm, which is consistent with a triple bond that consists of two covalent ones as well as one dative covalent bond. The bond dissociation energy of 1072 kJ/mol represents the strongest chemical bond known.¹ With a boiling point of -191.5 °C and a melting point of -205.02 °C it is a gas at normal conditions. The ground electronic state of carbon monoxide is a singlet state² since there are no unpaired electrons.

¹ T. L. Cottrell, *The Strengths of Chemical Bonds*, 2nd ed., Butterworths Scientific Publications, London, **1958**.

² D. A. Case, B. H. Huynh, M. Karplus, *J. Am. Chem. Soc.* **1979**, *101*, 4433-4453.

Known as “the silent killer”, carbon monoxide is a poisonous gas that has no odour, colour or taste. Carbon monoxide is produced from the partial oxidation of carbon-containing compounds; this is when there is not enough oxygen to produce carbon dioxide (CO₂), such as when operating a stove or an internal combustion engine in an enclosed space. Coal gas, which was widely used before the 1960s for domestic lighting, cooking, and heating, had carbon monoxide as a significant fuel constituent. Some processes in modern technology, such as iron smelting, still produce carbon monoxide as a byproduct.

The combustion of excess of carbon in air at high temperature is a major industrial source of CO. This is, in an oven air is passed through a bed of coke. The initially produced CO₂ equilibrates with the remaining hot carbon to give CO. Above 800 °C, CO is the predominant product.

Worldwide, the largest source of carbon monoxide is natural in origin, due to photochemical reactions in the troposphere that generate about 5×10^{12} kilograms per year.³ Other natural sources of CO include volcanoes, forest fires, and other forms of combustion.

Despite not being the anhydride of any acid, CO can be produced in the laboratory by the dehydration of formic acid, for example with sulfuric acid.

Carbon monoxide is a reactive gas which takes part in the synthesis of multiple organic compounds. For instance, aldehydes are produced by the hydroformylation of alkenes with CO and H₂. CO can be reduced to methanol by hydrogenation process. Moreover, CO and methanol can give acetic acid when in the presence of a rhodium catalyst and hydroiodic acid. Phosgene (COCl₂) is produced by passing purified CO and chlorine gas through a bed of porous activated carbon, which serves as a catalyst. From an inorganic point of view, carbon monoxide is involved in the industrial preparation of methane (natural gas). CO is also used as industrial reductor in the extraction of metals, from the corresponding metal oxide ores. Figure 1.1 attempts to summarize the above mentioned reactivity.

³ B. Weinstock, H. Niki, *Science* **1972**, 176, 290-292.

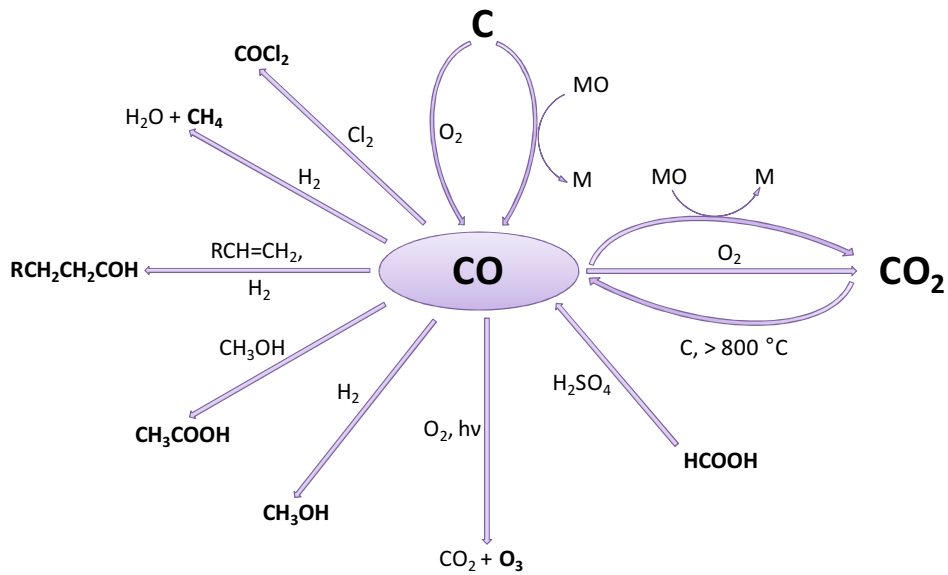


Figure 1.1. Carbon cycle flow diagram.

1.1.1 Pollutant role

Importance of CO detection

At high concentrations, CO is toxic to humans and animals. The greater danger of CO is its complexation with hemoglobin in the bloodstream. When inhaled, CO is readily absorbed from the lungs into the bloodstream, where it forms a tight but slowly reversible complex with hemoglobin (Hb) known as carboxyhemoglobin (COHb). CO binds 200 times more effectively to haemoglobin than oxygen. The presence of COHb in the blood decreases the oxygen carrying capacity, reducing the availability of oxygen to body tissues and resulting in tissue hypoxia. A reduction in oxygen delivery because of the elevated COHb level, exacerbated by impaired perfusion resulting from hypoxic cardiac dysfunction, potentially will impair cellular oxidative metabolism. COHb levels of greater than 20 % are typically associated with symptoms of clinical toxicity. Elevated or chronic

exposures may lead to neurotoxicity, cognitive and visual impairment, and unconsciousness, with death occurring in the range of 50 to 80 % COHb.⁴

The health risks associated with CO vary with its concentration and duration of exposure. Effects range from subtle cardiovascular and neurobehavioral effects (headache, nausea, dizziness, fatigue) at low concentrations to unconsciousness and death after prolonged exposures or acute exposures to high concentrations of CO. Risks associated with the relatively low ambient concentrations found in the environment and in contaminated work places have been extensively studied and reviewed⁵ and are listed in Table 1.1.

Indoor levels⁶ of CO range from 0.5 to 5 parts per million (ppm) but may reach much higher values (e.g. 100 ppm) with inefficient heating or ventilation, or in the presence of environmental tobacco smoke. In urban areas, ambient levels⁷ are typically 20 to 40 ppm, but may peak at much higher levels in heavily congested areas or alongside highways.

Carbon monoxide poisoning is a major public health problem and may be responsible for more than one-half of all fatal poisonings that are reported worldwide each year. Because of the risk of occult poisoning, some communities now require the installation of CO detectors in residences, along with smoke detectors and fire alarms.

⁴ D. Gorman, A. Drewry, Y. L. Huang, C. Sames, *Toxicology*, **2003**, *187*, 25-38.

⁵ a) D. G. Penney, *Carbon Monoxide*, CRC Press, Boca Raton, FL, **1996**; b) R. Bascom, P. A. Bromberg, D. L. Costa, R. Devlin, D. W. Dockery, M. W. Frampton, W. Lambert, J. M. Samet, F. E. Speizer, M. Utell, *Am. J. Respir. Crit. Care Med.* **1996**, *153*, 477-498; c) US Environmental Protection Agency, *Air Quality Criteria for Carbon Monoxide*, EPA/600/P-99/001. *National Center for Environmental Assessment*, Research Triangle Park, NC, **1999**.

⁶ D. Penney, V. Benignus, S. Kephelopoulos, D. Kotzias, M. Kleinman, A. Verrier, *WHO Guidelines for Indoor Air Quality: Selected Pollutants*, Copenhagen, **2010**, 55.

⁷ J. Raub, *WHO Environmental Health Criteria: Carbon Monoxide*, Geneva, **1999**, 70.

Table 1.1. Symptoms derived from exposure to different levels of CO.

Level of CO (ppm)	Health effects and other information
0.2	Natural CO levels in air
9	Maximum recommended indoor CO level (ASHRAE)
10-24	Possible health effects with long-term exposure
25	Max. TWA exposure for 8-hour-work-day (ACGIH)
35	Max. exposure allowed by OSHA in the workplace over an 8-hour-period
50	Max. permissible exposure in workplace (OSHA)
100	Slight headache after 1-2 hours
200	Dizziness, nausea, fatigue, headache after 2-3 hours
400	Headache and nausea after 1-2 hours. Life threatening in 3 hours
800	Headache, nausea, dizziness after 45 min; collapse and unconsciousness after 1 hour. Death within 2-3 hours
1000	Loss of consciousness after 1 hour of exposure

Existing methods for CO detection

When reviewing the existing methods for CO detection one has to go back in 1911, when canaries were traditionally used in coal mines to early detect life threatening gases, including CO. First analytical detectors were issued by the *Bureau of Mines*, for the first time in 1938 and extended in following publications.⁸ The main methods for detecting and determining CO are discussed below, outlining briefly the reactions or principles upon which are based, the range of concentrations that may be determined, the accuracy of determination; as well as the deficiencies that might have. The choice of method of analysis depends on such factors as: required accuracy, range of concentration involved, convenience, speed of analysis required, quantity of sample available, qualitative composition of sample or atmosphere to be analyzed, and possible effects of

⁸ J. J. Forbes, G. W. Grove, *Bureau of Mines Miners' Circ.*, **1954**, 33.

interfering gases. Some of the methods described require only adequate understanding of operational techniques, whereas others require thorough appreciation and skill in applying the principles involved.

The *National Bureau of Standards colourimetric carbon monoxide indicator*⁹ is a sensitive, hand-operated device for rapid detection and determination of low, physiologically significant concentrations of CO in air. It is sensitive to 0.001 % CO and will detect 0.01 to 0.04 % at ground level and 0.0025 to 0.05 % CO aboard aircraft in 1 to 5 minutes. The indicator is operated by squeezing a rubber bulb to aspirate the air sample through a small glass tube, which contains silica gel impregnated with palladous sulfate and ammonium molybdate. The colour change of the indicating gel, from yellow to progressively darker green is due to formation of molybdenum blue¹⁰ by reduction of initial palladous silicomolybdate, depends on the CO concentration and the volume of air drawn through the indicator tube. By matching the obtained test colour with a series of permanent colour standards, the CO concentration in the sampled air may be estimated. However, the indicating gel is sensitive to other oxidizable gases present in mine air samples, such as, ethylene and paraffin hydrocarbons with increasing numbers of carbon atoms; and produces similar colour changes. Oxides of nitrogen have been found to bleach CO test colours, thereby interfering with CO estimations in air that is contaminated with blasting fumes or diesel-engine exhaust gases.

By use of the *hoolamite detector*¹¹ the sampled atmosphere is first aspirated through an activated carbon cartridge, which removes interfering gases (acetylene, alcohol, ammonia, benzene, ether, hydrogen sulfide, hydrogen chloride, olefin hydrocarbons, and paraffin hydrocarbons above methane), then through a glass ampoule, which contains a mixture of iodine pentoxide, fuming sulfuric acid and pumice-stone granules. CO is oxidized, and the resultant colours range from blue-green to violet and finally black. The hoolamite detector may be used to determine semiquantitatively 0.1 to 1.0 % CO in air contaminated with smoke and fumes from fires and explosions. It is not sensitive enough, though, to

⁹ M. Shepherd, *Anal. Chem.*, **1947**, *19*, 77-81.

¹⁰ J. W. Cole, M. J. Salsbury, J. H. Yoe, *Anal. Chim. Acta*, **1948**, *2*, 115-126.

¹¹ S. H. Katz, J. J. Bloomfield, *Ind. Eng. Chem.*, **1922**, *14*, 304-306.

establish the absence of low, physiologically significant concentrations of CO in air.

The *carbon monoxide recorder*¹² is an instrument that may be used to sample, determine, and record continuously low concentrations of CO in air. Continuous determination of the CO content of the ventilating air of the tunnels allows automatic regulation of ventilation requirements in accordance with low, average, and peak traffic loads. The recorder operates as follows: The sampled air is drawn continuously through a cell containing hopcalite¹³ catalyst, where CO is oxidized at 100 °C. The heat liberated by oxidation of the CO is detected by a multiple-junction thermocouple circuit in the cell, and the electric potential generated, which is proportional to CO concentration, is measured by a recording potentiometer. CO concentrations as low as 1 to 2 ppm may be detected and recorded. Hydrogen is oxidized to some extent by passage over hopcalite, thus inducing a positive error.

The *carbon monoxide indicator* is a portable instrument that may be used for continuous determination of CO in air under various circumstances of suspected contamination. Two types of indicators are commercially available, a regular type, which aspirates the air sample through the indicator with a motor-driven pump; and a hand-cranked pump type for use where the possibility of the presence of flammable gases or solvent vapours must be considered. The portable indicator operates on the same principle as the CO recorder; sharing same drawbacks. CO is oxidized at room temperature in a hopcalite cell, and the heat of oxidation generates an electric potential in a thermocouple system connected to a millivoltmeter graduated in terms of CO concentration from 0 to 0.15 % volume.

The *carbon monoxide alarm*¹⁴ may be used to sample and continuously analyze the air of workshops and garages that may be contaminated by CO. The instrument operates on the same principle as the CO recorder and the portable indicator. CO

¹² H. W. Frevert, E. H. Francis, *Ind. Eng. Chem.*, **1934**, *6*, 226-228.

¹³ a) J. C. W. Frazer, *Jour. Phys. Chem.*, **1931**, *35*, 405-411; b) C. M. Loane, *Jour. Phys. Chem.*, **1933**, *37*, 615-622; c) E. C. Pitzer, J. C. W. Frazer, *Jour. Phys. Chem.*, **1941**, *45*, 761-776.

¹⁴ S. H. Katz, D. A. Reynolds, H. W. Frevert, J. J. Bloomfield, *Bureau of Mines Tech.*, **1926**, 335, 34.

is catalytically oxidized at 125 °C in a hopcalite cell containing a thermocouple circuit, and the instrument may be adjusted so that when 0.02 % or other predetermined concentration of CO is present, the thermoelectric potential generated is sufficient to close a relay, which activates an electrical circuit connected with a warning alarm such as flashing light or siren.

The *pyrotannic acid colourimetric method*¹⁵ may be used to determine the carboxyhemoglobin saturation in blood samples and the concentration of CO in air by using blood reagent solutions that have been equilibrated with air samples. The method is based upon the fact that a carmine-red suspension is formed by adding a mixture of pyrogalllic acid and tannic acid to a diluted sample of blood containing carboxyhemoglobin (COHb is formed by hemoglobin when CO is present). In absence of COHb a light gray-brown suspension is formed. In analyzing air samples, the method is particularly applicable in the concentration range from 0.01 to 0.20 % volume. Acid gases, such as sulfur dioxide, hydrogen sulfide, hydrogen cyanide, and hydrogen chloride, interfere with this method and should be removed.

The *iodine pentoxide method*¹⁶ is the standard laboratory procedure for the sensitive, accurate, chemical determination of carbon monoxide in air and in various gaseous mixtures. The method is based upon measurements of the iodine liberated by the oxidation of CO by heated iodine pentoxide according to the reaction: $5 CO + I_2O_5 \rightarrow I_2 + 5 CO_2$. Either the CO₂ or the I₂ can be collected and determined, and the volume of CO in the original gas sample can be calculated. Owing to the fact that the liberated I₂ partially oxidizes hydrogen, the determination of CO₂ is more precise. Besides, reactive and oxidizable gases, such as, ethylene interfere in the method. Likewise, moisture destroys the reactivity of I₂O₅. The analytical range of the procedure is from 0.0005 up to about 1.0 % CO volume.

¹⁵ F. Cook, *Ind. Eng. Chem.*, **1940**, *12*, 661-662.

¹⁶ a) E. G. Adams, N. T. Simmons, *Jour. Appl. Chem.*, **1951**, *1*, S20-S40; b) F. E. Vandaveer, *Gas*, **1942**, *18*, 24-29.

Low concentrations of CO in air may be determined by the *palladous chloride-phosphomolybdic acid-acetone colourimetric method*.¹⁷ The CO present in a 50 mL-air sample is absorbed and oxidized and the colour intensity of molybdenum blue formed is measured with a photoelectric colorimeter, and the CO concentration may be calculated from this reading. The range of this method is 0.002 to 0.06 %. However, the method is not specific for CO. Other commonly occurring oxidizable gases and vapours (ethylene, acetylene, hydrogen sulfide) have been found to show marked interfering effects.

In the mid-twentieth century, nondispersion-type infrared gas analyzers¹⁸ were developed and used to determine and record continuously the CO content of mine air, combustion gases, hydrogen, and other industrial process gases. The distinctive absorption of various regions of the infrared spectrum is a unique physical property of molecular gases; thus avoiding the interference of elemental diatomic gases. The use of different filters allows the specific determination of CO.

CO may be determined by gas-volumetric methods¹⁹ of analysis when it is present in appreciable concentrations as a component in various gaseous mixtures; however, all components that are reactive by absorption and combustion oxidation are directly determined by these procedures. CO may be determined by chemical absorption in cuprous salts reagents²⁰ by formation of the unstable molecular complex $\text{Cu}_2\text{Cl}_2 \cdot 2\text{CO} \cdot 4\text{H}_2\text{O}$ (cuprous salt reagents being the least satisfactory ones, as they readily absorb ethylene, acetylene and other unsaturates and oxygen; and need frequent replacement with fresh reagents to provide the assurance that CO will be completely absorbed); stoichiometric oxidation with cupric oxide²¹ heated at 300 °C according to the reaction $\text{CO} + \text{CuO} \rightarrow \text{CO}_2 + \text{Cu}^0$; slow combustion in air oxygen on heated platinum

¹⁷ J. T. Woods, M. G. Mollen, *Ind. Eng. Chem.*, **1941**, *13*, 760-764.

¹⁸ a) W. G. Fastie, A. H. Pfund, *Jour. Opt. Soc. America*, **1947**, *37*, 762-768; b) V. Z. Williams, *Rev. Sci. Instr.*, 1948, *19*, 135-178.

¹⁹ F. R. Brooks, L. Lyken, W. B. Milligan, H. R. Nebeker, V. Zahn, *Anal. Chem.*, **1949**, *21*, 1105-1116.

²⁰ H. Brückner, W. Gröbner, *Gas-u. Wasserfach*, **1935**, *78*, 269-273.

²¹ a) G. A. Burrell, G. G. Oberfell, *Ind. Eng. Chem.*, **1916**, *8*, 228-231; b) J. G. King, L. J. Edgcome, *Great Britain Fuel Res. Board Tech. Paper*, **1931**, *33*, 28.

filaments²² according to the reaction equation $2 CO + O_2 \rightarrow 2 CO_2$; and catalytic combustions in air or oxygen on platinised silica gel.²³ Errors are frequent with all these methods; as oxygen is also consumed in combustion of other gases such as hydrogen, methane and other paraffin hydrocarbons.

Many of the commonly used instruments and specialized procedures for detecting and determining CO are based on the use of oxidizing reagents. Various solid-state oxidants (platinum-group metals, reducible compounds, heavy metal oxides) may be used to oxidize CO either stoichiometrically or catalytically, at room temperature or at elevated temperatures, with formation of measurable amounts of CO₂, liberated I₂, or liberated heat of oxidation. In the latter case, the thermal effect can be detected and measured by multiple junction thermocouples, by thermopiles,²⁴ by thermistors,²⁵ and by thermometers.²⁶

Modern established methods for CO detection have been improved in terms of sensitivity. However, these methods that include gas chromatography,²⁷ laser infrared absorption²⁸ and electrochemical assays²⁹ have still some drawbacks to be solved. They cannot measure CO directly, require several time-consuming

²² J. R. Branham, M. Shepherd, S. Schuhmann, *Jour. Res. Nat. Bureau of Standards*, **1941**, *26*, 571-589.

²³ K. Kobe, R. A. MacDonald, *Ind. Eng. Chem.*, **1951**, *13*, 457-459.

²⁴ W. P. Kant, H. N. Cotabish, *United States Patent 2531592*, **1950**, Nov. 28.

²⁵ M. Katz, R. Riberdy, G. A. Grant, *Canadian Jour. Technol.*, **1952**, *30*, 303-310.

²⁶ C. H. Lindsley, J. H. Yoe, *Anal. Chimi. Acta*, **1948**, *2*, 127-132.

²⁷ a) M. J. van Rensburg, A. Botha, N. G. Ntsasa, J. Tshilongo, N. Leshabane, *Accred. Qual. Assur*, **2009**, *14*, 665-670; b) S. G. Walch, D. W. Lachenmeier, E-M. Sohnius, B. Madea, F. Musshoff, *Open Toxicology Journal*, **2010**, *4*, 21-25; c) J. Van Dam, P. Daenens, *J. Forens. Sci.*, **1994**, *39*, 473-478; d) A. M. Sundin, J. E. Larsson, *J. Chromatogr. B*, **2001**, *766*, 115-121; e) S. Oritani, B. L. Zhu, K. Ispida, K. Shimotouge, L. Quan, M. Q. Fujita, H. Maeda, *Forens. Sci. Intern.*, **2000**, *113*, 375-379.

²⁸ a) Y. Morimoto, W. Durante, D. G. Lancaster, J. Klattenhoff, F. K. Tittel, *Am. J. Physiol. Heart. Circ. Physiol.*, **2001**, *280*, H483-H488; b) S. V. Ivanov, A. A. Ionin, A. A. Kotkov, A. Y. Kozlov, L. V. Seleznev, D. V. Sinitsyn, O. G. Buzykin, *Combustion and Atmospheric Pollution*, **2003**, 631-634; c) S. Pei, F. Cui, X. Gao, W. Zhao, Y. Yong, H. Teng, H. Wei, W. Zhang, *Vib. Spectrosc.*, **2006**, *40*, 192-196; d) L. Li, F. Cao, Y. Wang, M. Cong, L. Li, Y. An, Z. Song, S. Guo, F. Liu, L. Wang, *Sensor. Actuat. B-Chem.*, **2009**, *142*, 33-38.

²⁹ a) S. S. Park, J. Kim, Y. Lee, *Anal. Chem.*, **2012**, *84*, 1792-1796; b) U. Hasegawa, A. J. van der Vlies, E. Simeoni, C. Wandrey, J. A. Hubbell, *J. Am. Chem. Soc.*, **2010**, *132*, 18273-18280.

intermediate steps (> 15 min) involving chemical reactions and/or are likely to generate false alarms in the presence of other chemicals or interfering gases.

Colourimetric CO sensing means, then, an excellent alternative to those methods. Only a few chromogenic probes are found in literature³⁰ able to detect CO in air but they lack sensitivity and/or selectivity. Therefore, the work described in this thesis features innovation, competitiveness and a promising future in the field of CO detection.

1.1.2 Therapeutic role

Importance of CO use in medical therapies

Despite the described dangerousness of carbon monoxide, this gas has recently attracted particular attention as a potential therapeutic agent. Although the endogenous production of CO as the natural product of haemoglobin turnover is known since the middle of the twentieth century (when CO was regarded as a metabolic elimination³¹ product); it was not until 1968 that, the heme oxygenase (HO) enzyme system responsible for the catalytic turnover of heme, was characterized and identified as a major source of CO in the body.³² Subsequent research sought to determine the physiological function of endogenously produced CO, as well as its role as a mediator of the cytoprotective properties of HO-1.³³ Moreover, recent works have revealed the impact of CO on some intracellular signaling pathways³⁴ (see Figure 1.2). CO can confer modulatory effects on the regulation of vascular function, inflammation, apoptosis, and cell proliferation, through stimulation of several signaling pathways. The sGC/cGMP axis has been implicated in vascular effects of CO with respect to vessel dilation, regulation of platelet aggregation, and regulation of fibrinolysis through PAI-1. The sGC/cGMP axis has also been implicated in downregulation of cell

³⁰ Previously described colourimetric probes have been reported in the introduction of the sixth article contained in this thesis.

³¹ T. Sjostrand, *Acta Physiol. Scand.*, **1952**, *26*, 338-344.

³² R. Tenhunen, H. S. Marver, R. Schmid, *Proc. Natl. Acad. Sci. USA*, **1968**, *61*, 748-755.

³³ See article contained in chapter 4 of this thesis.

³⁴ H. P. Kim, S. W. Ryter, A. M. Choi, *Annu. Rev. Pharmacol. Toxicol.*, **2006**, *46*, 411-449.

proliferation by CO, through upregulation of p38 mitogen activated protein kinase (MAPK) and p21. Anti-inflammatory and antiapoptotic effects of CO, including downregulation of proinflammatory cytokines production are also thought to be mediated by p38 MAPK. Additional mechanisms involving the inhibition of cytosolic reactive oxygen species (ROS) may play a role in regulation of apoptosis through inhibiting death-inducing signal complex (DISC) formation. Stimulation of mitochondrial ROS may upregulate PPAR γ leading to downregulation of the proinflammatory factor Egr-1. Additional signaling molecules such as heat shock factor-1 (HSF-1) and caveolin-1 have been shown to mediate the anti-inflammatory and antiproliferative effects of CO, respectively.

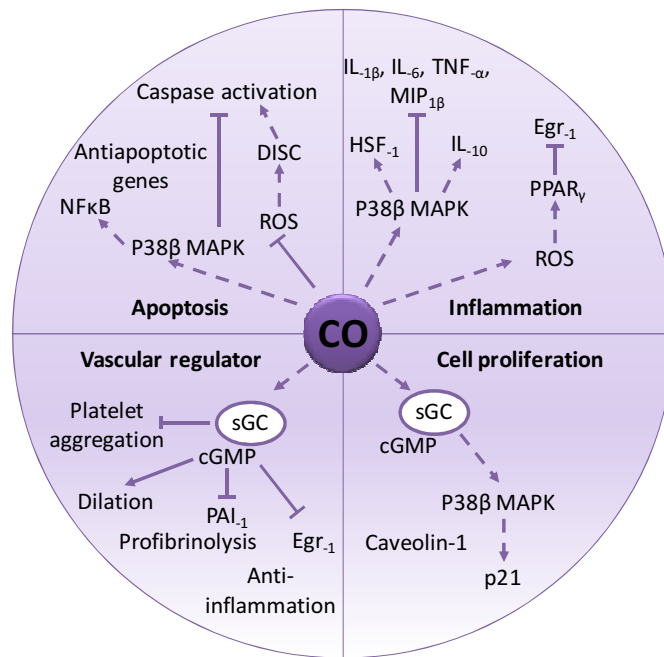


Figure 1.2. Signaling pathways regulated by CO.

New roles of CO have been identified on the regulation of several fundamental biological processes³⁵ including vascular tone,³⁶ inflammation,³⁷

³⁵ a) R. Motterlini, B. E. Mann, T. R. Johnson, J. E. Clark, R. Foresti, C. J. Green, *Curr. Pharm. Des.*, **2003**, *9*, 2525-2539; b) T. R. Johnson, B. E. Mann, J. E. Clark, R. Foresti, C. J. Green, R. Motterlini, *Angew. Chem. Int. Ed.*, **2003**, *42*, 3722-3729.

³⁶ W. Durante, F. K. Johnson, R. A. Johnson, *J. Cell. Mol. Med.*, **2006**, *10*, 672-686.

neurotransmission,³⁸ cell proliferation,³⁹ programmed cell death,⁴⁰ mitochondrial biogenesis⁴¹ and autophagy.⁴² Table 1.2 lists bioactivities mediated by CO and specifies the target system involved in each case.

Table 1.2. Bioactivities mediated by CO.

Bioactivity of CO	Target
Vasoactive effects	Cardiovascular and respiratory systems Nervous system Hepatic and renal circulation Gastrointestinal system
Anti-inflammatory effects	Cardiovascular and respiratory systems Gastrointestinal system
Inhibition of platelet aggregation	Cardiovascular system
Neurotransmission and neuroendocrine function	Nervous system
Activation of ion channels	Cardiovascular system
Oxygen sensing	Cardiovascular and nervous systems
Inhibition of smooth muscle cell proliferation	Cardiovascular and respiratory systems
Anti-apoptotic and cytoprotective effects	Cardiovascular and respiratory systems Gastrointestinal system

³⁷ L. E. Otterbein, F. H. Bach, J. Alam, *Nat. Med.*, **2000**, *6*, 422-428.

³⁸ A. Verma, D. J. Hirsch, C. E. Glatt, G. V. Ronnett, S. H. Snyder, *Science*, **1993**, *259*, 381-384.

³⁹ T. Morita, S. A. Mitsialis, H. Koike, Y. Liu, S. Kourembanas, *J. Biol. Chem.*, **1997**, *272*, 32804-32809.

⁴⁰ S. Brouard, L. E. Otterbein, J. Anrather, *J. Exp. Med.*, **2000**, *192*, 1015-1026.

⁴¹ H. B. Suliman, M. S. Carraway, L. G. Tatro, C. A. Piantadosi, *J. Cell. Sci.*, **2007**, *120*, 299-308.

⁴² S. J. Lee, S. W. Ryter, J. F. Xu, *Am. J. Respir. Cell. Mol. Biol.*, **2011**, *45*, 867-873.

The initial evidence supporting a beneficial action of CO originated from studies on lung injury in animals⁴³ and was reproduced later in almost all tissues examined, including heart, liver, kidney, intestine and reticulo-endothelial system.⁴⁴

Existing medical therapies involving CO

Despite the interesting biological activities discovered, the development of methods for delivering CO is in its infancy. Since CO is toxic at high concentrations, the precise control of the location, timing, and dosages of CO is the critical factor for appropriate therapeutic responses. In addition, the fact that CO is a gaseous molecule makes its controlled delivery more challenging. At the present, three different approaches have been proposed for examining the therapeutic potential of CO: direct administration of CO gas; use of prodrugs (i. e. methylene chloride) that are catabolized by hepatic enzymes to generate CO;⁴⁵ and transport and delivery of CO by means of specific CO carriers.

The simplest administration method is the *inhalation of CO* at a known and low concentration. The therapeutic benefit of CO inhalation has been shown in a number of preclinical animal models of acute lung injury, ischemia/reperfusion injury, sepsis, vascular injury, organ transplantation and others. As an example, anti-inflammatory studies with macaques exposed to 500 ppm CO during 6 hours (resulting in elevated COHb levels, > 30 %) have shown reduction of pulmonary neutrophilia.⁴⁶ In another example, the administration of 250 ppm CO to rodent models during hyperoxia exposure has provided protection against acute lung injury.⁴⁷ Also, the inclusion of 250 ppm CO during mechanical ventilation has

⁴³ L. E. Otterbein, L. L. Mantell, A. M. K. Choi, *Am. J. Physiol.*, **1999**, 276, L688-L694.

⁴⁴ a) H. P. Kim, S. W. Ryter, A. M. Choi, *Annu. Rev. Pharmacol. Toxicol.*, **2006**, 46, 411-449;

b) S. W. Ryter, J. Alam, A. M. Choi, *Physiol. Rev.*, **2006**, 86, 583-650.

⁴⁵ C. Chauveau, D. Bouchet, J. C. Roussel, P. Mathieu, C. Braudeau, K. Renaudin, L. Tesson, J. P. Souillou, S. Iyer, R. Buelow, I. Aegon, *Am. J. Transplant.*, **2002**, 2, 581-592.

⁴⁶ L. A. Mitchell, M. M. Channell, C. M. Royer, S. W. Ryter, A. M. Choi, J. D. McDonald, *Am. J. Physiol. Lung Cell. Mol. Physiol.*, **2010**, 299, L891-L897.

⁴⁷ L. E. Otterbein, L. L. Mantell, A. M. Choi, *Am. J. Physiol.*, **1999**, 276, L688-L694.

prevented lung injury.⁴⁸ Exogenous application of CO (500 ppm), significantly has protected the graft, and has reduced hemorrhage, fibrosis, and thrombosis after transplantation.⁴⁹ Moreover, exemplifying with human beings models, COHb levels of 10-20 % have been administrated after 250 ppm CO exposure, without poisonous effects.⁵⁰ In spite of all these successful examples, this method is a very nonspecific approach that can cause adverse effects.

As an alternative approach to the administration of CO gas by inhalation, *chemical CO-donor compounds* termed carbon monoxide releasing molecules (CORMs) have been developed as experimental therapeutics over the last decade.⁵¹ CORMs represent a good alternative to CO gas in terms of specificity of action. CO liberated from CORMs can be precisely controlled and delivered at given concentrations through all possible routes of administration. However, the main advantage of CORMs is that they deliver CO to tissues with less COHb buildup typical of inhalation CO (COHb level < 10 %), as is likely to bypass more effectively the biological trap represented by deoxyhemoglobin (rapidly converted to COHb through CO gas inhalation). Several prototypical CORMs have been extensively tested in experimental models (see Figure 1.3), including the original Mn₂CO₁₀ (**CORM-1**)⁵² and ruthenium compounds [Ru(CO)₃Cl₂]₂ (**CORM-2**)⁵³ and Ru(CO)₃Cl(glycinate) (**CORM-3**). **CORM-1** and **CORM-2** are commercially available hydrophobic transition metal carbonyls, while **CORM-3** is water-soluble and rapidly releases CO in physiological fluids (t_{1/2} < 1 min). A water-soluble boron-

⁴⁸ T. Dolinay, M. Szilasi, M. Liu, A. M. Choi, *Am. J. Respir. Crit. Care Med.*, **2004**, *170*, 613-620.

⁴⁹ R. Song, M. Kubo, D. Morse, *Am. J. Pathol.*, **2003**, *163*, 231-242.

⁵⁰ F. B. Mayr, A. Spiel, J. Leitner, C. Marsik, P. Germann, R. Ullrich, *Am. J. Respir. Crit. Care Med.*, **2005**, *171*, 354-360.

⁵¹ R. Motterlini, L. E. Otterbein, *Nat. Rev. Drug Discov.*, **2010**, *9*, 728-743.

⁵² a) R. Motterlini, J. E. Clark, R. Foresti, P. Sarathchandra, B. E. Mann, C. J. Green, *Circ. Res.*, **2002**, *90*, E17-E24; b) E. Fiumana, H. Parfenova, J. H. Jagger, C. W. Leffler, *Am. J. Physiol. Heart Circ. Physiol.*, **2003**, *284*, H1073-H1079; c) B. Arregui, B. Lopez, M. G. Salom, F. Valero, C. Navarro, F. J. Fenoy, *Kidney Int.*, **2004**, *65*, 564-574.

⁵³ a) J. Megias, J. Busserolles, M. J. Alcaraz, *Br. J. Pharmacol.*, **2007**, *150*, 977-986; b) B. W. Sun, Z. Y. Chen, X. Chen, C. Liu, *J. Burn. Care Res.*, **2007**, *28*, 173-181; c) M. Allanson, V. E. Reeve, *Cancer Immunol. Immunother.*, **2007**, *56*, 1807-1815; d) K. Srisook, S. S. Han, H. S. Choi, M. H. Li, H. Ueda, C. Kim, Y. N. Cha, *Biochem. Pharmacol.*, **2006**, *71*, 307-318.

containing CORM (**CORM-A1**)⁵⁴ has also been developed, which slowly releases CO ($t_{1/2} = 21$ min) in pH and temperature-dependent fashion. A new CORM (**CORM-S1**)⁵⁵ based on iron and cysteamine has recently been synthesized, which is soluble in water and releases CO under irradiation with visible light, while it is stable in the dark.

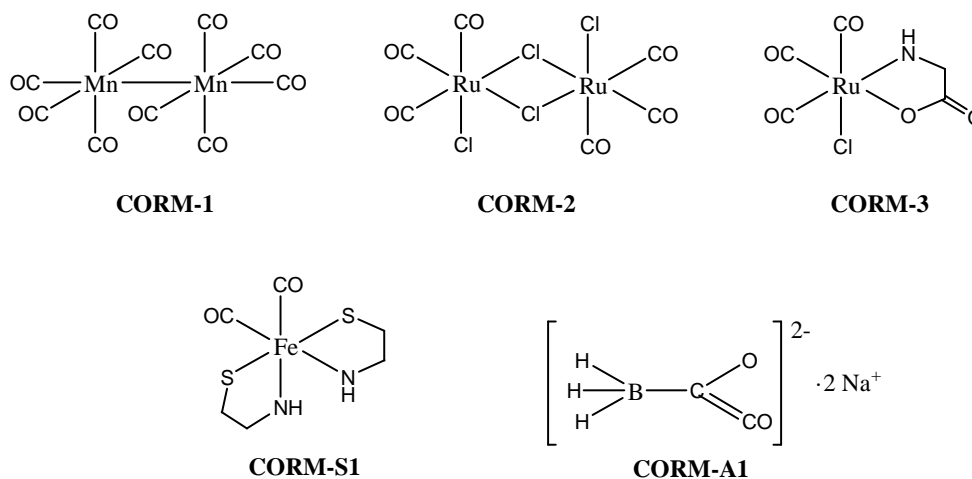


Figure 1.3. Structure of most common CORMs.

CORMs have demonstrated vasoactive effects. Table 1.3 summarizes the bioactive properties of most common CORMs. In particular, **CORM-3** has shown to produce a rapid vasodilatory response.⁵⁶ This compound has been shown to alleviate damage in ischemia/reperfusion injury, inhibit allograft rejection, suppress nitric oxide (NO) production from macrophages, and attenuate cardiovascular inflammation and thrombin-induced neuroinflammation. While **CORM-3** has been shown to prevent reoccurrence of sepsis and to reduce liver

⁵⁴ a) A. Sandouka, B. J. Fuller, B. E. Mann, C. J. Green, R. Foresti, R. Motterlini, *Kidney Int.*, **2006**, *69*, 239-247; b) H. Parfenova, S. Basuroy, S. Bhattacharya, D. Tcheranova, Y. Qu, R. F. Regan, C. W. Leffler, *Am. J. Physiol. Cell Physiol.*, **2005**, *290*, C1399-C1410; c) M. J. Ryan, N. L. Jernigan, H. A. Drummond, G. R. Jr. McLemore, J. M. Rimoldi, S. R. Poreddy, R. S. Gadepalli, D. E. Stec, *Pharmacol. Res.*, **2006**, *54*, 24-29.

⁵⁵ R. Kretschmer, G. Gessner Guido, H. Gorls, S. Heinemann, M. Westerhausen, *J. Inorg. Biochem.*, **2011**, *105*, 6-9

⁵⁶ R. Foresti, J. Hammad, J. E. Clark, *Br. J. Pharmacol.*, **2004**, *142*, 453-460.

injury after cecal ligation and puncture (CLP); **CORM-2** prolongs survival and reduces inflammation (see Figure 1.4).⁵⁷ In cardiac transplantation model, inclusion of **CORM-3** in the preservation fluid improved cardiac function following transplantation.⁵⁸ Though the discovery of these CO-releasing molecules opens up new possibilities, there are still several issues to overcome for medical applications, particularly those in which downstream tissue sites draining the injection site are targeted. These small molecular drugs diffuse rapidly within the body after administration and may liberate CO prior to reaching these target tissues. Thus, there is still a considerable need for developing a safe and efficient CO-delivery system.

Table 1.3. Bioactive properties of most common CORMs.

Compound	CO release kinetic and properties	Pharmacological action
CORM-1	Fast ($t_{1/2} < 1$ min) CO release is light-dependent Soluble in ethanol and DMSO	Vasodilator; Reno-protective
CORM-2	Fast ($t_{1/2} \approx 1$ min) CO release induced by ligand substitution Soluble in ethanol and DMSO	Vasodilator; Reno-protective; Anti-inflammatory; Anti-carcinogenic; Pro-angiogenic; Anti-apoptotic; Inhibitor of cell proliferation
CORM-3	Fast ($t_{1/2} \approx 1$ min, pH 7.4, 37 °C) CO release induced by ligand substitution Water-soluble	Vasodilator; Reno-protective; Cardioprotective; Anti-inflammatory; Anti-ischemic; Inhibitor of platelet aggregation
CORM-A1	Slow ($t_{1/2} \approx 21$ min, pH 7.4, 37 °C) CO release is pH-dependent Water-soluble	Vasodilator; Reno-protective; Anti-ischemic; Anti-apoptotic

⁵⁷ G. Cepinskas, K. Katada, A. Bihari, R. F. Potter, *Am. J. Physiol. Gastrointest. Liver Physiol.*, **2008**, *294*, G184-G191.

⁵⁸ M. D. Musameh, C. J. Green, B. E. Mann, B. J. Fuller, R. Motterlini, *J. Heart Lung Transplant*, **2007**, *26*, 1192-1198.

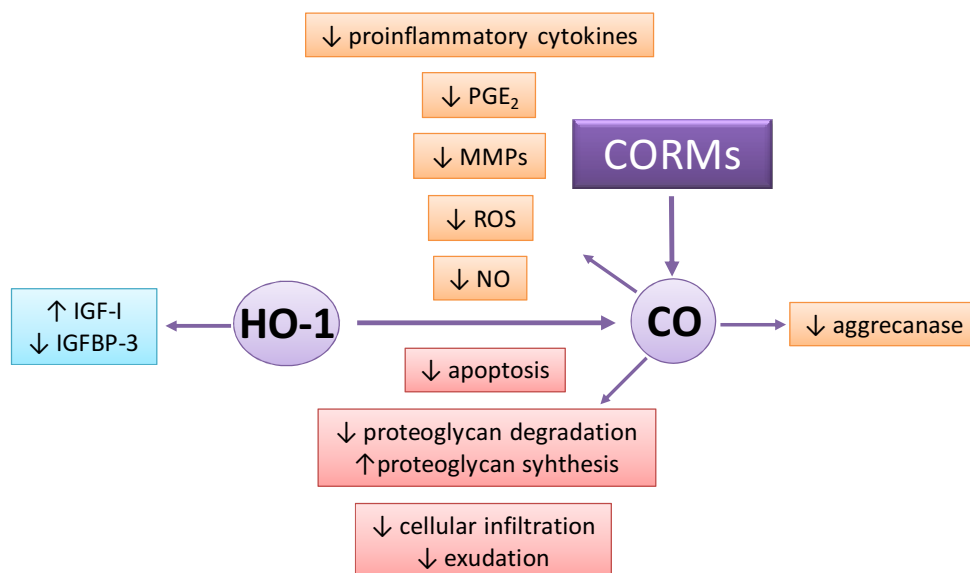


Figure 1.4. Protective effects of CO release via induction of HO-1, able to decrease production of inflammatory mediators and degradative enzymes; and reduce chondrocyte apoptosis.

1.2 Transition metal carbonyl complexes

In 1890, Ludwig Mond et al. published for the first time the synthesis of tetracarbonylnickel $[\text{Ni}(\text{CO})_4]$.⁵⁹ This colourless liquid was fortuitously obtained while attempting to recover the chlorine lost during the ammonia-soda process using the transition metal in the form of nickel oxide. The metal oxide was initially reacted in a combustion tube with CO and then heated with a flame in order to render the gases innocuous. After the reaction was completed, Mond noticed by accident that during the cooling process metallic nickel was formed. The discovery led Mond to recognize immediately the industrial potential of the interaction between metals and CO and he soon developed a new process for purifying metallic nickel. In the last step of this process, nickel contained in ores is

⁵⁹ W. A. Hermann, *J. Organomet. Chem.*, **1990**, *383*, 21-44.

volatilised as $[\text{Ni}(\text{CO})_4]$ by treatment with CO and the mixture of these two gases is finally heated to a temperature at which only extremely pure nickel is deposited.

In the subsequent years, numerous carbonyl derivatives containing iron, cobalt, molybdenum and ruthenium were synthesized and purified. The industrial exploitation of Mond's discovery is exemplified by the fact that nowadays formation of carbonyl complexes in the extraction of metals enables excellent yields of pure nickel on large scale productions and similar results can be obtained with iron pentacarbonyl for use in magnetic tapes.

With the growing interest in the characterization of a variety of metal carbonyls that could be used in organic synthesis and catalytic processes, the unique chemical reactivity of these compounds also began to unfold.

Most metals form coordination complexes containing covalently attached carbon monoxide. To better understand how CO bonds to transition metals. It is necessary to understand the bonding of CO itself. Figure 1.5 shows molecular orbital diagram of CO.

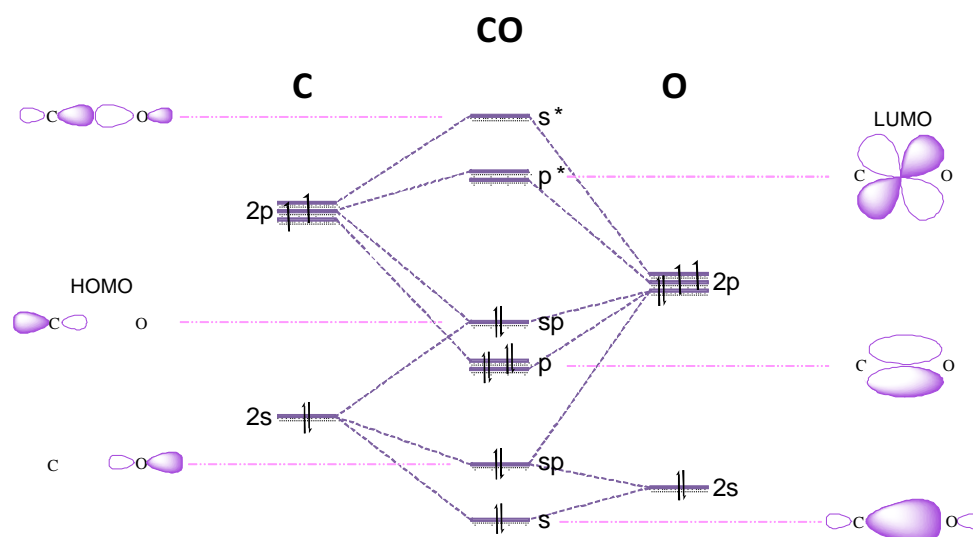


Figure 1.5. Molecular Orbital Diagram of CO.

Carbon monoxide, having two lone pair electrons, is a good Lewis base that can react as a ligand with metals through a σ -bond (homo). The formation of metal carbonyls is favoured by the fact that CO acts, as well, as π acceptor by a π -back bonding interaction with the π -anti-bonding orbital (lumo) placing electrons from the accessible filled d-orbitals from the metal. Therefore, carbon monoxide bonds preferentially to metals around the middle of the transition metals, i.e. groups 6 to 10. As represented in Figure 1.6, CO ligand in metal carbonyls acts as σ -donor and π -acceptor and so the bonding is covalent. This electron delocalization is responsible for the stabilization of low oxidation states of the metal.

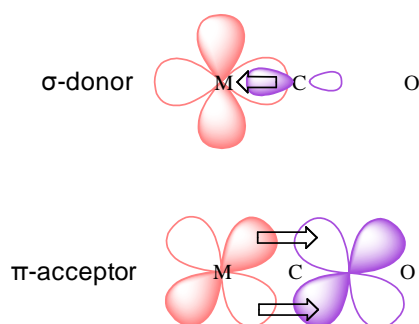


Figure 1.6. Schematic representation of π -back bonding between CO and a transition metal centre.

For stability, the metal of most metal carbonyls has 18 electrons available for bonding. As an example, iron pentacarbonyl $[\text{Fe}(\text{CO})_5]$ gives a total electron count of $18 = (8 + 2 \times 5)$; as group 8 iron (has 8 valence electrons in oxidation state 0) and each CO contributes 2 electrons from the carbon lone pair. For metals with 8 valence electrons, species with 16-electrons are also stable. This is the case of $[\text{Rh}(\text{CO})_2\text{I}_2]^-$ where group 9 Rh^+ (with $9 - 1 = 8$ valence electrons) and each of the four ligands (two CO and two I $^-$) provide a pair of electrons, giving a total electron count of $16 = (8 + 2 \times 4)$. These electron counts are very important in understanding reactivity. In general, metal carbonyls that do not meet these rules are unstable.

Shape of metal carbonyl

There are four main shapes for metal carbonyls depending on the number of groups attached to the metal.

When there are six ligands, the shape is octahedral with the ligands aligned along the directions of the Cartesian axes. See Figure 1.7a where L^1 , L^2 , L^3 and L^4 are *cis*-to the CO, and L^5 is *trans* to the CO.

When there are five ligands, the usual shape is trigonal bipyramidal. There are two different ligand positions, axial or equatorial. The first example in Figure 1.7b has the CO in the axial position; where L^1 , L^2 and L^3 are *cis*-to the CO and are equatorial, while L^4 is *trans* to the CO and is axial. The second example in Figure 1.7c has the CO equatorial; where L^1 and L^4 are *cis*-to the CO and are axial, while L^2 and L^3 are at 120° to the CO and are equatorial.

When there are four ligands, there are two possible geometries. If the electron count is 18, then the usual geometry is tetrahedral; where L^1 , L^2 and L^3 are all equivalent. Alternatively, if the electron count is 16, then the usual geometry is square planar; where L^1 and L^2 are *cis*-to the CO, while L^3 is *trans* to the CO.

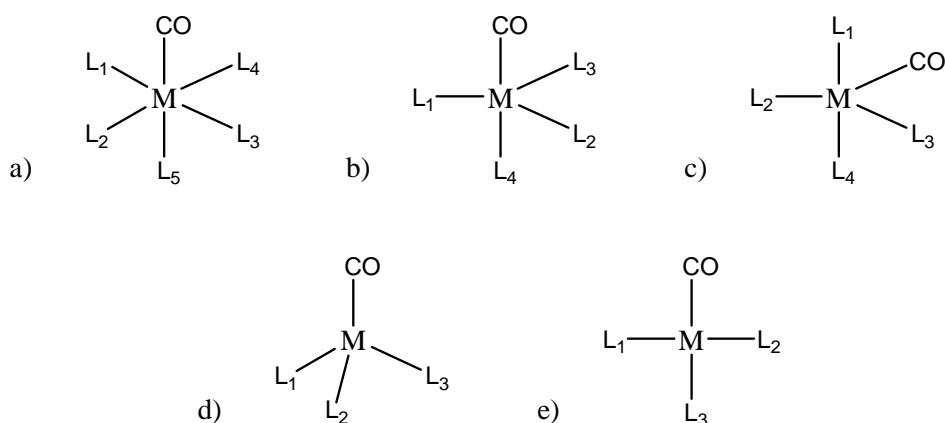


Figure 1.7. Structural shape of metal carbonyls depending on the number of ligands.

2. Objectives

In this thesis we focus on the detection of carbon monoxide in air and in solution by means of the use of different transition metal complexes (rhodium, ruthenium and osmium) that are able to coordinate carbon monoxide through colour and/or fluorescence changes. Particular, our aim was:

- To prepare a family of binuclear rhodium complexes and evaluate its use for the sensitive, selective and reversible chromogenic sensing of carbon monoxide in air.
- To implement the studied rhodium probes in an opto-chemical device able to quantitatively sense carbon monoxide present in air.
- To evaluate the use of binuclear rhodium complexes as Carbon Monoxide Releasing Molecules, considering CO as a potential therapeutic agent.
- To prepare a collection of vinyl ruthenium and osmium complexes and test its use for sensitive and selective chromo-fluorogenic sensing of carbon monoxide in air.

3. *Rhodium complexes for CO detection*

In this chapter, the sensitive, selective and reversible sensing of CO in air is described, by reporting three different publications.

In the first article (*Angew. Chem. Int. Ed.*, 2010, 49, 4934-4937), carbon monoxide is detected selectively and sensitively by the binuclear rhodium complex *cis*-[Rh₂(C₆H₄PPh₂)₂(O₂CCH₃)₂](HO₂CCH₃)₂ **A**. This complex, which contains two cyclometalated phosphine ligands, coordinates CO axially and undergoes a colour change from violet to orange-yellow (see Figure 3.1).

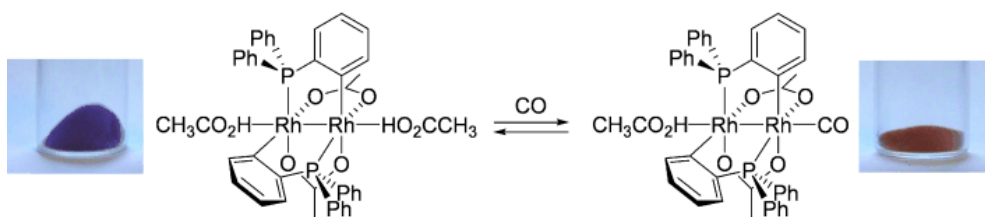


Figure 3.1. Mechanism of CO coordination in binuclear rhodium complex **A** and colour change observed upon CO sensing.

An extension of this preliminary work produced the second article (*J. Am. Chem. Soc.*, 2011, 133, 15762-15772) included in this doctoral dissertation. A collection of five rhodium (II) complexes **A-F** adsorbed on silica are used as probes for CO detection simply based in colour changes visible to the naked eye.

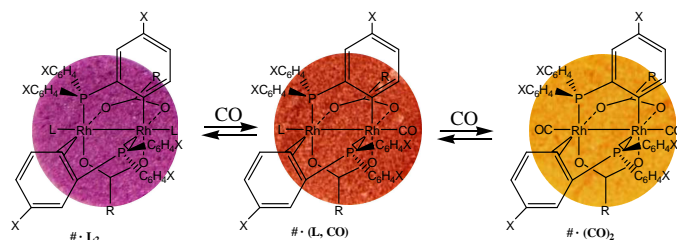


Figure 3.2. Two-step reversible CO coordination in binuclear rhodium complexes **A-F** and colour change induced.

The use of these complexes and its application in an optical device led to a third publication (*Sensors and Actuators B*, 2014, 191, 257-263). Complex **D** $[\text{Rh}_2[(\text{C}_6\text{H}_4)\text{P}(\text{C}_6\text{H}_5)_2]_2(\text{O}_2\text{CCF}_3)_2] \cdot (\text{CF}_3\text{CO}_2\text{H})_2$ was selected as the one with highest sensitivity to CO when deposited on cellulose paper. The improved handling of the sensing probe enabled the introduction in a simple portable opto-electronic system (see Figure 3.3) capable of quantifying CO present in air. The colour change occurred in the chemical probe is registered and transduced to an electrical signal, and this signal to a certain CO concentration value.

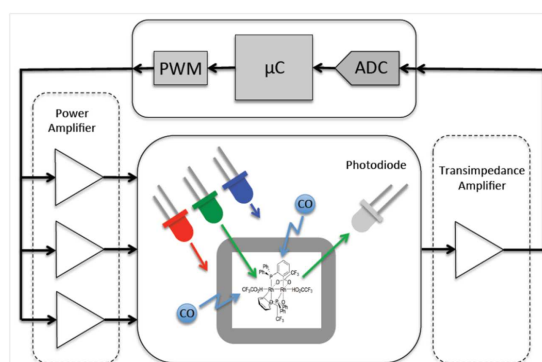


Figure 3.3. Schematic representation of the optoelectronic system used in an easy-to-use portable device for the selective and sensitive detection of CO in air.

***3.1. Sensitive and selective chromogenic sensing
of carbon monoxide by using binuclear rhodium
complexes***

Sensitive and Selective Chromogenic Sensing of Carbon Monoxide by Using Binuclear Rhodium Complexes

Julio Esteban, José Vicente Ros-Lis, Ramón Martínez-Máñez,
M. Dolores Marcos, María Moragues, Juan Soto and Félix
Sancenón*

*Instituto de Reconocimiento Molecular y Desarrollo Tecnológico (IDM), Centro
Mixto Universidad Politécnica de Valencia-Universidad de Valencia, Spain.*

*Departamento de Química, Universidad Politécnica de Valencia,
Camino de Vera s/n, 46022, Valencia, Spain.*

CIBER de Bioingeniería, Biomateriales y Nanomedicina (CIBER-BBN).

Received: March 5, 2010

Published online: June 2, 2010

*(Reprinted with permission from
Angewandte Chemie International Edition, 2010, 49, 4934–4937.
Copyright © 2010, WILEY-VCH Verlag GmbH & Co. KGaA, Weinheim)*

Carbon monoxide is an airborne contaminant that is toxic at low concentration levels and is difficult to detect as it is colorless and odorless. This hazard presents a real danger¹⁻⁴ in urban and indoor air, where concentrations of carbon monoxide can reach quite high levels. Typical anthropogenic sources of this pollutant involve combustion engines and improper burning of other fuels. For healthy adults, CO becomes toxic when it reaches a level higher than 50 ppm with continuous exposure over an eight-hour period. Medium exposure (a CO level between 150 ppm to 300 ppm) produces dizziness, drowsiness, and vomiting, whereas extreme exposure (a CO level of 400 ppm and higher) results in unconsciousness, brain damage, and death. Persons with CO poisoning often overlook the symptoms, and undetected exposure can be fatal. Unintentional CO exposure accounts for an estimated 15000 emergency department visits and 500 unintentional deaths in the United States alone each year.⁵

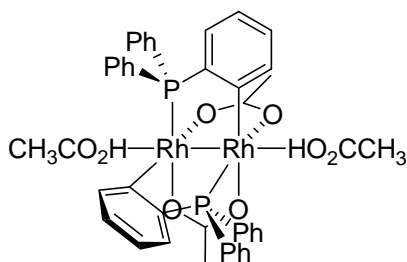
Most existing CO sensors use semiconducting metal oxides.⁶ As an alternative for certain applications, the development of chromogenic sensing systems that allow the presence of CO at poisonous concentrations to be easily detected with the naked eye may be of interest. However, colorimetric chromogenic probes for the detection of this deadly chemical are still rare. Reported chromogenic systems include the use of oxoacetatobridged triruthenium cluster complexes,⁷ rhodium complexes,⁸ polypyrrole functionalized with iron porphyrin derivatives,⁹ hybrid materials incorporating a cobalt(III) corrole complex,¹⁰ and iron compounds of diisopropylphosphinodiaminopyridine.¹¹ Important drawbacks to some of these reported systems involve poor color modulations, CO sensing in solution but not in air, and relatively large detection limits.

Following our interest in the design of novel chromogenic systems,¹² we report herein the development of a colorimetric probe that shows unambiguous color modulations for the sensitive and selective sensing of carbon monoxide.

The chromogenic probe involves the use of binuclear rhodium derivatives, and the sensing function is based on the well-known ability of these complexes to bind in axial sites.¹³ Furthermore, it was envisioned that a suitable selection of the bridging ligands in these binuclear derivatives may modulate the electron density of the metals in order to facilitate back donation from metal orbitals to the π^*

molecular orbital of CO. Moreover, it is also known that axial coordination on binuclear rhodium derivatives may result in color shifts.¹³

After preparing and testing a number of binuclear rhodium derivatives, we finally selected the compound of the formula $\text{cis-}[\text{Rh}_2(\text{C}_6\text{H}_4\text{PPh}_2)_2(\text{O}_2\text{CCH}_3)_2](\text{HO}_2\text{CCH}_3)_2$ (**1**·(**CH₃CO₂H**)₂) for CO signaling applications (Scheme 1). This product, prepared by Cotton et al. in 1985, was the first dirhodium(II) derivative containing two metalated phosphine ligands in a head-to-tail arrangement.¹⁴



Scheme 1. The complex **1**·(**CH₃CO₂H**)₂.

In a preliminary experiment, air samples containing CO were bubbled into chloroform containing **1**·(**CH₃CO₂H**)₂. A remarkable color change of the solutions from violet to orange-yellow was found. These changes are consistent with an axial coordination by CO. To corroborate the binding of carbon monoxide in **1**, crystals suitable for single X-ray diffraction were obtained from CH_2Cl_2 solution of **1**·(**CH₃CO₂H**)₂ in the presence of CO to which hexane was layered. Slow evaporation of this solution resulted in different yellow-orange crystals containing mixtures of the species **1**·(**CO,CH₃CO₂H**) and **1**·(**CO**)₂ (see the Supporting Information).

The structure of **1**·(**CO,CH₃CO₂H**) consists of a binuclear dirhodium core bridged by cisoid acetate groups, two orthometalated triphenylphosphines, and axial sites occupied by acetic acid and carbon monoxide (Figure 1).¹⁵ This complex is the first reported crystal structure of a binuclear rhodium derivative containing two different axial ligands. The isolation of this asymmetric compound **1**·(**CO,CH₃CO₂H**) can be explained by considering the inductive effect of the first

CO coordination, which is effectively transferred through the metal–metal bond to weaken the Lewis acidity of the second center. Furthermore, in this case, the ability of the axial ligand to behave as a π acceptor must also play an important role in the stability of the mono substituted adduct.

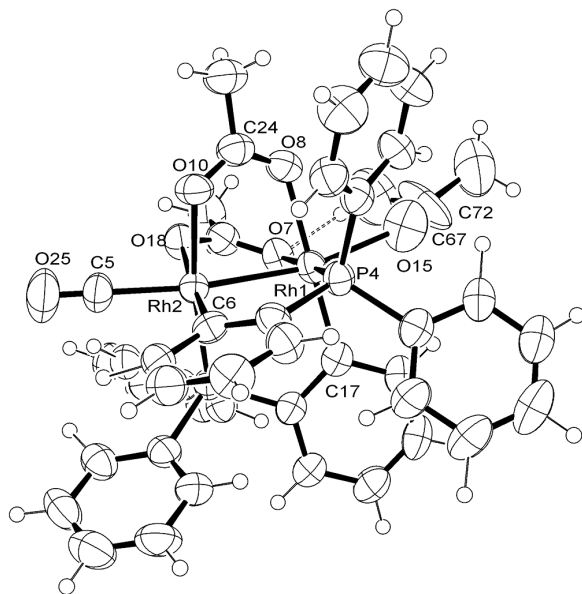


Figure 1. ORTEP of the crystal structure of **1·(CO, CH₃CO₂H)**; ellipsoids are set at 50% probability.

Selected bond lengths [Å] and angles [°]: Rh1–Rh2 2.5424(6), Rh1–P4 2.2118(12), Rh2–P3 2.2385(14), Rh1–O15 2.358(24), Rh2–C5 1.981(6), C5–O25 1.112(7); Rh2–C5–O25 178.1(5).

Further characterization of the **1·(CO,CH₃CO₂H)** complex demonstrated the existence of a C–O stretching frequency of 2028 cm⁻¹ which is considerably lower than the C–O stretching frequency of the free carbon monoxide (2143 cm⁻¹) suggesting a relatively high level of M→CO π back-bonding interaction. Additionally, the ¹³C NMR spectrum exhibited a resonance at $\delta = 128.4$ ppm assigned to the coordinated carbon monoxide ligand.

Motivated by the favorable chromogenic sensing features observed in chloroform by **1·(CH₃CO₂H)₂** in solution, we took a step forward towards the potential use of this compound for the detection of CO in air. With this idea in mind, compound **1·(CH₃CO₂H)₂** was adsorbed on silica gel, resulting in a modified

gray-violet solid. In a typical test, this colored silica support containing the rhodium probe was exposed to air containing different concentrations of carbon monoxide. A remarkable color modulation from violet to orange-yellow was observed after few minutes of exposure. Moreover, a more detailed look at the titration process, using an increasing concentration of carbon monoxide, clearly revealed that two products are formed. Thus, the visible diffuse reflectance spectrum of silica gel containing $1\cdot(\text{CH}_3\text{CO}_2\text{H})_2$ shows a unique band at 554 nm. The presence of air containing a large excess of CO resulted in the appearance of a new band at 398 nm, whereas at intermediate concentrations of CO, a band at 475 nm was observed (Figure 2). These changes are consistent with an axial coordination by CO and the formation of the derivatives $1\cdot(\text{CO})_2$ and $1\cdot(\text{CO}, \text{CH}_3\text{CO}_2\text{H})$ (Scheme 2).

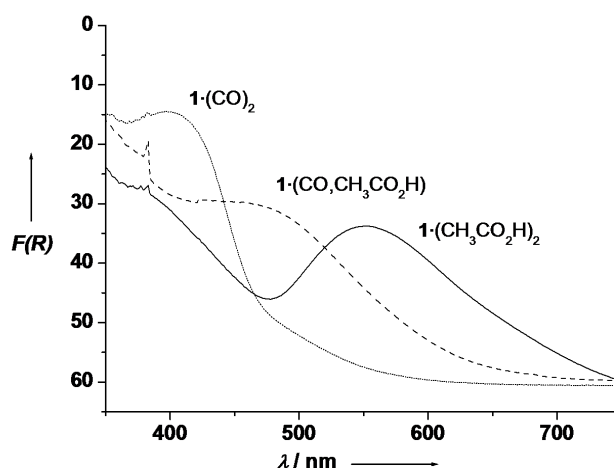
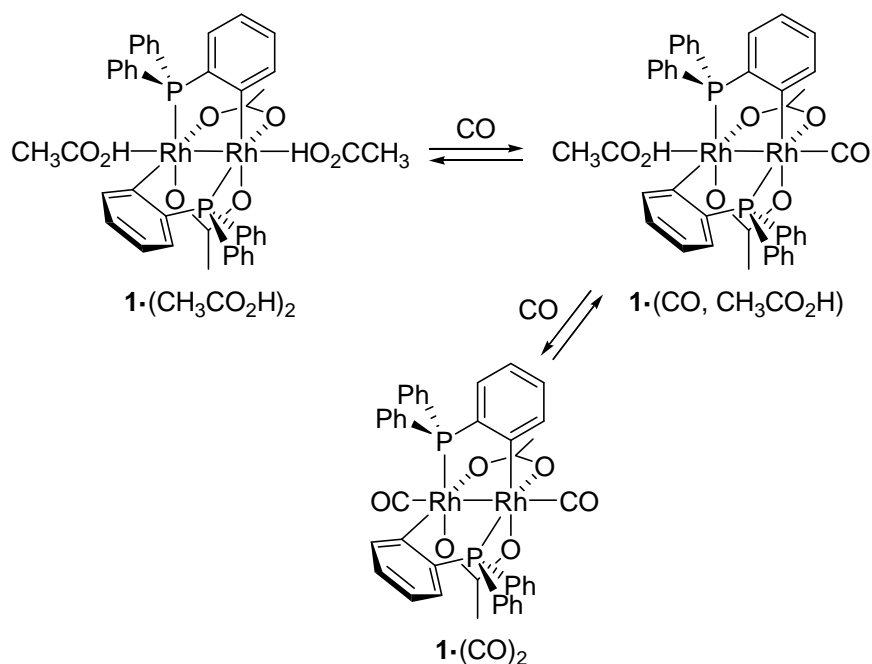


Figure 2. Diffuse reflectance spectra of $1\cdot(\text{CH}_3\text{CO}_2\text{H})_2$ adsorbed on silica gel (—) and the changes observed in the presence of CO to give the derivatives $1\cdot(\text{CO}, \text{CH}_3\text{CO}_2\text{H})$ (- - -) and $1\cdot(\text{CO})_2$ (·····).



Scheme 2. $1\cdot(\text{CH}_3\text{CO}_2\text{H})_2$ and the products $1\cdot(\text{CO}, \text{CH}_3\text{CO}_2\text{H})$ and $1\cdot(\text{CO})_2$ obtained upon coordination of carbon monoxide at axial positions.

Figure 3 shows a calibration curve using changes in the band at 554 nm of $1\cdot(\text{CH}_3\text{CO}_2\text{H})_2$ adsorbed on silica gel in the presence of increasing concentrations of CO in air. A linear dependence on CO concentration between 2 and 100 ppm was observed.

From further additional studies, a detection limit as low as 0.5 ppm of CO in air was obtained using a conventional UV/ Vis spectrophotometer and $1\cdot(\text{CH}_3\text{CO}_2\text{H})_2$ adsorbed on silica gel. A remarkable feature of this system is that for concentrations of CO in air at which it starts to become toxic (50 ppm) are able to induce a very clear and remarkable color change from violet to orange (see Figure 4).

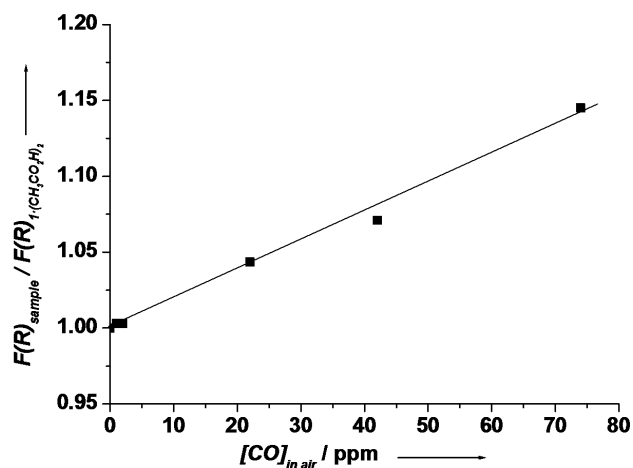


Figure 3. Intensity of the band in the diffuse reflectance spectrum in Figure 2 centered at 554 nm versus the concentration of CO in air for $1 \cdot (\text{CH}_3\text{CO}_2\text{H})_2$ adsorbed on silica gel.

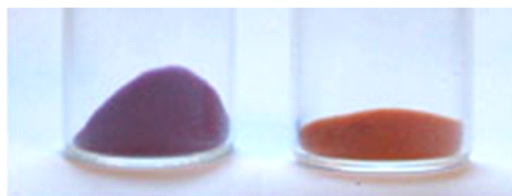


Figure 4. Photograph showing silica gel containing adsorbed $1 \cdot (\text{CH}_3\text{CO}_2\text{H})_2$ in contact with air in the absence (left) and the presence of 50 ppm of CO (right).

This system is highly selective toward CO. For example, no reaction was found in the presence of CO_2 , N_2 , O_2 , or Ar. Furthermore, no color change was observed in the presence of vapors of volatile organic compounds (VOCs), such as chloroform, hexane, ethanol, acetone, methane, toluene, xylene, or formaldehyde. Studies with coordinating species, such as SO_2 , NO, and NO_2 were also carried out; in these cases, no reaction between SO_2 and $1 \cdot (\text{CH}_3\text{CO}_2\text{H})_2$ adsorbed on silica gel was observed. The presence of the nitrogen oxides NO and NO_2 did induce a color modulation of the binuclear rhodium complex to yellow that is similar to that observed in the presence of CO but only when a very high

concentrations of NO or NO₂ were used (1320 ppm and 3450 ppm, respectively). The **1**·(CH₃CO₂H)₂ complex gave no response to water-saturated air.

In the course of these experiments, it was also observed that the binding of CO in this system was fully reversible. Figure 5 shows plots of the changes in intensity of the band at 400 nm in the diffuse reflectance spectrum of probe **1**·(CH₃CO₂H)₂ adsorbed on silica gel upon exposure to CO and CO-free air. This cyclic process was repeated at least 10 times without significant degradation of the sensing ability of the material.

Finally, to assess the effect that the metalated phosphines in complex **1**·(CH₃CO₂H)₂ have in the chromogenic sensing of carbon monoxide, the tetraacetate dirhodium complex [Rh₂(O₂CCH₃)₄] was used as control. In this case, even relatively high concentrations of CO resulted in no significant color variation, thus indicating poor or no coordination of the carbon monoxide molecule on the tetraacetate derivative.¹⁶ This result is in agreement with the observation that biscyclometalated dirhodium complexes show a higher ability for back donation to axial ligands than dirhodium tetracarboxylate, making the metalated derivative **1** more suitable for CO coordination. These comparative studies point to the importance of the selection of the bridging ligands in relation to the final chromogenic response observed.

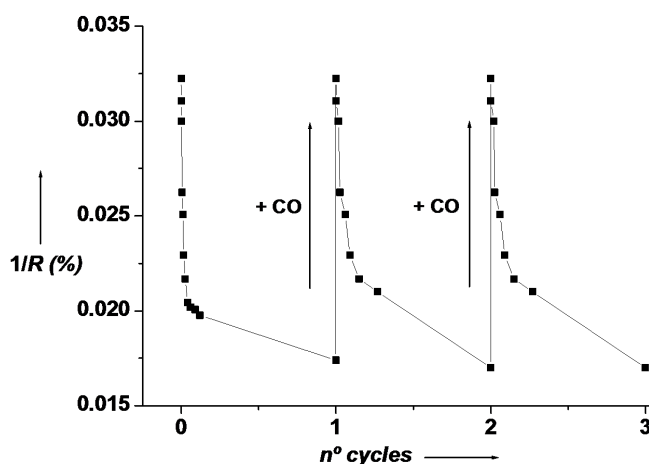


Figure 5. Reflectance changes in the band at 400 nm of silica containing **1**·(CH₃CO₂H)₂ upon exposure to CO and regeneration with a stream of air (900 min at room temperature).

In summary, we have demonstrated the use of a metalated binuclear rhodium complex as a chromogenic system for carbon monoxide sensing. Color modulations are due to coordination of CO at axial positions. The probe shows remarkable sensing properties, such as a clear color change to the naked eye at concentrations at which the carbon monoxide start to become toxic (50 ppm). As additional features, the system is selective and fully reversible. These results suggest that this or similar systems could have a potential application as efficient chemosensors for the simple colorimetric detection of this colorless and odorless hazard.

Acknowledgements

Financial support by the Spanish Government (project MAT2009-14564-C04-01) and the Generalitat Valencia (project PROMETEO/2009/016) is gratefully acknowledged. We thank M. Liu-Gonzalez of the SCSIE of the Universitat de Valencia (Spain) for single-crystal data collection and kind support in structure solution.

References

1. a) F. Wattel, R. Favory, S. Lancel, R. Neviere, D. Mathieu, *Bull. Acad. Natl. Med.* **2006**, *190*, 1961; b) J. J. McGrath, *Inhalation Toxicology (Carbon Monoxide)*, 2nd ed. (Eds.: H. Salem, S. A. Katz), CRC, Boca Raton, **2006**, p. 695; c) L. J. Wilkinson, *Molecules of Death (Carbon Monoxide—the Silent Killer)*, 2nd ed. (Eds.: R. H. Waring, G. B. Steventon, S. C. Mitchell), Imperial College Press, London, **2007**, p. 37.
2. <http://emedicine.medscape.com/article/1009092-overview>.
3. a) G. Claireaux, S. Thomas, B. Fievet, R. Motais, *Respir. Physiol.* **1988**, *74*, 91; b) M. G. Marsh, G. Marino, P. Pucci, P. Ferranti, A. Malorni, J. Kaeda, J. Marsh, L. Luzzatto, *Hemoglobin* **1991**, *15*, 43.
4. H. T. Benzon, E. A. Brunner, *J. Am. Med. Assoc.* **1978**, *240*, 1955.
5. CDC. Unintentional non-fire-related carbon monoxide exposures in the United States, 2001 – 2003. *MMWR* **2005**, *54*, 36.
6. a) B. Wang, Y. Zhao, D. Yu, L. M. Hu, J. S. Cao, F. L. Gao, Y. Liu, L. J. Wang, *Chin. Sci. Bull.* **2010**, *55*, 228; b) H. Ge, J. Liu, *Sens. Actuators B* **2006**, *117*, 408.
7. M. Itou, Y. Araki, O. Ito, H. Kido, *Inorg. Chem.* **2006**, *45*, 6114.

8. A. Gulino, T. Gupta, M. Altman, S. Lo Schiavo, P. G. Mineo, I. L. Fragalà, G. Evmenenko, P. Dutta, M. E. Van der Boom, *Chem. Commun.* **2008**, 2900.
9. S. Paul, F. Amalraj, S. Radhakrishnana, *Synt. Math.* **2009**, 159, 1019.
10. J. M. Barbe, G. Canard, S. Brandès, R. Guillard, *Chem. Eur. J.* **2007**, 13, 2118.
11. D. Benito-Garagorri, M. Puchberger, K. Mereiter, K. Kirchner, *Angew. Chem.* **2008**, 120, 9282; *Angew. Chem. Int. Ed.* **2008**, 47, 9142.
12. See for instance: a) E. Climent, M. D. Marcos, R. Martínez-Máñez, F. Sancenón, J. Soto, K. Rurack, P. Amorós, *Angew. Chem.* **2009**, 121, 8671; *Angew. Chem. Int. Ed.* **2009**, 48, 8519; b) E. Climent, A. Bernardos, R. Martínez-Máñez, A. Maquieira, M. D. Marcos, N. Pastor-Navarro, R. Puchades, F. Sancenón, J. Soto, P. Amorós, *J. Am. Chem. Soc.* **2009**, 131, 14075; c) R. Casasús, E. Aznar, M. D. Marcos, R. Martínez-Máñez, F. Sancenón, J. Soto, P. Amorós, *Angew. Chem.* **2006**, 118, 6813; *Angew. Chem. Int. Ed.* **2006**, 45, 6661.
13. P. Hirva, J. Esteban, P. Lahuerta, J. Pérez-Prieto, *Inorg. Chem.* **2007**, 46, 2619.
14. A. R. Chakravarty, F. A. Cotton, D. A. Tocher, J. H. Tocher, *Organometallics* **1985**, 4, 8.
15. CCDC 767560 contains the supplementary crystallographic data for this paper. These data can be obtained free of charge from The Cambridge Crystallographic Data Centre via www.ccdc.cam.ac.uk/data_request/cif.
16. M. C. Pirrung, A. T. Morehead, *J. Am. Chem. Soc.* **1994**, 116, 8991.

SUPPORTING INFORMATION

Sensitive and Selective Chromogenic Sensing of Carbon Monoxide by Using Binuclear Rhodium Complexes

Julio Esteban, José Vicente Ros-Lis, Ramón Martínez-Máñez,^{*} M. Dolores Marcos, María Moragues, Juan Soto and Félix Sancenón

General Considerations

$\text{Rh}_2(\text{O}_2\text{CMe})_4$, and the phosphine $\text{P}(\text{C}_6\text{H}_5)_3$ were commercially available. All solvents were of analytical grade. Column chromatography was performed on silica gel 60 (230-240 mesh). Solvent mixtures are volume/volume mixtures. All reactions were carried out in oven-dried glassware under argon atmosphere, although the isolated solids are air-stable. The solvent were degassed before used. The carbon monoxide was generated *in situ*, by reaction of sulphuric acid with formic acid.

Instrumentation

^1H , ^{13}C , spectra were recorded on a Bruker Avance 300 MHz spectrometer at 25 °C in CDCl_3 unless otherwise indicated. ^1H and ^{13}C NMR spectra were referenced to residual solvent peaks. Chemical shifts are reported in ppm and coupling constants (J) in hertz (Hz). Infrared Spectra in solution were recorded at room temperature on a JASCO FT-IR 460 Plus spectrometer. The UV-vis spectra were recorded using a spectrophotometer (Model Perkin Elmer Lambda) equipped with a diffuse reflectance accessory (Model RSA-PE-20, Labsphere, Inc., North Sutton, NH). Measurements were conducted at room temperature over a wavelength range of 350–800 nm with a wavelength step of 1 nm. The reflectance data were transformed using the Kubelka–Munk function $[F(R)]$:¹

$$F(R) = \frac{(1-R)^2}{2R}$$

In the above equation, R is the fraction of incident light reflected by sample.

Synthesis of Compound 1·(CH₃CO₂H)₂

Product 1·(CH₃CO₂H)₂ was obtained following a previously reported procedure, by refluxing triphenyl phosphine with $\text{Rh}_2(\text{O}_2\text{CMe})_4$ in a 2.2:1 molar ratio in toluene:acetic acid media (3:1 v/v) under an argon atmosphere during 3 hours.²

The compound was isolated via column chromatography on silica gel 60 (230-240 mesh) using CH₂Cl₂/Hexane 2:1 v/v mixtures as solvent.

Reactivity of 1·(CH₃CO₂H)₂ with CO

Air samples containing different concentrations of CO were bubbled on chloroform containing 1·(CH₃CO₂H)₂ and a remarkable color modulation from violet to orange-yellow or yellow was found depending on the concentration of CO. These changes are consistent with an axial coordination by CO to give the products 1·(CO,CH₃CO₂H) and 1·(CO)₂. Suitable crystals for single X-ray diffraction techniques were obtained from yellow CH₂Cl₂ solution obtained via reaction of 1·(CH₃CO₂H)₂ with a high concentration of CO to which hexane was layered. Slow evaporation of this solution resulted in different yellow-orange crystals containing mixtures of the 1·(CO,CH₃CO₂H) and 1·(CO)₂ species. Different crystals were obtained and solved via X-ray diffraction techniques (vide infra). Different crystals contained different proportions of 1·(CO,CH₃CO₂H) and 1·(CO)₂ derivatives. One of those crystals was used for structure determination procedures using single-crystal X-ray diffraction techniques.

Crystal structure

X-ray diffraction data was collected on a Nonius Kappa-CCD single crystal diffractometer, using Mo K_α radiation (λ=0.7173 Å) at 293 K. Data reduction and cell refinements were performed with the programs HKL DENZO and SCALEPACK.³ Crystal structure was solved by direct methods (SHELXS-97)⁴ with the aid of successive difference Fourier maps, and was refined using the SHELXL-97 program.⁵ All non-hydrogen atoms were refined anisotropically. The hydrogen atoms were assigned to ideal positions and refined using a riding model. At this moment, the refinement of the full expected molecular structure had converged to a value of R1 factor (F² > 2σ(F²)) of 0.046 but the position of the acetic carbonyl carbon (C67) was not well defined: the geometry of the axial acetic group was not correct and, additionally, the biggest residual electronic peak was situated very close to this carbon atom. Several trials of restrained refinement to keep the geometry of this axial acetic molecule were not successful. Then, a disordered

model in which the Rh1 atom axial position was shared by an acetic acid molecule and a monoxide molecule was essayed and a better geometry and lower R-factors were obtained. Only soft restrains to both carbon to oxygen distances for the acetic molecule were necessary. The final distribution of the Rh1 axial position was 64.4:35.6 % of occupancy for the acetic to carbon monoxide molecules. An ORTEP⁶ view of the obtained disorder is presented in Figure S1. Structure solution, refinement, molecular graphics and computing were accomplished with the WinGX⁷ graphical interface.

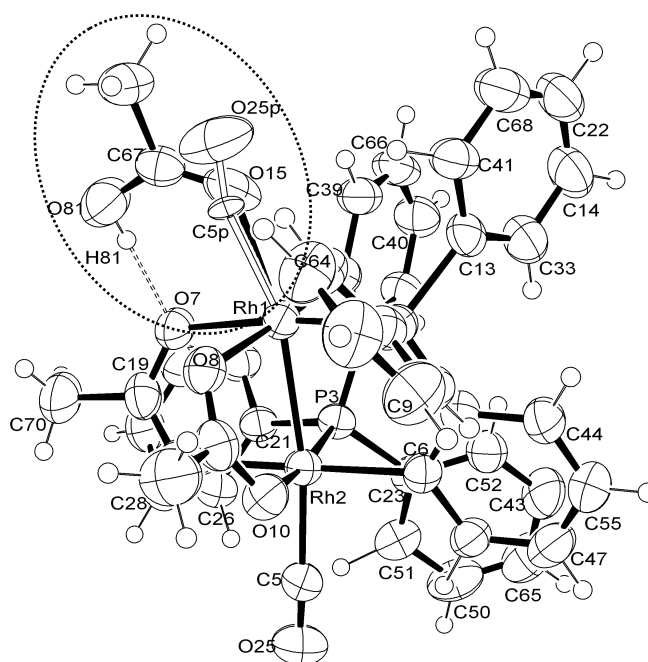


Figure S1. Overlapped ORTEP⁶ diagram of the $1 \cdot (\text{CH}_3\text{COOH}, \text{CO})$ and $1 \cdot (\text{CO}, \text{CO})$ molecules. Doted line remarks the only difference between them, the Rh1 axial position ligand (white bonds for CO and black bonds for CH_3COOH).

Table S1. Crystallographic data of Compound **1**·(CH₃COOH, CO) at 293 K.

Space Group	P2 ₁ /n
Z	4
Molecular Weight	934.49
Radiation	Mo K _α
Crystal dimensions:	
Lattice constants	
a	10.1790(2)
b	20.1240(4)
c	21.4590(4)
β	117.062(1)
Volume(Å ³)	3914.44(13)
Scan type	
T	20°C
Angular Range	(1.47-27.53) °2θ
Maximum <i>h,k,l</i>	13,26,27
Data examined	17632
Unique reflections	9003 R _{σv} = 0.0446
Merged data retained	986 I > 3σ(I)
Refinement:	
R ₁ for 5482 Fo > 4σ(Fo)	0.0393
wR ₁ for 5482 Fo > 4σ(Fo)	0.0935
R ₂ for all 9003 data	0.0887
wR ₂ for all 9003 data	0.1279
Weight: 1 / [σ ² (Fo ²) + (0.0665 * P) ² + 0.00 * P]	
where P = (Max (Fo ² , 0) + 2 * Fc ²) / 3	
No. of variables	507
Number of restraints	2
Max shift/esd	-0.001
Max and min electron density	
in final Fourier difference map (e ⁻ Å ⁻³)	0.66, -0.88

Table S2. Selected geometric data for Compound **1·(CH₃COOH, CO)** at 293 K.

SELECTED BOND DISTANCES (Å):			
Rh1 - C17	2.022 (5)	Rh2 - Rh2	2.5425 (5)
O7	2.138 (3)	C5	1.981 (5)
O8	2.167 (3)	C6	2.040 (4)
P4	2.2117 (11)	O10	2.131 (3)
O15	2.358 (18)	O18	2.173 (3)
C5P	2.14 (4)	P3	2.2384 (12)
C5P - O25P	1.11 (6)	C5 - O25	1.112 (6)
P3 - C36	1.805 (4)	P4 - C12	1.804 (5)
C21	1.834 (4)	C13	1.833 (5)
C23	1.838 (5)	C29	1.835 (5)
C19 - O18	1.251 (6)	C24 - O8	1.258 (6)
O7	1.267 (6)	O10	1.267 (6)
C70	1.502 (6)	C28	1.499 (7)
C67 - O15	1.229 (9)		
O81	1.311 (7)		
C72	1.512 (13)		
SELECTED BOND ANGLES (°)			
C17-Rh1-O7	92.91(14)	C5-Rh2-C6	91.71(18)
C17-Rh1-C5P	99.1(1.4)	C5-Rh2-O10	90.51(51)
C17-Rh1-O8	177.37(14)	C5-Rh2-O18	89.77(16)
C17-Rh1-P4	88.73(12)	C5-Rh2-P3	97.72(15)
C17-Rh1-O15	93.5(5)	C5-Rh2-Rh1	171.03(14)
C17-Rh1-Rh2	171.29(12)	C6-Rh2-O10	91.0(1.4)
O7-Rh1-C5P	83.8(1.4)	C6-Rh2-O18	175.63(14)
O7-Rh1-O8	84.54(12)	C6-Rh2-P3	90.11(12)
O7-Rh1-P4	174.36(9)	C6-Rh2-Rh1	96.36(12)
O7-Rh1-O15	86.2(5)	O10-Rh2-O18	84.93(12)
O7-Rh1-Rh2	86.74(8)	O10-Rh2-P3	171.67(9)
C5P-Rh1-O8	93.86(8)	O10-Rh2-Rh1	85.45(9)
C5P-Rh1-P4	101.3(1.4)	O18-Rh2-P3	93.76(9)
C5P-Rh1-O15	6.0(1.7)	O18-Rh2-Rh1	81.90(8)
C5P-Rh1-Rh2	161.4(1.3)	P3-Rh2-Rh1	86.2(4)
O8-Rh1-P4	93.86(8)	C36-P3-C21	104.37(20)

O8-Rh1-O15	85.7(5)	C36-P3-C23	106.04(21)
O8-Rh1-Rh2	83.24(9)	C36-P3-Rh2	113.38(15)
P4-Rh1-O15	99.0(5)	C21-P3-C23	105.09(20)
P4-Rh1-Rh2	87.7(3)	C21-P3-Rh2	112.80(15)
O15-Rh1-Rh2	167.4(4)	C23-P3-Rh2	114.28(15)
C12-P4-C13	104.78(21)	O25-C5-Rh2	178.1(5)
C12-P4-C29	106.12(21)	O25P-C5P-Rh1	156(4)
C12-P4-Rh1	113.38(15)	O18-C19-O7	124.4(4)
C13-P4-C29	103.68(21)	O18-C19-C70	118.8(5)
C13-P4-Rh1	115.31(15)	O7-C19-C70	116.8(5)
C29-P4-Rh1	112.81(15)	O8-C24-O10	124.9(4)
O15-C67-O81	125.0(1.6)	O8-C24-C28	118.2(5)
O15-C67-C72	124.2(1.4)	O10-C24-C28	116.8(5)
O81-C67-C72	110.5(9)		

 INTRAMOLECULAR HYDROGEN-BONDING

O81-H81	0.820(6)	O7.....H81	1.775(3)
O81...O7	2.580(7)	O81-H81...O7	166.7(4)

References

1. A. V. Zinchuk, B. C. Hancock, E. Y. Shalaev, R. D. Reddy, R. Govindarajan, E. Novak, *Eur. J. Pharm. Biopharm.*, **2005**, *61*, 158.
2. A. R. Chakravarty, F. A. Cotton, D. A. Tocher, J. H. Tocher, *Organometallics* **1985**, *4*, 8.
3. DENZO-SCALEPACK Otwinowski, Z. & Minor, W., "Processing of X-ray Diffraction Data Collected in Oscillation Mode ", *Methods in Enzymology, Volume 276: Macromolecular Crystallography, part A*, p.307-326, **1997**, Carter, C. W. Jr. & Sweet, R. M., Eds., Academic Press.
4. SHELXS86 - Program for Crystal Structure solution. Sheldrick, G. M., Institut für Anorganische Chemie der Universität, Tammanstrasse 4, D-3400 Göttingen, Germany, **1986**.
5. SHELX97 - Sheldrick, G. M. (1997). Programs for Crystal Structure Analysis (Release 97-2). University of Göttingen, Germany.
6. ORTEP3 for Windows - Farrugia, L. J. *J. Appl. Cryst.*, **1997**, *30*, 565. ORTEP-III - M. N. Burnett & C. K. Johnson, Oak Ridge National Laboratory Report ORNL- 6895, **1996**.

***3.2. Sensitive and selective chromogenic sensing
of carbon monoxide via reversible axial CO
coordination in binuclear rhodium
complexes***

***Sensitive and Selective Chromogenic Sensing of
Carbon Monoxide via Reversible Axial CO
Coordination in Binuclear Rhodium Complexes***

*María E. Moragues,^{†‡§} Julio Esteban,^{†‡} José Vicente Ros-
Lis,^{†‡} Ramón Martínez-Máñez,^{* †‡§} María Dolores Marcos,^{†‡§}
Manuel Martínez,^{* ††} Juan Soto,^{†‡} and Félix Sancenón^{†‡§}*

*† Centro de Reconocimiento Molecular y Desarrollo Tecnológico (IDM), Unidad
Mixta Universidad Politécnica de Valencia – Universidad de Valencia, Spain.*

*‡ Departamento de Química. Universidad Politécnica de Valencia, Camino de Vera
s/n, E-46022 Valencia, Spain.*

§ CIBER de Bioingeniería, Biomateriales y Nanomedicina (CIBER-BBN).

*†† Department de Química Inorgànica, Universitat de Barcelona, Martí I Franquès 1-
11, E-08028 Barcelona, Spain.*

Received: July 20, 2011

First published on the web: August 24, 2011

*(Reprinted with permission from
Journal of the American Chemical Society, 2011, 133, 15762–15772.*

Copyright © 2011, American Chemical Society)

Abstract

The study of probes for CO sensing of a family of binuclear rhodium(II) compounds of general formula $[\text{Rh}_2\{(\text{XC}_6\text{H}_3)\text{P}(\text{XC}_6\text{H}_4)\}_n(\text{O}_2\text{CR})_{4-n}] \cdot \text{L}_2$ containing one or two metalated phosphines (in a head-to-tail arrangement) and different axial ligands has been conducted. Chloroform solutions of these complexes underwent rapid color change, from purple to yellow, when air samples containing CO were bubbled through them. The binuclear rhodium complexes were also adsorbed on silica and used as colorimetric probes for “naked eye” CO detection in the gas phase. When the gray-purple colored silica solids containing the rhodium probes were exposed to air containing increasing concentrations of CO, two colors were observed, in agreement with the formation of two different products. The results are consistent with an axial coordination of the CO molecule in one axial position (pink-orange) or in both (yellow). The crystal structure of **3·(CO)** ($[\text{Rh}_2\{(\text{C}_6\text{H}_4)\text{P}(\text{C}_6\text{H}_5)_2\}_2(\text{O}_2\text{CCF}_3)_2] \cdot \text{CO}$) was solved by single X-ray diffraction techniques. In all cases, the binuclear rhodium complexes studied showed a high selective response to CO with a remarkable low detection limit. For instance, compound **5·(CH₃CO₂H)₂** ($[\text{Rh}_2\{(m\text{-CH}_3\text{C}_6\text{H}_3)\text{P}(m\text{-CH}_3\text{C}_6\text{H}_4)_2\}_2(\text{O}_2\text{CCH}_3)_2] \cdot (\text{CH}_3\text{CO}_2\text{H})_2$) is capable of detection of CO to the “naked eye” at concentrations as low as 0.2 ppm in air. Furthermore, the binding of CO in these rhodium complexes was found to be fully reversible, and release studies of carbon monoxide via thermogravimetric measurements have also been carried out. The importance of the silica support for the maintenance of the CO-displaced L ligands in the vicinity of the probes in a noninnocent manner has been also proved.

Introduction

Carbon monoxide is an airborne contaminant difficult to detect since it is colorless and odorless and toxic at low concentration levels. Moreover, this compound may present a real danger to humans¹ in automobiles, airplanes, industrial plants, mines, homes, and other environments in which persons may be present for extended periods of time. Typical anthropogenic sources of this deadly pollutant involve combustion engines and improper burning of other fuels.

Examples include residential furnaces, gasoline engines, charcoal grills, gas heaters, and others. Carbon monoxide toxicity lies in the fact that hemoglobin presents about 200 times higher affinity for carbon monoxide than for oxygen.

Therefore, carbon monoxide can readily displace oxygen on hemoglobin,² reducing the amount of the latter that can be carried to tissues and impairing the mechanisms of cellular respiration.³ For this reason, carbon monoxide is toxic to humans at relatively low concentrations.⁴ For healthy adults, CO becomes toxic when it reaches a level higher than 50 ppm with continuous exposure over an eight hour period. Mild exposure over a few hours (a CO level between 70 and 100 ppm) includes flu-like symptoms, such as headaches, sore eyes, and a runny nose. Medium exposure (a CO level between 150 and 300 ppm) will produce dizziness, drowsiness, and vomiting. Extreme exposure (a CO level of 400 ppm and higher) will result in unconsciousness, brain damage, and death. Unfortunately, it is quite usual that people with CO poisoning overlook the symptoms (e.g., headache, nausea, dizziness, or confusion), and unintentional CO exposure accounts for an estimated 15000 emergency department visits and 500 unintentional deaths in the United States alone each year.

Therefore, there is an increasing interest for the development of chemical sensor systems capable of detecting the presence of carbon monoxide in air at low concentrations. Most existing CO sensors use metal-oxide semiconductors (MOS)⁵ that have been widely chosen as gas-sensing devices and applied in monitoring quality air control. As an alternative to these methods, the development of chromogenic sensing systems for CO detection at poisonous concentrations is of great importance. Colorimetric methods are especially undemanding offering several advantages over other analytical procedures, such as real-time monitoring and the use of very simple and inexpensive instrumentation. Additionally, certain colorimetric changes, even at low concentration of analytes, can be observed to the “naked eye”, thus making chromogenic protocols unbeatable for certain applications.

However, colorimetric probes for the detection of this deadly chemical are still rare. An example involves the use of oxoacetatobridged triruthenium cluster complexes,⁶ which show color changes in acetonitrile. An electron transfer

process with a zinc tetraphenylporphyrin changes the oxidation state of the ruthenium metal center thus allowing its coordination to carbon monoxide. Polypyrrole functionalized with iron porphyrin has also been reported to act as a suitable material for carbon monoxide detection at low concentrations in water/methanol solutions.⁷ In a recent example, a stereospecific binding of CO at a pentacoordinated diisopropylphosphino diaminopyridine iron complex when exposed to high concentrations of carbon monoxide (1 atm of gaseous CO) has been reported; the corresponding hexacoordinated derivative is formed, as indicated by the color change from yellow to red.⁸ The optical detection of parts-per-million levels of carbon monoxide in air by UV-vis spectroscopy in the transmission mode using a monolayer of bimetallic rhodium complexes has also been reported, although with relatively poor changes in color.⁹ In all reported examples, until now, the modulations in the presence of carbon monoxide show certain shortcomings typically involving poor color changes. Additionally, in most cases colorimetric CO detection was performed in solution but not in air. Furthermore, relatively large detection limits hamper their use as reliable sensing systems.

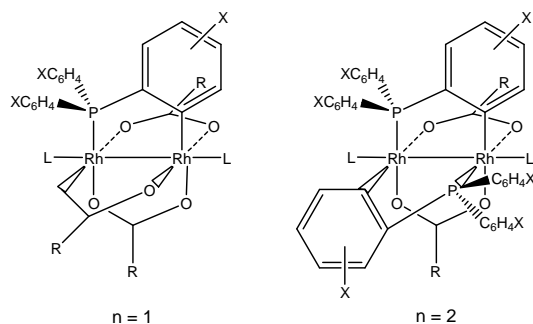
Following our interest in the design of novel chromogenic systems,¹⁰ we considered the application of binuclear rhodium compounds as potential colorimetric probes for the sensing of CO by exploiting the well-known ability of these complexes to coordinate different bases in their labile axial sites.¹¹ In a recent preliminary communication,¹² we have reported the development of a colorimetric probe based on the binuclear rhodium compound **2** · (CH₃CO₂H)₂ of formula [Rh₂{(C₆H₄)P(C₆H₄)₂}(O₂CCH₃)₂] · (CH₃CO₂H)₂. On the basis of the excellent sensing results obtained for this rhodium complex in terms of selectivity and sensitivity, we report herein an extended study using a family of binuclear rhodium(II) complexes of general formula [Rh₂{(XC₆H₃)P(XC₆H₄)₂}(O₂CR)_{4-n}] · L₂ containing one or two (in a head-to-tail arrangement) metalated phosphine ligands and different axial ligands. For these compounds, the color modulations observed in the presence of carbon monoxide, and induced via axial labile coordination of CO groups, have been studied.

Results and Discussion

Design of the Probe Complexes. The design of the chromogenic probes involves the use of binuclear rhodium(II) cyclometalated complexes and the well-documented labile coordination ability of these compounds in their axial sites. These have been demonstrated to act both in their own reactivity^{13,14} and as catalytic centers¹⁵ in a number of transformations.¹⁶ Additionally, some coordination studies on adduct formation between dirhodium compounds and different Lewis bases¹¹ have pointed out that even relatively simple systems such as tetra- μ -carboxylate-dirhodium(II) derivatives show an important π -back-bonding capability of the rhodium(II) atoms. This fact has been attributed to an extensive mixing of the orbitals with π symmetry on the two metal centers. This effect causes the rhodium(II) metal centers to be very effective in π -back-bonding to the axial ligands which is a very interesting feature for the design of CO binding complexes.¹⁷ In addition, when biscyclometalated compounds are compared with dirhodium tetracarboxylate derivatives, a higher ability of the former for π -back-donation to the axial ligand has been reported. Moreover, it has been observed, in much of the chemistry associated with dirhodium(II) cyclometalated complexes, that the presence of different ligands coordinated to the axial positions of these derivatives produce important changes in the UV-vis spectra in solution.^{18,19}

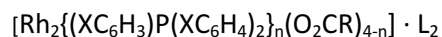
These enhanced π -back-donation properties of dirhodium(II) cyclometalated complexes and the color changes observed upon axial coordination with different ligands make these complexes suitable as potential chromogenic systems for CO detection. With these design concepts in mind, we have recently reported a colorimetric probe based on a binuclear cyclometalated rhodium compound. On the basis of the possible modulation of the sensing features via changes in the donor-acceptor properties of the π -bringing ligands, we have prepared a family of binuclear rhodium complexes (see Scheme 1) of general formula²⁰ $[\text{Rh}_2\{(\text{XC}_6\text{H}_3)\text{P}(\text{XC}_6\text{H}_4)_2\}_n(\text{O}_2\text{CR})_{4-n}] \cdot \text{L}_2$ containing one ($n = 1$) or two ($n = 2$) metalated phosphine ligands²¹ in a head-to-tail arrangement. Two different phosphines ($X = \text{H}$ or $m\text{-CH}_3$) and three different carboxylic acids ($R = \text{CH}_3, \text{CF}_3,$ or

$\text{C}(\text{CH}_3)_3$ as equatorial ligands, as well as four different axial ligands ($\text{L} = \text{CH}_3\text{CO}_2\text{H}$, $\text{CF}_3\text{CO}_2\text{H}$, $(\text{CH}_3)_3\text{CCO}_2\text{H}$, or H_2O), have been used. Table 1 shows the different compounds studied.



Scheme 1. General structure for binuclear rhodium compounds used in this work.

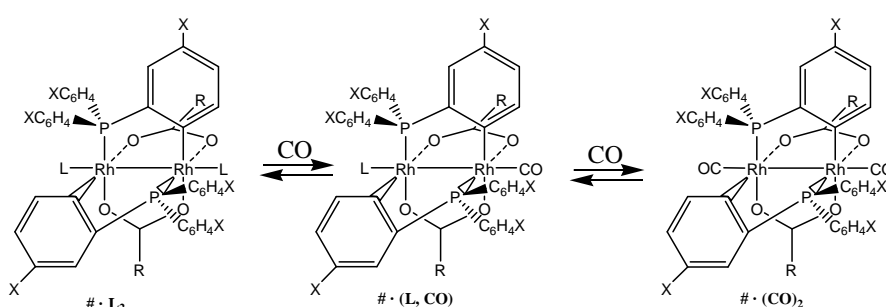
Table 1. Binuclear rhodium compounds used in this work with general formula



Compound	n	X	R	L
1 · $(\text{CH}_3\text{CO}_2\text{H})_2$	1	H	CH_3	$\text{CH}_3\text{CO}_2\text{H}$
2 · $(\text{CH}_3\text{CO}_2\text{H})_2$	2	H	CH_3	$\text{CH}_3\text{CO}_2\text{H}$
2 · $(\text{H}_2\text{O})_2$	2	H	CH_3	H_2O
3 · $(\text{CF}_3\text{CO}_2\text{H})_2$	2	H	CF_3	$\text{CF}_3\text{CO}_2\text{H}$
4 · $(\text{CH}_3)_3\text{CCO}_2\text{H})_2$	2	H	$\text{C}(\text{CH}_3)_3$	$(\text{CH}_3)_3\text{CCO}_2\text{H}$
5 · $(\text{CH}_3\text{CO}_2\text{H})_2$	2	<i>m</i> - CH_3	CH_3	$\text{CH}_3\text{CO}_2\text{H}$

Reactivity with Carbon Monoxide. Once the family of birhodium derivatives was prepared, UV-vis spectrophotometric studies for the CO coordination of all compounds, i.e., **1**· $(\text{CH}_3\text{CO}_2\text{H})_2$, **2**· $(\text{CH}_3\text{CO}_2\text{H})_2$, **2**· $(\text{H}_2\text{O})_2$, **3**· $(\text{CF}_3\text{CO}_2\text{H})_2$, **4**· $(\text{CH}_3)_3\text{CCO}_2\text{H})_2$, and **5**· $(\text{CH}_3\text{CO}_2\text{H})_2$, were carried out in chloroform solution. All

complexes, $\# \cdot L_2$, underwent a fast and distinct color change, from purple to yellow, when CO-containing air samples were bubbled through their chloroform solutions. Furthermore, depending on the concentration of CO in the air samples, two different products were obtained, with two distinct electronic spectra. For low CO concentrations, the purple solutions turned pink-orange, whereas at high CO concentration solutions became yellow. Interestingly, when CO-free air was bubbled on these final yellow solutions, the color reverted to purple, thus indicating that the process is reversible. All these observations agree with the formation of the corresponding mono-, $\# \cdot (L, CO)$, and bis-CO-substituted, $\# \cdot (CO)_2$, species (Scheme 2) of the dirhodium(II) starting materials.



Scheme 2. Complexes with general structure $[Rh_2\{(XC_6H_3)P(XC_6H_4)_2\}_n(O_2CR)_{4-n}] \cdot L_2$, simplified as $\# \cdot L_2$, and the corresponding products, simplified as $\# \cdot (L, CO)$ and $\# \cdot (CO)_2$, obtained upon coordination of carbon monoxide at labile axial positions.

Characterization of the Axial Carbon Monoxide Complexes. The crystal structures of dirhodium complexes containing cyclometalated phosphines have already been extensively reported.^{20,22,23} All the molecular structures of dirhodium(II) complexes **2-5** are very similar and can be rationalized with the single scheme in Figure 1a. All of them contain two bonded rhodium atoms that are also bridged by two carboxylate groups and two phosphine ligands. In the latter, metalation has occurred at one of the phenyl rings of each, producing a head-to-tail final conformation. Compound **1** $\cdot (CH_3CO_2H)_2$ is a little bit different as it contains three carboxylates and one phosphine ligand bridging the dirhodium(II)

lantern core. Additionally, the coordination spheres of the metal atoms are completed by means of two other ligands, mainly acetic acid and trifluoroacetic acid, that occupy the labile axial positions. In this way, a slightly distorted octahedral coordination exists around each of the metal atoms in the dirhodium(II) group.

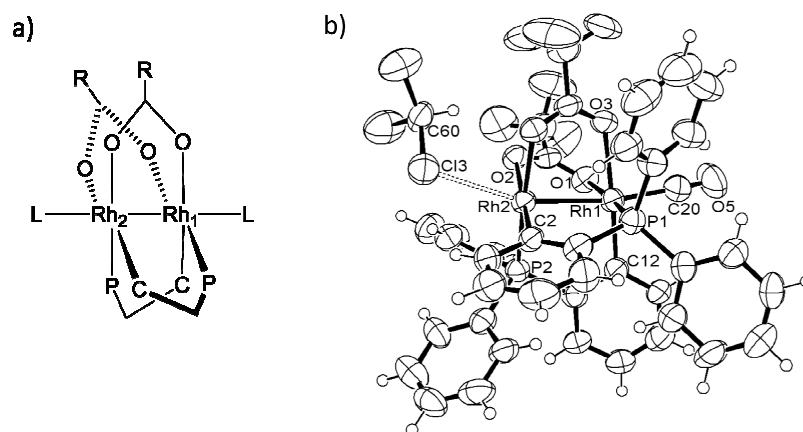


Figure 1. (a) Simplified scheme of the structures of compounds $2 \cdot L_2$ to $5 \cdot L_2$. (b) ORTEP plot of the crystal structure of $3 \cdot (CHCl_3, CO)$; thermal ellipsoids are set at the 50% probability level. Selected bond lengths [Å] and angles [°]: Rh1-Rh2, 2.5333(9); Rh1-P1, 2.2574(23); Rh1-C20, 1.9698(122); Rh2-P2, 2.2132 (21); Rh2-Cl3, 2.9023(31); C20-O5, 1.1042(152); Rh1-C20-O5, 176.63(1).

The values of the Rh-Rh bond distances in these bismetallated complexes present a very small variation (in the 2.499(2)-2.513(2) Å range), whereas a slightly shorter distance, 2.430(2) Å, is found for the monometallated analog. The d_{Rh-P} and d_{Rh-C} bond distances represent a wider range (2.193(6)-2.220(3) Å and 1.960(2)-2.020(2) Å, respectively), while the variation in the Rh- O_{axial} distances (2.301(4)-2.412(5) Å) represents the largest margin. It is interesting to note that the d_{Rh-L} and d_{Rh-Rh} bond distances do not show any significant trend upon variation of either the carboxylate R or the axial L groups, apart from that derived from the inherent steric hindrance caused by the more bulky groups. In this respect, the observed Rh-Rh- O_{axial} bond angles in the monometallated complex **1**, 169.0(1)° and 174.4(1)°, deviate only slightly from linearity, while for the doubly

metalated complexes deviations are more significant (within the 163.6(1)-166.9(1)° range).

To understand the ability of carbon monoxide to bind these dirhodium complexes in the axial positions, the comparison between the previously reported structures and those of the corresponding CO-substituted complexes should be conducted. Suitable crystals for single X-ray diffraction were obtained by slow evaporation of CO-bubbled chloroform solutions of the desired compounds layered with hexane. The crystal structures of two different families of compounds have been obtained: the first one (reported in a recent communication) is a mixture of $2 \cdot (\text{CH}_3\text{CO}_2\text{H}, \text{CO})$ and $2 \cdot (\text{CO})_2$,¹² while the second one, reported in this paper, corresponds to a $3 \cdot (\text{CHCl}_3, \text{CO})$ stoichiometry.²⁴

The molecular structure of compound $3 \cdot (\text{CHCl}_3, \text{CO})$ (Figure 1b) consists of a rhodium binuclear core with two metalated phosphine ligands in a head-to-tail conformation and two carboxylate (trifluoroacetate) ligands in the equatorial positions, as expected by comparison with the **2** to **5** family of complexes. In this case, however, the coordination on the axial labile positions of the rhodium(II) centers is completed with only one carbon monoxide molecule ligand at a bonding distance. The second axial position is occupied by a solvent molecule (chloroform) at a very long distance (2.902(3) Å). Relevant crystallographic data are collected in Tables S1 and S2 (Supporting Information).

The structure reported here, together with the one recently reported,¹² allows the comparison of the series of analogous $[\text{Rh}_2\{(\text{C}_6\text{H}_4)\text{P}(\text{C}_6\text{H}_5)_2\}_2(\text{O}_2\text{CR})_2]$ compounds differing only in the bridging carboxylate ligands ($\text{R} = \text{CH}_3$ or $\text{R} = \text{CF}_3$). Tables 2 and 3 collect the main metal-ligand distances and angles that allow a proper comparison between the two sets of data. The difference in the $d_{\text{Rh-Rh}}$ bond lengths when the R groups of the carboxylate ligands change from CH_3 to CF_3 is rather small, 0.009 Å, as has already been found for all **2-5** known complexes (0.005 Å between $2 \cdot (\text{CH}_3\text{CO}_2\text{H})_2$ and $3 \cdot (\text{CF}_3\text{CO}_2\text{H})_2$). It is clear that the important change in the electronic character of these carboxylates has only a small influence on the intermetallic distance. A more important effect is found when the carboxylic acid in the axial positions is substituted by a carbon monoxide. In this case, the differences found are 1 order of magnitude larger (0.0345 Å between

2·(CH₃CO₂H)₂ and **2**·(CH₃CO₂H, CO); 0.0203 Å between **3**·(CF₃CO₂H)₂ and **3**·(CHCl₃, CO)). This effect fits very nicely with the π-acceptor character of the carbon monoxide molecule that withdraws electron density from the metal-metal bond. A combination of the two above-mentioned facts may be the actual reason for the high asymmetry of the **3**·(CHCl₃, CO) complex. The complete coordination of the dirhodium(II) core in this complex can be achieved with only a simple solvent molecule, which supports the idea that the metal to axial ligand bond could not only be explained considering a pure sigma interaction.¹¹

Having a look at the Rh-equatorial ligand distances, a similar trend is evident. A longer d_{Rh-P} distance is, nevertheless, observed for metal atoms having carbon monoxide in their coordination sphere, which is balanced by a shortening in the corresponding d_{Rh-Oeq} bond lengths. Very similar averaged equatorial distances when changing the carboxylic acid by carbon monoxide are found in all cases.

With respect to the bond angles, a general deviation of linearity of the Rh-Rh-L unit, both for R = CH₃ and CF₃ (Table 3), is observed, probably due to the presence of the phosphine ligands in complexes **2** · (CH₃CO₂H, CO) and **3** · (CHCl₃, CO). The substitution of axial carboxylic acid molecules by carbon monoxide allows a relaxation in the Rh₂-Rh₁-L angles, producing less strained units.

Table 2. Relevant bond distances (Å) for biscyclometallated binuclear rhodium compounds used in this work^a

	$2\cdot(\text{CH}_3\text{CO}_2\text{H})_2$ ²⁰	$2\cdot(\text{CH}_3\text{CO}_2\text{H}, \text{CO})$ ¹²	$3\cdot(\text{CF}_3\text{CO}_2\text{H})_2$ ²⁶	$3\cdot(\text{CHCl}_3, \text{CO})$ ^b
$d_{\text{Rh1-Rh2}}$	2.508(1)	2.5425(5)	2.513(2)	2.5333(9)
$d_{\text{Rh1-Oax}}$	2.342(5)	-	2.340(2)	-
$d_{\text{Rh1-COax}}$	-	1.9810(5)	-	1.9698(122)
$d_{\text{Rh2-Oax}}$	2.342(5)	2.3580(18)	2.360(14)	-
$d_{\text{Rh2-COax}}$	-	-	-	-
$d_{\text{Rh1-Oav}}$	2.190(4)	2.1520(3)	2.210(2)	2.1832(54)
$d_{\text{Rh2-Oav}}$	2.136(4)	2.1525(3)	2.210(2)	2.16765(7)
$d_{\text{Rh1-P}}$	2.210(2)	2.2384(12)	2.218(7)	2.2574(23)
$d_{\text{Rh2-P}}$	2.210(1)	2.2117(11)	2.205(7)	2.2132(21)
$d_{\text{Rh1-C}}$	1.997(4)	2.0400(4)	2.020(2)	2.0326(79)
$d_{\text{Rh2-C}}$	1.996(6)	2.0220(5)	1.990(2)	1.9942(82)

^a Atom-labeling corresponds to the nomenclature shown in Figure 1b. ^b Present work.

Table 3. Rh-Rh-L angles (°) for biscyclometallated binuclear rhodium compounds used in this work

	$2\cdot(\text{CH}_3\text{CO}_2\text{H})_2$	$2\cdot(\text{CH}_3\text{CO}_2\text{H}, \text{CO})$	$3\cdot(\text{CF}_3\text{CO}_2\text{H})_2$	$3\cdot(\text{CHCl}_3, \text{CO})$
Rh ₂ -Rh ₁ -L	163.6(1)	171.03(14)	166.5(4)	170.71(33)
L-Rh ₂ -Rh ₁	163.6(1)	167.40(4)	166.3(4)	-

Carbon Monoxide Sensing Behaviour in Air. Despite the interesting spectrophotometric response of the studied dirhodium(II) complexes found in chloroform solutions, the detection of CO is of main importance in gas phase. Therefore we took a step forward towards the potential use of this kind of sensing derivatives as probes for the detection of carbon monoxide in air. Adsorption of compounds **1** to **5** on silica beads (via solution of each binuclear rhodium

compound in a minimum amount of chloroform followed by the addition of silica at a weight ratio 2-10 times) resulted in purple solids. The solids were separated after five minutes of stirring at room temperature and the solvent was removed on a rotary evaporator. The resulting solids were dried at 343 K for at least 48 h before use.

The colored silica supports containing the rhodium probes underwent important color changes in seconds when exposed to air containing different concentrations of carbon monoxide. As observed in chloroform solutions, a more detailed study of the titration process, using increasing concentrations of carbon monoxide, clearly revealed that two consecutive substitution reactions occur. As an example, Figure 2 shows the diffuse reflectance UV-Vis spectra of silica beads containing $5 \cdot (\text{CH}_3\text{CO}_2\text{H})_2$ and the changes observed in presence of air containing 8 and 2000 ppm of CO. Whereas $5 \cdot (\text{CH}_3\text{CO}_2\text{H})_2$ shows a band at 550 nm, a large excess of CO (2000 ppm) resulted in the appearance of a new band at 412 nm, whereas at lower concentrations of CO (8 ppm) a band at 495 nm was observed. These changes are consistent with an axial coordination by CO and the formation of the derivatives $5 \cdot (\text{CO})_2$ and $5 \cdot (\text{CH}_3\text{CO}_2\text{H}, \text{CO})$ (Scheme 2).

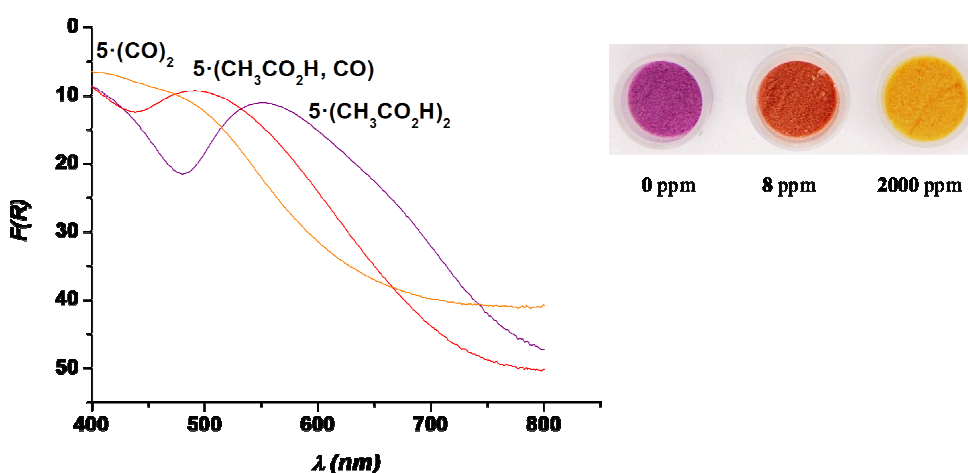


Figure 2. Diffuse reflectance UV-Vis spectra of a mixture of silica containing $5 \cdot (\text{CH}_3\text{CO}_2\text{H})_2$ and the changes observed in presence of air containing 8 and 2000 ppm of CO.

A very similar change in color and hypsochromic shift of the band was observed for all dirhodium(II) complexes studied. Table 4 shows the spectroscopic characteristics of the complexes in chloroform solutions, as well as adsorbed on silica, together with the data in the presence of an excess of carbon monoxide. Compounds **1** to **5** display an absorption band in the 550-570 nm range in chloroform that is not basically modified when adsorbed on silica beads. Upon addition of an excess of carbon monoxide, new bands centered in the 394-400 nm region were found for all complexes both in chloroform and on silica. The table also shows that the molar absorptivities of the corresponding carbon monoxide complexes are in general one order of magnitude larger than those of the starting derivatives.

Table 4. UV-Vis spectral data for the different binuclear rhodium(II) compounds studied in chloroform solution, as well as their diffuse reflectance spectra supported on silica beads, at room temperature^a

Compound	CHCl ₃ solution	solid	
	$\lambda_{\max}(\text{nm}), (\epsilon (\text{M}^{-1}\text{cm}^{-1}))$	$\lambda_{\max} (\text{nm})$	$\nu_{\text{CO}} (\text{cm}^{-1})$
1 ·(CH ₃ CO ₂ H) ₂	556, (157)	550	
1 ·(CO) ₂	394, (421)	400	2040
2 ·(CH ₃ CO ₂ H) ₂	567, (552)	545	
2 ·(CO) ₂	398, (7040)	398	2028
3 ·(CF ₃ CO ₂ H) ₂	571, (711)	537	
3 ·(CO) ₂	400, (6570)	402	2048
4 ·(CH ₃ CO ₂ H) ₂	547, (560)	539	
4 ·(CO) ₂	397, (3689)	400	2033
5 ·(CH ₃ CO ₂ H) ₂	564, (265)	550	
5 ·(CO) ₂	397, (1247)	412	2033

^a The bands assigned to the CO stretch in the IR spectrum are also included.

Table 4 also collects the carbon monoxide stretching frequency for the $\# \cdot (\text{CO})_2$ derivatives adsorbed on silica, which range from 2028 to 2048 cm^{-1} . These stretching ν_{CO} frequencies²⁵ are, in all cases, considerably lower than the CO stretching frequency of the free carbon monoxide (2143 cm^{-1}), which indicates the presence of highly acidic axial metal sites with relatively high levels of $\text{M} \rightarrow \text{CO}$ π -back-bonding. This effect is naturally stronger when donor groups are also present in the bringing carboxylate groups.

Perhaps one of the most remarkable behaviors in relation to the response of the tested dirhodium(II) complexes is that the chromogenic response is observed at relatively low concentrations of carbon monoxide. Titration studies of the derivatives **1** to **5** adsorbed on silica gel with increasing quantities of carbon monoxide in air allowed determining the detection limits for CO. From a chemosensing point of view, a low detection limit for carbon monoxide of less than 1.7 ppm was found for all studied complexes using a conventional UV-Vis spectrophotometer (see Table 5). Figure 3 shows the changes in absorbance of the band centered at 557 nm of **5**·($\text{CH}_3\text{CO}_2\text{H}$)₂ adsorbed on silica beads in the presence of different concentrations of CO in air; the response of complex **5**·($\text{CH}_3\text{CO}_2\text{H}$)₂ to CO shows a linear trend between 1 and 100 ppm at this wavelength. A similar linear behavior was also found for the other studied rhodium derivatives studied.

Table 5. Detection limits (ppm) for compounds $\# \cdot \text{L}_2$ in the presence of CO^a

Compound	Detection limits (ppm) of CO	
	UV-Vis spectrophotometer	naked eye
1 ·($\text{CH}_3\text{CO}_2\text{H}$) ₂	0.7	52
2 ·($\text{CH}_3\text{CO}_2\text{H}$) ₂	0.6	42
2 ·(H_2O) ₂	1.6	35
3 ·($\text{CF}_3\text{CO}_2\text{H}$) ₂	0.8	38
4 ·((CH_3) ₃ CCO ₂ H) ₂	1.7	50
5 ·($\text{CH}_3\text{CO}_2\text{H}$) ₂	0.2	0.2

^a Limits calculated from UV-Vis spectral data (first column) and the to the naked eye (second column).

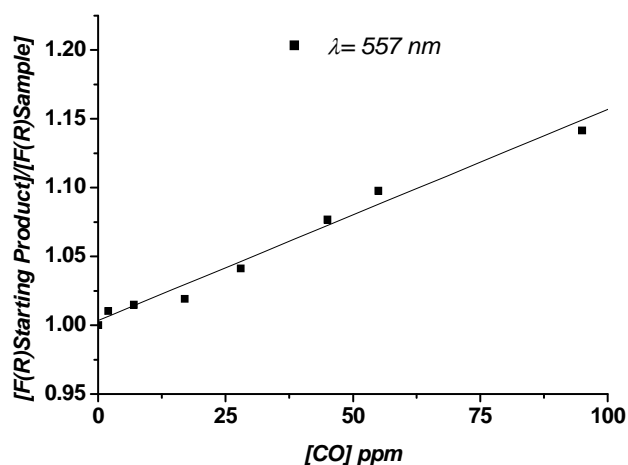


Figure 3. Loss of the intensity of the band centered at 557 nm vs concentration of CO in air for $5 \cdot (\text{CH}_3\text{CO}_2\text{H})_2$ adsorbed on silica.

Table 5 indicates the estimated detection limit to the “naked eye” for compounds **1** to **5** in the presence of CO; i.e. the minimum amount of CO necessary to observe a clear color change in the complexes. All the compounds display a chromogenic modulation to the “naked eye” at concentrations at which CO is toxic (i.e. 50-60 ppm), compound $5 \cdot (\text{CH}_3\text{CO}_2\text{H})_2$ even shows a very remarkable color modulation at CO concentrations as low as 0.2 ppm.

This range of visual CO detection values found for all compounds made it possible to design systems for semi-quantitative sensing of CO in air at different concentration ranges. For instance, a sensing array containing compounds $4 \cdot ((\text{CH}_3)_3\text{CCO}_2\text{H})_2$, $2 \cdot (\text{H}_2\text{O})_2$ and $5 \cdot (\text{CH}_3\text{CO}_2\text{H})_2$, displaying clear visual detection limits from CO concentration of 50, 35 and 0.2 ppm, respectively, will allow to sense the presence of CO in the ranges; $0.2 < C_{\text{CO}} < 35$ ppm; $35 < C_{\text{CO}} < 50$ ppm and $C_{\text{CO}} > 50$ ppm. Figure 4 shows such array and the color changes for $4 \cdot ((\text{CH}_3)_3\text{CCO}_2\text{H})_2$, $2 \cdot (\text{H}_2\text{O})_2$ and $5 \cdot (\text{CH}_3\text{CO}_2\text{H})_2$ derivatives for concentrations of CO of 0, 2, 35 and 50 ppm in air.

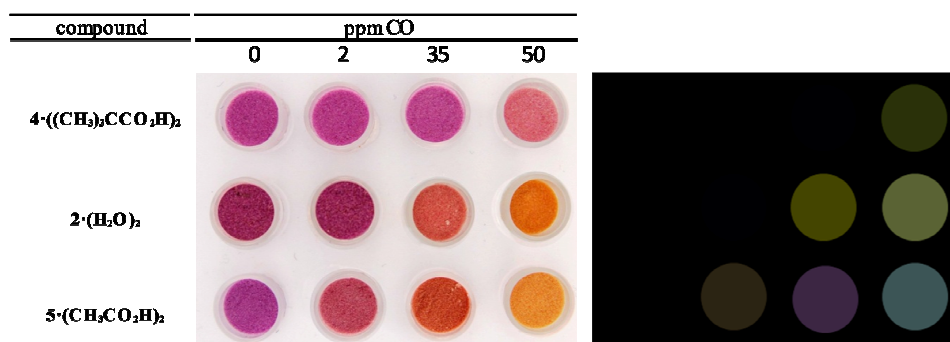


Figure 4. Sensing array of the studied complexes for CO detection in air. On the right, the increment of the RGB values is shown.

Selectivity. In all cases the binuclear rhodium complexes studied showed a remarkable selective response to carbon monoxide in air. For instance no reaction was observed in the presence of CO₂, N₂, O₂ or Ar at very high concentrations (up to 50000 ppm). Similarly, no color changes were observed in the presence of volatile organic compounds such as acetone, chloroform, ethanol, formaldehyde, hexane or toluene (up to 30000 ppm in air). Some color changes to yellow were observed in the presence of acetonitrile vapor, although only at concentrations of 4600 ppm. Studies with other coordinating oxygen-containing gaseous species, such as SO₂, NO and NO₂, were also carried out. No noticeable color changes were observed on any of the compounds adsorbed on silica beads in the presence of SO₂ (up to 38000 ppm in air), but NO and NO₂ produced color changes rather similar to those observed in the presence of CO. This reactivity, nevertheless, was only observed at very high concentrations of nitrogen mono- or dioxide. Additionally, whereas the reaction with NO was reversible, the reaction with NO₂ was irreversible. Thus, when the yellow compounds obtained by reaction of the binuclear rhodium derivatives supported on silica with high concentrations of NO were left in NO-free air the solid reverted to purple again, which was not observed for NO₂. All the reactivity and relevant concentrations conditions with VOCs and gases tested is summarized in Table 6 where concentrations in which color modulations of the complexes **1** to **5** were observed are shown.

Table 6. Summary of the observed behavior for VOCs and gases tested with all compounds^a

Solid	VOCs (ppm)						
	acetone	ACN	chloroform	ethanol	formaldehyde	hexane	toluene
1·(CH ₃ CO ₂ H) ₂	-	4600	-	-	-	-	-
2·(CH ₃ CO ₂ H) ₂	-	4600	-	-	-	-	-
2·(H ₂ O) ₂	-	4600	-	-	-	-	-
3·(CF ₃ CO ₂ H) ₂	-	4600	-	-	-	-	-
4·((CH ₃) ₃ CCO ₂ H) ₂	-	4600	-	-	-	-	-
5·(CH ₃ CO ₂ H) ₂	-	4600	-	-	-	-	-

Solid	gases (ppm)							
	water	CO ₂	N ₂	O ₂	Ar	SO ₂	NO	NO ₂
1·(CH ₃ CO ₂ H) ₂	-	-	-	-	-	-	8140	2650
2·(CH ₃ CO ₂ H) ₂	-	-	-	-	-	-	8140	2650
2·(H ₂ O) ₂	-	-	-	-	-	-	814	500
3·(CF ₃ CO ₂ H) ₂	-	-	-	-	-	-	4070	2650
4·((CH ₃) ₃ CCO ₂ H) ₂	-	-	-	-	-	-	4070	2650
5·(CH ₃ CO ₂ H) ₂	-	-	-	-	-	-	8140	5000

^a Both responses are shown: not induced color change (-) and concentrations (in ppm) necessary to induce color changes.

Reversibility of Carbon Monoxide Coordination. Ideal sensing systems do not only need to display selectively and sensing features at low concentration, but also must be able to show reversible binding with the target analyte. In line with the successful application of the above mentioned probes, binding of CO in the dinuclear rhodium complexes was found fully reversible. When the yellow solid corresponding to any $\# \cdot (\text{CO})_2$ complex embedded in silica was left in an open air atmosphere, the diffuse reflectance spectra evolve back to the initial corresponding purple complex probe. Although the uptake of CO in the adsorbed compounds occurs in the seconds/minutes time scale, the complete reverse transformation in air from $\# \cdot (\text{CO})_2$ to $\# \cdot \text{L}_2$ takes approximately 15 hours at room temperature. Noticeably, the desorption of carbon monoxide from $\# \cdot (\text{CO})_2$ occurs also in two consecutive steps producing initially $\# \cdot (\text{L}, \text{CO})$ and the further appearance of the purple dirhodium(II) starting materials, $\# \cdot \text{L}_2$. Figure 5 shows a representative example of the changes observed in the intensity of the band at 400 nm from the diffuse reflectance UV-Vis spectrum of the probe from complex $2 \cdot (\text{H}_2\text{O})_2$ upon cyclic contact with CO-containing and CO-free air. This cyclic process was repeated at least 10 times without significant degradation of the sensing ability of the material.

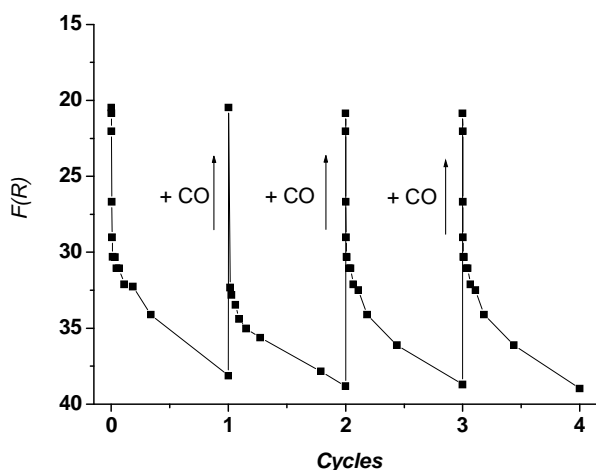


Figure 5. Diffuse reflectance UV-Vis spectral response for the band centered at $\lambda = 400$ nm for silica beads containing $2 \cdot (\text{CO})_2$ exposed to an open to air atmosphere. The cycling of the sensor is checked by letting CO-containing air in contact with the sample after full recovery (ca. 15 h) of the starting complex probe.

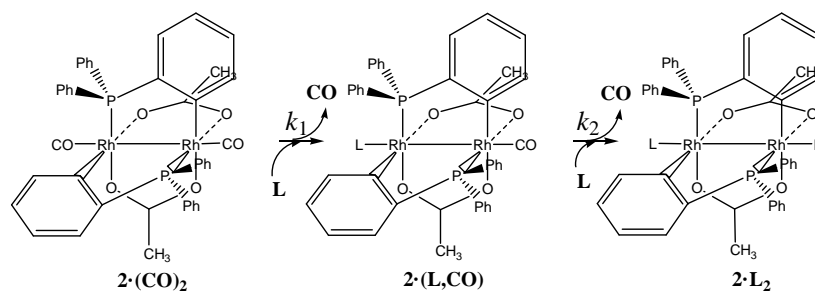
Moreover, the release of carbon monoxide from the corresponding $\# \cdot (\text{CO})_2$ was followed by thermogravimetry and in all cases the weight changes correspond to two equivalents of CO per molecule. Furthermore, no loss of the L ligands from the initial $\# \cdot \text{L}_2$ probe complexes was observed during the processes, thus indicating that these axial ligands remain adsorbed on the silica beads during all the cycles.

In this respect, and in order to determine the role played by the axial ligand in the reversible CO binding process, the formation and CO-release from $2 \cdot (\text{CO})_2$ using two different starting probe complexes ($2 \cdot (\text{CH}_3\text{CO}_2\text{H})_2$ and $2 \cdot (\text{H}_2\text{O})_2$) was monitored thermogravimetrically. Although in both cases two CO molecules are adsorbed/released reversibly, remarkable differences in the release kinetics were found. While for the $2 \cdot (\text{CO})_2$ derivative obtained from silica bead-supported $2 \cdot (\text{CH}_3\text{CO}_2\text{H})_2$ the loss of CO is complete in some hours, the complete CO release from the $2 \cdot (\text{CO})_2$ derivative obtained from the $2 \cdot (\text{H}_2\text{O})_2$ probe requires ca. two weeks at room temperature.

Kinetico-Mechanistic Studies of the Substitution of CO by L on the Immobilized Compounds. The uptake of carbon monoxide by the immobilized complexes occurs at room temperature in a time scale of minutes, much longer than the practically instant process observed for the systems in solution. Even though the diffusion of gaseous CO into the porous silica beads should play a crucial role in this process, as already established for other immobilized systems,^{26,27} no further studies have been carried out for the CO uptake process. The fully reversible character of the process for all adsorbed compounds indicated in Table 1 was confirmed by thermogravimetric and UV-Vis analyses (see Scheme 2). As indicated above, the results are especially relevant with respect to the presence of the CO-displaced axial L ligands of the starting material inside the silica beads, which creates the need for a further kinetico-mechanistic investigation of the process.

The release of CO from the $\# \cdot (\text{CO})_2$ derivatives obtained from silica immobilized samples of $\# \cdot \text{L}_2$, corresponds to the neat weight loss of two CO molecules per dirhodium unit and was studied in detail from a kinetico-

mechanistic perspective. The time monitoring at a fixed temperature of this weight loss provided an excellent handle for the measure of the rates of the process, when fitted to a double exponential decay, as corresponds to the intermediate formation of the $\# \cdot (\text{CO}, \text{L})$ species. Effectively, the weight loss associated to each one of fitted set of two consecutive exponentials is half that of the total decrease, in excellent agreement with the kinetic detection of the $\# \cdot (\text{CO}, \text{L})$ intermediate complexes (see above and Figure S1 for the $5 \cdot (\text{CO})_2$ complex). The observed first-order character of both consecutive processes can be associated either with a limiting CO dissociative process, or with a unimolecular reaction involving the L ligands already attached in an outer-sphere fashion to the dirhodium(II) probe complex.²⁸ Alternatively, instead of the back coordination of the CO-displaced L ligands, attachment of the available OH groups in the silica beads can also explain such behavior, the L ligands being mere spectators of the process. However, the latter possibility was rejected as complex **2** (which axial ligands have been extracted via thermal treatment)²⁹ adsorbed on silica beads was found to be brownish in color, in deep contrast to the purple color of the $2 \cdot \text{L}_2$ complexes. In the same line, the recycling of the silica beads on CO depletion also reverts to the original spectra for all the adsorbed $\# \cdot \text{L}_2$ complexes, a clear indication that the re-entry of the original axially bound ligands, L, on the dirhodium compounds is occurring. Consequently all the weight-loss/time traces (Figure S1) can be fully associated with Scheme 3, where L represents the axial ligands existing in the starting materials.



Scheme 3. Carbon monoxide liberation in $2 \cdot (\text{CO})_2$ in two consecutive kinetic steps, producing the regeneration of $2 \cdot \text{L}_2$.

The temperature dependence of both k_1 and k_2 rate constants has also been determined by the use of the Eyring equation.³⁰ Figure 6 shows the plots for two of the starting immobilized compounds studied, $2 \cdot (\text{CH}_3\text{CO}_2\text{H})_2$ and $2 \cdot (\text{H}_2\text{O})_2$; the relevant kinetic and thermal activation parameters for these processes on all studied compounds are collected in Table 7.

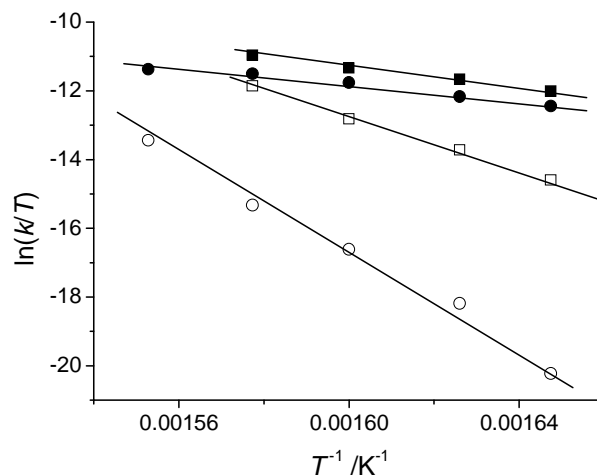


Figure 6. Eyring plot for k_1 (full) and k_2 (empty), rate constants corresponding to CO loss for immobilized compounds $2 \cdot (\text{CH}_3\text{CO}_2\text{H})_2$ (squares) and $2 \cdot (\text{H}_2\text{O})_2$ (circles).

The very different steric demands of the possible hydrogen bonding interactions for the immobilized complexes, as well as the dramatic change of the σ -donor character of the oxygen donors, are bound to produce important differences between the CO by $\text{CH}_3\text{CO}_2\text{H}$, $\text{CF}_3\text{CO}_2\text{H}$, $(\text{CH}_3)_3\text{CCO}_2\text{H}$ or H_2O substitution. As seen in the data collected in Table 7 the thermal activation parameters associated with the faster process (k_1) indicate that for all immobilized compounds the values determined for this step are surprisingly the same within experimental error, with rather low enthalpies and very negative entropies of activation. These indicate a mechanism with an important degree of ordering during the substitution process with very similar energetics. However, the total recovery of the $2 \cdot (\text{H}_2\text{O})_2$ system is much slower than for the rest of the probes, in

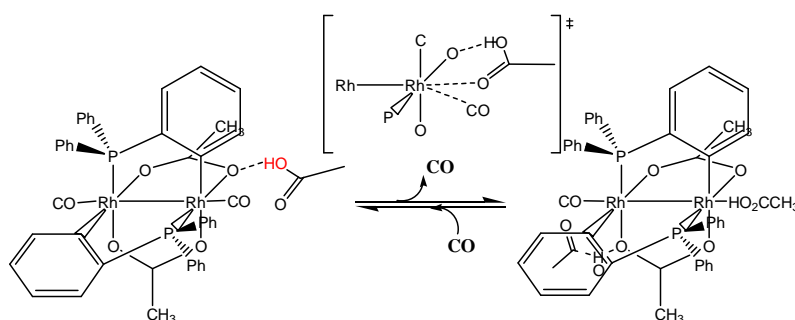
Table 7. Kinetic and thermal activation parameters for the processes indicated in Scheme 3 for immobilized complexes **#·L₂**^a

Compound	$10^3 \times^{342} k_1 / s^{-1}$	$\Delta H_1^\ddagger / kJ mol^{-1}$	$\Delta S_1^\ddagger / J K^{-1} mol^{-1}$	$10^4 \times^{342} k_2 / s^{-1}$	$\Delta H_2^\ddagger / kJ mol^{-1}$	$\Delta S_2^\ddagger / J K^{-1} mol^{-1}$
1·(CH₃CO₂H)₂	3.6	28±3	-210±8	3.3	60±5	-145±10
2·(CH₃CO₂H)₂	5.3	35±3	-190±11	6.8	100±5	-20±10
2·(H₂O)₂	3.2	30±3	-210±10	0.078	180±5	180±10
3·(CF₃CO₂H)₂	13	33±3	-185±11	16	21±5	-240±10
4·(CH₃)₃CCO₂H)₂	2.4	30±3	-210±10	2.2	85±15	-70±40
5·(CH₃CO₂H)₂	3.5	30±3	-200±11	6.0	75±10	-95±30

^a k_1 and k_2 were also determined at 334, 352, 361 and 371 K for the evaluation of the thermal activation parameters.

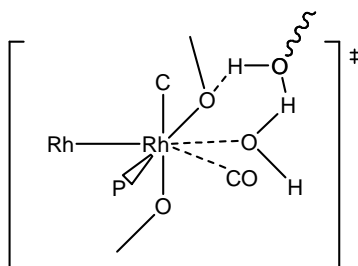
good agreement with the differences observed, due to the much lower value of k_2 for the recovery of compound $2 \cdot (\text{H}_2\text{O})_2$.

The only way to come to terms with the surprising homogeneity within the k_1 set of data between such different complexes, is by considering that the CO-displaced axial ligand (L) remains still attached *via* hydrogen bonding interactions to the neighbouring bridging carboxylato units of the dirhodium complex. Such interactions have already been described in some Pd(II) XRD data³¹ as well as in DFT³² and mechanistic studies on electrophilic C-H bond activation^{13,33} processes assisted by acid. By this attachment the important differences between the L ligands could be producing, *de facto*, a rather similar electronics in all cases. Scheme 4 represents a reasonable sequence for such process exemplified for the $2 \cdot (\text{CH}_3\text{CO}_2\text{H})_2$ complex. The transition state indicated presents an effective high degree of ordering with little enthalpic demands considering the already "initiated" Rh-carboxylate bonding.



Scheme 4. Mechanism proposed for CO liberation in compounds with carboxylic acid as axial ligands

Nevertheless, in the case of decoordinated H_2O arrangement, $2 \cdot (\text{H}_2\text{O})_2$, the involvement of the silica OH groups cannot be disregarded, given the existence of a single oxygen donor in the water molecule. An outer-sphere "solvent-assisted" interaction between one of the oxygens of the $\mu\text{-CH}_3\text{CO}_2^-$ group and the H_2O ligand ($\underline{\text{O}}\text{-C}(\text{CH}_3)\text{-}\underline{\text{O}}\text{..H-O..H-}\underline{\text{O}}\text{-H}$) should be considered as responsible of the similarity with the carboxylic acid systems ($\underline{\text{O}}\text{-C}(\text{R})\text{-}\underline{\text{O}}\text{...H-O-C}(\text{R})\text{-}\underline{\text{O}}$) (Scheme 5).



Scheme 5. Possible outer-sphere "solvent-assisted" interaction for the $2 \cdot (\text{H}_2\text{O})_2$ system

Examination of the kinetic and thermal activation data for k_2 for the systems studied (Table 7) indicate a general increase of the activation enthalpy accompanied by a decrease of the ordering during the process (less negative or positive activation entropies) with respect to k_1 , the exception being for the $3 \cdot (\text{CF}_3\text{CO}_2\text{H})_2$ complex with very poor σ -donors in its axial positions. Furthermore, the values for ΔH^\ddagger and ΔS^\ddagger are even much more positive for the $2 \cdot (\text{H}_2\text{O})_2$ system, thus implying a much more dissociated transition state than for the systems derived from its analogous $2 \cdot (\text{CH}_3\text{CO}_2\text{H})_2$ probe. Given the fact that the lack of a statistical factor in the value of the rate constants is a clear indicative of the electronic transmission *via* de Rh-Rh bond, already established in equilibrium studies,¹¹ the better the σ -donor character of the already coordinated first L ligand, the better π -back-donation into the remaining axially bound CO. As a consequence, the process becomes slower, with higher enthalpic demands that promote an important degree of decooordination of CO before the new ligand L can be coordinated to the fairly electron enriched rhodium centre. This effect should be very pronounced for L = H₂O and minimal (or even opposite) for L = CF₃CO₂H as effectively observed. Figure 7 shows the $\Delta H^\ddagger/\Delta S^\ddagger$ compensation plot for all the systems studied, which corroborates the homogeneity of the mechanism operating for all the reactions.

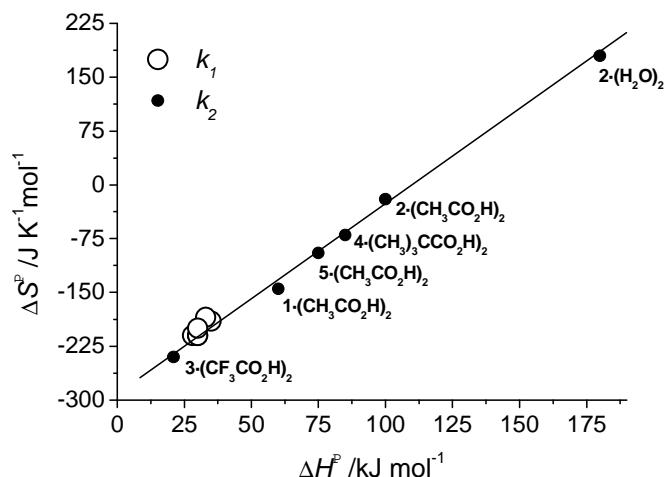


Figure 7. $\Delta H^\ddagger/\Delta S^\ddagger$ compensation plot for all the systems studied. The values for k_1 cannot be distinguished given its similarity.

Conclusions

A family of binuclear rhodium compounds of general formula $[\text{Rh}_2\{(\text{XC}_6\text{H}_3)\text{P}(\text{XC}_6\text{H}_4)_2\}_n(\text{O}_2\text{CR})_{4-n}] \cdot \text{L}_2$ containing one or two, in a head-to-tail arrangement, metallated phosphine ligands and different equatorial and axial ligands has been used as chromogenic chemosensors for CO detection. UV-Vis studies were carried out, both in solution and immobilized on silica beads, resulting in hypsochromic shifts. In the case of compounds adsorbed on silica beads in the presence of CO, two different spectra were observed due to the axial coordination of CO groups: orange (one CO in axial position) and yellow (two CO). The crystal structure of **3**·(CHCl₃, CO) was solved by single X-ray diffraction techniques. In all cases the binuclear rhodium complexes studied showed a remarkable low detection limit for CO, and a high selective response. From all VOCs and gases tested as possible interferences, the only sensing was observed in the presence of acetonitrile, NO and NO₂; nevertheless, this only occurs at high concentrations (4600, 4070 and 2650 ppm, respectively). As a special feature, all the complexes tested display a very clear and remarkable color change to the “naked eye” at concentrations at which CO becomes toxic (i.e. 50-60 ppm). In

particular, compound **5**·(CH₃CO₂H)₂ displays clear color modulations at CO concentrations as low as 0.2 ppm, even allowing the quantification CO in air, based on simple and visual color changes. Binding of CO in these systems was found fully reversible, and the release of carbon monoxide can be monitored by thermogravimetric measurements. The kinetic and thermal activation data obtained for the depletion of CO indicate that the outer-sphere coordination of the L ligands, even in the presence of axially bound CO, is determinant for the easiness and reproducibility of the reversibility of the process. The silica support behaves, especially for L= H₂O, as a non-innocent solvent assisting important interactions that avoid the total removal of the CO-substituted L groups.

Experimental Section

General Considerations. Commercially available reagents, [Rh₂(O₂CCH₃)₄], as well as the different phosphines (P(C₆H₅)₃, P(*m*-CH₃C₆H₄)₃) and carboxylic acids (CF₃CO₂H, CH₃CO₂H, (CH₃)₃CO₂H) were used as purchased. All solvents were of analytical grade. Column chromatography was carried out on silica gel 60 (230-240 mesh). Solvent mixtures are volume/volume mixtures, unless specified otherwise. All reactions were carried out in oven-dried glassware under argon atmosphere, although the isolated solids are air-stable. The solvents were degassed before use. All the gases used in this work were generated *in situ*: carbon monoxide by reaction of sulfuric acid with formic acid; carbon dioxide by adding chloride acid to sodium carbonate; nitrogen monoxide and nitrogen dioxide by oxidation of copper with nitric acid; sulfur dioxide by copper oxidation with sulfuric acid.

Compounds. [Rh₂{(XC₆H₃)P(XC₆H₄)₂]₂(O₂CR)₂·L₂. [Rh₂{(XC₆H₃)P(XC₆H₄)₂]₂·(O₂CCH₃)₂·(CH₃CO₂H)₂ complexes, **2**·(CH₃CO₂H)₂ and **5**·(CH₃CO₂H)₂, were obtained by refluxing the corresponding phosphine with [Rh₂(O₂CCH₃)₄] in toluene:acetic acid media (3:1) under argon atmosphere as described in the literature.^{15,34,35} For these compounds with two cyclometallated phosphines the molar ratio phosphine:dirhodium(II) tetraacetate was 2:1. These compounds containing two

ortho-metallated aryl phosphines and two carboxylates as bridging ligands show fast and quantitative interchange of both carboxylate ligands by other bridging ligands,³⁶ which facilitates the interchange with other carboxylates. Thus other derivatives with the same *ortho*-metallated dirhodium(II) skeleton can be easily obtained (see below).

Compounds of general formula $[\text{Rh}_2\{(\text{XC}_6\text{H}_3)\text{P}(\text{XC}_6\text{H}_4)_2\}_2(\text{O}_2\text{CR})_2] \cdot \text{L}_2$, **3**·(**CF₃CO₂H**)₂ and **4**·(**(CH₃)₃CCO₂H**)₂ were obtained by stirring the starting product, **2**·(**CH₃CO₂H**)₂, in presence of an excess of the substituting carboxylic acid (trifluoroacetic and pivalic acid respectively) in chloroform solution. The mixture was then heated under reduced pressure to dryness. The procedure was repeated until the complete interchange was produced (5-6 times). The excess of the acid was then eliminated by column chromatography (CH₂Cl₂:Hexane 2:1).

$[\text{Rh}_2\{(\text{C}_6\text{H}_4)\text{P}(\text{C}_6\text{H}_5)_2\}_2(\text{O}_2\text{CCH}_3)_2] \cdot (\text{H}_2\text{O})_2$, **2**·(**H₂O**)₂, was obtained by stirring **2**·(**CH₃CO₂H**)₂ in the presence of an excess of sodium carbonate in acetone. In this procedure, the water contained in the acetone is the origin of the substituting axial ligand. The resulting compounds were obtained after removal of the solvent under reduced pressure.

$[\text{Rh}_2\{(\text{XC}_6\text{H}_3)\text{P}(\text{XC}_6\text{H}_4)_2\}(\text{O}_2\text{CR})_3] \cdot \text{L}_2$. $[\text{Rh}_2\{(\text{C}_6\text{H}_4)\text{P}(\text{C}_6\text{H}_5)_2\}(\text{O}_2\text{CCH}_3)_3] \cdot (\text{CH}_3\text{CO}_2\text{H})_2$ complex, **1**·(**CH₃CO₂H**)₂, was obtained following the same synthetic procedure used than for compounds with general formula $[\text{Rh}_2\{(\text{XC}_6\text{H}_3)\text{P}(\text{XC}_6\text{H}_4)_2\}_2(\text{O}_2\text{CR})_2] \cdot \text{L}_2$, but using a phosphine:dirhodium(II) tetraacetate molar ratio of 0.9:1.

Silica Gel Immobilization of the Dirhodium(II) Complexes. Each binuclear rhodium compound was dissolved in a minimum volume of CHCl₃. An excess of silica (230-240 mesh, weight ratio 2-10 fold), was added to the coloured solution and the resulting mixture was stirred at room temperature for five minutes. After removal of the solvent on a rotary evaporator, the solid was dried in an oven at 343 K during at least two days prior to its use. A careful weight control of the samples was carried out, indicating that the effective final weight corresponds to

the mass of silica plus the mass of the $\# \cdot L_2$ complex, and that no evolution from the silica beads of the axially bound ligands, L, has occurred under the working conditions.

Instrumentation. Infrared Spectra were recorded at room temperature on a JASCO FT-IR 460 Plus Spectrometer. UV-Vis spectra were recorded using a Jasco V-650 Spectrophotometer equipped with a diffuse reflectance Sphere (Model ISV-722 Sphere) for measurements on solids. In the latter case, measurements were conducted at room temperature over a wavelength range of 350–800 nm with a wavelength step of 1 nm. The reflectance data were transformed using Kubelka–Munk function $[F(R)]$,³⁷ where R is the fraction of incident light reflected by sample.

$$F(R) = \frac{(1-R)^2}{2R}$$

For kinetic studies, CO loss was monitored via thermogravimetric analyses carried out on a TGA/SDTA 851e Mettler Toledo balance, set at a fixed temperature, using nitrogen as purge gas. The fitting of the weight changes *versus* time to a double exponential decay with identical amplitudes was carried out by the standard software packages available. Carbon monoxide concentrations were measured by an ambient carbon monoxide analyzer (Testo 315-2 Model 0632 0317), properly validated with calibration certificate issued by Spanish Certification Entity (ENAC).

X-ray data collection was performed on a Bruker Kappa CCD diffractometer using graphite monochromated Mo-K α radiation ($\lambda = 0.71073 \text{ \AA}$) at 293 K. Data reduction and cell refinements were performed with HKL DENZO and SCALEPACK programs.²³ Crystal structures were solved by direct methods with the aid of successive difference Fourier maps, and were refined using the SHELXTL 6.1 software package.³⁸ All non-hydrogen atoms were refined anisotropically. High residual electronic density was found around the CF₃ groups in the trifluoroacetate ligands and very anisotropic thermal ellipsoids were obtained for fluorine atoms. Hence, a disordered model for CF₃ groups was applied using a

riding model refinement and constraining the occupancy to one for those groups bonded to the same carbon atom in both acetate ligands. The hydrogen atoms were assigned to ideal positions and refined using a riding model. The details of the data collection, cell dimensions, and structure refinement are given in the supplementary material. Full crystallographic data has been deposited in the Cambridge Crystallographic Data Centre with the number CCDC 820952.

RGB values were analyzed using Adobe Photoshop Elements 7.0 software.

Associated Content

Supporting Information. Crystallographic data and structure refinement of $[\text{Rh}_2[(\text{C}_6\text{H}_4)\text{P}(\text{C}_6\text{H}_5)_2]_2(\text{O}_2\text{CCH}_3)_2]\cdot(\text{CO})$ (**3·CO**). Selected geometric data for $[\text{Rh}_2[(\text{C}_6\text{H}_4)\text{P}(\text{C}_6\text{H}_5)_2]_2(\text{O}_2\text{CCH}_3)_2]\cdot(\text{CO})$ (**3·CO**) at 293 K. Weight loss of a sample of **5·(CO)₂** with time at 50 °C. This material is available free of charge via the Internet at <http://pubs.acs.org>.

Author Information

Corresponding Author

rmaez@qim.upv.es; manel.martinez@qi.ub.es.

Acknowledgment

The authors wish to express their gratitude to the Spanish Ministerio de Ciencia e Innovación (projects MAT2009-14564-C04-01 and CTQ2009-14443-C02-02) and Generalitat Valenciana (project PROMETEO/2009/016) for their support. M.E.M. is grateful to the Spanish Ministerio de Ciencia e Innovación for an FPU grant.

References

1. (a) Wattel, F.; Favory, R.; Lancel, S.; Neviere, R.; Mathieu, D. *Bulletin de l'Academie Nationale de Medecine* **2006**, *190*, 1961-1975. (b) J. J. McGrath, *Carbon Monoxide*, **2006**, 695. Ed. H. Salem, S. A. Katz, 2nd Ed. (c) Wilkinson, L. J.; Waring, R. H.; Steventon, G. B.; Mitchell, S. C. *Molecules of death. Carbon monoxide-the silent killer*, (2n Ed.) **2007**.
2. <http://emedicine.medscape.com/article/1009092-overview>
3. (a) Claireaux, G.; Thomas, S.; Fievet, B.; Motais, R. *Respiration physiology* **1988**, *74*, 91-98. (b) Marsh, M. G.; Marino, G.; Pucci, P.; Ferranti, P.; Malorni, A.; Kaeda, J.; Marsh, J.; Luzzatto, L. *Hemoglobin* **1991**, *15*, 43-51.
4. Benzon, H. T.; Brunner, E. A. *JAMA* **1978**, *240*, 1955-1964.
5. Wang, B.; Zhao, Y.D.; Hu, L.M.; Cao, J.S.; Gao, F.L.; Liu, Y.; Wang, L.J. *Chinese Sci. Bull.* **2010**, *55*, 3, 228-232.
6. Itou, M.; Araki, Y.; Ito, O.; Kido, H. *Inorg. Chem.* **2006**, *45*, 6114-6116.
7. Paul, S.; Amalraj, F.; Radhakrishnana, S. *Synt. Math.* **2009**, *159*, 1019-1061.
8. Benito-Garagorri, D.; Puchberger, M.; Mereiter, K.; Kirchner, K. *Angew. Chem. Int. Ed.* **2008**, *47*, 9142-9145.
9. Giulino, A.; Gupta, T.; Altman, M.; Lo Schiavo, S.; Mineo, P. G.; Fragalà, I. L.; Evmenenko, G.; Dutta, P.; Van der Boom, M. E. *Chem. Commun.* **2008**, 2900-2902.
10. See for instance: (a) Climent, E.; Marcos, M.D.; Martínez-Máñez, R.; Sancenón, F.; Soto, J.; Rurack, K.; Amorós, P. *Angew. Chem. Int. Ed.* **2009**, *48*, 8519-8522. (b) Climent, E.; Bernardos, A.; Martínez-Máñez, R.; Maquieira, A.; Marcos, M.D.; Pastor-Navarro, N.; Puchades, R.; Sancenón, F.; Soto, J.; Amorós, P. *J. Am. Chem. Soc.* **2009**, *131*, 14075-14080. (c) Comes, M.; Aznar, E.; Moragues, M.; Marcos, M.D.; Martínez-Máñez, R.; Sancenón, F.; Soto, J.; Villaescusa, L.A.; Gil, L.; Amorós, P. *Chem. Eur. J.* **2009**, *15*, 9024-9033. (d) Ábalos, T.; Royo, S.; Martínez-Máñez, R.; Sancenón, F.; Soto, J.; Costero, A.M.; Gil, S.; Parra, M. *New. J. Chem.* **2009**, *33*, 1641-1645. (e) Aznar, E.; Coll, C.; Marcos, M.D.; Martínez-Máñez, R.; Sancenón, F.; Soto, J.; Amorós, P.; Cano, J.; Ruiz, E. *Chem. Eur. J.* **2009**, *15*, 6877-6888. (f) Climent, E.; Calero, P.; Marcos, M.D.; Martínez-Máñez, R.; Sancenón, F.; Soto, J. *Chem. Eur. J.* **2009**, *15*, 1816-1820.
11. Hirva, P.; Esteban, J.; Lahuerta, P.; Pérez-Prieto, J. *Inorg. Chem.* **2007**, *46*, 2619-2626.
12. Esteban, J.; Ros-Lis, J.V.; Martínez-Mañez, R.; Marcos, M.D.; Moragues, M.; Soto, J.; Sancenón, F. *Angew. Chem. Int. Ed.* **2010**, *49*, 4934-4937.
13. Estevan, F.; González, G.; Lahuerta, P.; Martínez, M.; Peris, E.; van Eldik, R. *J. Chem. Soc., Dalton Trans.* **1996**, 1045-1050.
14. Esteban, J.; Hirva, P.; Lahuerta, P.; Martínez, M. *Inorg. Chem.* **2006**, *45*, 8776-8784.
15. Hirva, P.; Lahuerta, P.; Pérez-Prieto, J. *Theor. Chem.* **2005**, *113*, 63-68.
16. (a) Estevan, F.; Lahuerta, P.; Pérez-Prieto, J.; Pereira, I.; Stiriba, S. E. *Organometallics*, **1998**, *17*, 3442-3447. (b) Estevan, F.; Lahuerta, P.; Pérez-Prieto, J.; Sanaú, M.; Stiriba, S. E.; Úbeda, M. A.

- Organometallics* **1997**, *16*, 880–886. (c) Barberis, M.; Lahuerta, P.; Pérez-Prieto, J.; Sanaú, M. *Chem. Commun.* **2001**, 439–440. (d) Barberis, M.; Pérez-Prieto, J.; Stiriba, S. E.; Lahuerta, P. *Org. Lett.* **2001**, *3*, 3317–3319. (e) Estevan, F.; Herbst, K.; Lahuerta, P.; Barberis, M.; Pérez-Prieto, J. *Organometallics* **2001**, *20*, 950–957.
17. Drago, R. S.; Tanner, S. P.; Ritchman, R. M.; Long, J. R. *J. Am. Chem. Soc.* **1979**, *101*, 2897–2903.
18. González, G.; Martínez, M.; Estevan, F.; García-Herbosa, G.; Lahuerta, P.; Peris, E.; Ubeda, M.; Diaz, M.R.; Garcia-Granda, S.; Tejerina, B. *New J. Chem.* **1996**, *20*, 83–94.
19. Esteban, J. *PhD Thesis* **2006**, *Universitat de València*.
20. Chakravarty, A. R.; Cotton, F. A.; Tocher, D. A.; Tocher, J. H. *Organometallics* **1985**, *4*, 8–13.
21. (a) Barcel, F.; Cotton, F. A.; Lahuerta, P.; Llusar, R.; Sanaú, M.; Schwotzer, W.; Úbeda, M. A. *Organometallics* **1986**, *5*, 808–811. (b) Barcel, F.; Cotton, F. A.; Lahuerta, P.; Sanaú, M.; Schwotzer, W.; Úbeda, M. A. *Organometallics* **1987**, *6*, 1105–1110. (c) Cotton, F. A.; Dunbar, K. R.; Verbruggen, M. G.; *J. Am. Chem. Soc.* **1987**, *109*, 5498–5506. (d) Cotton, F. A.; Dunbar, K. R. *J. Am. Chem. Soc.* **1987**, *109*, 3142–3143. (e) Cotton, F. A.; Dunbar, K. R.; Eagle, C. T. *Inorg. Chem.* **1987**, *26*, 4127–4130. (f) Lahuerta, P.; Paya, J.; Peris, E.; Pellinghelli, M. A.; Tiripicchio, A. *J. Organomet. Chem.* **1989**, *373*, C5–C7. (g) Morrison, E. C.; Tocher, D. A. *Inorg. Chim. Acta* **1989**, *156*, 99–105. (h) Morrison, E. C.; Tocher, D. A. *Inorg. Chim. Acta* **1989**, *157*, 139–140. (i) Lahuerta, P.; Payá, J.; Peris, E.; Aguirre, A.S.; García-Granda, A.; Gómez-Beltrán, F. *Inorg. Chim. Acta* **1992**, *192*, 43–49. (j) Lahuerta, P.; Payá, J.; Solans, X.; Úbeda, M. A. *Inorg. Chem.* **1992**, *31*, 385–391. (k) Lahuerta, P.; Peris, E. *Inorg. Chem.* **1992**, *31*, 4547–4551. (l) Borrachero, M. V.; Estevan, F.; Lahuerta, P.; Payá, J.; Peris, E. *Polyhedron* **1993**, *12*, 1715–1717. (m) Estevan, F.; Lahuerta, P.; Latorre, J.; Peris, E.; García-Granda, S.; Gómez-Beltrán, F.; Aguirre, A.; Salvad, M. A. *J. Chem. Soc. Dalton Trans.* **1993**, 1681–1688. (n) Lahuerta, P.; Úbeda, M. A.; Payá, J.; García-Granda, S.; Gómez-Beltrán, F.; Anillo, A. *Inorg. Chim. Acta* **1993**, *205*, 91. (o) Lahuerta, P.; Latorre, J.; Peris, E.; Sanaú, M.; Ubeda, M. A.; Garcia-Granda, S. *J. Organomet. Chem.* **1993**, *445*, C10–12. (p) Pruchnik, F. P.; Starosta, R.; Lis, T.; Lahuerta, P. *J. Organomet. Chem.* **1998**, *568*, 177–183. (q) Pruchnik, F. P.; Starosta, R.; Smolenski, P.; Shestakova, E.; Lahuerta, P. *Organometallics* **1998**, *17*, 3684–3689.
22. (a) Taber, D. F.; Malcolm, S. C.; Bieger, K.; Lahuerta, P.; Sanaú, M.; Stiriba, S. E.; Pérez-Prieto, J.; Monge, M. A. *J. Am. Chem. Soc.* **1999**, *121*, 860–861. (b) Lahuerta, P.; Martínez-Mañez, R.; Payá, J.; Peris, E. *Inorg. Chim. Acta* **1990**, *173*, 99–105. (c) Lahuerta, P.; Payá, J.; Pellinghelli, M. A.; Tiripicchio, A. *Inorg. Chem.* **1992**, *31*, 1224–1232.
23. Otwinowski, Z.; Minor, W. *Methods Enzymol.* **1997**, *276*, 307–326.
24. The crystal structure of $[\text{Rh}_2[(\text{C}_6\text{H}_4)\text{P}(\text{C}_6\text{H}_5)_2]_2(\text{O}_2\text{CCH}_3)_2]\cdot(\text{CO})$ (**3·CO**) has been deposited at the Cambridge Crystallographic Data Centre and allocated the deposition number CCDC 820952
25. Kou, X.; Rasika Dias, H. V. *Dalton Trans.* **2009**, 7529–7536.
26. Basallote, M. G.; Bozoglian, F.; Fernandez-Trujillo, M. J.; Martínez, M. *New J. Chem.* **2007**, *32*, 264–272.

27. Basallote, M. G.; Blanco, E.; Blázquez, M.; Fernández-Trujillo, M. J.; Litrán, R.; Máñez, M. A.; Ramírez del Solar, M. *Chem. Mater.* **2003**, 15, 2525-2532.
28. Espenson, J. H. *Chemical Kinetics and Reaction Mechanisms*, McGraw-Hill, **1981**.
29. A sample of silica containing the complex was heated at a rate of 5 degrees per minute until a weight loss equivalent to the two L ligands is observed. Alternatively when stirring a suspension of the prepared silica-adsorbed sample in chloroform at 70 °C for prolonged periods, followed by reduced pressure drying, a sample of axially free dirhodium complex was also produced.
30. Tobe, M. L.; Burgess, J. *Inorganic Reaction Mechanisms*, Longman, **1999**.
31. Albert, J.; Andrea, L.; Bautista, J.; Gonzalez, A.; Granell, J.; Font-Bardía, M.; Calvet, T. *Organometallics* **2008**, 27, 5108-5117.
32. Aullón, G.; Chat, R.; Favier, I.; Font-Bardía, M.; Gómez, M.; Granell, J.; Martínez, M.; Solans, X. *Dalton Trans.* **2009**, 8292-8300.
33. (a) Gómez, M.; Granell, J.; Martínez, M. *Eur. J. Inorg. Chem.* **2000**, 217-224. (b) Gómez, M.; Granell, J.; Martínez, M. *J. Chem. Soc., Dalton Trans.* **1998**, 37-44. (c) González, G.; Lahuerta, P.; Martínez, M.; Peris, E.; Sanau, M. *J. Chem. Soc., Dalton Trans.* **1994**, 545-550.
34. Esteban, J.; Esteban, F.; Sanau, M. *Inorg. Chim. Acta* **2009**, 362, 1179-1184.
35. Esteban, J.; Esteban, F.; Sanau, M. *Inorg. Chim. Acta* **2008**, 361, 1274-1280.
36. Lahuerta, P.; Peris, E. *Inorg. Chem.* **1992**, 31, 4547-4551.
37. Zinchuk, A. V.; Hancock, B. C.; Shalaev, E. Y.; Reddy, R. D.; Govindarajan, R.; Novak, E. *Eur. J. Pharm. Biopharm.* **2005**, 61, 158-170.
38. Sheldrick, G.M. *SHELXTL, v. 5.1 Bruker AXS*, Inc. ed.; Madison, WI, **2000**.

SUPPORTING INFORMATION

Sensitive and Selective Chromogenic Sensing of Carbon Monoxide via Reversible Axial CO Coordination in Binuclear Rhodium Complexes

María E. Moragues, Julio Esteban, José Vicente Ros-Lis, Ramón Martínez-Máñez,* M. Dolores Marcos, Manuel Martínez,* Juan Soto, Félix Sancenón.

Table S1. Crystallographic data and structure refinement of $[\text{Rh}_2[(\text{C}_6\text{H}_4)\text{P}(\text{C}_6\text{H}_5)_2]_2(\text{O}_2\text{CCH}_3)_2] \cdot (\text{CO})$ (**3-CO**) at 293 K.

$[\text{Rh}_2[(\text{C}_6\text{H}_4)\text{P}(\text{C}_6\text{H}_5)_2]_2(\text{O}_2\text{CCH}_3)_2] \cdot (\text{CO})$ (3-CO) at 293 K	
Empirical formula	C42 H29 Cl3 F6 O5 P2 Rh2
Formula weight	1101.80
Crystal system, Space group	Monoclinic, P21/c
Z, Calculated density	4, 1.6962 Mg/m ³
Volume	4314.50(29) Å ³
Lattice constants:	
A	10.0960(3)
B	21.7150(9)
C	21.0090(9)
β	110.490(2)
Temperature	293 K
Radiation	Mo K α
Absorption coefficient	10.946 cm ⁻¹
F (000)	2184.0
Wavelength	0.71073 Å
Crystal size	0.1 x 0.08 x 0.08 mm
Angular range	(1.4-27.5) °2 θ
Minimu, Maximum $h; k; l$	-13, 13; -26, 28; -27, 24
Data examined	17622
Unique reflections	9827 $R_{\text{ov}}=0.0955$
Refinement:	
R_1 for 4365 $F_o > 4\sigma(F_o)$	0.0634
wR_1 for 4365 $F_o > 4\sigma(F_o)$	0.1368
R_2 for all 9827 data	0.1711

wR ₂ for all 9827 data	0.2019
Weight: $1 / [\sigma^2(F_o^2) + (0.0903 * P)^2 + 0.00 * P]$ where $P = (\text{Max}(F_o^2, 0) + 2 * F_c^2) / 3$	
No. of variables	598
Number of restraints	0
Max shift/esd	0.003
Max and min electron density in final Fourier difference map	0.803, -1.004 e [·] Å ⁻³

Table S2. Selected geometric data for [Rh₂[(C₆H₄)P(C₆H₅)₂]₂(O₂CCH₃)₂](CO) (**3-CO**) at 293 K.

Selected bond distances (Å)			
Rh1 - Rh2	2.5333(9)		
Rh1 - P1	2.2574(23)	Rh2 - P2	2.2132(21)
Rh1 - O1	2.1662(55)	Rh2 - O2	2.1878(54)
Rh1 - O3	2.2002(53)	Rh2 - O4	2.1475(52)
Rh1 - C12	2.0326(79)	Rh2 - C2	1.9942(82)
Rh1 - C20	1.9698(122)	Rh2 - Cl3	2.9023(31)
C20 - O5	1.1042(152)		
P1 - C1	1.8110(105)	P2 - C11	1.8031(98)
P1 - C21	1.8377(80)	P2 - C31	1.8384(81)
P1 - C41	1.8323(94)	P2 - C51	1.8306(99)
O1 - C7	1.2466(112)	O2 - C7	1.2661(129)
O3 - C9	1.2543(132)	O4 - C9	1.2499(126)
Selected bond angles (°)			
Rh2 - Rh1 - P1	86.72(6)	Rh1 - Rh2 - P2	88.23(7)
Rh2 - Rh1 - O1	85.36(16)	Rh1 - Rh2 - O2	84.24(15)
Rh2 - Rh1 - O3	81.96(15)	Rh1 - Rh2 - O4	88.22(17)
Rh2 - Rh1 - C12	96.83(24)	Rh1 - Rh2 - C2	97.10(24)
Rh2 - Rh1 - C20	170.71(33)	Rh1 - Rh2 - Cl3	161.48(6)

P1 - Rh1 - O1	171.81(17)	P2 - Rh2 - O2	94.92(15)
P1 - Rh1 - O3	94.77(16)	P2 - Rh2 - O4	174.92(17)
P1 - Rh1 - C12	90.48(25)	P2 - Rh2 - C2	90.11(24)
P1 - Rh1 - C20	98.30(30)	P2 - Rh2 - C13	107.09(8)
C12 - Rh1 - C20	90.96(38)	C2 - Rh2 - C13	93.29(24)
C12 - Rh1 - O1	92.52(28)	C 2 - Rh2 - O 2	174.84(27)
C12 - Rh1 - O3	174.53(27)	C 4 - Rh2 - O 2	93.92(28)
O1 - Rh1 - O3	82.07(21)	O2 - Rh2 - O4	81.12(21)
O1 - Rh1 - C20	89.27(33)	O2 - Rh2 - C13	84.14(15)
O3 - Rh1 - C20	89.81(32)	O4 - Rh2 - C13	75.78(17)
Rh1 - C20 - O5	176.63(1.0)	Rh2 - C13 - C60	101.98(33)
Rh1 - P1 - C1	111.84(30)	Rh2 - P2 - C11	112.09(29)
Rh1 - P1 - C21	108.81(30)	Rh2 - P2 - C31	110.51(30)
Rh1 - P1 - C41	117.90(30)	Rh2 - P2 - C51	119.76(31)
Rh1 - C12 - C11	120.15(61)	Rh2 - C2 - C1	123.40(61)
P1 - C1 - C2	116.71(67)	P2 - C11 - C12	119.01(66)
Rh1 - O1 - C7	116.59(53)	Rh2 - O2 - C7	118.08(52)
Rh1 - O3 - C9	119.98(53)	Rh2 - O4 - C9	114.05(56)
O1 - C7 - O2	127.53(84)	O3 - C9 - O4	128.67(91)

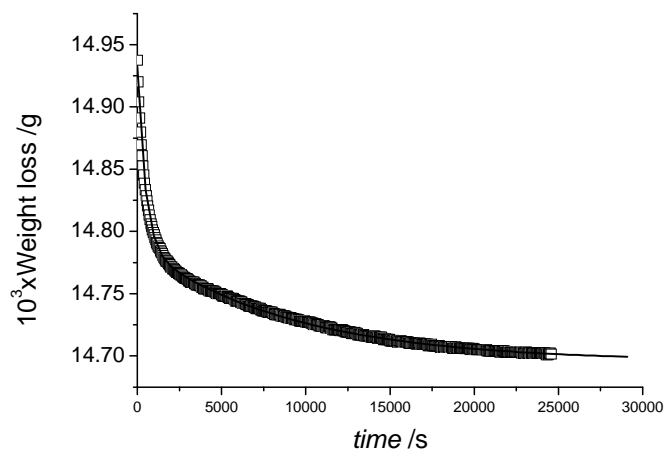


Figure S1. Weight loss of a sample of $5 \cdot (\text{CO})_2$ with time at 50°C .

***3.3. An optoelectronic sensing device for CO
detection in air based on a binuclear
rhodium complex***

***An optoelectronic sensing device for CO
detection in air based on a binuclear rhodium
complex***

*María E. Moragues,^[a,b] Roberto Montes-Robles,^[a] José
Vicente Ros-Lis,^[a] Miguel Alcañíz,^[a] Javier Ibañez,^[a] Teresa
Pardo,^[a,b] Ramón Martínez-Máñez,^{*[a,b]}*

^a *Centro de Reconocimiento Molecular y Desarrollo Tecnológico (IDM), Unidad
Mixta Universitat Politècnica de València – Universitat de València. Camino de
Vera s/n. 46022, Valencia, Spain.*

^b *CIBER de Bioingeniería, Biomateriales y Nanomedicina (CIBER-BBN), Spain.*

Received: April 5, 2013

Available online: October 10, 2013

*(Reprinted from
Sensors and Actuators B, 2014, 191, 257-263.
Copyright © 2014, with permission from Elsevier)*

Abstract

The design, fabrication and validation of an optoelectronic sensor implemented in an easy-to-use portable device for the selective and sensitive detection of CO in air is reported herein. The system is based on the colour changes observed in the binuclear rhodium complex of formula $[\text{Rh}_2[(\text{C}_6\text{H}_4)\text{P}(\text{C}_6\text{H}_5)_2]_2(\text{O}_2\text{CCF}_3)_2](\text{CF}_3\text{CO}_2\text{H})_2$ (**1**) upon coordinating CO molecules in axial positions. Complex **1** is used supported on cellulose chromatography paper. In this support, colour changes to the naked eye are observed for CO concentrations above 50 ppm. The probe is also implemented in a simple portable optoelectronic device. The cellulose support containing probe **1** in this device is placed inside a small dark chamber, is illuminated with a tricolour LED emitting at 624, 525 and 470 nm, respectively corresponding to red (R), green (G) and blue (B) light, and reflected light is detected by a photodiode. With a transimpedance amplifier, the current generated by the photodiode is transformed into a voltage compatible with the 10-bit analogue-to-digital converter (ADC) port. Colour changes are measured as the distance d between the R, G and B data of the blank (probe without CO) and that for a certain CO concentration. Typical calibration curves are fitted using a bi-exponential equation. This system offers a typical response time of a few minutes (ca. 7 min) and a limit of detection of 11 ppm. The probe in the cellulose supports is also highly reversible. The optoelectronic device is portable (dimensions 14 × 8.5 × 3.5 cm; weighs approximately 270 g) and is powered by AA batteries. In addition, no variations in experimental parameter d upon exposure to CO₂, N₂, O₂, Ar, water-saturated air and vapours of chloroform, hexane, ethanol, acetone, methane, toluene or formaldehyde are observed. Besides, colour changes are found for acetonitrile vapour, NO and NO₂, but only at high concentrations. For validation purposes, the device was used to determine the CO present in the 4-shed accumulated smoke of two cigarette types after passing smokers' lungs.

Keywords: Carbon monoxide · Optical device · Gas sensor · Chromogenic · Rhodium

Introduction

Carbon monoxide is a potentially deadly common substance which has no colour, odour or taste. This hazardous gas is invisible, toxic and notoriously difficult to detect, and is colloquially known as the silent killer.¹ The effects of CO exposure can vary greatly from person to person depending on age, overall health, and the concentration and length of exposure.² At low levels, CO causes mild flu-like symptoms, including headaches, dizziness, disorientation, nausea and fatigue. Moreover, high levels of CO or constant exposure can cause angina, impaired vision, reduced brain function, and eventually death. Although there is an increasing awareness of the effects and dangers of carbon monoxide poisoning, still thousands of people die worldwide each year and many people remain blissfully unaware that they are constantly exposed to a source of this deadly gas.

In general, carbon monoxide exposure is produced as a result of the incomplete burning of natural gas or carbon-based fuels (i.e., propane, gasoline, kerosene, wood, coal, charcoal, etc.) in combination with improperly vented heaters and furnaces. In fact, in some of those places with systems that function improperly, the amount of carbon monoxide can reach dangerous levels. Moreover, small concentrations of carbon monoxide can be found, among others, in auto exhausts, tobacco smoke, kitchens, chimneys, fireplaces or central heating systems. Apart from these general sources, carbon monoxide poisoning is also an occupational hazard.³ In particular, welders, mechanics, engine operators, forklift operators, fire fighters, marine workers, toll-booth attendants, customs inspectors, police officers, taxi drivers, and carbon-black makers are at constant risk of carbon monoxide poisoning. It is therefore vital to periodically check that all appliances and ventilation systems in both the home and workplace function properly, and it is also important to be able to detect carbon monoxide leaks.

Traditionally, electrochemical cells, solid-state sensors and thermocouples have been used to measure CO with varying degrees of success. Some portable CO sensors are commercially available which can detect low CO concentrations in air at low temperature. They are mainly electrochemical sensors based on technologies of metal oxide semiconductors. These instruments consist of a set of

three electrodes (working, auxiliary and reference electrodes) covered by a gas permeable membrane. Carbon monoxide is quantified through the semi-reactions that take place in the anode and cathode of an electrochemical cell, where the oxidation of CO to CO₂ and the reduction of O₂ to H₂O occur.⁴ With these electrochemical devices, good resolutions and measuring ranges (i.e., 0–2000 ± 5–10 ppm) are obtained. However, these technologies need periodical validations, are very sensitive to temperature (working temperatures between 5 and +45 °C with signal drifts induced by variations of only ±0.1 °C) and pressure (with signal drifts due to pressure variations lower than 10⁻⁵ bar). Furthermore, these systems do not withstand pressures above 1 atmosphere and cannot be used under vacuum conditions. Improved electrochemical CO sensors use a very low concentration of alkaline electrolyte, integrate an extremely small amount of noble metal catalyst into the catalyst layer and use a dry battery structure, thus avoiding the risk of electrolyte leakage.⁵ Despite improvements, these portable devices for CO detection are likely to generate false alarms in the presence of other chemicals or interfering gases.⁶⁻⁸

Among solid-state CO gas sensors, ZnO and SnO₂^{9,10} are two of the most studied materials given their chemical stability and high electron mobility. However, SnO₂ is often operated at high temperatures, typically above 400 °C, to achieve a catalytic oxidation of the gas. Some authors have reported that ZnO¹¹ and SnO₂,¹²⁻¹⁴ doped with Pt or Au nanoparticles, nanorods or nanowires, display catalytic CO spillover oxidation, thus improving gas detection in semiconductors and requiring low practical temperatures. In recent years, other materials have been developed to improve CO sensing; such as, nanostructured BiOCl ribbons doped with Au nanoparticles¹⁵ or nanostructured WO₃ films doped with Fe.¹⁶ With BiOCl/Au nanoparticles, the quantitative detection of CO has been demonstrated in the 100 to 400 ppm range to work at temperatures of ca. 200–300 °C, while WO₃/Fe films have responded to CO from 10 to 1000 ppm at a minimum temperature of 150 °C. These working temperature ranges and the consequent high energy consumption required for these solid-state sensors restrict their use to certain applications.

One alternative to these electrochemical systems is the design of optical CO sensors. Reported CO sensors are mainly based on two technologies: the use of spectrally narrowband lasers¹⁷ (primarily diode electrodes) and the use of non-dispersive infrared (broadband) systems. The non-dispersive infrared method (NDIR) is among the most reliable and accurate methods to measure carbon monoxide concentrations in urban air.¹⁸ NDIR systems are commercially available with limits of detection of approximately 0.02 ppm. These optical CO measuring techniques are sensitive, but relatively low concentrations of other common gases, such as CO₂, NO_x, hydrocarbons or water vapour, may interfere.¹⁹

An alternative to these systems is the use of molecular-based probes for the design of opto-chemical devices for CO sensing, including fluorescent probes in living cells based in palladium²⁰ and iron compounds.²¹ However, most existing CO-sensing probes based on the use of chromogenic probes, such as oxoacetatobridged triruthenium cluster complexes,²² rhodium complexes,²³ polypyrrole functionalized with iron porphyrin derivatives,²⁴ hybrid materials incorporating a cobalt(III) corrole complex,²⁵ and iron compounds of diisopropylphosphino-diaminopyridine,²⁶ either behave as CO probes only in solution or offer very limited colour changes, which hinder their application. In this field, we have recently reported a family of binuclear rhodium(II) compounds of the general formula $[\text{Rh}_2[(\text{XC}_6\text{H}_3)\text{P}(\text{XC}_6\text{H}_4)]_n(\text{O}_2\text{CR})_{4-n}] \cdot \text{L}_2$ containing one or two metallated phosphines (in a head-to-tail arrangement) and different axial ligands as CO-sensing probes. Chloroform solutions of these complexes undergo rapid colour change, from purple to yellow, when air samples containing CO are bubbled through them. Moreover, the binuclear rhodium complexes were also adsorbed on silica and used as colorimetric probes for “naked eye” CO detection in the gas phase.^{27,28}

Based on these previous findings, we report herein the development and validation of an easy-to-use, robust and portable optoelectronic CO device capable of displaying a selective and sensitive optical response to carbon monoxide in air, which is based on the use of a binuclear rhodium(II) derivative.

Experimental

Chemicals and materials. The commercially available reagents $[\text{Rh}_2(\text{O}_2\text{CCH}_3)_4]$, $\text{P}(\text{C}_6\text{H}_5)_3$ and $\text{CF}_3\text{CO}_2\text{H}$ carboxylic acid were used as purchased. All the solvents were of analytical grade. Compounds $[\text{Rh}_2[(\text{C}_6\text{H}_4)\text{P}(\text{C}_6\text{H}_5)_2]_2(\text{O}_2\text{CCF}_3)_2] \cdot (\text{CF}_3\text{CO}_2\text{H})_2$ (**1**), $[\text{Rh}_2[(\text{C}_6\text{H}_3\text{CH}_3)\text{P}(\text{C}_6\text{H}_4\text{CH}_3)_2]_2(\text{O}_2\text{CCH}_3)_2] \cdot (\text{CH}_3\text{CO}_2\text{H})_2$ (**2**), $[\text{Rh}_2[(\text{C}_6\text{H}_4)\text{P}(\text{C}_6\text{H}_5)_2]_2(\text{O}_2\text{CCH}_3)_2] \cdot (\text{CH}_3\text{CO}_2\text{H})_2$ (**3**), $[\text{Rh}_2[(\text{C}_6\text{H}_4)\text{P}(\text{C}_6\text{H}_5)_2]_2(\text{O}_2\text{CC}(\text{CH}_3)_3)_2] \cdot (\text{C}(\text{CH}_3)_3\text{CO}_2\text{H})_2$ (**4**) and $[\text{Rh}_2[(\text{C}_6\text{H}_4)\text{P}(\text{C}_6\text{H}_5)_2]_2(\text{O}_2\text{CCH}_3)_3] \cdot (\text{CH}_3\text{CO}_2\text{H})_2$ (**5**) were synthesised according to known procedures.²⁸ Cellulose paper (Whatman Grade no. 3MM Chromatography Paper) was purchased from VWR. Carbon monoxide was provided by the Abelló Linde Company. Dry air was obtained from a compressor (ATLAS COPCO, SF 4FF). The rest of the gases used in this work were generated in situ: carbon dioxide by adding chloride acid to sodium carbonate; nitrogen monoxide and nitrogen dioxide by oxidation of copper with nitric acid and sulphur dioxide by copper oxidation with sulphuric acid.

Preparation of the probe. The probe was supported on cellulose paper for chromatographic use (Whatman Grade no. 3MM Chromatography Paper). Probes were prepared easily by dropping 0.2 mL of a solution of the corresponding binuclear rhodium(II) complex in dichloromethane (40 mg/mL) on a piece of paper of 1 cm^2 and further drying at air under ambient conditions.

Characterisation of the probe response. Gas mixtures were prepared at $25 \text{ }^\circ\text{C}$ by a computer-driven gas mixing system composed of two mass flow controllers (model F-201CV, Bronkhorst High-Tech). In addition, CO concentrations were validated with a Testo analyzer (315_2 model 0632 0317), which was previously calibrated and certified by the Spanish Certification Agency (ENAC). The colorimetric response of the strips was studied by UV-vis spectra in a Jasco V-650 spectrophotometer equipped with a diffuse reflectance sphere (model ISV-722, Sphere). Measurements were taken at room temperature over a wavelength range of 350–700 nm with a wavelength step of 1 nm.

Electronic system. Fig. 1 shows the block diagram of the optical sensing device for CO detection. The system is controlled by a microcontroller (μC) Microchip PIC18F2550. It handles all the device's functions, such as: sensor reading, communication with the computer, data storage control in the memory and real-time date and time monitoring. Data can be downloaded to a PC through the serial port using the UART protocol. A USB2.0 port can also be used, including an UART to USB2.0 converter. The LCD display is directly connected to the microcontroller, while the temperature sensor (MCP9803 of Microchip), real-time clock (RTC DS1307 of Maxim) and the EEP-ROM are included in the microcontroller through an I2C module.

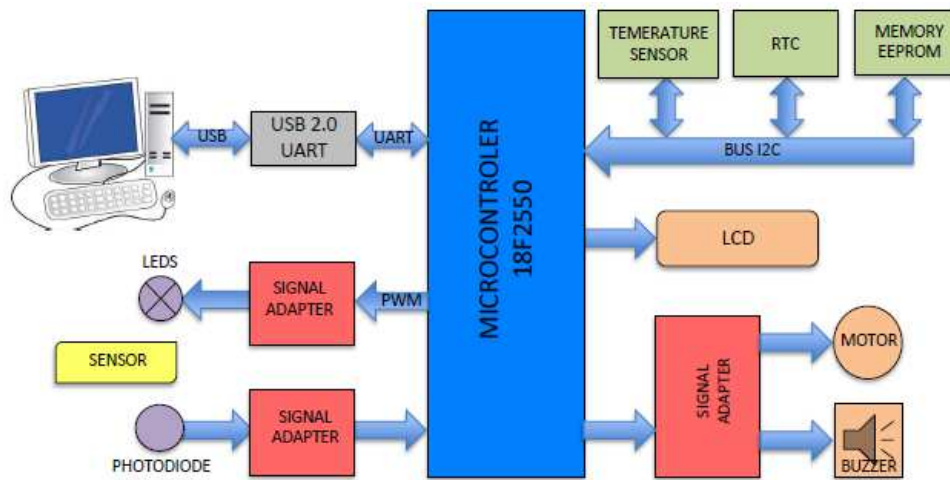


Figure 1. Block diagram of the CO optoelectronic equipment.

The equipment allows two inward airflow options: naturally or forced by a pump. All the experiments reported herein were carried out without using the intern pump. Hence the uptake of gas mixtures was not directly forced to pass through the probe. The equipment is also equipped with a buzzer to set alarms, if required. The device is portable (dimensions $14 \times 8.5 \times 3.5$ cm and weighs approximately 270 g) and power is provided by two AA batteries that offers a battery duration of up to 72 h under continuous monitoring conditions (with the

pump switched on). Battery duration can be prolonged substantially by reducing the measuring frequency and by switching off the air pump. Sampling times are configurable with ranks ranging from a few seconds to 30 min. Apart from sporadic measurements, the system is equipped with a clock, and an internal memory that stores colour measurements and times. Finally, the device is completed with an alphanumeric LCD display for the configurations and readings of the CO concentrations and there are two front buttons to set the configuration options (i.e., alarm on/off, motor on/off, sampling time, intensity of each light emission in the triple-LED sensor, internal memory usage or removal).

Optical system. The optical detection of CO is achieved using a CO sensitive layer (a cellulose strip), a tricolour LED as the light source and a photodiode as the detector. The emissive part of the optical system is composed of a tricolour LED (PLCC6 Full-Colour SMD LED FCL-P5RR from Forge Europa)²⁹ which emits at 624, 525 and 470 nm, corresponding to red (R), green (G) and blue (B) light, respectively. A photodiode (BPX65 from Osram) was used for the detection of colour changes. Through illumination, the probe reflects the LED light that energises the photodiode. This signal is adapted and captured by the analogue-to-digital converter (ADC) port available on the microcontroller. The intensities collected by the red, green and blue LED are stored in RAM memory as R, G and B values, respectively, which are subsequently processed for noise removal.³⁰ The resulting RGB data, along with the temperature, date and time of the experiment, are stored in the EEPROM. By taking the values obtained in the absence of CO (R_0 , G_0 and B_0) as a reference, the Euclidean distance d for a certain sample i (R_i , G_i and B_i) is calculated by Eq. (1). This Euclidean distance is related to the concentration level of CO present in air.

$$d = \sqrt{(R_0 - R_t)^2 + (G_0 - G_t)^2 + (B_0 - B_t)^2} \quad (1)$$

Colorimetric performance and the stability of the equipment overtime were evaluated using a collection of strips of diverse colours, which were measured several times. In all cases, reproducible RGB values were obtained.

Results and discussion

Optoelectronic sensor. As mentioned above, we have recently reported that some cyclometallated binuclear rhodium complexes are capable of reacting reversibly with CO in air to result in colour changes that are visible to the naked eye.²⁸ Specifically for this work, five rhodium complexes of the formulas $[\text{Rh}_2[(\text{C}_6\text{H}_4)\text{P}(\text{C}_6\text{H}_5)_2]_2(\text{O}_2\text{CCF}_3)_2] \cdot (\text{CF}_3\text{CO}_2\text{H})_2$ (**1**), $[\text{Rh}_2[(\text{C}_6\text{H}_3\text{CH}_3)\text{P}(\text{C}_6\text{H}_4\text{CH}_3)_2]_2(\text{O}_2\text{CCH}_3)_2] \cdot (\text{CH}_3\text{CO}_2\text{H})_2$ (**2**), $[\text{Rh}_2[(\text{C}_6\text{H}_4)\text{P}(\text{C}_6\text{H}_5)_2]_2(\text{O}_2\text{CCH}_3)_2] \cdot (\text{CH}_3\text{CO}_2\text{H})_2$ (**3**), $[\text{Rh}_2[(\text{C}_6\text{H}_4)\text{P}(\text{C}_6\text{H}_5)_2]_2(\text{O}_2\text{CC}(\text{CH}_3)_3)_2] \cdot (\text{C}(\text{CH}_3)_3\text{CO}_2\text{H})_2$ (**4**) and $[\text{Rh}_2[(\text{C}_6\text{H}_4)\text{P}(\text{C}_6\text{H}_5)_2]_2(\text{O}_2\text{CCH}_3)_3] \cdot (\text{CH}_3\text{CO}_2\text{H})_2$ (**5**) were synthesised according to known procedures.²⁸ These complexes have been reported to offer significant colour changes supported on silica, from purple to orange-salmon and yellow, in seconds when exposed to air containing carbon monoxide given the consecutive axial coordination of two CO molecules and the formation of the corresponding derivatives $\mathbf{n} \cdot \text{CO}$ and $\mathbf{n} \cdot (\text{CO})_2$, respectively. Fig. 2 shows a representation of the CO reaction with binuclear rhodium(II) complex **1**.

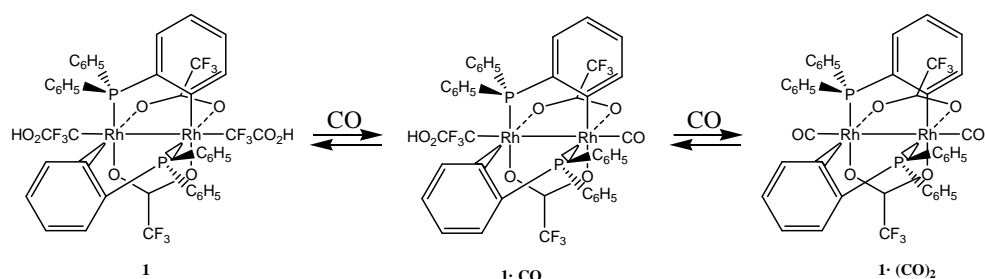


Figure 2. Complex of the general formula $[\text{Rh}_2[(\text{C}_6\text{H}_4)\text{P}(\text{C}_6\text{H}_5)_2]_2(\text{O}_2\text{CCF}_3)_2] \cdot (\text{CF}_3\text{CO}_2\text{H})_2$ (**1**) and the corresponding $\mathbf{1} \cdot \text{CO}$ and $\mathbf{1} \cdot (\text{CO})_2$ products obtained upon the coordination of carbon monoxide at axial positions.

Despite the good colorimetric response recently observed by us for the **1–5** complexes on silica in the presence of CO,²⁸ we found that this support was not easy to handle and it was difficult to integrate it into the optoelectronic device. Therefore in a first step, different supports were tested to incorporate binuclear rhodium(III) probes. Attempts were made with a number of organic (e.g., polymers) and inorganic supports. However most of them proved unsuitable

because, in most cases, the probes displayed a considerable loss of sensing properties or loss of reversibility. The rhodium complexes retained clear and reversible naked-eye colour changes in only two supports: in silica gel plates for thin layer chromatography; in a cellulose paper for chromatographic use. Silica gel plates proved fragile and were also ruled out as supports. Conversely, chromatographic paper was flexible and it was easy to prepare reproducible homogeneous sensing systems by dropping 0.2 mL of a solution of the corresponding binuclear rhodium(II) complex in dichloromethane (40 mg/mL) on a piece of paper (1 cm²) with further drying. As described in Section 2, the chromatographic paper containing the rhodium probe was placed inside a small dark chamber, illuminated with a tricolour LED emitting at 624, 525 and 470 nm and reflected light was detected by a photodiode. Colour changes were then measured as the distance d between the RGB data of the blank (probe without CO) and that of the probe at a certain CO concentration (see Eq. (1)).

Optical response of the probe and calibration of the optoelectronic device. By way of example of the response observed for the binuclear rhodium(II) complexes in the presence of CO, Fig. 3 shows the evolution of the UV–vis diffuse reflectance of the cellulose paper containing probe **1** in the presence of air containing 50 and 500 ppm of CO. Apart from probe **1**, the remaining binuclear rhodium(II) complexes **2–5** were also tested in the cellulose support. However the latter displayed a less sensitive colour change and poorer reversibility. Therefore, the remaining studies were carried out only with the films containing probe **1**.

It is worth mentioning that although the limit of detection of CO, when using complex **1**, increases in the cellulose strip as compared to silica, the cellulose support proved suitable to detect carbon monoxide in a wide range of concentrations (vide infra). For instance, Fig. 4 shows the colour changes observed on the cellulose substrates of **1** for different CO concentrations in air. Clear changes can be seen by the naked eye at concentrations as low as 50 ppm. Moreover, Fig. 4 suggests that these cellulose strips can be implemented as a suitable colour scale for CO sensing to the naked eye. In relation to the colour changes observed in the figure, it is interesting to note that the CO concentrations

of ca. 50 ppm are the concentration at which CO becomes toxic for healthy adults who are submitted to continuous exposure. Moreover, CO concentrations of ca. 300–400 ppm are the limit at which carbon monoxide starts to become highly toxic for adults over short exposure periods.³¹

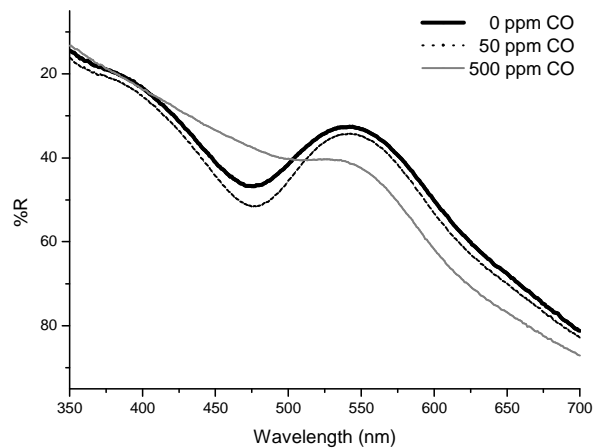


Figure 3. Diffuse reflectance UV-vis spectra of the cellulose paper probe containing **1** (solid black line) and the changes observed in the presence of air containing 50 and 500 ppm of CO (dashed line and grey line, respectively).

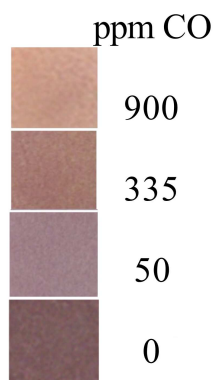


Figure 4. Colour scale for the semi-quantification of CO (from 0 to 900 ppm) using complex **1** on cellulose strips.

Fig. 5 shows a typical calibration curve of the colour differences (d values, see Eq. (1)) measured using the optoelectronic above-described equipment when employing probe **1** on a cellulose support upon the addition of increasing concentrations of CO in air (0–7000 ppm). An almost linear dependence on the CO concentration of between 2 and 80 ppm was observed. However, d loses linearity when the concentration is increased and approaches saturation when the carbon monoxide concentration is of ca. 7000 ppm. An important issue relating to implementing the calibration curve in the optoelectronic sensing device is fitting the obtained d values in accordance with the CO concentration. In the first attempt made, the response was empirically fitted to a single exponential to obtain Eq. (2) with a regression coefficient of 0.9759. Regardless of this relatively good regression coefficient, it was not possible to properly fit the resulting equation to the experimental data (see Fig. 5a), especially at low CO concentrations.

$$y = 62.92 - 58.00 \cdot e^{-0.001x} \quad (2)$$

In the equation, y is the value of d and x is the CO concentration in ppm. At this point it should be noted that, as expressed in Fig. 1, the CO coordination to the binuclear rhodium compound, and therefore the colour change, is a two-step process given the presence of two consecutive CO molecules which coordinate at the axial positions of the probe. Thus by bearing this concept in mind, the optical response in Fig. 5 was fitted to a bi-exponential equation (see Eq. (3)).

$$y = 62.65 - 50.07 \cdot e^{-0.0006x} - 13.24 \cdot e^{-0.0184x} \quad (3)$$

A regression coefficient of 0.9983 was calculated for the bi-exponential model in agreement with the excellent fit to the experimental values within the whole concentration range (see Fig. 5b). Having programmed the bi-exponential equation, the optochemical device herein reported was able to determine CO concentrations from 0 to 7000 ppm with an error of ± 4 ppm. Some additional information can be obtained from the fit parameters of the bi-exponential equation. By bearing in mind the characteristic $a \cdot e^{-bx}$ structure for the exponential equations, values of 50.07 and 13.24 were obtained for the “a” terms of the

equation. These values correlated directly with the contribution of each term to the global change. Conversely, “b” reflects the strength of the CO-ligand interaction, that is: the higher the value, the greater the strength and the lower the concentration needed to induce spectroscopic changes. Thus the exponential equation with the highest “b” value (0.0184) responds to low CO concentrations and is responsible for most colour variation (d) up to 500 ppm. We believe that this can be tentatively assigned to the coordination of the first CO molecule to probe **1** in agreement with the CO response range.

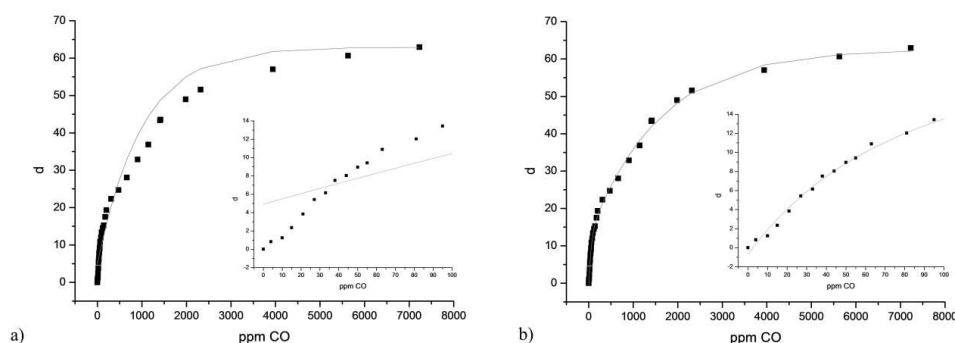


Figure 5. (a) Simple exponential regression and (b) double exponential regression of the d values of cellulose strips of **1** upon the addition of CO (0–8000 ppm). The inset shows a magnification in the 0–100 ppm range. Square dots are experimental data, whereas the line depicts exponential fitting.

Selectivity and reversibility studies. From the calibration curve, a limit of detection (LOD) as low as 11 ppm of CO in air was obtained using the experimental data (d) registered by the optoelectronic device with the cellulose strip containing probe **1**. In comparison with the LOD of 0.8 ppm CO for complex **1** when adsorbed on silica gel, the LOD was clearly affected when the probe was on the cellulose strip. Nevertheless, this did not hamper device performance since it was still lower than 50 ppm, which is the concentration at which CO becomes toxic for healthy adults who are continuously exposed beyond an 8-h period. Moreover, typical response times of ca. 7 min were determined.

The cellulose strips of **1** exhibited very high selectivity towards CO. No variations in experimental parameter d upon exposure to CO₂, N₂, O₂, Ar or water-

saturated air were observed. Thus, it can be stated that the CO response of the strips are not affected by relative humidity. Furthermore, no colour change was registered by the optoelectronic device in the presence of vapours of volatile organic compounds (VOCs), such as chloroform, hexane, ethanol, acetone, methane, toluene or formaldehyde. Reversible colour changes to yellow were observed in the presence of acetonitrile vapour, but only at concentrations of 4900 ppm. Studies with coordinating species, such as SO₂, NO, and NO₂, were also carried out. In these cases, no reaction between SO₂ and the strips of probe **1** was observed. The presence of nitrogen oxides NO and NO₂ induced a reversible orange-brown colour modulation of the binuclear rhodium(II) complex, which slightly differed from that observed in the presence of CO, but only when very high concentrations of NO or NO₂ were being used (8900 ppm and 3162 ppm, respectively). All these results are consistent with the behavior observed for the binuclear rhodium(II) complexes adsorbed on silica.²⁸ However, the interfering concentrations of acetonitrile, NO and NO₂ were even higher for probe **1** on cellulose strips since in silica, interfering concentrations for acetonitrile, NO and NO₂ were 4600, 4070 and 2700 ppm, respectively.

Reversibility was also extensively evaluated for the cellulose strips containing complex **1**. The optoelectronic device was exposed to air containing 30 ppm of CO at room temperature for 7 min and then parameter *d* was determined. After measurements were taken, the device was placed in CO-free air for 7 min and the *d* value was determined again. This process was repeated several times and the results are shown in Fig. 6. A basically reversible sensing process was clearly observed.

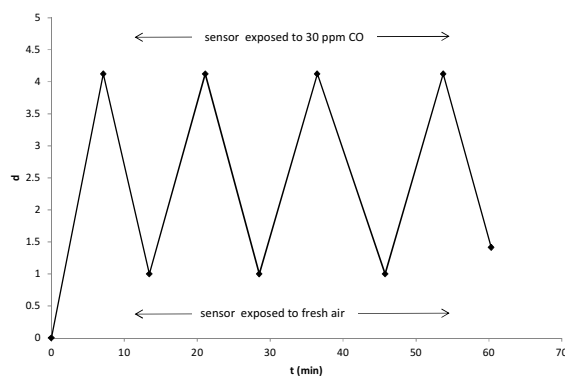


Figure 6. Colorimetric response of the cellulose strips of **1** upon four cyclic exposures to 30 ppm of CO and CO-free air.

Tests in real environments and samples. The response effectiveness of the optoelectronic device was tested in a chemistry laboratory environment, which was assumedly CO-free; working at 25.0 °C. As expected, the device registered concentrations of CO of ca. 0 ppm for days, thus the typical solvent vapours in a laboratory did not affect the optoelectronic device response. Finally the device was used to determine the CO present in the 4-shed accumulated smoke of two cigarette types after passing smokers' lungs. In accordance with the values reported in previous studies, 9 and 25 ppm of CO were measured for normal and fine-cut tobacco cigarettes, respectively.³²

Conclusions

An optoelectronic device for CO monitoring in air has been developed. It is based on the reversible reaction of CO with binuclear rhodium(II) complex $[\text{Rh}_2\{[(\text{C}_6\text{H}_4)\text{P}(\text{C}_6\text{H}_5)_2]_2(\text{O}_2\text{CCF}_3)_2\} \cdot (\text{CF}_3\text{CO}_2\text{H})_2$ (**1**) which is coupled with colour changes. Probe **1** is incorporated into a cellulose paper for chromatography and this simple system has proven to be suitable for the naked eye detection of CO in air at concentrations as low as 50 ppm. Moreover the cellulose strips containing probe **1** were used as the sensing part of an optoelectronic device for CO monitoring. The device illuminated the probe with a tricolour LED, which emits at 624, 525 and 470 nm, and the reflected light was detected by a photodiode. The

electronic system is portable (dimensions 14 × 8.5 × 3.5 cm, weighing approximately 270 g) and is powered by AA batteries, which offer good battery duration. Colour variations in this device were measured as the distance *d* between the RGB values of the blank (probe without CO) and that of the probe with a certain CO concentration. A typical response time of 7 min and a limit of detection of 11 ppm were obtained using the optoelectronic device. Moreover, the system proved highly selective to the presence of CO and no changes were found in the presence of other common gases (CO₂, N₂, O₂, Ar) and saturated vapour of common solvents (chloroform, hexane, ethanol, acetone, methane, toluene or formaldehyde). Only acetonitrile vapour, NO and NO₂ were found to be interferents, but only at very high concentrations.

Acknowledgements

We thank the Spanish Government (Project MAT2012-38429-C04-01), Generalitat Valenciana (Projects PROMETEO2009/016 and ISIC/2012/005) and the UPV (Project INNOVA-04-10) for support. M.E.M thanks the Spanish Ministry of Education for a Doctoral FPU Fellowship.

References

1. L.J. Wilkinson, R.H. Waring, G.B. Steventon, S.C. Mitchell, *Molecules of Death. Carbon Monoxide: The Silent Killer*, 2nd ed., Imperial College Press, London, **2007**.
2. K. Rajiah, E.M. Mathew, *Clinical manifestation, effects, diagnosis, monitoring of carbon monoxide poisoning and toxicity*, *Afr. J. Pharm. Pharmacol.* **5** (2011) 259–264.
3. J-C. Normand, C. Durand, B. Delafosse, *Acute carbon monoxide poisoning: a persistent occupational risk*, *Archives des Maladies Professionnelles et de l'Environnement* **72** (2011) 240–245.
4. <http://www.testo.com>
5. <http://www.figarosensor.com>
6. D. Gutmacher, C. Foelmli, W. Vollenweider, U. Hofer, J. Wöllenstein, *Comparison of gas sensor technologies for fire gas detection*, *Procedia Eng.* **25** (2011) 1121–1124.
7. <http://www.intlsensor.com>

8. C. Kaminski, A. Poll, *Electrochemical or Solid State H₂S Sensors: Which is Right For You?*, InTech, ISA, **1985**, pp. 55.
9. G. Korotcenkov, V. Brynzari, S. Dmitriev, *SnO₂ films for thin film gas sensor design*, Mater. Sci. Eng. B **63** (**1999**) 195–204.
10. N. Yamazoe, Y. Kurokawa, T. Seiyama, *Effects of additives on semiconductor gas sensors*, Sens. Actuators **4** (**1983**) 283–289.
11. P. Rai, Y.-S. Kim, H.-M. Song, M.-K. Song, Y.-T. Yu, *The role of gold catalyst on the sensing behavior of ZnO nanorods for CO and NO₂ gases*, Sens. Actuators B **165** (**2012**) 133–142.
12. N. Yamazoe, *New approaches for improving semiconductor gas sensors*, Sens. Actuators B **5** (**1991**) 7–19.
13. N. Barsan, M. Schweizer-Berberich, W. Göpel, *Fundamental and practical aspects in the design of nanoscaled SnO₂ gas sensors: a status report*, Fresenius J. Anal. Chem. **365** (**1999**) 287–304.
14. T. Yanagimoto, Y.-T. Yu, K. Kaneko, *Microstructure and CO gas sensing property of Au/SnO₂ core-shell structure nanoparticles synthesized by precipitation method and microwave-assisted hydrothermal synthesis method*, Sens. Actuators B **166** (**2012**) 31–35.
15. C.R. Michel, N.L. López, A.H. Martínez-Preciado, *CO₂ and CO gas sensing properties of nanostructures BiOCl ribbons doped with gold nanoparticles*, Sens. Actuators B **173** (**2012**) 100–105.
16. M. Ahsan, T. Tesfamichael, M. Ionescu, J. Bell, N. Motta, *Low temperature CO sensitive nanostructures WO₃ thin films doped with Fe*, Sens. Actuators B **162** (**2012**) 14–21.
17. J. Wolfrum, *Lasers in combustion: from basic theory to practical devices*, Proc. Combust. Inst. **27** (1) (**1998**) 1–41.
18. K-H. Cho, S-W. Lee, J-H. Lee, K-S. Choi, *Development and properties of carbon monoxide detector for ambient air monitoring*, Anal. Sci. Technol. **13** (**2000**) 222–228.
19. <http://www.draeger.com>
20. B.W. Michel, A.R. Lippert, C.J. Chang, *A reaction-based fluorescent probe for selective imaging of carbon monoxide in living cells using a palladium-mediated carbonylation*, J. Am. Chem. Soc. **134** (**2012**) 15668–15671.
21. J. Wang, J. Karpus, B.S. Zhao, Z. Luo, P.R. Chen, C. He, *A selective fluorescent probe for carbon monoxide imaging in living cells*, Angew. Chem. Int. Ed. **51** (**2012**) 9652–9656.
22. M. Itou, Y. Araki, O. Ito, H. Kido, *Carbon monoxide ligand-exchange reaction of triruthenium cluster complexes induced by photosensitized electron transfer: a new type of photoactive CO color sensor*, Inorg. Chem. **45** (**2006**) 6114–6116.
23. A. Gulino, T. Gupta, M. Altman, S. Lo Schiavo, P.G. Mineo, I.L. Fragal, G. Evmenenko, P. Dutta, M.E. Van der Boom, *Selective monitoring of parts per million levels of CO by covalently immobilized metal complexes on glass*, Chem. Commun. **25** (**2008**) 2900–2902.
24. S. Paul, F. Amalraj, S. Radhakrishnan, *CO sensor based on polypyrrole functionalized with iron porphyrin*, Synth. Metals **159** (**2009**) 1019–1023.
25. J.M. Barbe, G. Canard, S. Brandès, R. Guillard, *Selective chemisorptions of carbon monoxide by organic-inorganic hybrid materials incorporating cobalt(III) corroles as sensing components*, Chem. Eur. J. **13** (**2007**) 2118–2129.
26. D. Benito-Garagorri, Puchberger M., Mereiter K., Kirchner K., *Stereospecific and reversible CO binding at iron pincer complexes*, Angew. Chem. **120** (**2008**) 9282–9285;

- D. Benito-Garagorri, Puchberger M., Mereiter K., Kirchner K., *Stereospecific and reversible CO binding at iron pincer complexes*, *Angew. Chem. Int. Ed.* **47** (2008) 9142–9145.
27. J. Esteban, J.V. Ros-Lis, R. Martínez-Mañez, M.D. Marcos, M.E. Moragues, J. Soto, F. Sancenón, *Sensitive and selective chromogenic sensing of carbon monoxide by using binuclear rhodium complexes*, *Angew. Chem. Int. Ed.* **49** (2010) 4934–4937.
28. M.E. Moragues, J. Esteban, J.V. Ros-Lis, R. Martínez-Mañez, M.D. Marcos, M. Martínez, J. Soto, F. Sancenón, *Sensitive and selective chromogenic sensing of carbon monoxide via reversible axial CO coordination in binuclear rhodium complexes*, *J. Am. Chem. Soc.* **133** (2011) 15762–15772.
29. S.W. Brown, C. Santana, G.P. Eppeldauer, *Development of a tunable LED-based colorimetric source*, *Res. Natl. Inst. Stand. Technol.* **107** (2002) 363–371.
30. M.T. Fairchild, *Color Appearance Models*, Wiley, Chichester, UK, **2005**.
31. UNE 23301:1988 *Detection equipments of carbon monoxide concentration in the garages and parkings*; UNE 23300:1984/1M:2005 *Detection and measuring equipments of carbon monoxide concentration*.
32. T. Castaño, C. Hebert, M.T. Campo, M. Ysa, A. Pons, *Fine-cut tobacco: a priority for public health and consumer advocacy*, *Gac. Sanit.* **26** (2012) 267–269.

Biographies

María Esperanza Moragues graduated in Chemistry at the University of Valencia (UV) in 2008. She is a Ph.D. Student at the Polytechnic University of Valencia (UPV). Her main areas of interest are the development of chemical chemosensors and probes, especially those centred on CO detection.

Roberto Montes-Robles graduated in Industrial Engineering in Automation and Electronics in 2012 at the Polytechnic University of Valencia (UPV). He is working in the Electronic Engineering Department of the UPV in association with the Centre of Molecular Recognition and Technological Development (IDM). His collaboration involves the development of electronic sensors.

José Vicente Ros-Lis obtained a degree in Chemistry in 2000 at the University of Valencia and a PhD in 2005 at the Polytechnic University of Valencia. Currently, he is a member of the Centre of Molecular Recognition and Technological Devel-

opment (IDM). His research interests include the development of chemical sensors and technology transfer.

Miguel Alcañiz received his M.S. degree in Physics from the University of Valencia, Spain, in 1991. He is an assistant professor in the Electronic Engineering Department of the UPV. He is a member of the Centre of Molecular Recognition and Technological Development (IDM) of UPV. His research interest includes digital systems, electrochemical impedance spectroscopy and multivariable analysis.

Javier Ibañez is a Maîtrise in Power Electronic and Control at the Université Pierre et Marie Curie (Paris VI) in 1994 and he received his Ph.D. in 2009 at the Polytechnic University of Valencia (UPV). He is an assistant professor of Electronic Technology in the Electronic Engineering Department of the UPV. He is a member of the Institute of Molecular Recognition and Technological Development (IDM). His main areas of interest are optical devices for water and air contamination detection.

Teresa Pardo obtained a degree in Chemistry and joined the Polytechnical University of Valencia in 1982. After her PhD entitled “phenolic composition of grapes and red wines from the Valencia region” she joined the Centre of Molecular Recognition and Technological Development in the area of chemical sensors.

Ramón Martínez-Máñez graduated in Chemistry at the University of Valencia in 1986, and he received his Ph.D. in 1990 at the same university. After a postdoctoral period at Cambridge (UK), he joined the Department of Chemistry at the UPV. He became a full professor in 2002. His main areas of interest fall in the field of chromo-fluorogenic and electrochemical sensors and molecular probes for anions, cations and neutral chemical species.

4. Rhodium complexes as CO-RMs

As it has been reported above in the general introduction, carbon monoxide is much more than a contaminant. In this chapter the use of carbon monoxide as a therapeutic agent has been considered and thus, the cited dirhodium complexes **A** and **F** have been used as CO-releasing molecules. (*Inorg. Chem.*, 2013, 52, 13806-13808).

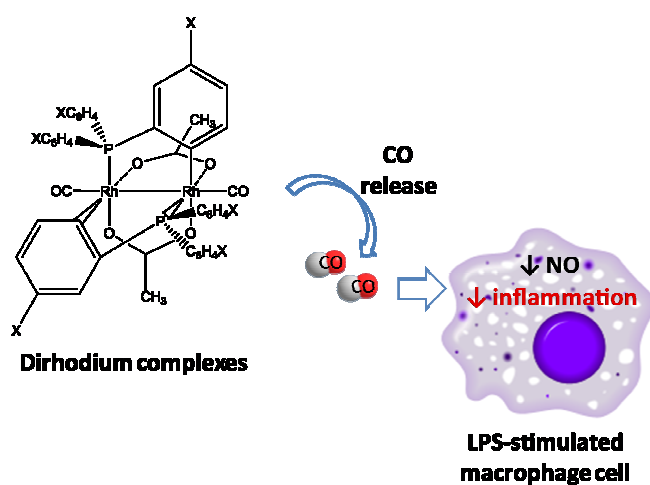


Figure 4.1. Dirhodium complexes as CORMs involved in anti-inflammatory test.

***4.1. CO-releasing binuclear rhodium complexes
as inhibitors of nitric oxide generation in
stimulated macrophages***

**CO-Releasing Binuclear Rhodium Complexes as
Inhibitors of Nitric Oxide Generation in
Stimulated Macrophages**

María E. Moragues,^{†‡} Rita Brines,[†] M^a Carmen Terencio,^{†§}
Félix Sancenón,^{†‡} Ramón Martínez-Máñez,^{*†‡} and M^a José
Alcaraz^{*†§}

[†] Centro de Reconocimiento Molecular y Desarrollo Tecnológico, Unidad Mixta
Universitat Politècnica de València – Universitat de València, Camino de Vera s/n,
46022 Valencia, Spain.

[‡] CIBER de Bioingeniería, Biomateriales y Nanomedicina, 50018, Zaragoza, Spain.

[§] CIBER de Bioingeniería, Biomateriales y Nanomedicina (CIBER-BBN).

^{||} Department de Farmacologia, Universitat de València, Av. Vicent Andrés Estellés
s/n, 46100 Burjassot, València, Spain.

Received: July 30, 2013

Published: November 27, 2013

(Reprinted with permission from
Inorganic Chemistry, 2013, 52, 13806–13808.
Copyright © 2013, American Chemical Society)

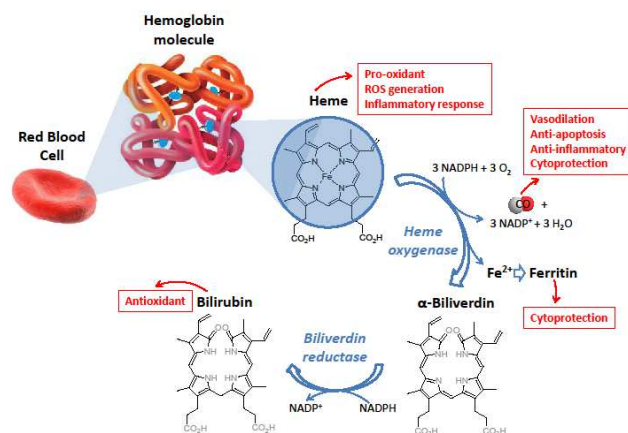
Abstract.

Nontoxic CO-releasing dirhodium complexes act as inhibitors of NO in stimulated macrophage cells, suggesting that novel antiinflammatory treatments could involve the use of these types of binuclear complexes.

Within the last 10 years, the reputation of carbon monoxide (CO) has started to shift from a noxious, polluting gas to an essential molecule involved in the modulation of several biological processes¹ as a signaling pathways regulator, fundamental for almost all living organisms including humans. These vital roles of CO, including regulation of neurotransmission,² vascular tone,³ inflammation,⁴ cell proliferation,⁵ in vitro and in vivo programmed cell death,⁶ mitochondrial biogenesis,⁷ and autophagy,⁸ make CO gas promising in molecular medicine as experimental and clinical therapeutic.⁹

Production of this gaseous molecule in the organism is mediated by heme oxygenase (HO-1) activity.¹⁰ This enzyme catabolizes heme to iron, biliverdin, and CO, which mediates many of the biological effects of induced HO-1 (Scheme 1). The protective role of the HO-1/CO pathway has been demonstrated in numerous experimental models of inflammation, tissue damage, and cardiovascular diseases.¹¹ In inflammatory and immune conditions, the expression of HO-1 by many cell types could be part of an adaptive mechanism against stress through scavenging of reactive oxygen or nitrogen species, regulation of cell proliferation, and prevention of apoptosis.¹² The therapeutic benefit of CO inhalation has been shown in a number of preclinical animal models of lung and vascular diseases.¹³ Inhaled CO diffuses rapidly across alveolar and capillary membranes, forming a tight-binding complex with the oxygen carrier protein hemoglobin to form carboxyhemoglobin (COHb). To avoid CO poisoning, the COHb levels associated with CO inhalation must be heeded. In spite of the probed benefits obtained, the administration route for gaseous compounds is restricted to inhalation through the lung, with difficulty in controlling the absorption, distribution, and specificity of CO. In this context, the biological effects of CO can be reproduced by the administration of CO-releasing molecules (CO-RMs), which are capable of carrying

and delivering small amounts of CO in biological systems.¹⁴ The use of CO-RMs represents a good alternative to CO gas in terms of controlled delivery through all possible routes of administration and also reduces COHb to nondangerous levels (<10%). The beneficial effect of these molecules has been shown after administration in various experimental models of arthritis.¹⁵ In these conditions, CORMs reduce several proinflammatory parameters including nitric oxide (NO)¹⁶ and prostaglandin E2 (PGE2) produced by activation of inducible NO synthase (iNOS) and cyclooxygenase-2, respectively.



Scheme 1. Schematic Representation of Metabolites Derived from HO-1 Activity and Their Physiological Effects.

CO-RMs have been extensively studied over the last years and can be classified into several types.¹⁷ In particular, the most common CO-RMs are organometallic carbonyl complexes (mainly of chromium, molybdenum, manganese, rhenium, iron, and ruthenium).¹⁸ However, also α,α -dialkylaldehydes, oxalates, boroncarboxylates, and silacarboxylates have recently been studied for their application in CO-release processes. Among all of these types of CO-RMs, metal carbonyls are perhaps the most well-suited for their use in pharmaceutical applications.¹⁷ Employment of aldehydes as CO-RMs is limited by their slow release rate and medium toxicity.¹⁹ Moreover, the CO delivery rate from oxalates

is too slow,²⁰ whereas silicacarboxylates need an activator (fluoride, methoxide, or tertbutoxide anions) to induce CO release.²¹ On the other hand, boron carboxylates show a limited scope for chemical transformation that makes them unsuitable for the generation of compounds with appropriate pharmaceutical characteristics.²²

From another point of view, a family of binuclear rhodium complexes of the general formula $[\text{Rh}_2\{(\text{XC}_6\text{H}_3)\text{P}(\text{XC}_6\text{H}_4)_2\}_n(\text{O}_2\text{CR})_{4-n}]\cdot\text{L}_2$ containing one or two, in a head-to-tail arrangement, metalated phosphine ligands and different equatorial and axial ligands had recently been used by us as chromogenic probes for CO detection.²³ In this context, these ideal sensing systems not only display sensing features at low concentration but also show reversible binding with the target CO molecule.

On the basis of these observations and interest in the design of new CO-RMs, it occurred to us that CO-containing binuclear rhodium complexes could be used as suitable systems as physiological CO donors. In this context, we report herein, as far as we know for the first time, the use of binuclear rhodium complexes bearing coordinated CO molecules as CO-RMs and have tested them in the generation of inflammatory mediators NO and PGE2 in murine macrophage cell line RAW 264.7.

In particular, we used for this study the complexes $[\text{Rh}_2\{(\text{C}_6\text{H}_4)\text{P}(\text{C}_6\text{H}_5)_2\}_2(\text{O}_2\text{CCH}_3)_2]\cdot(\text{CO})_2$ (**1**·(CO)₂) and $[\text{Rh}_2\{(m\text{-CH}_3\text{C}_6\text{H}_3)\text{P}(m\text{-CH}_3\text{C}_6\text{H}_4)_2\}_2(\text{O}_2\text{CCH}_3)_2]\cdot(\text{CO})_2$ (**2**·(CO)₂) (see Figure 1). The starting complexes, i.e., $[\text{Rh}_2\{(\text{C}_6\text{H}_4)\text{P}(\text{C}_6\text{H}_5)_2\}_2(\text{O}_2\text{CCH}_3)_2]\cdot(\text{CH}_3\text{CO}_2\text{H})_2$ (**1**·(CH₃CO₂H)₂) and $[\text{Rh}_2\{(m\text{-CH}_3\text{C}_6\text{H}_3)\text{P}(m\text{-CH}_3\text{C}_6\text{H}_4)_2\}_2(\text{O}_2\text{CCH}_3)_2]\cdot(\text{CH}_3\text{CO}_2\text{H})_2$ (**2**·(CH₃CO₂H)₂), were obtained by refluxing the corresponding phosphines, P(C₆H₅)₃ for **1**·(CH₃CO₂H)₂ and P(m-CH₃C₆H₄)₃ for **2**·(CH₃CO₂H)₂, with $[\text{Rh}_2(\text{O}_2\text{CCH}_3)_4]$ in toluene/acetic acid. The molar ratio phosphine–dirhodium(II) tetraacetate was fixed to 2:1. Both complexes **1**·(CH₃CO₂H)₂ and **2**·(CH₃CO₂H)₂ (simplified as #·(CH₃CO₂H)₂) contain two orthometalated arylphosphines and two acetates as bridging ligands.²³ The design of CO-RM derivatives involves the use of these binuclear rhodium(II) cyclometalated complexes and the well-documented labile coordination ability in their axial sites. Moreover, coordination studies on adduct formation between

dirhodium compounds and different Lewis bases²⁴ have demonstrated that even systems such as dirhodium(II) tetra- μ -carboxylate are very effective in π -back-bonding to the axial ligands, which is a very interesting feature for the design of CO binding complexes. Besides, when biscyclometalated compounds are compared with dirhodium tetracarboxylate derivatives, a higher ability of the former for π -back-donation to the axial ligand has been reported. In fact, the simple exposure of solutions of $\mathbf{1}\cdot(\text{CH}_3\text{CO}_2\text{H})_2$ and $\mathbf{2}\cdot(\text{CH}_3\text{CO}_2\text{H})_2$ in methanol to a CO stream allowed one to obtain the corresponding $\mathbf{1}\cdot(\text{CO})_2$ and $\mathbf{2}\cdot(\text{CO})_2$ complexes. Moreover, the formation of $\mathbf{1}\cdot(\text{CO})_2$ and $\mathbf{2}\cdot(\text{CO})_2$ from $\mathbf{1}\cdot(\text{CH}_3\text{CO}_2\text{H})_2$ and $\mathbf{2}\cdot(\text{CH}_3\text{CO}_2\text{H})_2$ can easily be monitored through the naked eye because the color of the complexes changes from purple ($\mathbf{1}\cdot(\text{CH}_3\text{CO}_2\text{H})_2$ absorbance at ca. 560 nm) to orange [$\mathbf{1}\cdot(\text{CH}_3\text{CO}_2\text{H},\text{CO})$ absorbance at ca. 510 nm] to yellow ($\mathbf{1}\cdot(\text{CO})_2$ absorbance at ca. 390 nm) upon reaction with CO.^{23a} Moreover, when the yellow complexes $\mathbf{1}\cdot(\text{CO})_2$ and $\mathbf{2}\cdot(\text{CO})_2$ were left in an open-air atmosphere, the color changed slowly (in about 15 h) to purple because of the release of axially coordinated CO molecules. This release of axial CO molecules from $\mathbf{1}\cdot(\text{CO})_2$ and $\mathbf{2}\cdot(\text{CO})_2$ complexes was also studied by thermogravimetry, and in both cases, the weight changes correspond to the release of 2 equiv of CO per molecule (see the Supporting Information). Bearing in mind the adequate uptake and release features of both complexes, we intend to use them as CO-RMs. For this purpose, the cytotoxicity of both $\mathbf{1}\cdot(\text{CO})_2$ and $\mathbf{2}\cdot(\text{CO})_2$ complexes was first evaluated.

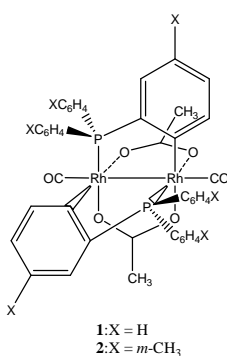


Figure 1. Structure for dirhodium complexes $\mathbf{1}\cdot(\text{CO})_2$ and $\mathbf{2}\cdot(\text{CO})_2$ with the general formula $[\text{Rh}_2\{(\text{XC}_6\text{H}_3)\text{P}(\text{XC}_6\text{H}_4)_2\}_2(\text{O}_2\text{CCH}_3)_2]\cdot(\text{CO})_2$.

In particular, RAW 264.7 macrophages were treated with $1 \cdot (\text{CO})_2$ and $2 \cdot (\text{CO})_2$ at different concentrations over a 60 min period at 37 °C, and the cell viability was determined by MTT assay. The obtained results are shown in Figure 2a. As seen, both complexes are essentially nontoxic in the concentration tested (1 and 10 μM). In fact, absorbance values after treatments were not statistically different with respect to the stimulated control (C; see the Supporting Information for details).

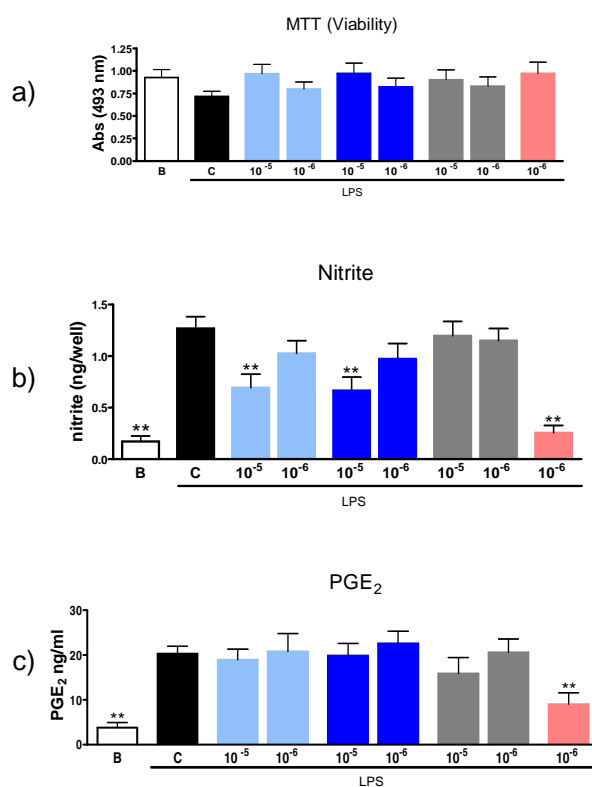


Figure 2. (a) MTT assay, (b) nitrite release, and (c) PGE₂ generation. Data are expressed as mean \pm SEM ($n = 12-18$). ** $p < 0.01$. Compared to stimulated control cells (C) and nonstimulated or blank cells (B); (light blue) complex $1 \cdot (\text{CO})_2$ (30-days stock); (sky blue) complex $1 \cdot (\text{CO})_2$ (recently prepared); (gray) complex $2 \cdot (\text{CO})_2$; (salmon) dexamethasone.

Once the nontoxicity of both complexes was demonstrated, the inhibition of nitrite and PGE₂ in RAW 264.7 macrophages in the presence of $1 \cdot (\text{CO})_2$ and

$2 \cdot (\text{CO})_2$ was studied. Incubation of RAW 264.7 macrophages with lipopolysaccharide (LPS) produced the expression of iNOS and a consequent increase of the nitrite levels (Figure 2b), which were significantly inhibited after preincubation with complex $1 \cdot (\text{CO})_2$ (10 μM) and the reference compound dexamethasone (1 μM). In contrast, complex $2 \cdot (\text{CO})_2$ had no effect at this level. As shown by the results, complex $1 \cdot (\text{CO})_2$ was able to maintain its inhibitory properties even 30 days after preparation (maintained under a CO atmosphere), thus demonstrating its stability and ability to donate CO molecules even after this time period. In a parallel assay, complex $1 \cdot (\text{CH}_3\text{CO}_2\text{H})_2$ (without coordinated CO molecules) was tested in the same conditions, demonstrating that this compound had no antiinflammatory properties per se (data not shown). Finally, none of the tested compounds showed an inhibitory effect with respect to the generation of PGE2 in stimulated macrophages (Figure 2c).

In summary, we have reported herein, for the first time, the potential use of cyclometalated binuclear rhodium complexes containing CO molecules as axial ligands as CO-releasing systems. This was demonstrated using complex $1 \cdot (\text{CO})_2$, which was found to clearly inhibit the nitrite levels in biological assays carried out in mouse macrophage cells where inflammation had been stimulated by LPS. We believe that this first proof-of-concept may open new studies in the use of binuclear rhodium complexes as potential CO-RMs able to carry and deliver small amounts of CO in biological systems and may allow advancement in the study of the pathophysiological and therapeutical role of CO.

Associated Content

Supporting Information. Materials and methods, general considerations, synthesis of the rhodium complexes, cell culture, cell viability assay, determination of nitrite and PGE2, statistical analysis, diffuse reflectance UV-vis and thermogravimetric studies. This material is available free of charge via the Internet at <http://pubs.acs.org>.

Author Information

Corresponding Author

rmaez@qim.upv.es; Maria.J.Alcaraz@uv.es.

Notes

The authors declare no competing financial interest.

Acknowledgments

Financial support from the Spanish Government (Projects MAT2012-38429-C04-01 and SAF2010-22048) and the Generalitat Valencia (Projects PROMETEO2009/016, ISIC/2012/005, and PROMETEO2010/047) is gratefully acknowledged. M.E.M. thanks the Spanish Ministry of Education for a Doctoral FPU Fellowship.

References

1. Piantadosi, C. A. *Antioxid. Redox Signaling* **2002**, *4*, 259.
2. (a) Verma, A.; Hirsch, D. J.; Glatt, C. E.; Ronnett, G. V.; Snyder, S. H. *Science* **1993**, *259*, 381. (b) Maines, M. D. *Mol. Cell. Neurosci.* **1993**, *4*, 389.
3. (a) Wagner, C. T.; Durante, W.; Christodoulides, N.; Hellums, J. D.; Schafer, A. I. *J. Clin. Invest.* **1997**, *100*, 589. (b) Motterlini, R.; Gonzales, A.; Foresti, R.; Clark, J. E.; Green, C. J.; Winslow, R. M. *Circ. Res.* **1998**, *83*, 568.
4. Otterbein, L. E.; Bach, F. H.; Alam, J.; Soares, M.; Tao, L. H.; Wysk, M.; Davis, R. J.; Flavell, R. A.; Choi, A. M. *Nat. Med.* **2000**, *6*, 422.
5. Morita, T.; Mitsialis, S. A.; Koike, H.; Liu, Y.; Kourembanas, S. *J. Biol. Chem.* **1997**, *272*, 32804.
6. Brouard, S.; Otterbein, L. E.; Anrather, J.; Tobiasch, E.; Bach, F. H.; Choi, A. M.; Soares, M. P. *J. Exp. Med.* **2000**, *192*, 1015.
7. Suliman, H. B.; Carraway, M. S.; Tatro, L. G.; Piantadosi, C. A. *J. Cell Sci.* **2007**, *120* (Pt2), 299.
8. Lee, S. J.; Ryter, S. W.; Xu, J. F.; Nakahira, K.; Kim, H. P.; Choi, A. M.; Kim, Y. S. *Am. J. Respir. Cell Mol. Biol.* **2011**, *45*, 867.
9. (a) Wu, L.; Wang, R. *Pharm. Rev.* **2005**, *57*, 585. (b) Ryter, S. W.; Choi, A. M. K. *Korean J. Int. Med.* **2013**, *28*, 123.
10. Maines, M. D. *Annu. Rev. Pharmacol. Toxicol.* **1997**, *37*, 517.

11. (a) Motterlini, R.; Otterbein, L. E. *Nat. Rev. Drug Discovery* **2010**, *9*, 728. (b) Fernandez-Gonzalez, A.; Mitsialis, A. S.; Liu, X.; Kourembanas, S. *Am. J. Physiol. Lung Cell Mol. Physiol.* **2012**, *302*, L775.
12. Bainbridge, S. A.; Belkacemi, L.; Dickinson, M.; Graham, C. H.; Smith, G. N. *Am. J. Pathol.* **2006**, *169*, 774.
13. Schallner, N.; Fuchs, M.; Schwer, C. I.; Loop, T.; Buerkle, H.; Lagrèze, W. A.; van Oterendorp, C.; Biermann, J.; Goebel, U. *PLoS One* **2012**, *7*, e46479.
14. (a) Winburn, I. C.; Gunatunga, K.; McKernan, R. D.; Walker, R. J.; Sammut, I. A.; Harrison, J. C. *Basic Clin. Pharmacol. Toxicol.* **2012**, *111*, 31. (b) Alcaraz, M. J.; Guillen, M. I.; Ferrandiz, M. L.; Megías, J.; Motterlini, R. *Curr. Pharm. Des.* **2008**, *14*, 412.
15. (a) Ibáñez, L.; Alcaraz, M. J.; Maicas, N.; Guede, D.; Caeiro, J. R.; Ferrándiz, M. L. *Calcif. Tissue Int.* **2012**, *91*, 69. (b) García-Arnandis, I.; Guillén, M. I.; Gomar, F.; Castejón, M. A.; Alcaraz, M. J. *PLOS One* **2011**, *6*, 24591.
16. Romanski, S.; Kraus, B.; Schatzschneider, U.; Neudörfl, J.-M.; Amslinger, S.; Schmalz, H.-G. *Angew. Chem., Int. Ed.* **2011**, *50*, 2392.
17. Romao, C. C.; Blättler, W. A.; Seixas, J. D.; Bernardier, G. J. L. *Chem. Soc. Rev.* **2012**, *41*, 3571.
18. Hartinger, G. C.; Dyson, P. J. *Chem. Soc. Rev.* **2009**, *38*, 391.
19. De Matos, M. N.; Romao, C. C. *U.S. Patent* 2007219120A1, **2007**.
20. Alberto, R.; Motterlini, R. *Dalton Trans.* **2007**, 1651.
21. Friis, S. D.; Taaning, R. H.; Lindhart, A. T.; Skrydstrup, T. *J. Am. Chem. Soc.* **2011**, *133*, 18114.
22. Pitchumony, T. S.; Spingler, B.; Motterlini, R.; Alberto, R. *Org. Biomol. Chem.* **2010**, *8*, 4849.
23. (a) Moragues, M. E.; Esteban, J.; Ros-Lis, J. V.; Martínez-Máñez, R.; Marcos, M. D.; Martínez, M.; Soto, J.; Sancenón, F. *J. Am. Chem. Soc.* **2011**, *133*, 15762. (b) Esteban, J.; Ros-Lis, J. V.; Martínez-Máñez, R.; Marcos, M. D.; Moragues, M. E.; Soto, J.; Sancenón, F. *Angew. Chem., Int. Ed.* **2010**, *49*, 4934.
24. Hirva, P.; Esteban, J.; Lahuerta, P.; Pérez-Prieto, J. *Inorg. Chem.* **2007**, *46*, 2619.

SUPPORTING INFORMATION

CO-Releasing Binuclear Rhodium Complexes as Inhibitors of Nitric Oxide Generation in Stimulated Macrophages

María E. Moragues, Rita Brines, M^a Carmen Terencio, Félix Sancenón,
Ramón Martínez-Máñez and M^a José Alcaraz

MATERIALS AND METHODS

General considerations

Synthesis of $[\text{Rh}_2\{(\text{XC}_6\text{H}_3)\text{P}(\text{XC}_6\text{H}_4)_2\}_2(\text{O}_2\text{CCH}_3)_2] \cdot (\text{CH}_3\text{CO}_2\text{H})_2$

Cell culture of mouse macrophage cell line RAW 264.7

Cell viability assay (MTT)

Determination of nitrite and PGE2

Statistical analysis

Diffuse reflectance UV-vis studies

Thermogravimetric studies

REFERENCES

Materials and Methods

General considerations. Commercially available reagents, $[\text{Rh}_2(\text{O}_2\text{CCH}_3)_4]$, as well as the different phosphines ($\text{P}(\text{C}_6\text{H}_5)_3$, $\text{P}(m\text{-CH}_3\text{C}_6\text{H}_4)_3$) and $\text{CH}_3\text{CO}_2\text{H}$, were used as purchased. All solvents were of analytical grade. All reactions were carried out in oven-dried glassware under an argon atmosphere, although the isolated solids are air-stable. The solvents were degassed before use. Carbon monoxide was provided by a commercially available CO cylinder.

Synthesis of $[\text{Rh}_2\{\text{X}(\text{C}_6\text{H}_3)\text{P}(\text{X}(\text{C}_6\text{H}_4)_2\}_2(\text{O}_2\text{CCH}_3)_2]\cdot(\text{CH}_3\text{CO}_2\text{H})_2$. Complexes **1**· $(\text{CH}_3\text{CO}_2\text{H})_2$ ($\text{X} = \text{H}$) and **2**· $(\text{CH}_3\text{CO}_2\text{H})_2$ ($\text{X} = m\text{-CH}_3$) were obtained by refluxing the corresponding phosphine, $\text{P}(\text{C}_6\text{H}_5)_3$ or $\text{P}(m\text{-CH}_3\text{C}_6\text{H}_4)_3$, respectively with $[\text{Rh}_2(\text{O}_2\text{CCH}_3)_4]$ in toluene:acetic acid media (3:1) under argon atmosphere as described in the literature.^{1,2,3} The molar ratio phosphine:dirhodium(II) tetraacetate was 2:1. These compounds containing two ortho-metalated aryl phosphines and two carboxylates as bridging ligands show ability to coordinate different bases in their labile axial sites.⁴

Synthesis of **1· $(\text{CO})_2$ and **2**· $(\text{CO})_2$.** Compounds **1**· $(\text{CO})_2$ and **2**· $(\text{CO})_2$ were obtained by slow evaporation of CO-bubbled methanol solutions of **1**· $(\text{CH}_3\text{CO}_2\text{H})_2$ and **2**· $(\text{CH}_3\text{CO}_2\text{H})_2$. Both yellow complexes containing CO as axial ligands could be isolated and remained stable under a CO atmosphere. Crystal structure of dirhodium complex **1**· $(\text{CO})_2$ has been reported by us in a previous work.⁵

Cell culture of mouse macrophage cell line RAW 264.7. Macrophages were cultivated in DMEM/HAM F-12 medium supplemented with penicillin (100 U/ml), streptomycin (100 $\mu\text{g}/\text{ml}$) and fetal bovine serum (FBS) (10%) in an incubator at 37°C and 5% CO_2 . For the experiments, cells were removed from the tissue culture flask using a cell scraper, seeded in sterile 96-well microplates (400,000 cells/well) and incubated for 2 hours to allow cell adherence. The medium was then removed and new DMEM/HAM F-12 medium supplemented with 5% FBS was added. Blank cells (**B**) were cultivated in normal conditions, whereas control cells (**C**) were stimulated with bacterial lipopolysaccharide (LPS) derived from

Escherichia coli (serotype O111: B4) (1 µg/ml) for 18h. Macrophages under study were preincubated with compounds **1**·(CO)₂ and **2**·(CO)₂ (0.1% EtOH) for 30 minutes and then stimulated with LPS as described for control cells. At the end of each experiment, cellular supernatants were collected to determine nitrite (stable metabolite of NO) and PGE₂ levels. Dexamethasone⁶ (10⁻⁶ M) was used as anti-inflammatory reference compound. The adherent cells were used to discard the possible cytotoxic effect of tested compounds by the mitochondrial reduction of 3-(4,5-dimethylthiazol-2-yl)-2,5-diphenyl tetrazolium bromide (MTT) to formazan.

Cell viability assay (MTT). The MTT assay is a colorimetric method based on the ability of cells to reduce the yellow tetrazolium salt (MTT) to purple formazan by the mitochondrial succinyl dehydrogenase activity.⁷ Thus, the amount of formazan is directly correlated to the number of metabolically active cells. A solution of MTT (0.25 mg/ml) in culture media was added to cells and incubated for 60 min at 37°C. Then, supernatant was removed and dimethylsulfoxide was added to the wells to produce cell lysis and dissolve the formazan. Absorbance was measured at 490 nm. The average value of the absorbance of the blank at 490 nm is considered as 100% cell viability, and based on it, the percentage of cytotoxicity of the complexes in study is calculated.

Determination of nitrite and PGE₂. Nitrite concentration was determined in culture supernatants as reflection of NO released by stimulated cells. Based on the fluorometrically method of Misko,⁸ aliquots of culture supernatants were incubated with 2,3-diaminonaphthalene (0.05 mg / mL in 0.62 M HCl) in white microplates and maintained in the dark for 10 min. The reaction was stopped with 2.8 M NaOH and fluorescence was measured at 365 nm excitation and 450 nm emission. The amount of nitrite was obtained by extrapolation from standard curve with sodium nitrite. PGE₂ levels in cell culture supernatants were determined by radioimmunoassay (RIA) by competition with [5,6,8,11,12,14,15 (n)-³H]PGE₂.⁹

Statistical analysis. Results are presented as mean \pm SEM (n = 12-18). Statistical significance was determined by analysis of variance (one-way-ANOVA) followed by Dunnett's test for multiple comparisons. $**p < 0.01$ compared to stimulated cells (C).

Diffuse reflectance UV-vis studies. UV-vis spectra were recorded using a Jasco V-650 spectrophotometer equipped with a diffuse reflectance Sphere (model ISV-722). Measurements were conducted at room temperature over a wavelength range of 350-800 nm with a wavelength step of 1 nm. The reflectance data were transformed using Kubelka-Munk function $[F(R)]$,¹⁰ where R is the fraction of incident light reflected by the sample.

$$F(R) = \frac{(1-R)^2}{2R}$$

Absorption of compounds **1·(CH₃CO₂H)₂** and **2·(CH₃CO₂H)₂** on silica beads (via solution of each binuclear rhodium compound in a minimum amount of chloroform followed by the addition of silica at a molar ratio 250 times) resulted in purple solids. Exposure of these solids to CO stream allowed to obtain **1·(CO)₂** and **2·(CO)₂** as yellow solids. Figure S1 shows the diffuse reflectance UV-vis spectra of silica beads containing **1·(CO)₂** and **2·(CO)₂** and the changes observed as CO is released. Bathochromic shifts of approximately 150 nm are registered for both complexes as the two CO molecules are released from axial positions. The intermediate bands formed at 470 and 510 nm, correspond to the **1·(CH₃CO₂H, CO)** and **2·(CH₃CO₂H, CO)** derivatives, respectively.

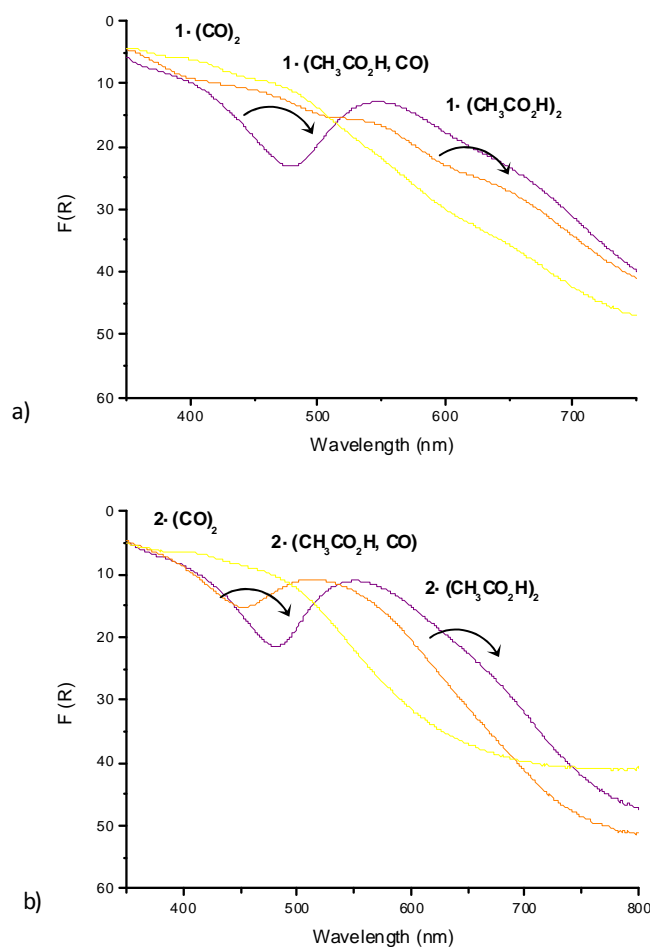


Figure S1. Diffuse reflectance UV-vis spectra of compounds a) $1\cdot(\text{CO})_2$ and b) $2\cdot(\text{CO})_2$ embedded in silica gel and the changes observed through the release of CO coordinated at axial positions.

Termogravimetric studies. Thermogravimetric analyses were carried out on a TGA/SDTA 851e Mettler Toledo balance under a flow of N_2 and with an isothermal heating programme at $37\text{ }^\circ\text{C}$ for 60 minutes. The CO release from compounds $1\cdot(\text{CO})_2$ and $2\cdot(\text{CO})_2$ adsorbed on silica gel was studied through registration of mass loss in $1\cdot(\text{CO})_2$ and $2\cdot(\text{CO})_2$ as well as in $1\cdot(\text{CH}_3\text{CO}_2\text{H})_2$ and $2\cdot(\text{CH}_3\text{CO}_2\text{H})_2$. By subtracting each pair of curves, the amount of CO released from the dicarbonyl

compounds was calculated being 0.093 mg for $1 \cdot (\text{CO})_2$ and 0.1091 mg for $2 \cdot (\text{CO})_2$. Figure S2 shows the curves resulting from the subtraction of the registered ones and the consequent amount of CO released.

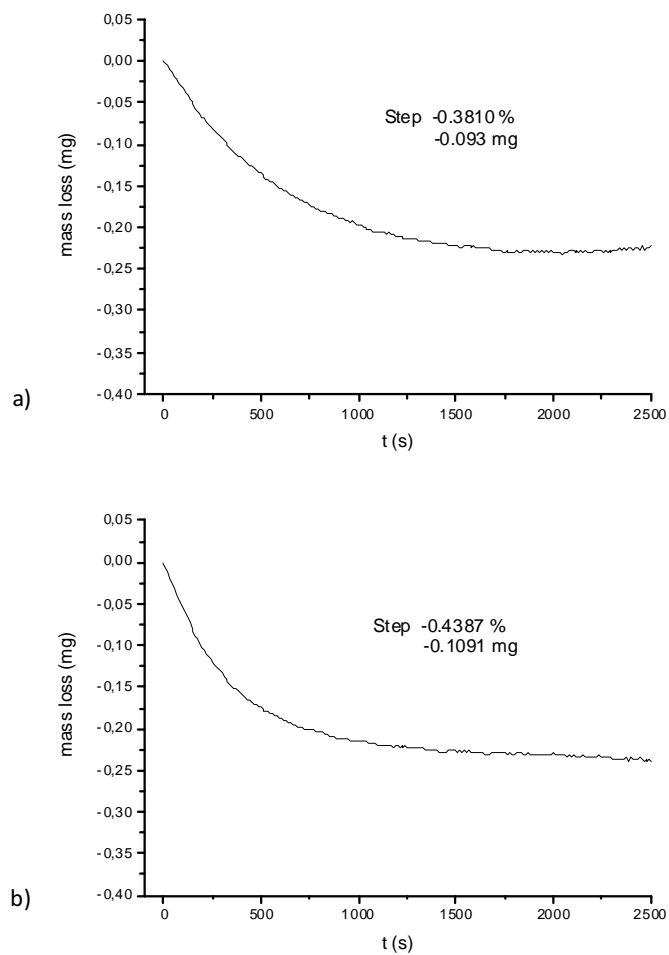


Figure S2. Mass loss (mg) in silica solids of a) $1 \cdot (\text{CO})_2$ and b) $2 \cdot (\text{CO})_2$ at 37 °C.

References

1. Hirva, P.; Lahuerta, P.; Pérez-Prieto, J. *Theor. Chem.* **2005**, 113, 63.
2. Esteban, J.; Esteban, F.; Sanau, M. *Inorg. Chim. Acta* **2009**, 362, 1179.
3. Esteban, J.; Esteban, F.; Sanau, M. *Inorg. Chim. Acta* **2008**, 361, 1274.
4. Hirva, P.; Esteban, J.; Lahuerta, P.; Pérez-Prieto, J. *Inorg. Chem.* **2007**, 46, 2619.
5. Esteban, J.; Ros-Lis, J.V.; Marínez-Máñez, R.; Marcos, M.D.; Moragues, M.E.; Soto, J.; Sancenón, F. *Angew. Chem. Int. Ed.* **2010**, 49, 4934.
6. Bunim, J.J.; Black, R.L.; Lutwak, L.; Peterson, R. E.; Whedon, G.D. *Arthritis & Rheumatism* **1958**, 1 (4), 313.
7. Borenfreund, E.; Babick, H.; Martin-Alguacil, N. *Toxic In Vitro* **1988**, 2, 1.
8. Misko, T.P.; Schilling, R.J.; Salvemini, D.; Moore, W.M.; Currie, M.G. *Anal. Biochem.* **1993**, 214, 11.
9. Moroney, M.A.; Alcaraz, M.J.; Forder, R.A.; Carey, F.; Hoult, J.R. *J. Pharm. Pharmacol.* **1998**, 40, 787.
10. Zinchuk, A.V.; Hancock, B. C.; Chalaev, E.Y.; Reddy, R.D.; Govindarajan, R.; Novak, E. *Eur. J. Pharm. Biopharm.* **2005**, 61, 158.

***5. Ruthenium and osmium complexes for CO
detection***

In this chapter, the sensitive and selective sensing of CO in air is described, by reporting two publications.

In the fifth article reported here (*J. Am. Chem. Soc.*, 2014, 136,11930-11933), carbon monoxide can be chromo-fluorogenically detected by the use of an alkenyl-ruthenium(II) complex $[\text{Ru}(\text{CH}=\text{CHPyr-1})\text{Cl}(\text{CO})(\text{BTD})(\text{PPh}_3)_2]$ **G**. This complex, which contains a fluorogenic pyrenylvinyl ligand *trans* to a 2,1,3-benzothiadiazole (BTD) fluorescence-quencher molecule, coordinates CO by means of BTD displacement and undergoes a colour change from orange to yellow with a concomitant revival of the pyrene fluorescence. (See Figure 5.1).

An extension of this preliminary work produced the sixth article (*Chem. Sci.*, 2014, *submitted*) included in this doctoral dissertation. A collection of three ruthenium(II) and two osmium(II) complexes, **G**, **I**, **K** and **H**, **J**, respectively; adsorbed on silica are used as probes for CO detection simply based in colour changes visible to the naked eye. (See Figure 5.2).

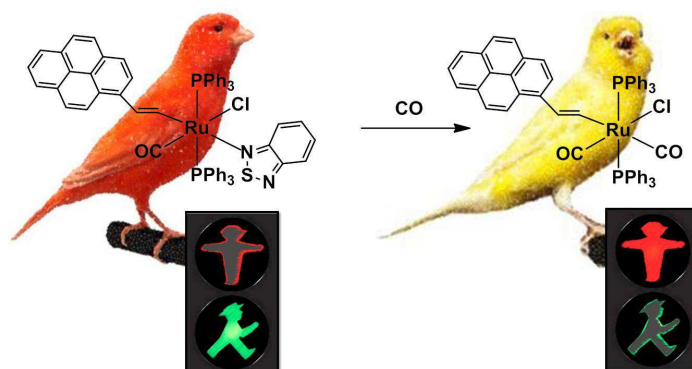


Figure 5.1. Scheme of the chromo-fluorogenic synthetic "canary" for CO detection based on pyrenylvinyl ruthenium(II) complex.



Figure 5.2. Scheme of the colour evolution of the colorimetric probes upon presence of increasing concentrations of CO.

***5.1. A chromo-fluorogenic synthetic
“canary” for CO detection based on a
pyrenylvinyl ruthenium(II) complex***

A Chromo-Fluorogenic Synthetic “Canary” for CO Detection Based on a Pyrenylvinyl Ruthenium(II) Complex

*María E. Moragues,^{†,‡,§} Anita Toscani,^{||} Félix Sancenón,^{†,‡,§}
Ramón Martínez-Máñez,^{*,†,‡,§} Andrew J. P. White,^{||} James D.
E. T. Wilton-Ely.^{*,||}*

[†]*Centro de Reconocimiento Molecular y Desarrollo Tecnológico (IDM), Unidad Mixta Universidad Politécnica de Valencia-Universidad de Valencia, Spain*

[‡]*Departamento de Química, Universidad Politécnica de Valencia, Camino de Vera s/n, 46022, Valencia, Spain*

[§]*CIBER de Bioingeniería, Biomateriales y Nanomedicina (CIBER-BBN)*

^{||}*Department of Chemistry, Imperial College London, South Kensington Campus, London SW7 2AZ, UK*

Received: July 15, 2014

Published: August 4, 2014

*(Reprinted with permission from
Journal of the American Chemical Society, 2014, 136, 11930–11933.*

Copyright © 2014, American Chemical Society)

Abstract

The chromo-fluorogenic detection of carbon monoxide in air has been achieved using a simple, inexpensive system based on ruthenium(II). This probe shows exceptional sensitivity and selectivity in its sensing behavior in the solid state. A color response visible to the naked eye is observed at 5 ppb of CO, and a remarkably clear color change occurs from orange to yellow at the onset of toxic CO concentrations (100 ppm) in air. Even greater sensitivity (1 ppb) can be achieved through a substantial increase in turn-on emission fluorescence in the presence of carbon monoxide, both in air and in solution. No response is observed with other gases including water vapor. Immobilization of the probe on a cellulose strip allows the system to be applied in its current form in a simple optoelectronic device to give a numerical reading and/or alarm.

The development of electronic household detectors for harmful gases dates from the 1980s and 90s. Back in 1911, canaries were traditionally used in coal mines as an early detection system against life threatening gases such as carbon dioxide, carbon monoxide and methane. The canary, normally a very songful bird, would stop singing and eventually die in the presence of these gases, signaling to the miners to exit the mine. Although considered as moderately toxic compared to other highly poisonous gases, carbon monoxide (CO) detection has always been of vital importance as it lacks color, odor or taste and it is present in numerous natural and artificial environments.¹ Carbon monoxide is a temporary atmospheric pollutant in some urban areas, mainly arising from the exhaust of internal combustion engines (such as vehicles, portable generators, lawn mowers and power washers), but also from incomplete combustion of other fuels (including wood, coal, charcoal, oil, paraffin, propane, natural gas, and waste). Many technologies and devices (electrochemical,² optical,³ and those based on metal-oxide semiconductors⁴) have been developed to detect, monitor, and alert the leakage of carbon monoxide. These systems suffer from drawbacks such as false alarms arising due to water vapor or airborne particulates. As an alternative to these systems the design of molecular probes for the chromo-fluorogenic

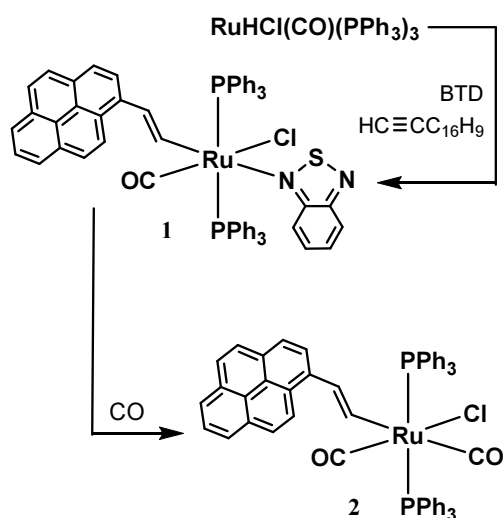
recognition of CO is of importance. In particular, colorimetric methods are undemanding, giving advantages such as real-time monitoring and the use of simple and inexpensive instrumentation. Moreover, certain colorimetric changes can be observed by the naked eye, thus making chromogenic protocols matchless for certain applications

Optical detection of carbon monoxide dates back to the late twentieth century when the presence of CO was revealed by a chemically infused paper that turned brown when exposed to the gas. However, only in the last few years has the number of chromogenic probes for CO detection based on new sensing concepts increased. In this field, oxoacetato-bridged triruthenium cluster complexes,⁵ glass-immobilized rhodium complexes,⁶ iron porphyrin functionalized polypyrroles⁷ and a phosphino diaminopyridine iron complex⁸ have been reported to display color modulations in the presence of carbon monoxide. More recently the optical detection of CO using bimetallic rhodium complexes has also been reported by some of us.⁹ Regardless of several advantages offered by chromogenic sensors, only a few probes for carbon monoxide detection using emission changes have been reported so far involving the use of iron¹⁰ and palladium¹¹ complexes. However, in some of these reported systems the modulations caused by the presence of carbon monoxide reveal particular shortcomings, typically involving poor color or emission changes, sensing in solution but not in air and high detection limits which hamper the use of these probes as viable sensing systems.

Within this context, we have taken advantage of the well-known ability of alkenyl-ruthenium(II) complexes to react with small donor ligands such as carbon monoxide¹² to explore their use as potential colorimetric probes for CO sensing. The organometallic probe, $[\text{Ru}(\text{CH}=\text{CHPyr-1})\text{Cl}(\text{CO})(\text{BTD})(\text{PPh}_3)_2]$ (**1**) (Scheme 1), consists of a Ru(II) metal center bonded to a fluorogenic pyrenylvinyl (CH=CH-Pyr-1) ligand *trans* to a 2,1,3-benzothiadiazole (BTD) molecule that acts as an emission quencher (*vide infra*). The coordination sphere in **1** is completed by two triphenylphosphine ligands, a chloride and a CO moiety. The probe was designed to express a dual chromo- and fluorogenic response to carbon monoxide. Thus, the presence in the complex of a pyrene donor group and a BTD acceptor was

expected to result in a ligand-to-ligand charge transfer band that would inhibit the fluorescence emission from pyrene. The interchange of the labile quencher BTD by CO to give **2** was envisaged to induce both a revival of the pyrene fluorescence and a color change due to the modification of the coordination sphere of the Ru(II) center.

Probe **1** was prepared in 96% yield following the simple and extensively utilized synthesis of alkenyl ruthenium complexes through hydroruthenation of a hydride complex by a suitable terminal alkyne.¹³ This process consists of the regio- and stereospecific insertion of a terminal alkyne into the Ru-H bond. Thus, the brightly colored σ -alkenyl 18-electron adduct **1** (see Scheme 1) was readily synthesized by reaction of the hydride $[\text{RuHCl}(\text{CO})(\text{PPh}_3)_3]$ ¹⁴ with 1-ethynylpyrene and BTD¹⁵ in dichloromethane at room temperature.



Scheme 1. Formation of complex $[\text{Ru}(\text{CH}=\text{CHPyr-1})\text{Cl}(\text{CO})(\text{BTD})(\text{PPh}_3)_2]$ **1** and complex $[\text{Ru}(\text{CH}=\text{CHPyr-1})\text{Cl}(\text{CO})_2(\text{PPh}_3)_2]$ **2**.

X-ray quality crystals of **1** were obtained by recrystallization of the complex via vapor diffusion of diethyl ether onto a dichloromethane solution of **1**. Figure 1 provides a plot of the complex showing the atomic numbering scheme. In the structure, the Ru(II) center adopts a distorted octahedral coordination environment with two triphenylphosphine ligands in axial positions and four ligands (Cl, CO, BTD and vinylpyrene) occupying the equatorial sites.

The electronic spectrum of a methanol solution of complex **1** in the visible region is dominated by low intensity band at ca. 500 nm attributed to a $\pi\text{-}\pi^*$ pyrenylvinyl-to-BTD ligand-to-ligand charge transfer transition and a moderately intense absorption band at 390 nm due to a pyrene $\pi\text{-}\pi^*$ transition.¹⁶

In a preliminary test, air samples containing CO were bubbled into dichloromethane or methanol solutions of **1** and an instantaneous and remarkable color change from red to yellow was observed. This color modulation is concomitant with significant reduction in intensity of the broad band at 390 nm which additionally reveals the typical absorption bands of the pyrene group at 339 and 355 nm.¹⁷

All these changes are consistent with displacement of the BTD ligand by CO and the formation of complex $[\text{Ru}(\text{CH}=\text{CHPyr-1})\text{Cl}(\text{CO})_2(\text{PPh}_3)_2]$ (**2**) (Scheme 1). Suitable crystals of **2** for X-ray single-crystal diffraction studies were obtained by diethyl ether diffusion onto a dichloromethane solution of **1** under an atmosphere of CO. Figure 2 shows a plot of **2** which reveals the presence of a CO molecule *trans* to the pyrenylvinyl ligand due to the displacement of the BTD group, supporting the proposed mechanism.

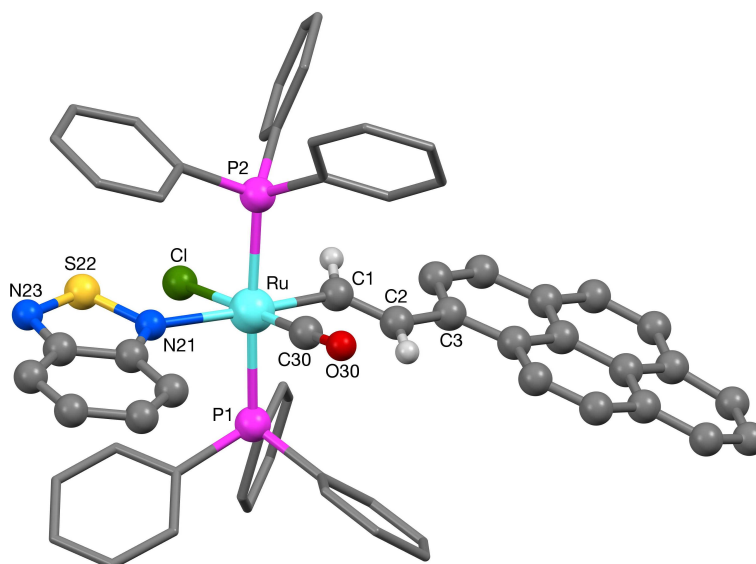


Figure 1. Crystal structure of [Ru(CH=CHPyr-1)Cl(CO)(BTD)(PPh₃)₂] (**1**). Selected bond lengths [Å] and angles [°]: Ru-C30 1.824(3), Ru-C1 2.048(3), Ru-N21 2.238(3), Ru-P1 2.4064(7), Ru-P2 2.4099(6), Ru-Cl 2.4663(7); O30-C30-Ru 178.2(3), C30-Ru-P1 92.25(8), N21-Ru-P2 92.35(6), C30-Ru-Cl 178.60(8), C1-Ru-N21 171.45(11).

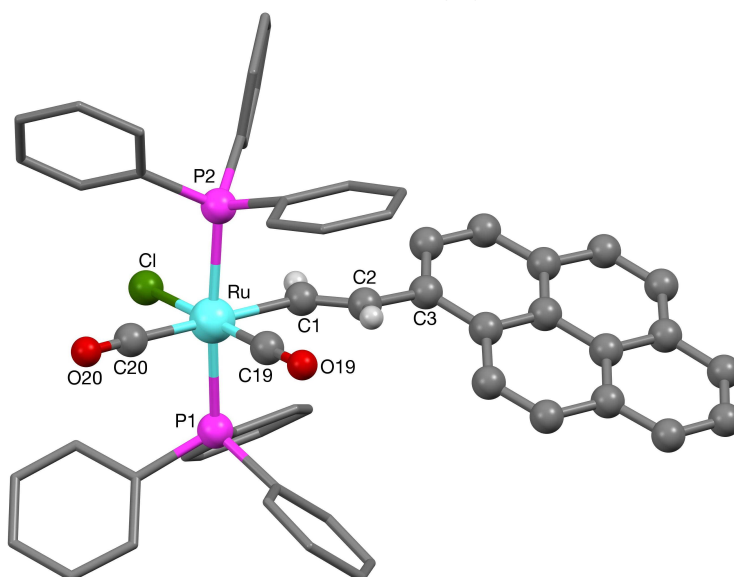


Figure 2. Crystal structure of [Ru(CH=CHPyr-1)Cl(CO)₂(PPh₃)₂] (**2**). Selected bond lengths [Å] and angles [°]: Ru-C19 1.857(2), Ru-C20 1.957(2), Ru-C1 2.104(2), Ru-P1 2.4126(5), Ru-P2 2.4060(5), Ru-Cl 2.4472(5); O19-C19-Ru 177.95(19), O20-C20-Ru 175.49(19), C19-Ru-P1 92.49(6), C19-Ru-Cl 175.94(6), C20-Ru-C1 178.37(8), C20-Ru-P2 93.09(6).

Moreover, the displacement of the BTD ligand by CO also results in the recovery of the fluorescence emission of the pyrene group. Thus, whereas **1** is very weakly fluorescent in methanol ($\lambda_{\text{exc}} = 355 \text{ nm}$, $\lambda_{\text{em}} = 458 \text{ nm}$) formation of **2** results in a remarkable 36-fold increase in emission. This can be seen in Figure 3 which shows the effect of bubbling increasing volumes of CO through a methanolic solution of compound **1**. Further experiments demonstrated that a similar chromo-fluorogenic response from **1** in the presence of CO was observed in methanol:water 1:1 v/v solutions (complex **1** is not soluble in higher proportions of water). Titration experiments with carbon monoxide in methanol:water 1:1 v/v allowed the determination of a limit of detection (LOD) as low as 1 ppb. The turn-on fluorescence is tentatively explained by the fact that BTD displacement eliminates the electron transfer between pyrenylvinyl and BTD ligands in **1** resulting in a revival of the emission.

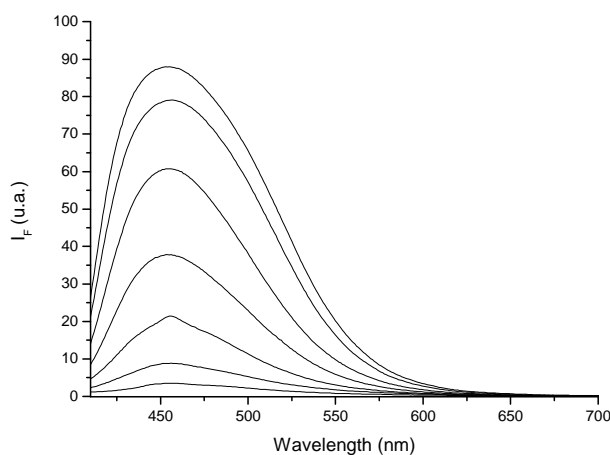


Figure 3. Turn-on fluorescence response ($\lambda_{\text{ex}} = 355 \text{ nm}$) of a $1 \times 10^{-4} \text{ mol dm}^{-3}$ methanol solution of **1** upon addition of increasing volumes of CO (0, 0.03, 0.08, 0.2, 0.5, 0.7, 1 mL).

Motivated by the favorable chromo-fluorogenic sensing features of **1** observed in solution, the system was developed with a view to exploiting the potential use of this compound for CO detection in air. With this aim in mind, compound **1** was adsorbed on silica gel resulting in an orange solid. In a typical test, this colored silica support containing the ruthenium probe was exposed to air containing

different concentrations of carbon monoxide. An instantaneous and remarkable modulation of color from orange to yellow was observed, consistent with the formation of **2** (Figure 4). From further titration studies a detection limit as low as 0.6 ppb of CO in air was obtained. Furthermore, a visual color change to the naked eye from orange to yellow was observed for CO concentrations in air as low as 5 ppb. At concentrations of ca. 100 ppm, which is the concentration at which CO becomes toxic for short-term exposure to humans, the color change is extremely clear (see Figure 4).

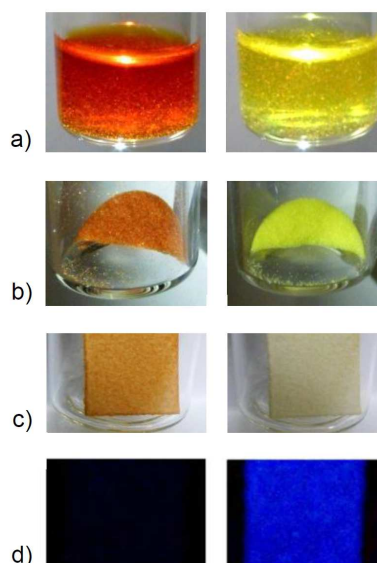


Figure 4. Summary of the visual color and/or fluorescence changes observed by the naked eye in the absence (left) and in the presence of 100 ppm of CO (right) for compound **1** a) dissolved in dichloromethane, b) adsorbed on silica gel, c) deposited on cellulose paper, and d) deposited on cellulose paper and detected by fluorescence emission under UV irradiation at 355 nm.

Furthermore, the chromogenic response to CO in air using **1** adsorbed on silica gel was found to be highly selective over other gases tested. For instance no color changes were found in the presence of Ar, N₂, O₂, CO₂, H₂S, and coordinating gases such as SO₂ and NO_x nor in the presence of common volatile organic compounds such as chloroform, formaldehyde, acetone, ethanol, toluene, and

hexane. Only acetonitrile induced some evident color change to yellow, but only at concentrations of ca. 5000 ppm. Importantly, in terms of potential applications (where steam may be present), exposure of **1** to water-saturated air did not trigger any chromogenic response.

These data show silica to be a simple and effective support for the chromogenic detection of CO in air using complex **1**. However, the fluorogenic response observed for **1** in the presence of carbon monoxide was relatively poor when using silica as the support. In contrast, **1** was found to display a clear turn-on emission enhancement at 495 nm in the presence of carbon monoxide when adsorbed on strips of cellulose paper. This support also offers many practical benefits, as it avoids the need for silica and is easier to handle. It is also compatible with simple optoelectronic devices which can convert color changes into numerical readings.^{9c} Using cellulose paper the response of the probe was studied by monitoring the emission changes upon exposure to increasing concentrations of CO and a remarkable LOD of 0.7 ppb was calculated from these experiments. A clear optical response to the naked eye can also be observed for concentrations of ca. 90 ppm (see Figure 4) using a conventional UV lamp, or simply the readily apparent color change. Complex **1** is also highly selective to CO on this support and it was confirmed that no changes in color or in emission were observed in the presence of Ar, N₂, O₂, CO₂, SO₂, NO_x, H₂S, and common volatile organic compounds (e.g., chloroform, formaldehyde, acetone, ethanol, toluene, and hexane).

In summary, we report the design and use of a ruthenium(II) complex (**1**) for the simple, selective chromo-fluorogenic detection of carbon monoxide. To our knowledge, this is the first complex capable of both chromogenic or fluorogenic sensing of CO in air. In addition, the combination of two sensing modalities allows both simple visible detection as well as greater sensitivity when desired. The probe shows a color change visible to the naked eye at CO concentrations of 5 ppb and a remarkably clear change from orange to yellow at CO concentrations of 100 ppm in air. This serves as a clear warning at levels which become toxic on prolonged exposure to the gas. Moreover, **1** also displays a turn-on fluorescence

emission in the presence of carbon monoxide. Both the color and turn-on emission modulations observed are highly selective and due to a displacement of the BTD ligand in **1** by CO to yield complex **2**. This exceptionally high selectivity for CO over water vapor is of crucial importance in the potential application of this system in a domestic setting where steam is present (a shortcoming of commercial devices). The high-yielding and straightforward synthetic procedure used to prepare **1** in air, coupled with the commercial availability and relatively low cost of ruthenium and other reagents, render compound **1** both accessible and inexpensive. These attributes make this system suitable for implementation in an easy-to-use portable optoelectronic device,^{9c} allowing **1** to be applied as an efficient chemosensor for the simple chromo-fluorogenic detection of this colorless and odorless killer.

Associated Content

Supporting Information. General considerations. Instrumentation. Synthesis of [Ru(CH=CHPyr-1)Cl(CO)(BTD)(PPh₃)₂] (**1**) and [Ru(CH=CHPyr-1)Cl(CO)₂(PPh₃)₂] (**2**), silica gel immobilization of complex **1**, preparation of cellulose probe of **1**, reactivity of **1** with CO, crystallographic data and structure of **1** and **2**, selected geometric data for compounds **1** and **2** at 173 K, fluorescence calibration curve for **1** in aqueous methanol solution and response upon addition of CO, Rehm-Weller calculations, sensitivity studies with **1** adsorbed on silica upon addition of CO, selectivity studies with **1** adsorbed on silica, and sensitivity studies with **1** deposited on cellulose strip upon addition of CO. This material is available free of charge via the Internet at <http://pubs.acs.org>.

Author Information

Corresponding Author

rmaez@qim.upv.es; j.wilton-ely@imperial.ac.uk.

Notes

The authors declare no competing financial interest.

Acknowledgment

Financial support from the Spanish Government (project MAT2012-38429-C04) and the Generalitat Valenciana (project PROMETEO/2009/016) is gratefully acknowledged. M.E.M is grateful to the Spanish Ministerio de Ciencia e Innovación for an FPU grant. J.D.E.T.W.-E. and A. T. acknowledge the Leverhulme Trust for a grant (RPG-2012-634).

References

1. (a) Wilkinson, L. J.; Waring, R. H.; Steventon, G. B.; Mitchell, S. C. *Molecules of Death. Carbon Monoxide: The Silent Killer*, 2nd ed., Imperial College Press, London, **2007**, p. 37. (b) Rajiah, K.; Mathew, E. M. *Afr. J. Pharm. Pharmacol.* **2011**, *5*, 259. (c) Normand, J. -C.; Durand, C.; Delafosse, B. *Arch. Prof. Mal. Environ.* **2011**, *72*, 240.
2. (a) <http://www.testo.com>. (b) <http://www.figarosensor.com>. (c) Gutmacher, D.; Foelml, C.; Vollenweider, W.; Hofer, U.; Wöllenstein, J. *Procedia Eng.* **2011**, *25*, 1121. (d) <http://www.intlsensor.com>. (e) Kaminski, C.; Poll, A. *Electrochemical or Solid State H₂S Sensors: Which is Right For You?* InTech, USA, **1985**, p. 55.
3. (a) Wolfrum, J. *Proc. Combust. Inst.* **1998**, *27*, 1. (b) Cho, K. -H.; Lee, S. -W.; Lee, J. -H.; Choi, K. -S. *Anal. Sci. Technol.* **2000**, *13*, 222. (c) <http://www.draeger.com>.
4. (a) Wang, B.; Zhao, Y.; Yu, D.; Hu, L. M.; Cao, J. S.; Gao, F. L.; Liu, Y.; Wang, L. J. *Chin. Sci. Bull.* **2010**, *55*, 228. (b) Ge, H.; Liu, J. *Sens. Actuators B* **2006**, *117*, 408.
5. Itou, M.; Araki, Y.; Ito, O.; Kido, H. *Inorg. Chem.* **2006**, *45*, 6114.
6. Gulino, A.; Gupta, T.; Altman, M.; Lo Schiavo, S.; Mineo, P. G.; Fragalà, I. L.; Evmenenko, G.; Dutta, P.; Van der Boom, M. E. *Chem. Commun.* **2008**, 2900.
7. Paul, S.; Amalraj, F.; Radhakrishnana, S. *Synth. Met.* **2009**, *159*, 1019.
8. Benito-Garagorri, D.; Puchberger, M.; Mereiter, K.; Kirchner, K. *Angew. Chem. Int. Ed.* **2008**, *47*, 9142.
9. (a) Esteban, J.; Ros-Lis, J. V.; Martínez-Máñez, R.; Marcos, M. D.; Moragues, M. E.; Soto, J.; Sancenón, F. *Angew. Chem. Int. Ed.* **2010**, *49*, 4934. (b) Moragues, M. E.; Esteban, J.; Ros-Lis, J. V.; Martínez-Máñez, R.; Marcos, M. D.; Martínez, M.; Soto, J.; Sancenón, F. *J. Am. Chem. Soc.* **2011**, *133*, 1576. (c) Moragues, M. E.; Montes-Robles, R.; Ros-Lis, J. V.; Alcañiz, M.; Ibañez, J.;

- Pardo, T.; Martínez-Máñez, R. *Sens. Actuators B* **2014**, 191, 257. (d) Alba, M.; Pazos-Perez, N.; Vaz, B.; Formentin, P.; Tebbe, M.; Correa-Duarte, M. A.; Granero, P.; Ferré-Borrull, J.; Alvarez, R.; Pallares, J.; Fery, A.; de Lera, A. R.; Marsal, L. F.; Alvarez-Puebla, R. A. *Angew. Chem. Int. Ed.* **2013**, 52, 6459. (e) Courbat, J.; Pascu, M.; Gutmacher, D.; Briand, D.; Wöllenstein, J.; Hofer, U.; Severin, K.; de Rooij, N. F. *Procedia Engineering* **2011**, 25, 1329.
10. Wang, J.; Karpus, J.; Zhao, B. S.; Luo, Z.; Chen, P. R.; He, C. *Angew. Chem. Int. Ed.* **2012**, 51, 9652.
11. Michel, B. W.; Lippert, A. R.; Chang, C. J. *J. Am. Chem. Soc.* **2012**, 134, 15668.
12. (a) Loumrhari, H.; Ros, J.; Torres, M. R.; Santos, A.; Echavarren, A. M. *J. Organomet. Chem.* **1991**, 411, 255. (b) Harris, M. C. J.; Hill, A. F. *Organometallics* **1991**, 10, 3903.
13. (a) Torres, M. R.; Vegas, A.; Santos, A.; Ros, J. *J. Organomet. Chem.* **1986**, 309, 169. (b) Alcock, N. W.; Cartwright, J.; Hill, A. F.; Marcellin, M.; Rawles, H. M. *J. Chem. Soc., Chem. Commun.* **1995**, 369.
14. (a) Vaska, L. *J. Am. Chem. Soc.* **1964**, 86, 1943. (b) Schunn, R. A.; Wonchoba, E. R.; Wilkinson, G. *Inorg. Synth.* **1972**, 13, 131.
15. (a) Harris, M. C. J.; Hill, A. F.; *J. Organomet. Chem.* **1992**, 438, 209. (b) Herberhold, M.; Hill, A. F. *J. Organomet. Chem.* **1989**, 377, 151. (c) Alcock, N. W.; Hill, A. F.; Roe, M. S. *J. Chem. Soc., Dalton Trans.*, **1990**, 1737.
16. Maurer, J.; Linseis, M.; Sarkar, B.; Schwederski, B.; Niemeyer, M.; Kaim, W.; Zális, S.; Anson, C.; Zabel, M.; Winter, R. F. *J. Am. Chem. Soc.* **2008**, 130, 259.
17. Marsh, N. D.; Mikolajczak, C. J.; Wornat, M. J. *Spectrochimica Acta Part A*, **2000**, 56, 1499.

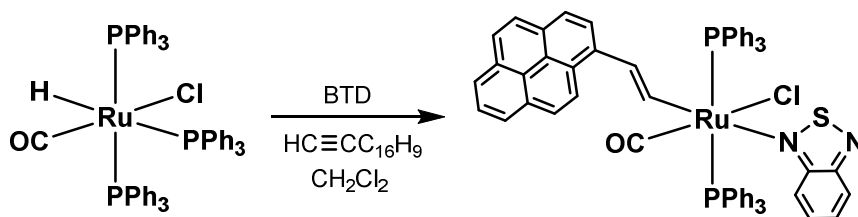
SUPPORTING INFORMATION

A chromo-fluorogenic synthetic “canary” for CO detection based on a pyrenylvinyl ruthenium(II) complex

María E. Moragues, Anita Toscani, Félix Sancenón, Ramón Martínez-Máñez,* Andrew J. P. White, James D. E. T. Wilton-Ely.*

General considerations. The complex [RuHCl(CO)(PPh₃)₃] was prepared by a published procedure.^{S1} The chemicals 1-ethynylpyrene and 2,1,3-benzothiadiazole were provided by Alfa-Aesar and Sigma-Aldrich, respectively. Tris(2,2'-bipyridyl)dichlororuthenium(II) hexahydrate was purchased from Sigma-Aldrich and used as a reference compound for quantum yield calculations. All solvents were of analytical grade. Solvent mixtures are volume/volume mixtures. Solvents used for UV-Vis and fluorescence measurements were thoroughly degassed with N₂. All experiments and manipulations of compounds were conducted in air, unless otherwise specified. Carbon monoxide was provided by a commercially available CO cylinder. The procedures given provide materials of sufficient purity for synthetic and spectroscopic purposes.

Instrumentation. NMR spectroscopy was performed at 25°C using a Bruker AV400 spectrometer in CDCl₃ unless stated otherwise. Chemical shifts are reported in ppm and coupling constants (*J*) are in Hertz. Elemental analysis data were obtained by London Metropolitan University. Mass spectrometry analyses were performed at the Servei d'Espectrometria de Masses of the Universitat de València, Spain, on a Quadrupole time of flight (QqTOF) 5600 system (Applied Biosystems-MDS Sciex) spectrometer for high resolution mass spectra. The HRMS was operated in positive mode under the following conditions: Gas1 35 psi, GS2 35, CUR 25, temperature 450 °C, ion spray, voltage 5500 V. UV-Vis spectra were recorded using a Jasco V-650 spectrophotometer equipped with a diffuse reflectance sphere (model ISV-722) for measurements on solids. In the latter case, measurements were conducted at room temperature over a wavelength range of 350-800 nm with a wavelength step of 1 nm. Fluorescence measurements were carried out using a Jasco FP-8500 spectrophotometer. Carbon monoxide concentrations were measured using an ambient carbon monoxide analyzer (Testo 315-2 model 0632 0317), properly validated with an ISO calibration certificate issued by Instrumentos Testo, Cabrils, Spain.

Synthesis of [Ru(CH=CHPyr-1)Cl(CO)(BTD)(PPh₃)₂] (1)

Scheme S1. Synthesis of compound [Ru(CH=CHPyr-1)Cl(CO)(BTD)(PPh₃)₂] (1).

2,1,3-benzothiadiazole (BTD, 25 mg, 0.184 mmol) was added to a dichloromethane (10 mL) solution of [RuHCl(CO)(PPh₃)₃] (101.8 mg, 0.107 mmol). The mixture was stirred at room temperature until a color change from colorless to orange was observed. Then 1-ethynylpyrene (36.5 mg, 0.161 mmol) was added and the reaction mixture was stirred at room temperature for 1 h. Methanol (25 mL) was then added and the mixture was left to stand for 30 min. On slow concentration under reduced pressure and subsequent cooling at -20 °C, red-orange crystals formed. These were isolated by filtration, washed with ethanol (2 x 10 mL) and dried under vacuum. Yield: 105.5 mg (96%). X-ray quality crystals of [Ru(CH=CHPyr-1)Cl(CO)(BTD)(PPh₃)₂] (1) were obtained by recrystallization by vapor diffusion (diethyl ether/dichloromethane). NMR (CDCl₃, 25 °C): ¹H NMR δ 9.06 (d, *J* = 15 Hz, 1H, RuCH=C), 8.05 (m, 2H, BTD), 7.95-7.70 (m, 9H, pyrenyl), 7.93 (m, 2H, BTD), 7.64-7.18 (m, 30H, PPh₃), 7.01 (d, *J* = 15 Hz, 1H, RuC=CH); ³¹P NMR δ 29.4 (s, PPh₃). HRMS: Calcd. for C₆₁H₄₆ClN₂OP₂RuS⁺: *m/z* 1054.1616; Found: *m/z* 1054.0870. EA: Calcd. for C₆₁H₄₅ClN₂OP₂RuS: C 69.5, H 4.3, N 2.7%; Found: C 69.4, H 4.5, N 2.6%.

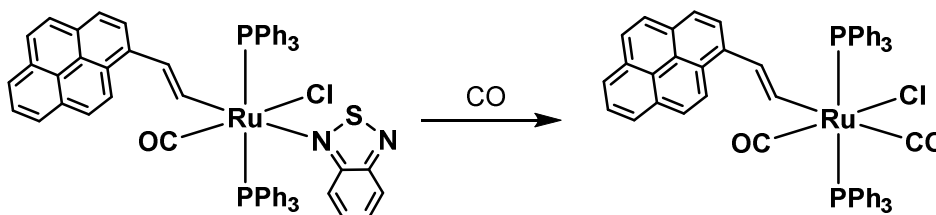
Silica gel immobilization of complex 1. Complex 1 (5 mg) was dissolved in the minimum amount of chloroform (5 mL). This solution was then added to silica gel (150 mg), yielding 1 as an orange solid after evaporation of chloroform (see Figure S1).



Figure S1. From left to right: color of ruthenium compound **1**, silica-adsorbed **1**, and the silica-adsorbed solid upon reaction with CO (to form **2**).

Preparation of cellulose probe of 1. Complex **1** was supported on cellulose paper for chromatographic use (Whatman Grade no. 3MM Chromatography Paper). Probes were prepared in simple fashion by dropping 0.2 mL of a solution of **1** in dichloromethane (5 mg/mL) on the cellulose paper strip and then were dried in air under ambient conditions.

Reactivity of 1 with CO.



Scheme S2. Reactivity of **1** with CO to give dicarbonyl complex **2**.

Air samples containing different concentrations of CO were bubbled through methanol : water, 12:10 (v/v) solutions of **1** (2 mL, 1.9×10^{-3} mol dm⁻³) to yield a remarkable color modulation from red to bright yellow (see Figure S2). These changes are consistent with coordination of CO and the concomitant displacement of the BTD molecule to give product **2**. Compound **2** was prepared on a larger scale by treating a dichloromethane solution (10 mL) of **1** (7 mg, 0.007

mmol) with a stream of carbon monoxide for 1 minute. Ethanol (5 mL) was added and the precipitate isolated by rotary evaporation. The yellow product was filtered, washed with ethanol (10 mL) and dried. Yield: 6.4 mg (97%). X-ray quality crystals of $[\text{Ru}(\text{CH}=\text{CHPyr}-1)\text{Cl}(\text{CO})_2(\text{PPh}_3)_2]$ (**2**) were obtained by vapor diffusion (diethyl ether/dichloromethane) under a CO atmosphere. NMR (CDCl_3 , 25 °C): ^1H NMR δ 8.53 (d, $J = 15$ Hz, 1H, $\text{RuCH}=\text{C}$), 8.10-7.83 (m, 9H, pyrenyl), 7.76-7.30 (m, 30H, PPh_3), 7.13 (d, $J = 15$ Hz, 1H, $\text{RuC}=\text{CH}$); ^{31}P NMR δ 23.7 (s, PPh_3). MS(ES⁺): Calcd. For $\text{C}_{56}\text{H}_{41}\text{ClO}_2\text{P}_2\text{Ru}$: m/z 944.39; Found: m/z 945.4157. EA: Calcd. for $\text{C}_{56}\text{H}_{41}\text{ClO}_2\text{P}_2\text{Ru}$: C 71.1, H 4.3%; Found: C 70.8, H 4.4%.

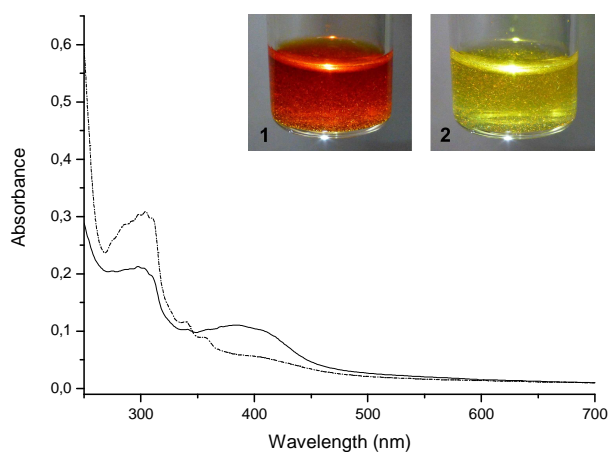


Figure S2. UV-Vis spectra of probe **1** (1×10^{-4} mol dm^{-3}) in methanol (solid line) and compound **2** obtained upon displacement of BTD by CO coordination in **1** (dashed line).

Crystallography. Crystals of compounds **1** and **2** were grown by vapor diffusion of diethyl ether onto dichloromethane solutions of the complexes. Suitable crystals were mounted on a fiber and measured on an Oxford Diffraction Xcalibur 3 diffractometer.

Crystal data for 1: $C_{61}H_{45}ClN_2OP_2RuS$, $M = 1052.51$, monoclinic, Pn (no. 7), $a = 10.14297(19)$, $b = 15.8652(3)$, $c = 15.3256(3)$ Å, $\beta = 93.3717(17)^\circ$, $V = 2461.93(8)$ Å³, $Z = 2$, $\rho_{\text{calcd}} = 1.420$ g cm⁻³, $\mu(\text{Mo}_{K\alpha}) = 0.526$ mm⁻¹, $T = 173$ K, orange blocky needles, 10246 independent measured reflections ($R_{\text{int}} = 0.0296$), F^2 refinement,² $R_1(\text{obs}) = 0.0289$, $wR_2(\text{all}) = 0.0583$, 9260 independent observed absorption-corrected reflections [$|F_o| > 4\sigma(|F_o|)$], $2\theta_{\text{max}} = 59^\circ$], 622 parameters. The absolute structure of **1** was determined by a combination of R -factor tests [$R_1^+ = 0.0289$, $R_1^- = 0.0346$] and by use of the Flack parameter [$x^+ = 0.000(15)$, $x^- = 1.028(15)$]. CCDC 988548.

Crystal data for 2: $C_{56}H_{41}ClO_2P_2Ru \cdot 0.5(\text{CH}_2\text{Cl}_2)$, $M = 986.81$, triclinic, $P-1$ (no. 2), $a = 10.2934(2)$, $b = 14.2153(4)$, $c = 17.9941(5)$ Å, $\alpha = 101.858(3)$, $\beta = 99.784(2)$, $\gamma = 104.373(2)^\circ$, $V = 2427.39(12)$ Å³, $Z = 2$, $\rho_{\text{calcd}} = 1.350$ g cm⁻³, $\mu(\text{Mo}_{K\alpha}) = 0.540$ mm⁻¹, $T = 173$ K, yellow tabular needles, 10499 independent measured reflections ($R_{\text{int}} = 0.0186$), F^2 refinement,^{S2} $R_1(\text{obs}) = 0.0309$, $wR_2(\text{all}) = 0.0885$, 9115 independent observed absorption-corrected reflections [$|F_o| > 4\sigma(|F_o|)$], $2\theta_{\text{max}} = 58^\circ$], 559 parameters. CCDC 988549.

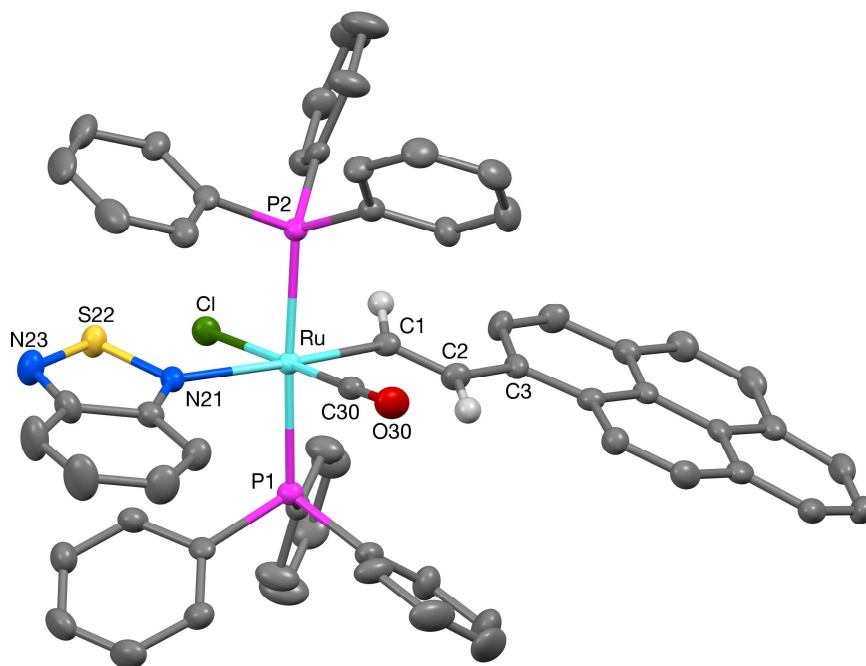


Figure S3. The crystal structure of [Ru(CH=CHPyr-1)Cl(CO)(BTD)(PPh₃)₂] (**1**) with 50% probability ellipsoids.

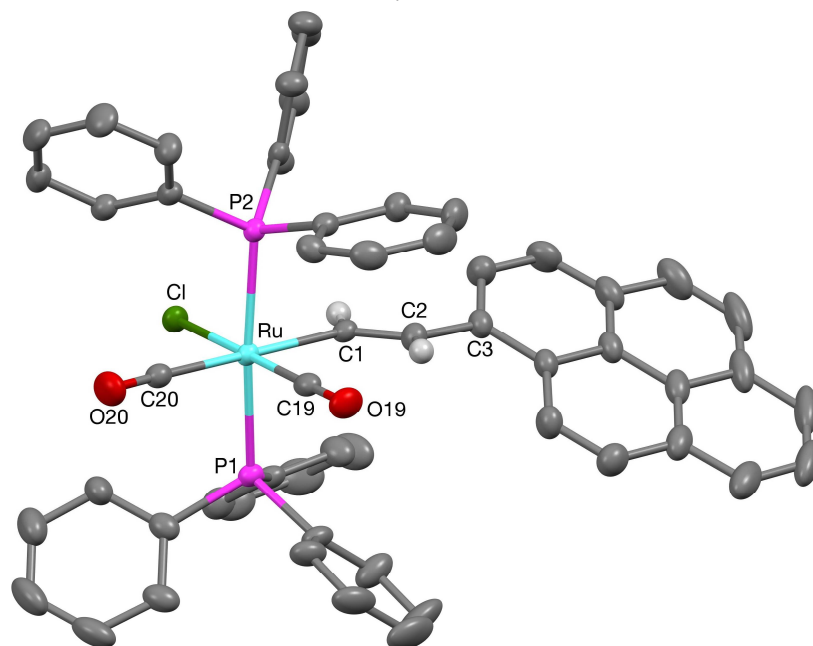


Figure S4. The crystal structure of [Ru(CH=CHPyr-1)Cl(CO)₂(PPh₃)₂] (**2**) with 50% probability ellipsoids.

The included solvent in the structure of **2** was found to be highly disordered, and the best approach to handling this electron density was found to be the SQUEEZE routine of PLATON.^{S3} This suggested a total of 36 electrons per unit cell, equivalent to 18 electrons per complex. During the synthesis and crystallization of the compound, both dichloromethane [CH₂Cl₂, 42 electrons] and ethanol [C₂H₆O, 26 electrons] were employed, but unfortunately before the use of SQUEEZE the electron density distribution did not clearly favor either. However, as dichloromethane was the most recently used, and as the crystals showed some signs of desolvation, dichloromethane was assumed as the solvent present. 50% Dichloromethane equates to 21 electrons, and so this was used as the solvent present. The atom list for the asymmetric unit is thus low by 0.5(CH₂Cl₂), and that for the unit cell is low by one molecule of CH₂Cl₂.

Table S1. Selected geometric data for compound **1** at 173 K.

Selected bond lengths [Å]			
Ru-C(30)	1.824(3)	C(1)-C(2)	1.323(4)
Ru-C(1)	2.048(3)	C(2)-C(3)	1.471(4)
Ru-N(21)	2.238(3)	C(3)-C(4)	1.410(4)
Ru-P(1)	2.4064(7)	C(3)-C(16)	1.416(4)
Ru-P(2)	2.4099(6)	C(4)-C(5)	1.370(4)
Ru-Cl	2.4663(7)	C(5)-C(6)	1.394(4)
P(1)-C(31)	1.833(3)	N(21)-C(29)	1.346(4)
P(1)-C(43)	1.835(3)	N(21)-S(22)	1.649(2)
P(1)-C(37)	1.841(3)	S(22)-N(23)	1.610(3)
		N(23)-C(24)	1.329(4)
P(2)-C(61)	1.818(3)	C(24)-C(25)	1.410(4)
P(2)-C(55)	1.837(3)	C(24)-C(29)	1.444(4)
P(2)-C(49)	1.852(3)	C(25)-C(26)	1.358(5)
		C(26)-C(27)	1.422(4)
C(30)-O(30)	1.146(3)	C(27)-C(28)	1.352(4)

Selected bond angles [°]			
C(30)-Ru-C(1)	88.71(12)	O(30)-C(30)-Ru	178.2(3)
C(30)-Ru-N(21)	99.83(10)	C(1)-Ru-N(21)	171.45(11)
C(30)-Ru-P(1)	92.25(8)	C(1)-Ru-P(1)	87.14(7)
C(30)-Ru-P(2)	88.48(8)	C(1)-Ru-P(2)	88.27(7)
C(30)-Ru-Cl	178.60(8)	C(1)-Ru-Cl	90.60(8)
N(21)-Ru-P(1)	92.07(6)	P(1)-Ru-Cl	86.50(2)
N(21)-Ru-P(2)	92.35(6)	P(2)-Ru-Cl	92.72(2)
N(21)-Ru-Cl	80.85(7)	P(1)-Ru-P(2)	175.34(3)
C(31)-P(1)-C(43)	104.27(12)	C(61)-P(2)-C(55)	104.44(13)
C(31)-P(1)-C(37)	100.72(12)	C(61)-P(2)-C(49)	104.12(13)
C(43)-P(1)-C(37)	102.29(12)	C(55)-P(2)-C(49)	100.04(12)
C(31)-P(1)-Ru	114.66(8)	C(61)-P(2)-Ru	112.14(8)
C(43)-P(1)-Ru	115.15(8)	C(55)-P(2)-Ru	114.71(8)
C(37)-P(1)-Ru	117.71(9)	C(49)-P(2)-Ru	119.58(9)
C(2)-C(1)-Ru	133.2(2)	C(29)-N(21)-S(22)	106.80(19)
C(1)-C(2)-C(3)	127.0(3)	C(29)-N(21)-Ru	132.04(19)
C(4)-C(3)-C(16)	117.0(3)	S(22)-N(21)-Ru	121.11(14)
C(4)-C(3)-C(2)	120.6(3)	N(23)-S(22)-N(21)	99.61(13)
C(16)-C(3)-C(2)	122.3(3)	C(24)-N(23)-S(22)	107.6(2)
C(36)-C(31)-C(32)	118.3(2)	N(23)-C(24)-C(25)	126.0(3)
C(36)-C(31)-P(1)	125.3(2)	N(23)-C(24)-C(29)	113.9(3)
C(32)-C(31)-P(1)	116.3(2)	C(25)-C(24)-C(29)	120.1(3)
C(50)-C(49)-C(54)	118.9(3)	N(21)-C(29)-C(28)	128.5(3)
C(50)-C(49)-P(2)	122.3(2)	N(21)-C(29)-C(24)	112.1(3)
C(54)-C(49)-P(2)	118.8(2)	C(28)-C(29)-C(24)	119.4(3)

Table S2. Selected geometric data for compound **2** at 173 K.

Selected bond lengths [Å]			
Ru-C(19)	1.857(2)	C(1)-C(2)	1.331(3)
Ru-C(20)	1.957(2)	C(2)-C(3)	1.471(3)
Ru-C(1)	2.104(2)	C(3)-C(4)	1.394(3)
Ru-P(1)	2.4126(5)	C(3)-C(16)	1.421(3)
Ru-P(2)	2.4060(5)	C(4)-C(5)	1.382(3)
Ru-Cl	2.4472(5)	C(5)-C(6)	1.385(4)
P(1)-C(27)	1.829(2)	P(2)-C(45)	1.824(2)
P(1)-C(21)	1.835(2)	P(2)-C(51)	1.832(2)
P(1)-C(33)	1.839(2)	P(2)-C(39)	1.840(2)
C(19)-O(19)	1.141(2)	C(20)-O(20)	1.132(3)
Selected bond angles [°]			
O(19)-C(19)-Ru	177.95(19)	O(20)-C(20)-Ru	175.49(19)
C(19)-Ru-C(1)	86.84(8)	C(20)-Ru-C(1)	178.37(8)
C(19)-Ru-C(20)	91.73(9)	C(20)-Ru-P(1)	93.72(6)
C(19)-Ru-P(1)	92.49(6)	C(20)-Ru-P(2)	93.09(6)
C(19)-Ru-P(2)	89.52(6)	C(20)-Ru-Cl	91.48(6)
C(19)-Ru-Cl	175.94(6)		
C(1)-Ru-P(1)	87.15(6)	P(1)-Ru-Cl	84.819(18)
C(1)-Ru-P(2)	86.10(6)	P(2)-Ru-Cl	92.796(18)
C(1)-Ru-Cl	89.98(6)	P(2)-Ru-P(1)	172.838(18)
C(27)-P(1)-C(21)	105.66(10)	C(45)-P(2)-C(51)	106.96(10)
C(27)-P(1)-C(33)	102.45(10)	C(45)-P(2)-C(39)	102.80(9)
C(21)-P(1)-C(33)	103.71(10)	C(51)-P(2)-C(39)	100.35(9)
C(27)-P(1)-Ru	113.38(7)	C(45)-P(2)-Ru	109.03(7)
C(21)-P(1)-Ru	116.36(7)	C(51)-P(2)-Ru	115.36(7)
C(33)-P(1)-Ru	113.85(7)	C(39)-P(2)-Ru	120.90(7)
C(2)-C(1)-Ru	128.69(16)	C(22)-C(21)-C(26)	118.6(2)
C(1)-C(2)-C(3)	126.7(2)	C(22)-C(21)-P(1)	121.35(17)
C(4)-C(3)-C(16)	118.5(2)	C(26)-C(21)-P(1)	120.06(17)
C(4)-C(3)-C(2)	121.1(2)	C(44)-C(39)-C(40)	118.87(19)
C(16)-C(3)-C(2)	120.39(19)	C(44)-C(39)-P(2)	122.22(16)
		C(40)-C(39)-P(2)	118.79(16)

Fluorescence calibration curve to 1 aqueous methanol solution response upon addition of CO.

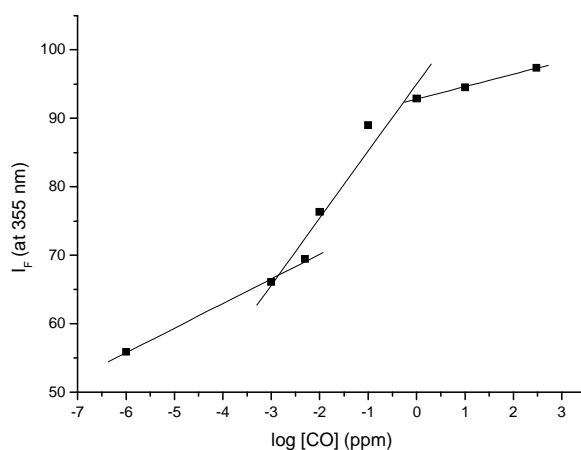


Figure S5. Calibration curve of fluorescence intensity at 458 nm ($\lambda_{\text{ex}} = 355$ nm) of methanol:water, 1:1 (v/v) solution of **1** as a function of CO concentration (0-300 ppm).

Rehm-Weller calculations. In complex **1**, the occurrence of an electron transfer process between vinylpyrene and BTD ligands is thermodynamically favorable as can be demonstrated from electrochemical and photophysical data. The free energy of the process ($\text{BTD} + \text{vinylpyrene} \rightleftharpoons \text{BTD}^- + \text{vinylpyrene}^+$) in which the vinylpyrene acts as an electron donor and the BTD as an electron acceptor can be calculated by the Rehm-Weller equation:⁵⁴

$$\Delta G = -\frac{hcN_A}{\lambda} + F[E_{\text{vinylpyrene}^+/\text{vinylpyrene}}^o - E_{\text{BTD}^-/\text{BTD}}^o]$$

where $E_{\text{vinylpyrene}^+/\text{vinylpyrene}}^o$ and $E_{\text{BTD}^-/\text{BTD}}^o$ are the literature redox potentials of the processes: $\text{vinylpyrene}^+ + 1e^- \rightarrow \text{vinylpyrene}$ (-2.48 v) and $\text{BTD} + 1e^- \rightarrow \text{BTD}^-$ (-1.56 v), respectively, and λ (458 nm) can be obtained from the emission fluorescence spectrum. Taking into account these data, ΔG is $-89.03 \text{ kJ mol}^{-1}$, indicating that the electron transfer process from the vinylpyrene to the BTD can occur. These calculations supported the fact that the weak emission observed for complex **1** is due to an electron transfer process between vinylpyrene and BTD ligands and also pointed to BTD displacement by CO as the mechanism behind the *turn on* fluorescence observed.

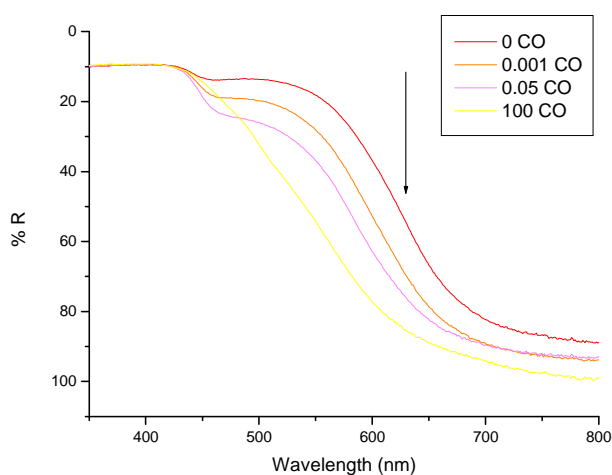
Sensitivity studies with **1 adsorbed on silica upon addition of CO.**

Figure S6. Diffuse reflectance UV-Vis spectra of silica-adsorbed **1** and the changes obtained in the presence of increasing concentration of CO.

Figure S7 shows the calculation of the detection limit, based on visual examination of the reflectance measure at a certain wavelength (474 nm) versus logarithm of CO concentration. The detection limit concurs with the inflection point of the two slopes observed for the concentration range studied.

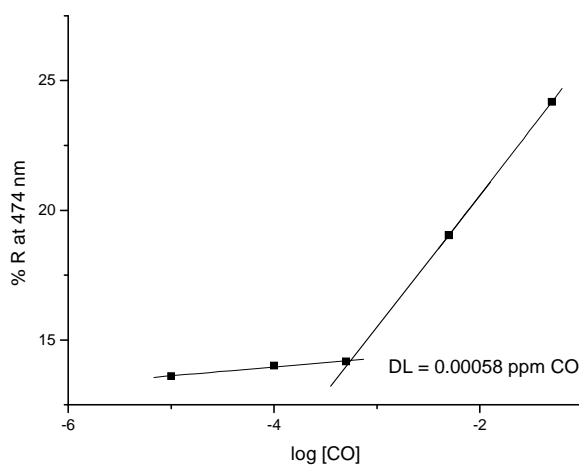


Figure S7. Detection limit of CO within the concentration range from 0 to 0.05 ppm of CO.

Selectivity studies with **1 adsorbed on silica.** Silica-adsorbed **1** showed a remarkably selective response to carbon monoxide in air. For instance, no reaction was observed in the presence of gases such as Ar, N₂, O₂, CO₂, SO₂ and NO_x (see Figure S8) at very high concentrations (up to 50,000 ppm). The same was true of H₂S at (lethal) concentrations of 200 ppm. Similarly, no color changes were observed in the presence of volatile organic compounds (see Figure S9) such as chloroform, formaldehyde, acetone, ethanol, toluene or hexane (up to 30,000 ppm). Only acetonitrile (ACN) induced some evidence of a color change to yellow, although only at concentrations of approximately 5000 ppm (see Figure S10). The reaction of **1** with ACN was found to be reversible.

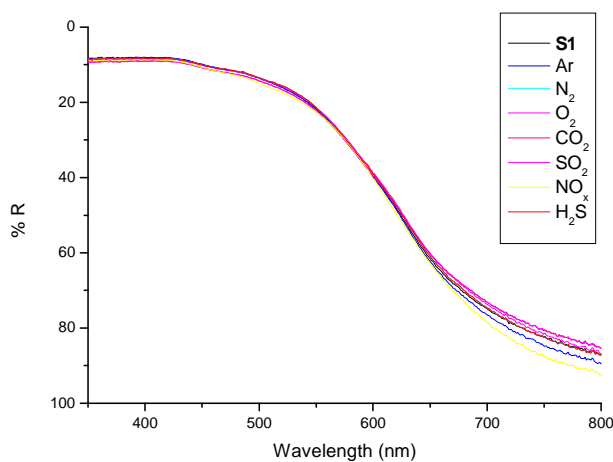


Figure S8. Diffuse reflectance UV-Vis spectra of silica-adsorbed **1** and the changes obtained in the presence of different gases.

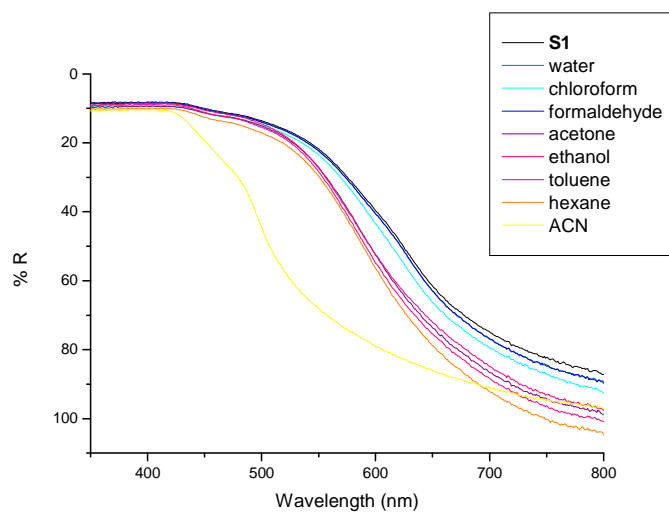


Figure S9. Diffuse reflectance UV-Vis spectra of silica-adsorbed **1** and the changes obtained in the presence of different volatile organic compounds (VOCs).

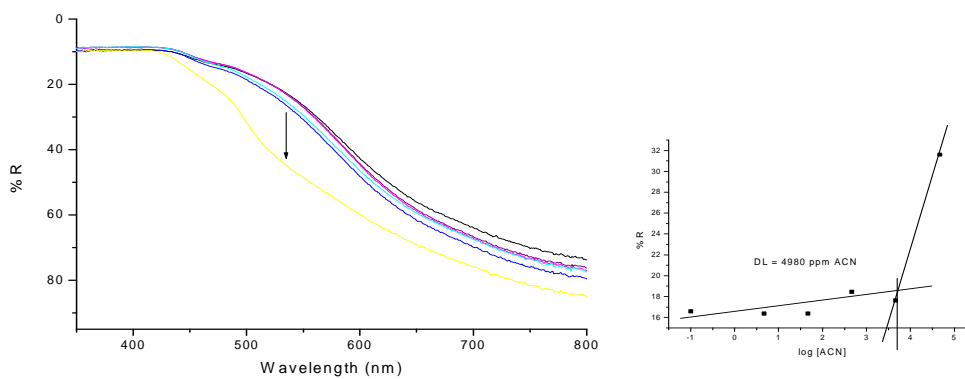


Figure S10. Diffuse reflectance UV-Vis spectra of silica-adsorbed **1** and the changes observed in the presence of air containing increasing quantities of ACN (4.6, 46, 460, 4600, 46,000 ppm). Inset: detection limit calculation from diffuse reflectance measured at 500 nm.

Sensitivity studies with 1 deposited on cellulose strip upon addition of CO.

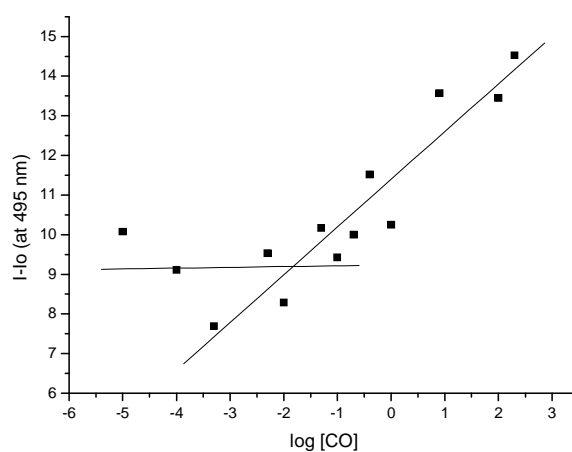


Figure S11. Emission intensity at 495 nm ($\lambda_{\text{ex}} = 382$ nm) of **1** deposited on a cellulose strip upon exposure to increasing concentrations of CO.

References

- S1. Laing, K. R.; Roper, W. R. *J. Chem. Soc. A* **1970**, 2149.
- S2. SHELXTL, Bruker AXS, Madison, WI; SHELX-97, Sheldrick, G.M. *Acta Cryst.*, **2008**, *A64*, 112-122; SHELX-2013, <http://shelx.uni-ac.gwdg.de/SHELX/index.php>.
- S3. Spek, A.L. (2008) PLATON, A Multipurpose Crystallographic Tool, Utrecht University, Utrecht, The Netherlands. See also Spek, A. L. *J. Appl. Cryst.*, **2003**, *36*, 7.
- S4. Rehm, D.; Weller, A. *Isr. J. Chem.* **1970**, *8*, 259.

5.2. Ruthenium(II) and osmium(II) alkenyl complexes for highly sensitive chromogenic sensing of carbon monoxide in air

***Ruthenium(II) and Osmium(II) Alkenyl Complexes
as Highly Sensitive and Selective Chromogenic
Probes for the Sensing of Carbon Monoxide in air***

*María E. Moragues,^{a,b,c} Anita Toscani,^d Félix Sancenón,^{a,b,c}
Paul Dingwall,^d Neil J. Brown,^d Ramón Martínez-Máñez,^{*a,b,c}
Andrew J. P. White,^d James D. E. T. Wilton-Ely^{*d}*

^a *Centro de Reconocimiento Molecular y Desarrollo Tecnológico, (IDM), Unidad Mixta Universidad Politécnica de Valencia – Universitat de València, Spain.*

^b *Departamento de Química. Universidad Politécnica de Valencia. Camino de Vera s/n. E-46022, Valencia, Spain.*

^c *CIBER de Bioingeniería, Biomateriales y Nanomedicina (CIBER-BBN).*

^d *Department of Chemistry, Imperial College London, SW7 2AZ, London, UK.*

Submitted: October 12, 2014

*(Submitted to
Chemical Science, 2014)*

Abstract

The detection of carbon monoxide in both solution and air has been achieved using simple, inexpensive systems based on the vinyl complexes $[M(\text{CH}=\text{CHR})\text{Cl}(\text{CO})(\text{BTD})(\text{PPh}_3)_2]$ (R = aryl, BTD = 2,1,3-benzothiadiazole). Depending on the nature of the vinyl group, chromogenic and fluorogenic responses signalled the presence of this odourless, tasteless, invisible and toxic gas. Chloroform solutions of the complexes underwent rapid change between easily differentiated colours when exposed to air samples containing CO. More significantly, adsorbing the complexes on silica produced colorimetric probes for the 'naked eye' detection of CO in the gas phase. Structural data for key species before and after addition of carbon monoxide were obtained by single X-ray diffraction techniques. In all cases the ruthenium and osmium vinyl complexes studied showed a highly selective response to CO with exceptionally low detection limits. Naked eye detection of CO at concentrations as low as 5 ppb in air was achieved with the onset of toxic levels (100 ppm) resulting in a remarkably clear colour change. Even greater sensitivity (1 ppb) was achieved through a 36-fold increase in turn-on emission fluorescence in the presence of carbon monoxide, both in air and in solution. This behaviour was explored computationally using TDDFT experiments. Additionally, the systems were shown to be selective for CO over all other gases tested, including water vapour and common organic solvents. Supporting the metal complexes on cellulose strips for use in an existing optoelectronic device provides numerical readings for CO concentration and an alarm.

Introduction

The selective detection of gases which are toxic at low concentrations is one of the most promising applications of optical sensors. Among such gases, carbon monoxide stands out due to its high toxicity and its common presence in both domestic and work settings as well as other environments frequented by the general public. Traditionally, electrochemical cells, solid-state sensors and thermocouples have been used to accomplish routine CO detection.

Electrochemical sensors based on metal-oxide semiconductors generally possess reasonably good resolution and measuring ranges. However, these are very sensitive to temperature and pressure.¹ In relation to solid-state CO sensors, based on ZnO and SnO₂, these require such high working temperatures that their use is restricted to specific laboratory applications.² Moreover optical sensors which have been reported use either spectrally narrowband lasers³ or non-dispersive infrared (NDIR)⁴ systems. Although currently the most accurate method to measure CO concentrations in urban air, NDIR systems are sensitive to relatively low concentrations of other common gases (interferents), such as CO₂, NO_x, hydrocarbons or water vapour. Current commercial CO detectors have to be sited carefully in environments where water vapour (steam) or particulates (smoke) are generated, such as kitchens and bathrooms, in order to avoid false alarms. These can also be triggered by the presence of solvents (from cleaning products, hairspray) or fuels (e.g., in mechanical or automotive workshops). Therefore, there is an increasing interest in the development of chemical sensor systems capable of selectively detecting the presence of carbon monoxide in air at low concentrations. In this context, colorimetric methods are especially undemanding, offering several advantages over other analytical procedures, such as real-time monitoring and the use of very simple and inexpensive instrumentation. Additionally, certain colorimetric changes, even at low concentration of analytes, can be observed by the naked eye, making chromogenic approaches unbeatable for certain applications. In the context of these factors, several chromogenic probes for CO detection have been reported recently. One of the first examples, by Ito and co-workers, uses acetonitrile solutions of an oxo-acetato-bridged triruthenium cluster. In this system, a photosensitizing electron donor (zinc tetraphenylporphyrin) controls the redox state of the metal centre, allowing the exchange of weakly coordinating solvent molecules by CO, resulting in colour changes.⁵ Another example involves the selective optical monitoring of CO by covalently immobilized bimetallic rhodium complexes on glass substrates. Despite the poorly resolved changes in colour, a detection limit as low as 2.5 ppm of CO can be determined by UV-Vis

measurements on this monolayer-based sensor.⁶ Kirchner and co-workers prepared a penta-coordinate iron diisopropylphosphino diaminopyridine pincer complex that gives rise to a clear colour change (from yellow to red) in the solid state upon exposure to CO, but only with high concentrations of the gas (1 atm). However, the generation of the resultant hexa-coordinate derivative is stereospecific and the CO binding is fully reversible.⁷ Redox polymers functionalized with porphyrins have also been used for the recognition of CO. Polypyrrole can be functionalized with tetraphenylporphyrin iron(III) chloride units and the polymer formed is able to detect CO in water/methanol solutions with a detection limit as low as 100 ppm.⁸ Very recently, sensitive and selective CO detection in air was accomplished by some of us via the use of binuclear rhodium complexes. Silica probes of these rhodium(II) complexes allowed the 'naked eye' detection of CO concentrations of around 50 ppm, resulting from a colour change on axial coordination of the CO to the metal complexes.⁹ Finally, a P-S-N iron(II) complex was reported recently which achieves the chromogenic sensing of CO (albeit only in solution). Purple acetonitrile solutions of the complex become orange on exposure to high concentrations of CO (passing a 1 atm stream of CO through the solution for 5 mins). The colour change observed is ascribed to the reversible binding of CO to form the corresponding octahedral iron monocarbonyl complex.¹⁰

In spite of the significant progress made during the past decade, developing a readily applicable and highly sensitive molecular visual detection system for CO in air remains a challenge. The design of such systems requires not only selectivity and sensitivity towards a given analyte but, in the case of highly poisonous gases such as CO, the detection process must be both rapid and reliable (stable). While the systems described above display novel and ingenious approaches to CO sensing, they all have drawbacks such as detecting CO only in solution, requiring expensive, non-portable instrumentation or showing limits of detection unsuitable for the early warning of the presence of sub-acute levels of CO in air. In addition, the relative cost, synthetic difficulty and stability of these systems are also potential issues. Lastly, in order to compete with current electronic systems,

a molecular probe must be readily integrated into a device which can display a reading and sound an alarm.

In order to understand the extent of the issues surrounding human exposure to carbon monoxide, it is helpful to describe its occurrence. Carbon monoxide is produced as a result of the incomplete burning of carbon-based fuels (i.e., propane, gasoline, kerosene, wood, coal, charcoal etc.) in inadequately vented heaters and furnaces. Carbon monoxide levels can vary widely within an enclosed or semi-enclosed area such as a domestic room, office, garage or workshop; and can also fluctuate enormously over a short period of time as conditions change. For this reason, the level of CO concentration in air is often measured using the Time-Weighted Average (TWA). This determines an average exposure to CO over time (usually expressed in parts per million, ppm). Carbon monoxide poisoning symptoms vary widely between individuals. A person exposed to relatively low carbon monoxide levels over a longer period can display only mild symptoms while actually becoming seriously poisoned. Normal fresh air contains 0-0.2 ppm carbon monoxide. The American Society of Heating Refrigeration and Air Conditioning Engineers (ASHRAE) lists a maximum allowable short term limit of 9 ppm CO. The Environmental Protection Agency (EPA)¹¹ has set two national health protection standards for CO: a 1-hour TWA of 35 ppm, and an 8-hour TWA of 9 ppm. These standards make it clear that any carbon monoxide reading over 9 ppm should be investigated and acted upon. The UK Department of Health reported in 2013 that 50 people die each year from carbon monoxide poisoning in the UK.¹² Many factors play a role in the severity of symptoms while in the body. Some health effects due to prolonged exposure to various concentrations of CO are summarized in *Table 1*. From mild to extreme CO exposure; passing through medium exposure, symptoms evolve as stated to result in headache, nausea, dizziness, fatigue, collapse, loss of consciousness and danger of death. Significantly, the less severe of these symptoms can often be mistaken for other ailments, such as mild food poisoning or dehydration, leading to prolonged exposure.

Table 1. Health effects^a of CO upon exposure to levels^b of CO considered dangerous.

Level of CO exposure (ppm)	Time exposed (hours)						
	1	2	4	8	12	16	24
35							
50							
75							
100							
200							
400							

^a The images typify the following symptoms in order of harshness: headache, nausea, dizziness, fatigue, collapse and loss of consciousness.

^b US Environmental Protection Agency standards.

Taking into account the facts mentioned above and following our interest in the design of novel chromo-fluorogenic systems,¹³ we present here the application of ruthenium(II) and osmium(II) vinyl complexes as sensitive, selective, colorimetric probes for the sensing of CO using their well-known ability to react with small molecules, such as carbon monoxide.¹⁴ We have recently reported preliminary data on the development of a chromo-fluorogenic probe based on the ruthenium(II) pyrenylvinyl complex **1** of formula $[\text{Ru}(\text{CH}=\text{CHPyr}-1)\text{Cl}(\text{CO})(\text{BTD})(\text{PPh}_3)_2]$.¹⁵ Based on the initial sensing results obtained for this ruthenium complex in terms of selectivity and sensitivity, we report herein an extended study using a set of synthetically accessible and relatively inexpensive ruthenium(II) and osmium(II) vinyl complexes of general formula $[\text{M}(\text{CH}=\text{CHR})\text{Cl}(\text{CO})(\text{BTD})(\text{PPh}_3)_2]$ containing the 2,1,3-benzothiadiazole (BTD)

chromophore and various different vinyl ligands. For these compounds the colour modulations observed in the presence of carbon monoxide, induced by the displacement of the BTD ligand upon coordination of the CO group, have been studied spectroscopically and computationally.

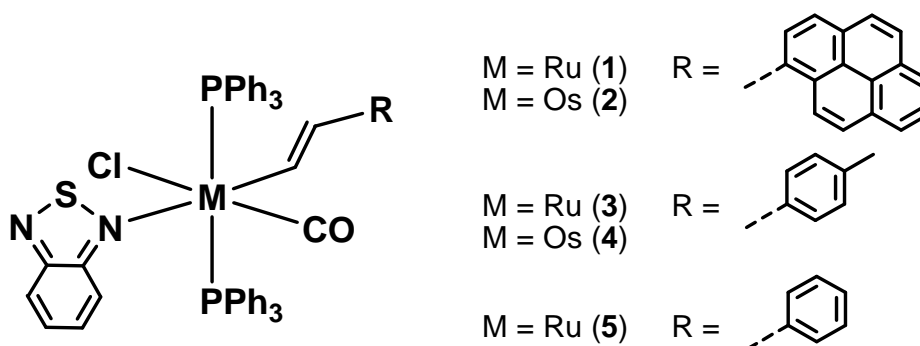
Results and Discussion

Design of the probe complexes. The design of the chromogenic probes involves the use of brightly coloured σ -vinyl 18-electron complexes and their well-documented ability to react with neutral, two-electron donors, such as carbon monoxide. The vinyl ligand is an important member of the σ -organyl ligand family, and is believed to be present as an intermediate in many catalytic reactions. Well-established synthetic routes such as hydrometallation and the reaction of coordinated alkynes with electrophiles or nucleophiles are known to yield vinyl complexes of many metals, often those belonging to group 8.¹⁶ Since the discovery of hydrometallation of alkynes by the compounds $[\text{RuHCl}(\text{CO})(\text{PPr}^i_3)_2]$ and $[\text{RuHCl}(\text{CO})(\text{PPh}_3)_3]$, the resulting vinyl complexes have been studied extensively by many researchers (see examples by Werner,¹⁷ Esteruelas,¹⁸ Santos,¹⁹ Caulton,²⁰ Hill²¹), as well as by some of us,²² covering functional-group transformation, ligand exchange and theoretical calculations.

The effect of nitrogen donor ligands on the reactivity of ruthenium hydrides²³ and vinyl ruthenium complexes^{21c} has been examined in detail. Yet, the most convenient triphenylphosphine-stabilised vinyl complexes to be used as starting materials are those of the form $[\text{M}(\text{CR}=\text{CHR})\text{Cl}(\text{CO})(\text{PPh}_3)_2]$ (M = Ru only)²⁴ or $[\text{M}(\text{CR}=\text{CHR})\text{Cl}(\text{CO})(\text{BTD})(\text{PPh}_3)_2]$ (M = Ru, Os). The BTD heterocycle confers both high crystallinity and enhanced visible properties to the materials and competes successfully with any excess triphenylphosphine present to avoid contamination by tris(phosphine) byproducts. Moreover, the lability of the BTD ligand in these complexes is remarkably well balanced, being displaced by better donors but resisting exchange with potentially coordinating solvents such as alcohols, tetrahydrofuran or even high

concentrations of acetonitrile. As a result, a rich and varied chemistry has been developed from vinyl complexes bearing this heterocycle.^{21c}

With these design concepts in mind, and based on the possible modulation of the sensing features via changes in the metal centre and the donor-acceptor properties of the vinyl ligands, a set of ruthenium and osmium vinyl complexes was prepared (structures **1-5** in Scheme 1) of general formula $[M(\text{CH}=\text{CHR})\text{Cl}(\text{CO})(\text{BTD})(\text{PPh}_3)_2]$; containing two different metals as central atoms (Ru or Os) and three different vinyl ligands ($R = \text{Pyr-1}$, $\text{C}_6\text{H}_4\text{Me-4}$ or C_6H_5) *trans* to the 2,1,3-benzothiadiazole (BTD) chromophore. Two triphenylphosphine ligands, a chloride and a carbonyl unit complete the coordination sphere of the 18-electron octahedral complexes. The synthesis and chromo-fluorogenic features of complex $[\text{Ru}(\text{CH}=\text{CHPyr-1})\text{Cl}(\text{CO})(\text{BTD})(\text{PPh}_3)_2]$ (**1**) have been recently published by us in a preliminary communication.¹⁵



Scheme 1. Structures of the ruthenium and osmium vinyl complexes (**1-5**) used in this work.

Reactivity with carbon monoxide in solution. Once the set of ruthenium and osmium derivatives had been prepared, UV-Vis spectrophotometric studies were performed for the coordination of CO to compounds **1-5**. Chloroform solutions of the ruthenium complexes **1**, **3** and **5** displayed an orange colour that changes to yellow when CO-containing air samples were bubbled through their solutions (see Table 2). In contrast, the osmium complexes **2** and **4** displayed a CO-induced colour change from purple to light yellow (see Table 2). The observed colour

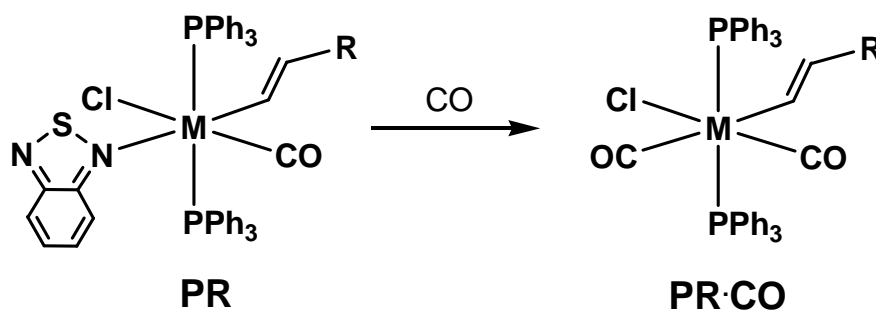
changes are consistent with the formation of the corresponding dicarbonyl complexes, through displacement of the BTD ligand (Scheme 2).

Table 2. UV-Vis and diffuse reflectance spectral data at room temperature for complexes **1-5** in chloroform solutions and supported on silica.

Compound	CHCl ₃ solution		Solid
	Absence of CO	Presence of CO	
	λ_{max} (nm)	λ_{max} (nm)	
1	500; 402; (361; 345) ^a	(361; 345) ^{a,b}	499
2	547; (418; 402) ^a	(395; 377) ^a	547
3	487; 400	-	513
4	540	-	558
5	483; 400	-	500

^a Pyrene signals

^b Enhanced signals



Scheme 2. Reactivity of the complexes acting as probes, simplified as **PR**, with carbon monoxide to give the corresponding dicarbonyl products, simplified as **PR·CO**.

Characterization of the dicarbonyl complexes. Crystal structures of transition metal complexes containing phosphines and vinyl ligands have already been extensively reported. The molecular structures of complexes **1** to **5** are very similar with all containing one metal centre bonded to two triphenylphosphine ligands, one chloride, a CO molecule and a BTD heterocycle *trans* to the vinyl

ligand. This results in a pseudo-octahedral arrangement around the metal centres. A significant structural feature of these complexes is the coplanar orientation of the vinyl and carbonyl ligands. Participation of the empty π^* orbitals of the vinyl ligands in back-bonding interactions will result in a strengthened metal-carbon bond. When a vinyl complex contains other π -acceptor ligands (e.g., the CO molecule), competition for back-donation, and therefore the relative orientation of the vinyl ligand, will have an impact on the stability of the complex.²⁵ Favourable back-donation is found for vinyl and carbonyl ligands due to their *trans* arrangement.

In order to understand the ability of carbon monoxide to bind to these divalent metal vinyl complexes, it is helpful to draw a comparison between related structures reported previously and those of the corresponding BTD and CO-substituted complexes. Suitable crystals for single X-ray diffraction were obtained (Figure 1) by vapour diffusion of diethyl ether onto (in the case of **5**·CO, CO-infused) dichloromethane solutions of the complexes. The crystal structures of BTD complexes with two different vinyl ligands have been obtained (**1** reported in a recent communication¹⁵ and **4** reported here) as well as two dicarbonyl examples, formed after addition of carbon monoxide (**1**·CO and **5**·CO reported in previous and present work, respectively).

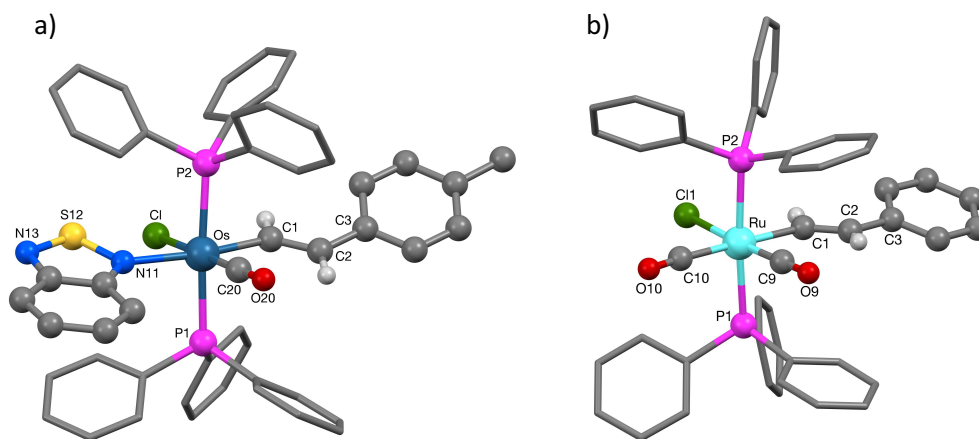


Figure 1. Crystal structures of a) $[\text{Os}(\text{CH}=\text{CHC}_6\text{H}_4\text{Me-4})\text{Cl}(\text{CO})(\text{BTD})(\text{PPh}_3)_2]$ (**4**) and b) $[\text{Ru}(\text{CH}=\text{CHC}_6\text{H}_5)\text{Cl}(\text{CO})_2(\text{PPh}_3)_2]$ (**5-CO**).

The molecular structure of compound **4** (Figure 1a) consists of an osmium centre with two triphenylphosphine ligands, while the labile BTD unit is situated *trans* to the tolylvinyl ligand. A chloride and a CO molecule complete the coordination sphere. Relevant crystallographic data are collected in Tables S1 and S2 (see ESI).

The structure reported here, together with the one recently reported for complex **1**,¹⁵ allows the comparison of the series of analogous $[\text{M}(\text{CH}=\text{CHR})\text{Cl}(\text{CO})(\text{BTD})(\text{PPh}_3)_2]$ compounds differing only in the metal ($\text{M} = \text{Ru}$ or Os) and in the vinyl substituents ($\text{R} = \text{Pyr-1}$ or $\text{C}_6\text{H}_4\text{Me-4}$). Table 3 collects the main metal-ligand structural data.

In both structures **4** and **5-CO**, an approximate octahedral arrangement is adopted. Somewhat surprisingly given their use over a number of decades, the structures of **1** and **4** are the first examples of structurally characterised vinyl complexes bearing the BTD ligand. The *trans* relationship adopted by **4** (and **1**) is in contrast to the mutually *cis* disposition of the BTD ligand and the hydride ligand in the complex $[\text{RuHCl}(\text{CO})(\text{BTD})(\text{PPh}_3)_2]$,²⁶ which is a precursor to the compounds $[\text{Ru}(\text{CH}=\text{CHR})\text{Cl}(\text{CO})(\text{BTD})(\text{PPh}_3)_2]$. This indicates that substantial reorganisation occurs on hydrometallation of the alkyne by the hydride precursor. Also, noteworthy is the fact that the $\text{M}-\text{C}_{\text{CO}}$ bond distances for the two carbonyl ligands

in the dicarbonyl complex (**5**·CO) differ substantially. This can be taken as evidence of the substantial *trans* influence exerted by the vinyl group, resulting in an elongation of the M-C_{CO} bond *trans* to the vinyl ligand. This effect is also observed in the pyrenylvinyl complex **1**·CO. Comparing the structure of the BTD complex **1** with that of the dicarbonyl **1**·CO, a greater M-C_{vinyl} distance is observed also for the vinyl ligand in the dicarbonyl structure. In the absence of significantly greater steric congestion, this must also be taken as evidence of the greater *trans* influence of the CO ligand compared to that of the BTD ligand. It would be expected that the Os-N distance (2.2073(19) Å) in **4** would be similar if not slightly longer than the Ru-N bond length in the analogous ruthenium complex (**1**). However, it is in fact substantially shorter ($d_{\text{Ru-N}}$ in **1** is 2.238(3) Å). This could be due to a release of steric congestion on replacing the pyrenylvinyl in **1** with the less bulky tolylvinyl in **4**. Otherwise, the structures are as expected and the bond data are in agreement with those reported previously for comparable compounds with monodentate N-donors such as [Ru(CH=CHBu^t)Cl(CO)(Me₂Hpz)(PPh₃)₂] (Me₂Hpz = 3,5-dimethylpyrazole).²⁷ Further details and bond data can be found in the Supplementary Information.

Table 3. Relevant bond distances (Å) for the divalent vinyl complexes used in this work.

	1 ^[15]	1 ·CO ^[15]	4	5 ·CO
$d_{\text{M-Cco}}$	1.824(3)	1.857(2)	1.831(2)	1.858(6)
$d_{\text{M-Cl}}$	2.4663(7)	2.4472(5)	2.4591(6)	2.4688(14)
$d_{\text{M-Cvinyl}}$	2.048(3)	2.104(2)	2.068(2)	2.115(5)
$d_{\text{M-N}}$	2.238(3)	-	2.2073(19)	-
$d_{\text{M-Cco2}}$	-	1.957(2)	-	1.971(6)
$d_{\text{M-P1}}$	2.4064(7)	2.4126(5)	2.3878(6)	2.4061(14)
$d_{\text{M-P2}}$	2.4099(6)	2.4060(5)	2.4158(6)	2.4037(14)

Carbon monoxide sensing behaviour in air. Despite the encouraging spectrophotometric response of the ruthenium and osmium vinyl complexes **1-5** in chloroform solution, the detection of CO in the gas phase was of paramount importance in the design of a probe to be used in air. In order to address this aim,

the five complexes were adsorbed on an inorganic matrix (thus hugely increasing the surface area exposed to the gas) and their chromogenic response toward CO in air studied. Adsorption of probes **1-5** on silica was achieved by dissolution of each complex in a minimum amount of chloroform followed by the addition of conventional lab silica at a weight ratio of 250 times. This resulted in orange (when **1**, **3** and **5** are used) and purple solids (using **2** and **4**) after solvent removal on a rotary evaporator. The resulting solids were left to stand at least 1 h before use, so that a stable initial colour is achieved. Diffuse reflectance maxima for the complexes adsorbed on silica are included in Table 2. This illustrates that the sensory materials show intense absorption bands in the 500-560 nm range.

The coloured silica probes containing the ruthenium and osmium vinyl complexes underwent significant colour changes within 2-4 seconds when exposed to air containing different concentrations of carbon monoxide inducing a progressive reduction in the absorbance of the visible bands in the 500-560 nm range (see Figure S4 in Supporting Information). As an example Figure 2 and Figure 3 show the diffuse reflectance spectra of complex **1** and **2** supported on silica and the changes observed upon addition of 100 ppm and 50 ppm of CO, respectively. The behaviour of the remaining complexes (**3**, **4** and **5**) on silica is also shown in Figure S4. All these changes are consistent with a displacement of BTD ligand by CO coordination to give the dicarbonyl derivative **PR·CO** (Scheme 2).

Using simple titration profiles of the five sensor materials with CO, the limits of detection were evaluated and the results are displayed in Table 4. Together with the values measured using a conventional UV-visible spectrophotometer (see Figure S4), Table 4 shows the estimated detection limit to the naked eye for complexes **1-5** in the presence of CO; i.e. the minimum amount of CO necessary to observe a clear colour change in the materials. As examples of CO response, the reduction of the intensity of the band centred at 535 nm vs. the log of the concentration of CO in air for **2** adsorbed on silica is shown in Figure 4, whereas pictures of the colour changes observed for **1** on silica gel upon exposure to 0.001, 0.005, 0.05, 50 and 100 ppm CO in air is shown in Figure 5.

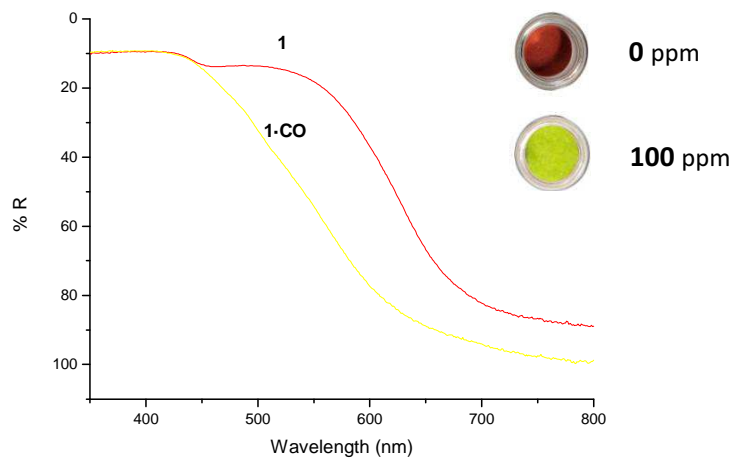


Figure 2. Diffuse reflectance UV-Vis spectrum of complex **1** supported on silica and the changes observed in the presence of air containing 100 ppm of CO.

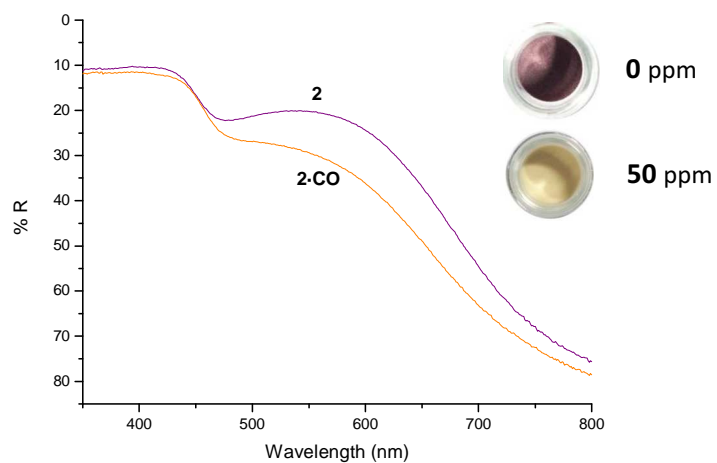


Figure 3. Diffuse reflectance UV-Vis spectrum of complex **2** on silica with the changes observed in the presence of air containing 50 ppm of CO.

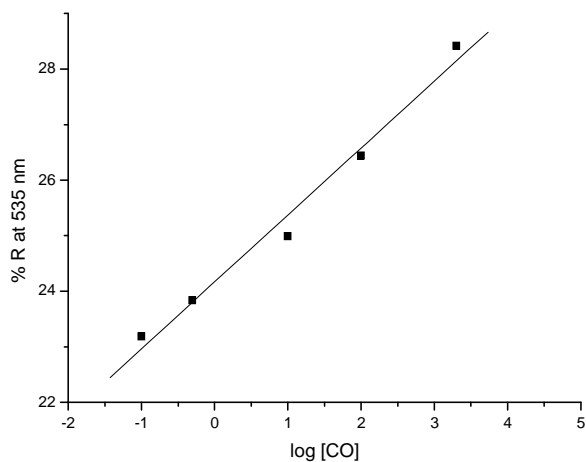


Figure 4. Reduction of the intensity of the band centred at 535 nm vs. the log of the concentration of CO in air for **2** adsorbed on silica.

Table 4. Detection limits (ppm) for complexes **1-5** in the presence of CO. Limits calculated from UV-visible spectral data and to the naked eye.

Compound	Detection limits (ppm) of CO	
	UV-Vis spectrophotometer	"Naked eye"
1	0.0006	0.005
2	0.19	0.5
3	0.1	0.5
4	0.015	0.5
5	0.084	0.5

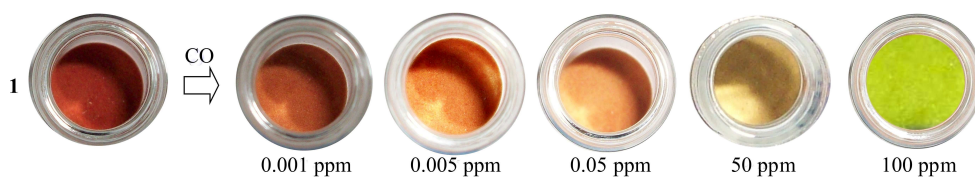


Figure 5. Colour changes observable to the naked eye for complex **1** on silica gel upon exposure to 0.001, 0.005, 0.05, 50 and 100 ppm CO in air.

One of the most remarkable aspects of the behaviour of complexes **1-5** is the clear chromogenic response observed at relatively low concentrations of carbon monoxide. In particular, and remarkably, across all the silica-supported complexes prepared, a chromogenic change to the 'naked eye' was observed at concentrations as low as 0.5 ppm. Moreover, complex **1** excels above the rest, due not only to its remarkable colour modulation observed at concentrations at which CO becomes toxic; but also to its ability to detect extremely low CO concentrations.

Moreover, another remarkable feature observed in **1** was that the displacement of the BTD ligand by CO also results in the recovery of the fluorescence emission of the pyrene group. This effect was observed both in solution and in air. For instance methanolic solutions of **1** were poorly fluorescent ($\lambda_{\text{exc}} = 355 \text{ nm}$, $\lambda_{\text{em}} = 458 \text{ nm}$) but addition of CO and formation of **1**·CO resulted in a remarkable 36-fold increase in emission. Moreover, **1** was also found to display a turn-on emission enhancement in the presence of carbon monoxide when the probe was adsorbed on strips of cellulose paper. Using this support, a remarkable LOD for CO of 0.7 ppb was calculated. In addition to this, a clear optical response to the naked eye was also found for concentrations of ca. 90 ppm using a conventional UV lamp.

Based on the observation that naked-eye colour changes for probes **2-5** are found at different CO concentrations it is possible to design systems for semi-quantitative *visual* sensing of CO in air. As an example, a sensing array containing compounds **2-5** and the colour changes observed at concentrations of CO of 0, 0.5, 1, 5, 10 and 50 ppm in air is shown in Figure 6.



Figure 6. Sensing array of probes **2-5** for CO detection in air showing naked eye colour changes upon exposure of 0.5, 1, 5, 10 and 50 ppm CO.

Selectivity. Once the sensitivity of the five silica-supported vinyl complexes towards CO had been established, the chromogenic response in the presence of other gases (CO_2 , N_2 , O_2 , Ar, SO_2 , NO_x and H_2S) and vapours (acetone, chloroform, ethanol, formaldehyde, hexane, toluene and acetonitrile) was studied. In all cases the ruthenium and osmium vinyl complexes displayed a remarkably selective response for carbon monoxide in air. For instance, no reaction was observed in the presence of CO_2 , N_2 , O_2 or Ar at very high concentrations (up to 50000 ppm). Similarly, no colour changes were observed in the presence of volatile organic compounds such as acetone, chloroform, ethanol, formaldehyde, hexane or toluene (up to 30000 ppm in air). However, some colour changes were observed for all complexes in the presence of acetonitrile vapour, although only at concentrations of 1500-5000 ppm (levels which are considered toxic to humans). Studies with other potentially coordinating gaseous species, such as SO_2 , NO_x and H_2S were also carried out. No noticeable colour changes were observed with any of the complexes adsorbed on silica in the presence of SO_2 (up to 38000 ppm) or H_2S (up to 200 ppm, well above the level toxic to humans). Exposure to NO_x produced colour changes to orange for all complexes except for **1** (that was already orange). However, this reactivity was only observed at very high concentrations of nitrogen oxides (around 2200 ppm). The reactivity towards the

VOCs and gases tested, together with relevant concentrations, are summarized in Table 5.

Table 5. Summary of the observed behaviour for VOCs and gases tested with complexes **1-5**. Responses are shown with the concentration (in ppm) necessary to induce a colour change or where no colour change was observed (-).

VOCs (ppm)								
Solid	acetone	acetonitrile	chloroform	ethanol	formaldehyde	hexane	toluene	
1	-	5000	-	-	-	-	-	-
2	-	2090	-	-	-	-	-	-
3	-	2146	-	-	-	-	-	-
4	-	3020	-	-	-	-	-	-
5	-	1574	-	-	-	-	-	-

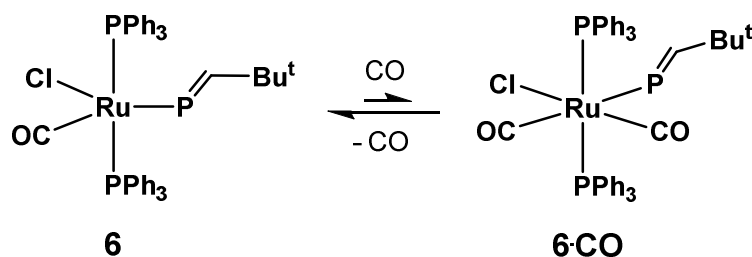
Gases (ppm)								
Solid	Water	CO ₂	N ₂	O ₂	Ar	SO ₂	NO _x	H ₂ S
1	-	-	-	-	-	-	- ^a	-
2	-	-	-	-	-	-	2570	-
3	-	-	-	-	-	-	2287	-
4	-	-	-	-	-	-	2582	-
5	-	-	-	-	-	-	2213	-

^a No visible spectroscopic changes

Reversibility. Coordination of CO with this set of vinyl complexes was found to be essentially irreversible both in solution and in air. Therefore the probes are better defined (and used) as chemodosimeters and will reflect the cumulative response towards the concentration of CO present in air during a prolonged period of time.

As an attempt to design probes that could be used for the reversible sensing of CO, we focused our attention on the phosphavinyl ruthenium complex [Ru(P=CHBu^t)Cl(CO)(PPh₃)₂] (**6**).²⁸ At first glance, complex **6** appears closely related to the conventional vinyl complexes [Ru(CH=CHR)Cl(CO)(PPh₃)₂]. However, in analogy to nitrosyl ligands, the phosphavinyl can act as either a one-electron or a

three-electron donor. There is evidence that, in the case of **6**, the reactivity of the phosphavinyl ligand resembles a 3-electron donor, rendering the coordination sphere of the metal coordinatively-saturated. For example, the analogue $[\text{Ru}(\text{P}=\text{CHBu}^t)\text{Cl}(\text{CO})(\text{BTD})(\text{PPh}_3)_2]$ cannot be prepared as the BTD ligand is ejected after reaction between $[\text{RuHCl}(\text{CO})(\text{BTD})(\text{PPh}_3)_2]$ and $\text{P}\equiv\text{CBu}^t$ to form **6** exclusively. In this system it has been shown that coordination of carbon monoxide is reversible (Scheme 3) and even solid samples of **6**·CO precipitated under an atmosphere of CO lose carbon monoxide over a period of hours to reform **6**.²⁸



Scheme 3. Reversible reaction of phosphavinyl compound **6** with CO.

In order to explore the possibility of exploiting this in the current study, solutions of **6** in dichloromethane were exposed to a mixture of carbon monoxide in air, resulting in a colour change from yellow-orange to colourless. The colour could be regenerated by purging the solution with air. In the solid state, addition of pure carbon monoxide led to a colour change from orange to pale yellow, which was reversed on removal of the carbon monoxide atmosphere. However, supporting complex **6** on silica under the same conditions used for the other complexes led to the orange colour being lost and so the exploration of **6** as a probe for the detection of CO in air was not pursued further.

Density functional theory (DFT) study. To further investigate the colour change observed on exposure of the vinyl complexes to carbon monoxide, a computational study was performed using a high level of theory. Four ruthenium vinyl complexes containing either a pyrene (**1**) or phenyl (**3**) substituent on the vinyl ligand were modelled, both as the BTD precursor (**1** and **3**) and with CO

bound (**1**·CO and **3**·CO). Calculations were conducted using the B3LYP functional with explicit inclusion of dispersion corrections using the D3 procedure by Grimme, employing the MW28 pseudopotential and basis set for Ru and the TZVP basis set for all other atoms. Solvent effects were included via CPCM. Time-dependent Density Functional Theory (TD-DFT) experiments were conducted at the same level of theory for the first 100 states.

In both BTM probes **1** and **3** (before CO is added), the strong colour of the complexes originate from a low intensity π - π^* transition between the aromatic vinyl group and the BTM chromophore (at around 624 nm for **1** and 576 nm for **3**) and a more intense π - π^* aromatic vinyl transition (at ca. 300-400 nm). Predicted UV-Vis spectra are shown in Figure 7 and selected MOs can be found in the ESI (Tables S4-S7). Upon coordination of CO, the transitions change depending on the identity of the vinyl group but both compounds lose their distinct coloured transitions above 500 nm, whereas the π - π^* aromatic vinyl transition remain and are hypsochromically shifted.

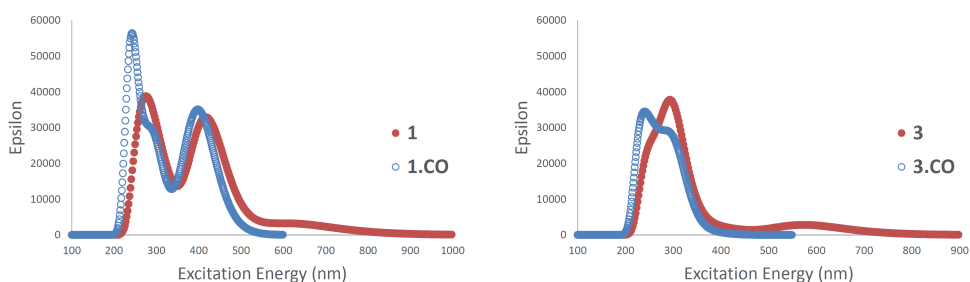


Figure 7. TD-DFT UV spectra for **1** and **1**·CO (left); **3** and **3**·CO (right).

Conclusions

Ruthenium(II) and osmium(II) vinyl complexes (**1-5**) of general formula $[M(\text{CH}=\text{CHR})\text{Cl}(\text{CO})(\text{BTD})(\text{PPh}_3)_2]$ containing two different metal centres (Ru or Os) and three different vinyl ligands ($R = \text{Pyr-1}$, $\text{C}_6\text{H}_4\text{Me-4}$ or C_6H_5) *trans* to a 2,1,3-benzothiadiazole (BTD) chromophore have been investigated as chromogenic probes for CO detection. Spectroscopic studies (UV-Vis) were carried out on the complexes, both in solution and immobilized on silica, showing colour changes in

the visible region due to coordination of CO and displacement of BTD ligand. These changes were associated with remarkable colour modulations from orange to yellow (in case of ruthenium complexes **1**, **3** and **5**) and from purple to yellow (for osmium complexes **2** and **4**). Further information on these modulations in colour was provided by a TD-DFT computational study. Examples of the probes before (**4**) and after CO additions (**5•CO**) were also investigated structurally using single crystal X-ray diffraction techniques. In all cases the ruthenium and osmium vinyl complexes studied showed a highly selective response to CO with remarkably low detection limits. Of all VOCs and gases tested as possible interferents, only acetonitrile and NO_x gave any indication of colour changes, yet in both cases this was only observed at extremely high (and well above toxic) concentrations unlikely to be encountered in any setting requiring CO sensing. Most notably, the exceptional selectivity for CO over water vapour and all organic solvents tested is of crucial importance in the potential application of this system in domestic or workplace settings where steam, cleaning products or fuel fumes are present (addressing this shortcoming in commercial devices).

While this very high selectivity is vital for a viable CO detector, good sensitivity and a clear indication of the presence of this odourless, tasteless, toxic gas are of great importance. All the complexes tested (**1-5**) display a very clear and remarkable colour change, easily visible to the naked eye at very low concentrations of CO. In particular, complex **1** demonstrates distinct changes in colour at CO concentrations as low as 0.005, even allowing the visual quantification of CO in air. Critically, the chromogenic responses observed cover a wide spectrum of concentrations, encompassing the toxicity range for humans (Table 1). This would allow the system described here to be employed in its current form to monitor acute or cumulative exposure to CO in the home or workplace (using a comparison colour chart for various amounts of CO). Cellulose strips impregnated with the complexes¹⁵ would also allow the colour change to be converted to a numerical reading (and hence alarm) using a simple, portable optoelectronic device, such as described by some of us previously.²⁹ The attributes described above for complexes **2-5** complement the dual chromo-

fluorogenic detection of carbon monoxide by complex **1**, but using simpler and less expensive reagents. Both the colour (**1-5**) and turn-on emission modulations (**1**) observed are highly selective and due to a displacement of the BTD ligand in the probes by CO to yield the dicarbonyl complexes. Furthermore, the high-yielding and straightforward synthetic procedure used to prepare **1-5** in air, coupled with the commercial availability and relatively low cost of ruthenium and other reagents render the metal complexes both accessible and inexpensive. The combination of sensitivity, selectivity, simple synthesis and low cost (for complex **1** around £10/g and less than a penny for the amount on a cellulose strip) make the system described here a very attractive and efficient chemosensor for the simple chromogenic (and for **1**, fluorogenic) detection of this colourless, odourless and highly toxic gas.

Acknowledgements

The authors wish to express their gratitude to the Spanish Government (project MAT2012-38429-C04) and Generalitat Valenciana (project PROMETEOII/2014/047) for their support. M.E.M. is grateful to the Spanish Ministerio de Ciencia e Innovación for an FPU grant as well as for the short-stay fellowship, which allowed this profitable collaboration. The authors thank Johnson Matthey Ltd for a generous loan of ruthenium and osmium salts. A.T. gratefully acknowledges the support of the Leverhulme Trust (Grant RPG-2012-634) for a studentship. The authors thank Prof. C. K. Williams, Prof. N. J. Long and Dr P. Hunt (Imperial College) for the use of apparatus and assistance.

References

1. a) D. Gutmacher, C. Foelml, W. Vollenweider, U. Hofer, J. Wöllenstein, *Procedia Eng.*, **2011**, 25, 1121-1124; b) C. Kaminski, A. Poll, *Electrochemical or Solid State H₂S Sensors: Which is Right for You?* InTech, USA, **1985**.

2. a) G. Korotcenkov, V. Brynzari, S. Dmitriev, *Mater. Sci. Eng. B*, **1999**, *63*, 195-204; b) N. Yamazoe, Y. Kurokawa, T. Seiyama, *Sens. Actuators*, **1983**, *4*, 283-289.
3. J. Wolfrum, *Proc. Combust. Inst.*, **1998**, *27*, 1, 1-41.
4. K. -H. Cho, S. -W. Lee, J. -H. Lee, K. -S. Choi, *Anal. Sci. Technol.*, **2000**, *13*, 222-228.
5. M. Itou, Y. Araki, O. Ito, H. Kido, *Inorg. Chem.*, **2006**, *45*, 6114-6116.
6. A. Giulino, T. Gupta, M. Altman, S. Lo Schiavo, P. G. Mineo, I. L. Fragalà, G. Evmenenko, P. Dutta, M. E. van der Boom, *Chem. Commun.*, **2008**, 2900-2902.
7. D. Benito-Garagorri, M. Puchberger, K. Mereiter, K. Kirchner, *Angew. Chem. Int. Ed.*, **2008**, *47*, 9142-9145.
8. S. Paul, F. Amalraj, S. Radhakrishnana, *Synt. Met.*, **2009**, *159*, 1019-1023.
9. a) M. E. Moragues, J. Esteban, J. V. Ros-Lis, R. Martínez-Máñez, M.D. Marcos, M. Martínez, J. Soto, F. Sancenón, *J. Am. Chem. Soc.*, **2011**, *133*, 15762-15772; b) J. Esteban, J. V. Ros-Lis, R. Martínez-Máñez, M. D. Marcos, M. Moragues, J. Soto, F. Sancenón, *Angew. Chem. Int. Ed.*, **2010**, *49*, 4934-4937.
10. C. W. Tate, A. deMello, A. D. Gee, S. Kealey, R. Vilar, A. J. P. White, N. J. Long, *Dalton Trans.*, **2012**, *41*, 83-89.
11. US Environmental Protection Agency, *Air Quality Criteria for Carbon Monoxide*, EPA/600/P-99/001. *National Center for Environmental Assessment*, Research Triangle Park, NC, **1999**.
12. <https://www.gov.uk/government/publications/carbon-monoxide-poisoning>.
13. See for instance: a) L. E. Santos-Figueroa, C. Giménez, A. Agostini, E. Aznar, M. D. Marcos, F. Sancenón, R. Martínez-Máñez, P. Amorós, *Angew. Chem. Int. Ed.*, **2013**, *52*, 13712-13716; b) E. Climent, M.D. Marcos, R. Martínez-Máñez, F. Sancenón, J. Soto, K. Rurack, P. Amorós, *Angew. Chem. Int. Ed.*, **2009**, *48*, 8519-8522; c) E. Climent, A. Bernardos, R. Martínez-Máñez, A. Maquieira, M.D. Marcos, N. Pastor-Navarro, R. Puchades, F. Sancenón, J. Soto, P. Amorós, *J. Am. Chem. Soc.*, **2009**, *131*, 14075-14080; d) Comes, E. Aznar, M. Moragues, M.D. Marcos, R. Martínez-Máñez, F. Sancenón, J. Soto, L.A. Villaescusa, L. Gil, P. Amorós, *Chem. Eur. J.*, **2009**, *15*, 9024-9033; e) T. Ábalos, S. Royo, R. Martínez-Máñez, F. Sancenón, J. Soto, A.M. Costero, S. Gil, M. Parra, *New. J. Chem.*, **2009**, *33*, 1641-1645; f) E. Aznar, C. Coll, M.D. Marcos, R. Martínez-Máñez, F. Sancenón, J. Soto, P. Amorós, J. Cano, E. Ruiz, *Chem. Eur. J.*, **2009**, *15*, 6877-6888; g) E. Climent, P. Calero, M.D. Marcos, R. Martínez-Máñez, F. Sancenón, J. Soto, *Chem. Eur. J.*, **2009**, *15*, 1816-1820.
14. a) H. Loumrhari, J. Ros, *J. Organomet. Chem.*, **1991**, *411*, 255-261; b) M. C. J. Harris, A. F. Hill, *Organometallics* **1991**, *10*, 3903-3906; c) B. R. James, L. D. Markham, B. C. Hui, G. L. Rempel, *J. Chem. Soc., Dalton Trans.*, **1973**, 2247-2252.
15. M. E. Moragues, A. Toscani, F. Sancenón, R. Martínez-Máñez, A. J. P. White, J. D. E. T. Wilton-Ely, *J. Am. Chem. Soc.*, **2014**, *136*, 11930-11933.
16. E. W. Abel, F. G. A. Stone, G. Wilkinson (Eds.), *Comprehensive Organometallic Chemistry II*, vol. 7, Pergamon, Oxford, **1995**.

17. a) S. Jung, K. Ilg, C. D. Brandt, J. Wolf, H. Werner, *Eur. J. Inorg. Chem.*, **2004**, 469-480; b) S. Jung, C. D. Brandt, J. Wolf, H. Werner, *Dalton Trans.*, **2004**, 375-383; c) H. Werner, S. Jung, P. Gonzalez-Herrero, K. Ilg, J. Wolf, *Eur. J. Inorg. Chem.*, **2001**, 1957-1961; d) S. Jung, K. Ilg, J. Wolf, H. Werner, *Organometallics*, **2001**, *20*, 2121-2123; e) H. Werner, W. St üer, S. Jung, B. Weberndörfer, J. Wolf, *Eur. J. Inorg. Chem.*, **2002**, 1076-1080; f) H. Werner, A. Stark, P. Steinert, C. Grunwald, J. Wolf, *Chem. Ber.*, **1995**, *128*, 49-62.
18. a) M. A. Esteruelas, A. M. López, E. Oñate, *Organometallics*, **2007**, *26*, 3260-3263; b) T. Bolano, R. Castarlenas, M. A. Esteruelas, E. Oñate, *J. Am. Chem. Soc.*, **2006**, *128*, 3965-3973; c) B. Eguillar, M. A. Esteruelas, M. Oliván, E. Oñate, *Organometallics*, **2005**, *24*, 1428-1438; d) R. Castarlenas, M. A. Esteruelas, E. Oñate, *Organometallics*, **2001**, *20*, 3283-3292; e) R. Castarlenas, M. A. Esteruelas, E. Oñate, *Organometallics*, **2001**, *20*, 2294-2302; f) M. A. Esteruelas, C. García-Yebra, M. Oliván, E. Oñate, M. Tajada, *Organometallics*, **2000**, *19*, 5098-5106; g) R. Castarlenas, M. A. Esteruelas, E. Oñate, *Organometallics*, **2000**, *19*, 5454-5463; h) M. L. Buil, M. A. Esteruelas, C. García-Yebra, E. Gutiérrez-Puebla and M. Oliván, *Organometallics*, **2000**, *19*, 2184-2193; i) C. Bohanna, M. L. Buil, M. A. Esteruelas, E. Oñate, C. Valero, *Organometallics*, **1999**, *18*, 5176-5179; j) C. Bohanna, B. Callejas, A. Edwards, M. A. Esteruelas, F. J. Lahoz, L. A. Oro, N. Ruiz, C. Valero, *Organometallics*, **1998**, *17*, 373-381; k) M. A. Esteruelas, A. V. Gómez, A. M. López, E. Oñate, *Organometallics*, **1998**, *17*, 3567-3573; l) M. A. Esteruelas, F. Liu, E. Oñate, E. Sola, B. Zeier, *Organometallics*, **1997**, *16*, 2919-2928; m) M. L. Buil, S. Elipe, M. A. Esteruelas, E. Oñate, E. Peinado, N. Ruiz, *Organometallics*, **1997**, *16*, 5748-5755; n) M. A. Esteruelas, F. J. Lahoz, E. Oñate, L. A. Oro, E. Sola, *J. Am. Chem. Soc.*, **1996**, *118*, 89-99; o) C. Bohanna, M. A. Esteruelas, J. Herrero, A. M. López, L. A. Oro, *J. Organomet. Chem.*, **1995**, *498*, 199-206; p) C. Bohanna, M. A. Esteruelas, F. J. Lahoz, E. Oñate, L. A. Oro, E. Sola, *Organometallics*, **1995**, *14*, 4825-4831; q) C. Bohanna, M. A. Esteruelas, F. J. Lahoz, E. Oñate, L. A. Oro, *Organometallics*, **1995**, *14*, 4685-4696.
19. a) B. Gómez-Lor, A. Santos, M. Ruiz, A. M. Echavarren, *Eur. J. Inorg. Chem.*, **2001**, 2305-2310; b) A. M. Castaño, A. M. Echavarren, J. López, A. Santos, *J. Organomet. Chem.*, **1989**, *379*, 171-175; c) J. Montoya, A. Santos, A. M. Echavarren, J. Ros, *J. Organomet. Chem.*, **1990**, *390*, C57-C60; d) H. Loumrhari, J. Ros, M. R. Torres, A. Santos, A. M. Echavarren, *J. Organomet. Chem.*, **1991**, *411*, 255-261; e) J. Montoya, A. Santos, J. López, A. M. Echavarren, J. Ros, A. Romero, *J. Organomet. Chem.*, **1992**, *426*, 383-398; f) J. López, A. Romero, A. Santos, A. Vegas, A. M. Echavarren, P. Noheda, *J. Organomet. Chem.*, **1989**, *373*, 249-258; g) A. M. Echavarren, J. López, A. Santos, J. Montoya, *J. Organomet. Chem.*, **1991**, *414*, 393-400; h) M. R. Torres, A. Vegas, A. Santos, J. Ros, *J. Organomet. Chem.*, **1987**, *326*, 413-421; i) M. R. Torres, A. Santos, J. Ros, X. Solans, *Organometallics*, **1987**, *6*, 1091-1095.
20. a) D. J. Huang, K. B. Renkema, K. G. Caulton, *Polyhedron*, **2006**, *25*, 459-468; b) A. V. Marchenko, H. Gérard, O. Eisenstein, K. G. Caulton, *New J. Chem.*, **2001**, *25*, 1382-1388; c) A. V. Marchenko, H. Gérard, O. Eisenstein, K. G. Caulton, *New J. Chem.*, **2001**, *25*, 1244-1255; d) J. N.

- Coalter, W. E. Streib, K. G. Caulton, *Inorg. Chem.*, **2000**, *39*, 3749–3756; e) A. Pedersen, M. Tilset, K. Folting, K. G. Caulton, *Organometallics*, **1995**, *14*, 875–888.
21. a) A. F. Hill, R. P. Melling, *J. Organomet. Chem.*, **1990**, *396*, C22–C24; b) A. F. Hill, M. C. J. Harris, R. P. Melling, *Polyhedron*, **1992**, *11*, 781–787; c) M. C. J. Harris, A. F. Hill, *Organometallics*, **1991**, *10*, 3903–3906; d) R. B. Bedford, A. F. Hill, A. R. Thompsett, A. J. P. White, D. J. Williams, *Chem. Commun.*, **1996**, 1059–1060; e) A. F. Hill, A. J. P. White, D. J. Williams, J. D. E. T. Wilton-Ely, *Organometallics*, **1998**, *17*, 4249–4258; f) J. C. Cannadine, A. F. Hill, A. J. P. White, D. J. Williams, J. D. E. T. Wilton-Ely, *Organometallics*, **1996**, *15*, 5409–5415; g) A. F. Hill, C. T. Ho and J. D. E. T. Wilton-Ely, *Chem. Commun.*, **1997**, 2207–2208; h) A. F. Hill, J. D. E. T. Wilton-Ely, *J. Chem. Soc., Dalton Trans.*, **1999**, 3501–3510; i) R. B. Bedford, A. F. Hill, C. Jones, A. J. P. White, D. J. Williams, J. D. E. T. Wilton-Ely, *Organometallics*, **1998**, *17*, 4744–4753; j) R. B. Bedford, A. F. Hill, C. Jones, A. J. P. White, J. D. E. T. Wilton-Ely, *J. Chem. Soc., Dalton Trans.*, **1997**, 139–140.
22. a) J. D. E. T. Wilton-Ely, M. Wang, D. Benoit, D. A. Tocher, *Eur. J. Inorg. Chem.*, **2006**, 3068–3078; b) J. D. E. T. Wilton-Ely, P. J. Pogorzelec, S. J. Honarkhah, D. A. Tocher, *Organometallics*, **2005**, *24*, 2862–2874; c) J. D. E. T. Wilton-Ely, S. J. Honarkhah, M. Wang, D. A. Tocher, *Dalton Trans.*, **2005**, 1930–1939; d) J. D. E. T. Wilton-Ely, M. Wang, S. J. Honarkhah, D. A. Tocher, *Inorg. Chim. Acta*, **2005**, *358*, 3218–3226.
23. A. Santos, J. López, A. Galán, J. J. González, P. Tinoco, A. M. Echavarren, *Organometallics*, **1997**, *16*, 3482–3488.
24. M. R. Torres, A. Vegas, A. Santos, J. Ros, *J. Organomet. Chem.*, **1986**, *309*, 169–177.
25. S.-H. Choi, I. Bytheway, Z. Lin, G. Jia, *Organometallics*, **1998**, *17*, 3974–3980.
26. N. W. Alcock, A. F. Hill, M. S. Roe, *J. Chem. Soc., Dalton Trans.*, **1999**, 1737–1740.
27. A. Romero, A. Santos, A. Vegas, *Organometallics*, **1988**, *7*, 1988–1993.
28. R. B. Bedford, A. F. Hill, C. Jones, A. J. P. White, D. J. Williams, J. D. E. T. Wilton-Ely, *Organometallics*, **1998**, *17*, 4744–4753.
29. M. E. Moragues, R. Montes-Robles, J. V. Ros-Lis, M. Alcañiz, J. Ibañez, T. Pardo, R. Martínez-Mañez, *Sens. Actuators B*, **2014**, *191*, 257–263.

SUPPORTING INFORMATION

Ruthenium(II) and Osmium(II) Alkenyl Complexes as Highly Sensitive and Selective Chromogenic Probes for the Sensing of Carbon Monoxide in air

María E. Moragues, Anita Toscani, Félix Sancenón, Paul Dingwall, Neil J. Brown, Ramón Martínez-Máñez,* Andrew J. P. White, James D. E. T. Wilton-Ely*

EXPERIMENTAL PROCEDURES

Reagents

Instrumentation

Synthesis

Silica gel immobilisation of vinyl complexes **1-5**

Crystallography

Carbon monoxide sensing studies

DFT Studies

Calculated UV-Vis Spectra

REFERENCES

Experimental procedures

Reagents. The compounds 1-ethynylpyrene, 4-ethynyltoluene, 4-ethynylbenzene and 2,1,3-benzothiadiazole (BTD) were used as purchased. All solvents were of analytical grade. Solvents used for UV-Vis measurements were thoroughly degassed with N₂. Petroleum ether refers to the fraction boiling between 40-60°C. All experiments and manipulations of compounds were conducted in air, unless otherwise specified. Carbon monoxide was provided by commercially available CO cylinders. Mixtures of different concentrations of CO were prepared by mixing CO with CO-free synthetic air. The rest of gases used in this work were generated *in situ*, carbon dioxide (by adding hydrochloric acid to sodium carbonate), nitrogen oxides (by oxidation of copper with nitric acid), sulfur dioxide (by copper oxidation with sulfuric acid) and H₂S (by adding hydrochloric acid to sodium sulphide). The procedures given provide materials of sufficient purity for synthetic and spectroscopic purposes.

Instrumentation. NMR spectroscopy was performed at 25°C using a Bruker AV400 spectrometer, operating at 400.32 MHz for ¹H nuclei and 162.05 MHz for ³¹P nuclei. Spectra were recorded in CDCl₃ unless stated otherwise. Chemical shifts are reported in ppm and coupling constants (*J*) are in Hertz. Elemental analysis data were obtained by London Metropolitan University. Solvates were confirmed by integration of the ¹H NMR spectrum. Electrospray (ES) mass analyses were performed at Imperial College London on a Micromass LCT Premier spectrometer. UV-Vis spectra were recorded using a Jasco V-650 spectrophotometer equipped with a diffuse reflectance sphere (model ISV-722) for measurements on solids. In the latter case, measurements were conducted at room temperature over a wavelength range of 350-800 nm with a wavelength step of 1 nm. Carbon monoxide concentrations were measured using an ambient carbon monoxide analyser (Testo 315-2 model 0632 0317), properly validated with an ISO calibration certificate issued by Instrumentos Testo, Cabrils, Spain. Computational calculations were performed using the B3LYP functional, dispersion corrections were added using the empirical dispersion keyword and Grimme's D3 procedure.

MWB28 was used as the pseudo potential and basis set for Ru. Initially, all other atoms were calculated at 6-31G(d) and then refined using the TZVP basis set. Solvent (methanol) was included in all calculations using the CPCM methodology. An ultrafine grid and tight convergence criteria, scf=9, was employed throughout. TD-DFT calculations were carried out on fully optimised structures for the first 100 states using the same functional and basis sets. Molecular orbital diagrams were generated using Gauss view. Full crystallographic data have been deposited in the Cambridge Crystallographic Data Centre with the numbers CCDC 1011581 and 1011582.

Synthesis.

General Comments. The complexes $[\text{RuHCl}(\text{CO})(\text{PPh}_3)_3]$,¹ $[\text{OsHCl}(\text{CO})(\text{BTD})(\text{PPh}_3)_2]$,² $[\text{Os}(\text{CH}=\text{CHC}_6\text{H}_4\text{Me-4})\text{Cl}(\text{CO})(\text{BTD})(\text{PPh}_3)_2]$ (**4**),² $[\text{Os}(\text{CH}=\text{CHC}_6\text{H}_4\text{Me-4})\text{Cl}(\text{CO})_2(\text{PPh}_3)_2]$ (**4·CO**),² $[\text{Ru}(\text{P}=\text{CH}^t\text{Bu})\text{Cl}(\text{CO})(\text{PPh}_3)_2]$ (**6**),³ $[\text{Ru}(\text{P}=\text{CH}^t\text{Bu})\text{Cl}(\text{CO})_2(\text{PPh}_3)_2]$ (**6·CO**)³ and $[\text{Ru}(\text{CH}=\text{CHC}_6\text{H}_5)\text{Cl}(\text{CO})_2(\text{PPh}_3)_2]$ (**5·CO**)⁴ were prepared according to published procedures. Further data are provided for the compounds $[\text{Ru}(\text{CH}=\text{CHPyr-1})\text{Cl}(\text{CO})(\text{BTD})(\text{PPh}_3)_2]$ (**1**),⁵ $[\text{Ru}(\text{CH}=\text{CHPyr-1})\text{Cl}(\text{CO})_2(\text{PPh}_3)_2]$ (**1·CO**).⁵

$[\text{Ru}(\text{CH}=\text{CHPyr-1})\text{Cl}(\text{CO})(\text{BTD})(\text{PPh}_3)_2]$ (1**)**

2,1,3-benzothiadiazole (25 mg, 0.184 mmol) was added to a dichloromethane (10 mL) solution of $[\text{RuHCl}(\text{CO})(\text{PPh}_3)_3]$ (102 mg, 0.107 mmol) and the resulting orange solution was stirred at room temperature for few minutes. 1-ethynylpyrene (37 mg, 0.164 mmol) was then added and the reaction mixture was stirred at room temperature for 1 h, after which methanol (25 mL) was added and the dichloromethane slowly removed under reduced pressure (rotary evaporator). The resulting red-orange crystals were isolated by filtration, washed with ethanol (2 x 10 mL) and dried *in vacuo*. Yield: 106 mg (94%). IR ($\bar{\nu}_{\text{max}}/\text{cm}^{-1}$): 1928 (CO), 1432, 1232, 1088, 846, 740, 692. NMR δ_{H} (CDCl_3) 7.01 (1H, dt, $J_{\text{HH}} = 15.0$ Hz, J_{HP}

unresolved, H β), 7.64 – 7.18 (30H, m, Ph), 7.93 (2H, m, BTD), 7.70 – 7.95 (9H, m, pyrenyl), 8.05 (2H, m, BTD), 9.06 (1H, dt, $J_{\text{HH}} = 15.0$ Hz, J_{HP} unresolved, H α); δ_{P} (CDCl₃) 29.4 (s, PPh₃). MS (ES +ve) m/z 1053 (M⁺, 5%). Elemental analysis: Found: C, 69.4; H, 4.5; N, 2.6. C₆₁H₄₅ClN₂OP₂RuS requires C, 69.6; H, 4.3; N, 2.7%.

[Ru(CH=CHPyr-1)Cl(CO)₂(PPh₃)₂] (1·CO)

Compound **1·CO** was prepared by treating a dichloromethane solution (10 mL) of **1** (7.0 mg, 0.007 mmol) with a stream of carbon monoxide for 1 minute. Ethanol (5 mL) was added, forming a yellow precipitate which was filtered, washed with ethanol (10 mL), and dried *in vacuo*. Yield: 6.4 mg (97%). IR ($\bar{\nu}_{\text{max}}/\text{cm}^{-1}$): 2031 (CO), 1874 (CO) 1481, 1433, 1346, 1160, 1091, 847, 740, 691. NMR δ_{H} (CDCl₃) 7.13 (1H, dt, $J_{\text{HH}} = 15.0$ Hz, J_{HP} unresolved, H β), 7.76 - 7.30 (30H, m, PPh₃), 8.10 - 7.83 (9H, m, pyrenyl), 8.53 (1H, dt, $J_{\text{HH}} = 15.0$ Hz, J_{HP} unresolved, H α); δ_{P} (CDCl₃) 23.7 (s, PPh₃). MS (ES +ve) m/z 945 (M⁺, 10%). Elemental Analysis: Found: C, 70.8; H, 4.4; C₅₆H₄₁ClO₂P₂Ru requires C, 71.2; H, 4.4%.

[Os(CH=CHPyr-1)Cl(CO)(BTD)(PPh₃)₂] (2)

A dichloromethane solution (10 mL) of [OsHCl(CO)(BTD)(PPh₃)₂] (70 mg, 0.076 mmol) was treated with 1-ethynylpyrene (19 mg, 0.084 mmol). The resulting dark red solution was stirred for 3 hours at room temperature and then filtered through Celite. Addition of methanol (15 mL) followed by slow reduction of the solvent volume, resulted in a dark red solid, which was washed with cold methanol (10 mL), petroleum ether (10 mL) and dried. Yield: 60 mg (69%). IR ($\bar{\nu}_{\text{max}}/\text{cm}^{-1}$): 1919 (CO), 1434, 1183, 1117, 745, 719, 691. NMR δ_{H} (CD₂Cl₂) 7.08-7.21 (18H, m, Ph), 7.46 (12H, m, Ph), 7.80 – 7.99 (9H + 1H, m, pyrenyl + H β), 8.15 (2H, d, $J_{\text{HH}} = 7.6$ Hz, BTD), 8.15 (2H, m, BTD), 9.70 (1H, dt, $J_{\text{HH}} = 16.8$ Hz, J_{HP} unresolved, H α); δ_{P} (CD₂Cl₂) -1.2 (s, PPh₃). MS (ES +ve) m/z 1188 (M⁺ + 2Na, 60%).

Elemental Analysis: Found: C, 60.3; H, 3.5; N, 2.5. $C_{61}H_{45}ClN_2OOSp_2S \cdot CH_2Cl_2$ requires C, 60.7; H, 3.9; N, 2.3%.

[Os(CH=CHPyr-1)Cl(CO)₂(PPh₃)₂] (2 CO)

Compound **2 CO** was prepared by treating a dichloromethane solution (3 mL) of **2** (25 mg, 0.022 mmol) with a stream of carbon monoxide for 1 minute. Methanol (5 mL) was added and the resulting mustard yellow precipitate was isolated by filtration. The compound was washed with methanol (10 mL) and dried. Yield: 19 mg (84%). IR ($\bar{\nu}_{max}/cm^{-1}$): 2017 (CO), 1954 (CO), 1434, 1092, 847, 740, 692. NMR δ_H (CD_2Cl_2) 7.25 (1H, dt, $J_{HH} = 18.1$ Hz, $J_{HP} = 2.3$ Hz, H β), 7.33 – 7.43 (18H, m, Ph), 7.58 (1H, d, $J_{HH} = 8.1$ Hz, pyrenyl), 7.68 – 7.73 (12H, m, Ph), 7.87 (2H, s, pyrenyl), 7.92 – 8.00 (4H, m, pyrenyl), 8.06 (1H, dt, 1H, $J_{HH} = 18.1$ Hz, $J_{HP} = 3.0$ Hz, H α), 8.07 – 8.12 (2H, m, pyrenyl); δ_P (CD_2Cl_2) –7.3 (s, PPh₃). MS (ES +ve) m/z 1034 (M^+ , 100%). Found: C, 65.0; H, 4.2. $C_{56}H_{41}ClO_2OsP_2$ requires C, 65.1; H, 4.0 %.

[Ru(CH=CHC₆H₄Me-4)Cl(CO)(BTD)(PPh₃)₂] (3)

4-ethynyltoluene (26 μ l, 0.236 mmol) was added to a dichloromethane solution (10 mL) of [RuHCl(CO)(PPh₃)₃] (150 mg, 0.158 mmol) to give a dark red solution. BTD (32 mg, 0.235 mmol) was then added and the solution was stirred for 1 hour at room temperature. EtOH (20 mL) was added and the dichloromethane was slowly removed under vacuum to yield a bright orange crystalline product. This was filtered and washed with EtOH (2 x 10 mL) and petroleum ether (20 mL) and dried under vacuum. Yield: 131 mg (88 %). IR ($\bar{\nu}_{max}/cm^{-1}$): 1914 (CO), 1482, 1434, 1091, 979, 837, 741, 693. NMR δ_H (CD_2Cl_2) 2.29 (3H, s, CH₃), 5.75 (1H, dt, $J_{HH} = 16.0$ Hz, $J_{HP} =$ unresolved, H β), 6.77, 6.79 (2 x 2H, AB, $J_{AB} = 7.9$ Hz, C₆H₄Me), 7.12 (12H, t, $J_{HH} = 7.0$ Hz, Ph), 7.23 (6H, t, $J_{HH} = 7.0$ Hz, Ph), 7.50 – 7.44 (12H, m, Ph), 7.72 – 7.67 (2H, m, BTD), 7.91 (2H, s br, BTD), 8.63 (1H, dt, $J_{HH} = 16.0$ Hz, $J_{HP} = 3.2$ Hz, H α); δ_P

(CD₂Cl₂) 26.7 (s, PPh₃). MS (ES +ve) *m/z* 943 (M⁺, 40%). Elemental Analysis: Found: C, 62.1; H, 4.7; N, 2.9. C₅₂H₄₃ClN₂OP₂RuS·CH₂Cl₂ requires C, 62.0; H, 4.4; N, 2.7%.

[Ru(CH=CHC₆H₄Me-4)Cl(CO)₂(PPh₃)₂] (3 CO)

Compound **3-CO** was prepared by treating a dichloromethane solution (3 mL) of **3** (30 mg, 0.032 mmol) with a stream of carbon monoxide for 1 minute. Methanol (5 mL) was added and the resulting precipitate was isolated by filtration. The pale pink compound was washed with methanol (10 mL) and dried. Yield: 25 mg (94 %). IR ($\bar{\nu}_{\text{max}}/\text{cm}^{-1}$): 2030 (CO), 1968 (CO), 1481, 1434, 1091, 990, 741, 733, 690. NMR δ_{H} (CD₂Cl₂) 2.31 (3H, s, CH₃), 5.85 (1H, dt, $J_{\text{HH}} = 18.0$ Hz, J_{HP} unresolved, H β), 6.80, 7.01 (2 x 2H, AB, $J_{\text{AB}} = 7.9$ Hz, C₆H₄Me), 7.37 – 7.47 (18H, m, Ph), 7.52 (1H, dt, $J_{\text{HH}} = 18.0$ Hz, $J_{\text{HP}} = 3.5$ Hz, H α), 7.69-7.74 (12H, m, Ph); δ_{P} (CD₂Cl₂) 23.8 (s, PPh₃). MS (ES +ve) *m/z* 853 (M⁺ + H₂O, 9%). Elemental analysis: Found: C, 63.7; H, 4.6. C₄₇H₃₉ClO₂P₂Ru· $\frac{3}{4}$ CH₂Cl₂ requires C, 63.9; H, 4.5%.

[Ru(CH=CHC₆H₅)Cl(CO)(BTD)(PPh₃)₂] (5)

Ethynylbenzene (25 μ l, 0.236 mmol) was added to a dichloromethane solution (10 mL) of [RuHCl(CO)(PPh₃)₃] (150 mg, 0.158 mmol) to give a dark red solution. BTD (32 mg, 0.235 mmol) was then added and the solution was left to stir for 1 hour at room temperature. EtOH (20 mL) was added and dichloromethane was slowly removed under vacuum to yield a bright red crystalline product, which was filtered and washed with EtOH (2 x 10 mL) and petroleum ether (20 mL). Yield: 125 mg (85 %). IR ($\bar{\nu}_{\text{max}}/\text{cm}^{-1}$): 1917 (CO), 1481, 1433, 1090, 738, 689. NMR δ_{H} (CD₂Cl₂) 5.82 (1H, d, $J_{\text{HH}} = 16.0$ Hz, H β), 6.91 (2H, d, $J_{\text{HH}} = 7.3$ Hz, CPh), 6.98 (1H, t, $J_{\text{HH}} = 7.3$ Hz, CPh), 7.14 – 7.20 (12H + 2H, m, PPh + CPh), 7.30 (6H, m, PPh), 7.46 – 7.51 (12H, m, PPh), 7.54 (2H, m, BTD), 7.95 (2H, m, BTD), 8.70 (1H, dt, $J_{\text{HH}} = 16.0$ Hz, $J_{\text{HP}} = 3.0$ Hz, H α); δ_{P} (CD₂Cl₂) 27.0 (s, PPh₃). MS (ES +ve) *m/z* 839 (M⁺ – BTD +

2Na, 34%). Elemental analysis: Found: C, 65.9; H, 4.5. $C_{51}H_{41}ClN_2OP_2RuS$ requires C, 66.0; H, 4.5%.

Silica gel immobilisation of the vinyl complexes 1-5. Each vinyl complex (0.007-0.022 mmol) was dissolved in a minimum volume of $CHCl_3$. An excess (5 mmol) of silica (particle size 40-63 μm), was added to the coloured solution and the resulting mixture was stirred at room temperature for five minutes. After removal of the solvent on a rotary evaporator, the solid was left to stand for 1 hour at room temperature prior to its use (see Figure S3).

Crystallography. The dichloromethane solvent molecule included in the structure of **5•CO** was found to be disordered. Two orientations were identified of approximately 86 and 14% occupancy. The geometries of these orientations were optimized, the thermal parameters of adjacent atoms were restrained to be similar, and only the non-hydrogen atoms of the major occupancy orientation were refined anisotropically (those of the minor occupancy orientation were refined isotropically).

Crystal data for 4: $C_{52}H_{43}ClN_2OOS_2P_2S \cdot CH_2Cl_2$, $M = 1116.46$, triclinic, $P-1$ (no. 2), $a = 11.8215(3)$, $b = 13.0465(4)$, $c = 15.3904(4)$ Å, $\alpha = 92.606(2)$, $\beta = 99.286(2)$, $\gamma = 91.790(2)^\circ$, $V = 2338.33(11)$ Å³, $Z = 2$, $D_c = 1.586$ g cm⁻³, $\mu(Mo-K\alpha) = 3.053$ mm⁻¹, $T = 173$ K, red blocky needles, Oxford Diffraction Xcalibur 3 diffractometer; 10837 independent measured reflections ($R_{int} = 0.0201$), F^2 refinement,⁶ $R_1(obs) = 0.0232$, $wR_2(all) = 0.0501$, 9915 independent observed absorption-corrected reflections [$|F_o| > 4\sigma(|F_o|)$], $2\theta_{max} = 59^\circ$], 570 parameters. CCDC 1011581.

Crystal data for 5•CO: $C_{46}H_{37}ClO_2P_2Ru \cdot CH_2Cl_2$, $M = 905.14$, monoclinic, $P2_1/n$ (no. 14), $a = 10.13508(17)$, $b = 18.4651(3)$, $c = 22.6080(5)$ Å, $\beta = 97.2599(18)^\circ$, $V = 4197.06(14)$ Å³, $Z = 4$, $D_c = 1.432$ g cm⁻³, $\mu(Cu-K\alpha) = 5.798$ mm⁻¹, $T = 173$ K, colourless needles, Oxford Diffraction Xcalibur PX Ultra diffractometer; 8157

independent measured reflections ($R_{\text{int}} = 0.0479$), F^2 refinement, $R_1(\text{obs}) = 0.0625$, $wR_2(\text{all}) = 0.1657$, 7081 independent observed absorption-corrected reflections [$|F_o| > 4\sigma(|F_o|)$], $2\theta_{\text{max}} = 145^\circ$, 509 parameters. CCDC 1011582.

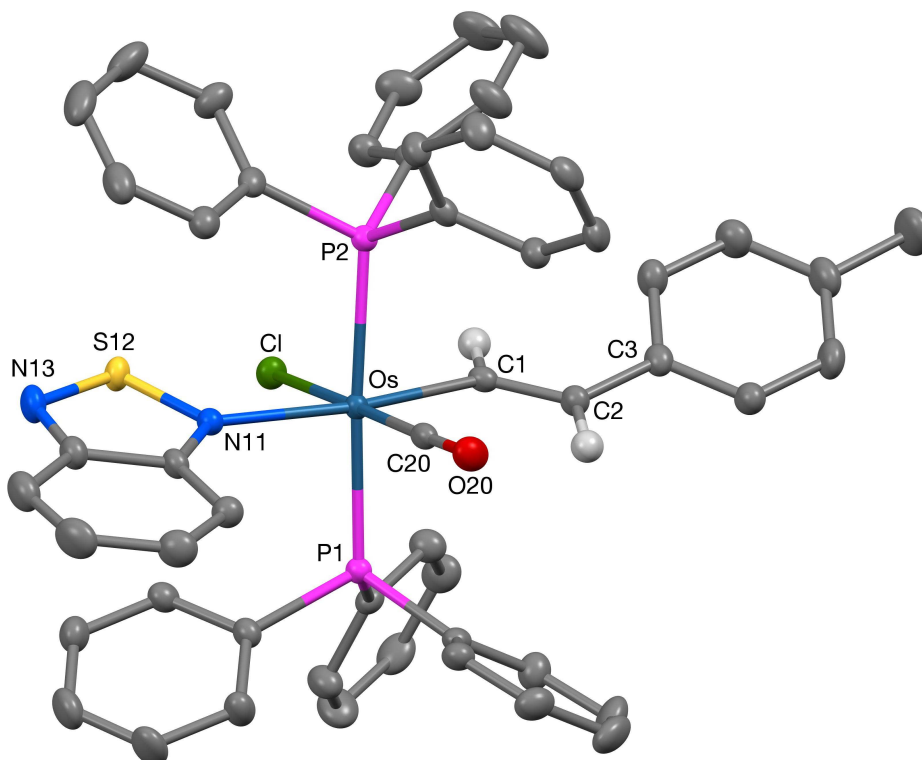


Figure S1. Crystal structure of $[\text{Os}(\text{CH}=\text{CHC}_6\text{H}_4\text{Me-4})\text{Cl}(\text{CO})(\text{BTD})(\text{PPh}_3)_2]$ (**4**) with 50% probability ellipsoids.

Table S1. Selected geometric data for $[\text{Os}(\text{CH}=\text{CHC}_6\text{H}_4\text{Me-4})\text{Cl}(\text{CO})(\text{BTD})(\text{PPh}_3)_2]$ **4** at 173 K.

Selected bond distances (\AA)			
Os-C20	1.831(2)	P1-C21	1.831(2)
Os-C1	2.068(2)	P1-C27	1.833(2)
Os-N11	2.2073(19)	P1-C33	1.839(2)

Os-P1	2.3878(6)	P2-C39	1.832(3)
Os-P2	2.4158(6)	P2-C45	1.840(2)
Os-Cl	2.4591(6)	P2-C51	1.841(2)
N11-C19	1.363(3)	C20-O20	1.164(3)
N11-S12	1.653(2)	C1-C2	1.336(3)
S12-N13	1.605(2)	C2-C3	1.473(3)
N13-C14	1.347(3)	C3-C8	1.394(4)
C14-C15	1.420(4)	C3-C4	1.405(4)
C14-C19	1.431(3)	C4-C5	1.387(4)
C15-C16	1.364(4)	C5-C6	1.391(4)
C16-C17	1.423(4)	C6-C7	1.394(4)
C17-C18	1.365(4)	C6-C9	1.510(4)
C18-C19	1.415(3)	C7-C8	1.388(4)
Selected bond angles (°)			
C1-Os-N11	170.79(8)	C1-Os-P1	91.29(7)
P1-Os-P2	175.48(2)	C1-Os-P2	84.26(7)
C20-Os-Cl	176.74(8)	C1-Os-Cl	87.61(7)
N11-Os-P1	91.78(5)	C20-Os-N11	98.40(9)
N11-Os-P2	92.50(5)	C20-Os-P1	91.24(8)
N11-Os-Cl	83.92(5)	C20-Os-C1	90.22(10)
P1-Os-Cl	86.38(2)	P2-Os-Cl	92.66(2)
O20-C20-Os	177.6(2)	C19-N11-Os	132.61(16)
C2-C1-Os	133.20(19)	S12-N11-Os	120.53(10)

C21-P1-Os	113.26(8)	C39-P2-Os	116.59(8)
C27-P1-Os	111.83(8)	C45-P2-Os	116.55(8)
C33-P1-Os	120.02(8)	C51-P2-Os	114.44(8)

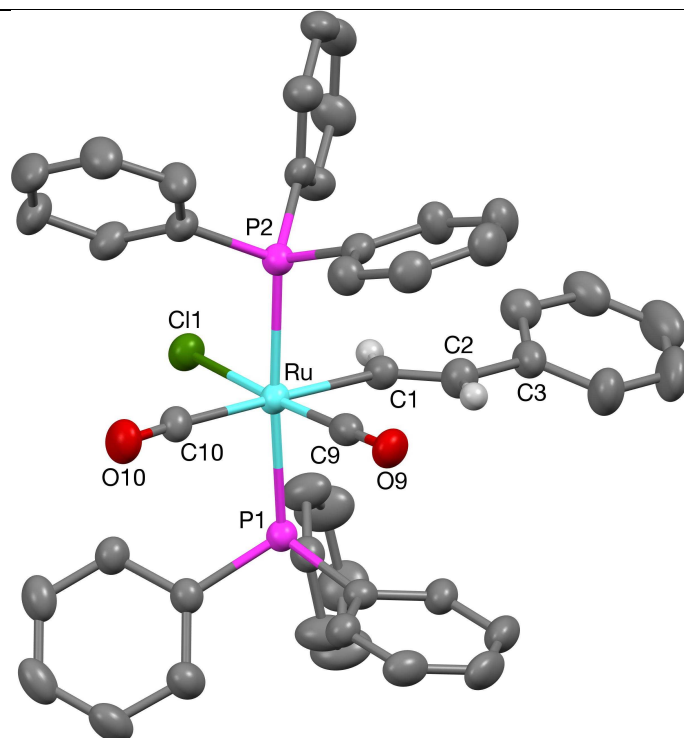


Figure S2. Crystal structure of $[\text{Ru}(\text{CH}=\text{CHC}_6\text{H}_5)\text{Cl}(\text{CO})_2(\text{PPh}_3)_2]$ (**5·CO**) with 50% probability ellipsoids.

Table S2. Selected geometric data for $[\text{Ru}(\text{CH}=\text{CHC}_6\text{H}_5)\text{Cl}(\text{CO})_2(\text{PPh}_3)_2]$ (**5·CO**) at 173 K.

Selected bond distances (Å)			
Ru-C9	1.858(6)	P1-C11	1.826(6)
Ru-C1	2.115(5)	P1-C17	1.837(6)
Ru-C10	1.971(6)	P1-C23	1.838(6)
Ru-P1	2.4061(14)	P2-C35	1.831(6)

Ru-P2	2.4037(14)	P2-C41	1.835(6)
Ru-Cl	2.4688(14)	P2-C29	1.845(6)
C9-O9	1.140(7)	C10-O10	1.120(7)
C1-C2	1.308(9)	C4-C5	1.373(10)
C2-C3	1.486(8)	C5-C6	1.361(12)
C3-C8	1.381(9)	C6-C7	1.362(14)
C3-C4	1.394(9)	C7-C8	1.397(11)
Selected bond angles (°)			
C10-Ru-C1	179.0(2)	C9-Ru-C10	93.0(2)
P1-Ru-P2	175.43(5)	C9-Ru-C1	86.2(2)
C9-Ru-Cl	176.39(18)	C9-Ru-P2	89.41(17)
C10-Ru-P2	91.79(17)	C1-Ru-P2	88.82(15)
C10-Ru-P1	92.69(17)	C1-Ru-P1	86.69(15)
C10-Ru-Cl	90.38(16)	C1-Ru-Cl	90.40(16)
P1-Ru-Cl	91.60(5)	P2-Ru-Cl	89.27(5)
O9-C9-Ru	179.8(6)	C2-C1-Ru	132.4(5)
O10-C10-Ru	175.1(5)		
C11-P1-Ru	109.64(17)	C35-P2-Ru	110.05(18)
C17-P1-Ru	115.10(19)	C41-P2-Ru	114.30(19)
C23-P1-Ru	121.6(2)	C29-P2-Ru	120.8(2)

Carbon monoxide sensing studies.

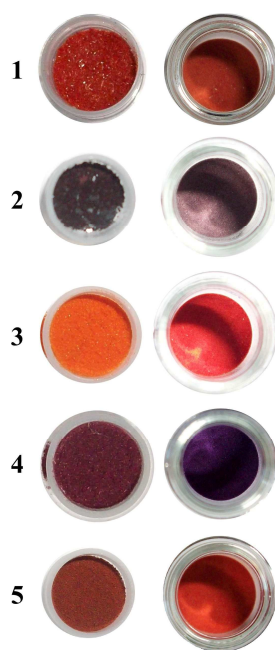


Figure S3. Left: the colour of ruthenium and osmium complexes **1-5**; right: the colour of **1-5** on silica.

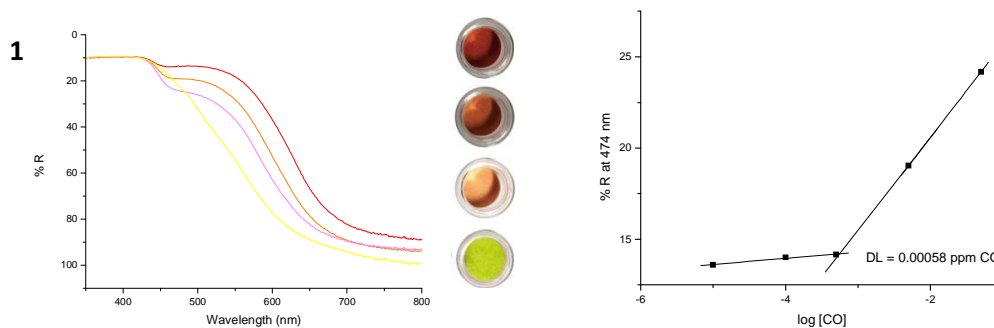


Figure S4a. Left: Spectroscopic changes of complex **1** on silica upon increasing concentrations of CO.

Right: calculation curve in the range 0.0001-100 ppm.

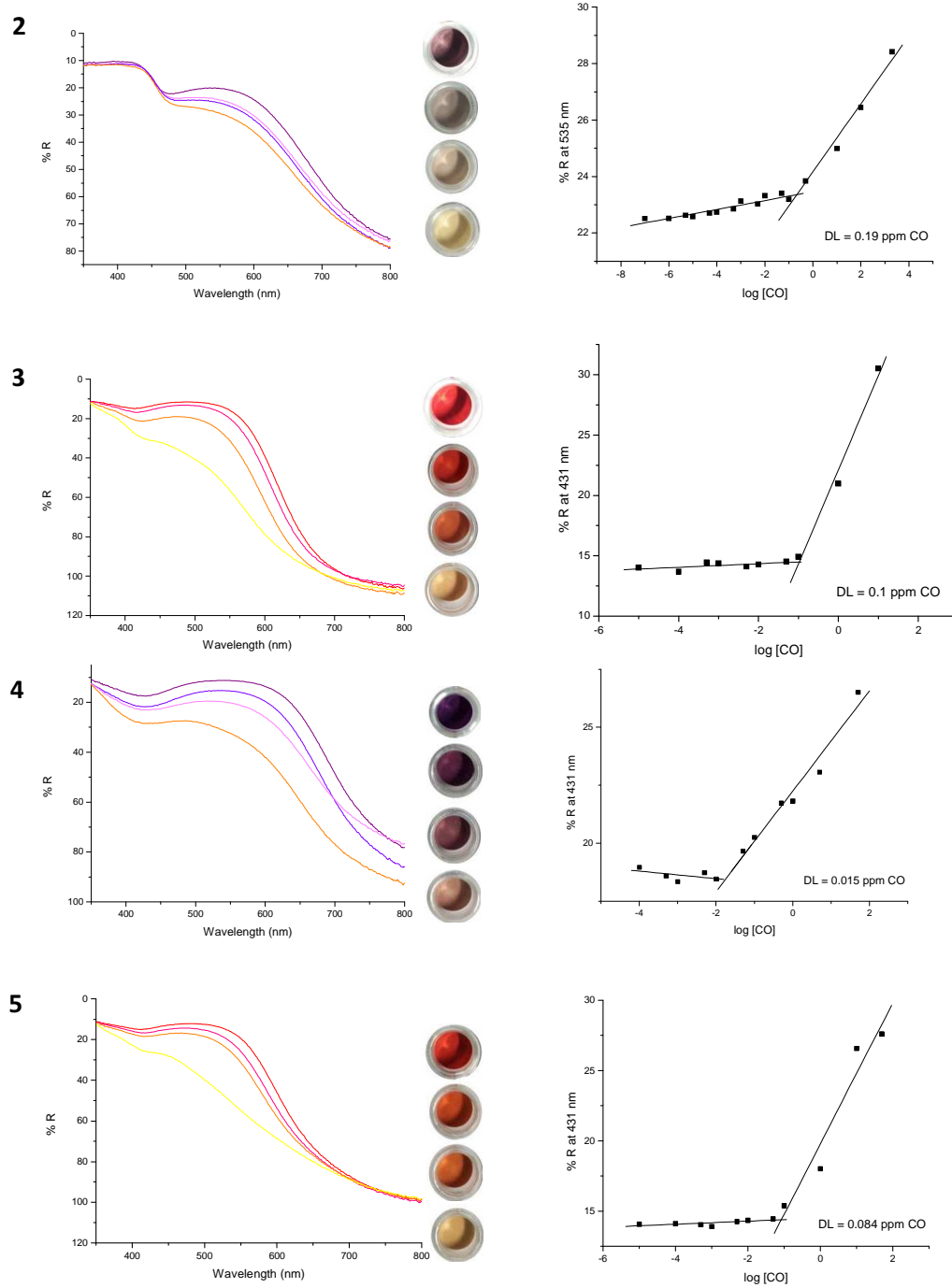
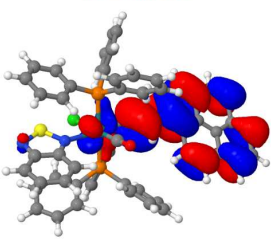
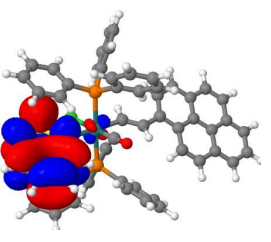
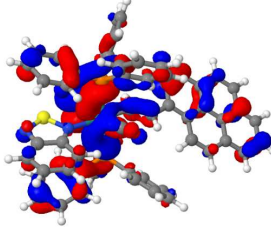
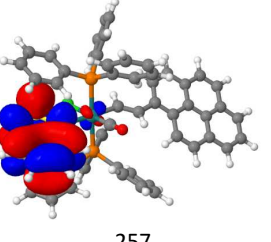


Figure S4b. Left: Spectroscopic changes of complexes 2-5 on silica upon increasing concentrations of CO. Right: calculation curves in the range 0.0001-100 ppm.

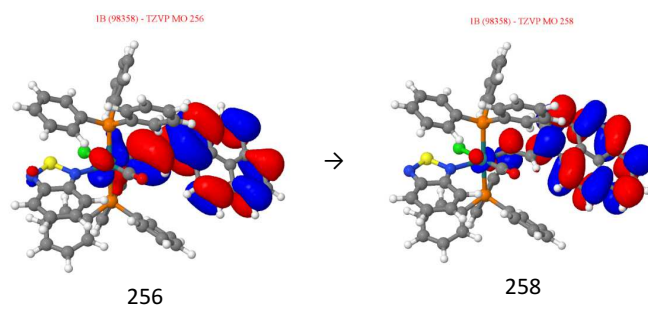
DFT Studies.**Table S3.** Calculated bond lengths in Å for complexes **1**, **1·CO**, **3** and **3·CO**.

Model	Ru-N or Ru-CO _(added CO)	Ru-P(3)	Ru-P(4)	Ru-Cl	Ru-CO	Ru-C ₁	C ₁ -C ₂
1	2.28483	2.45321	2.43757	2.54494	1.82511	2.05145	1.34432
3	2.28418	2.44656	2.43375	2.54531	1.82544	2.05911	1.34255
1·CO	1.96983	2.46679	2.44448	2.53908	1.85638	2.11228	1.34186
3·CO	1.96822	2.46190	2.44099	2.54352	1.85638	2.11463	1.33957

Table S4. Molecular orbitals for Compound **1**.

λ (nm)	MO	Transition	
624.16	 256	 257	Ru-vinyl → BTD
420.79	 254	 257	Ru-phosphine → BTD

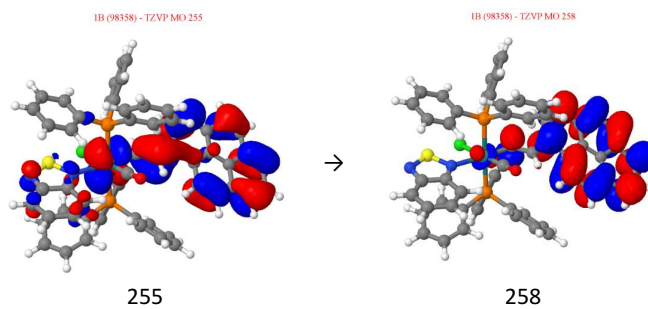
414.86



Ru-vinyl π

→ π^*

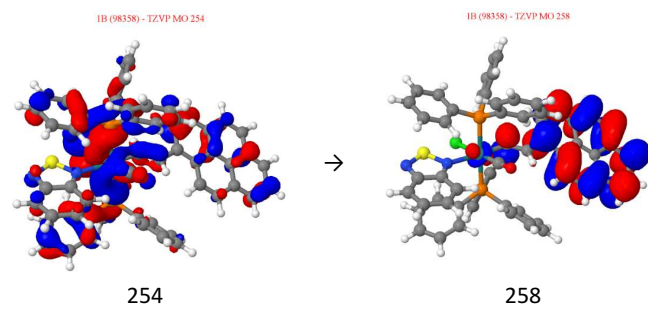
320.65



Ru-vinyl π

→ π^*

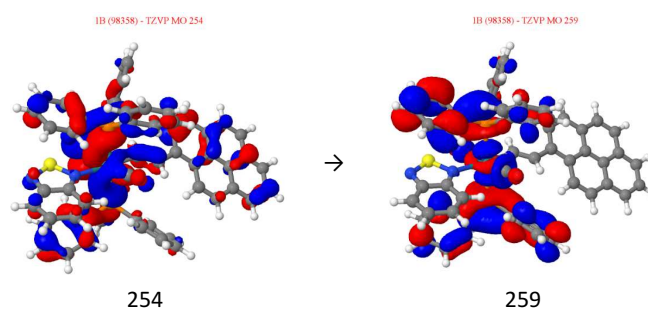
302.90



Ru-phosphine

→ Ru-vinyl

280.68



Ru-phosphine π

→ π^*

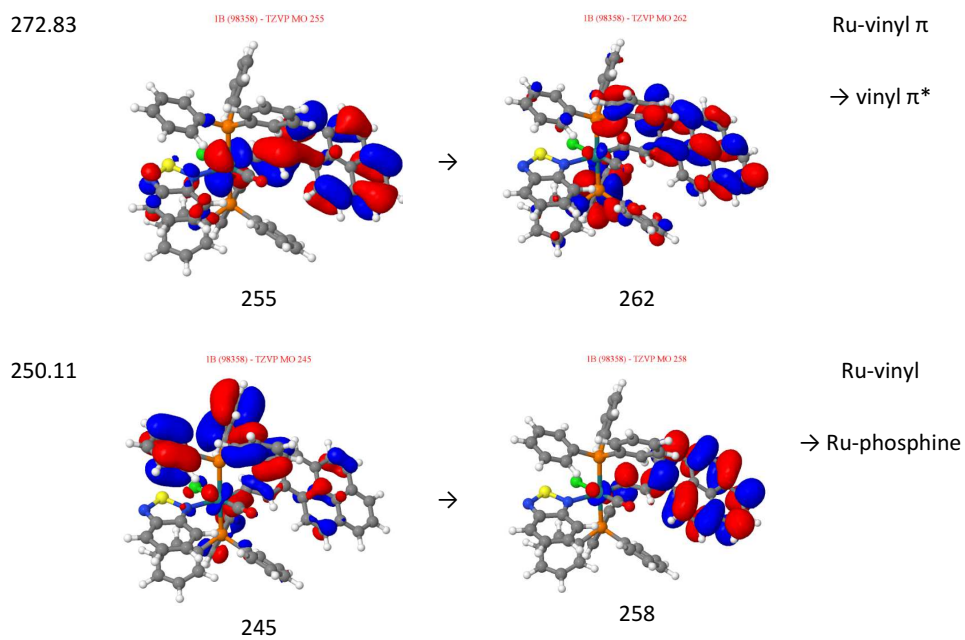
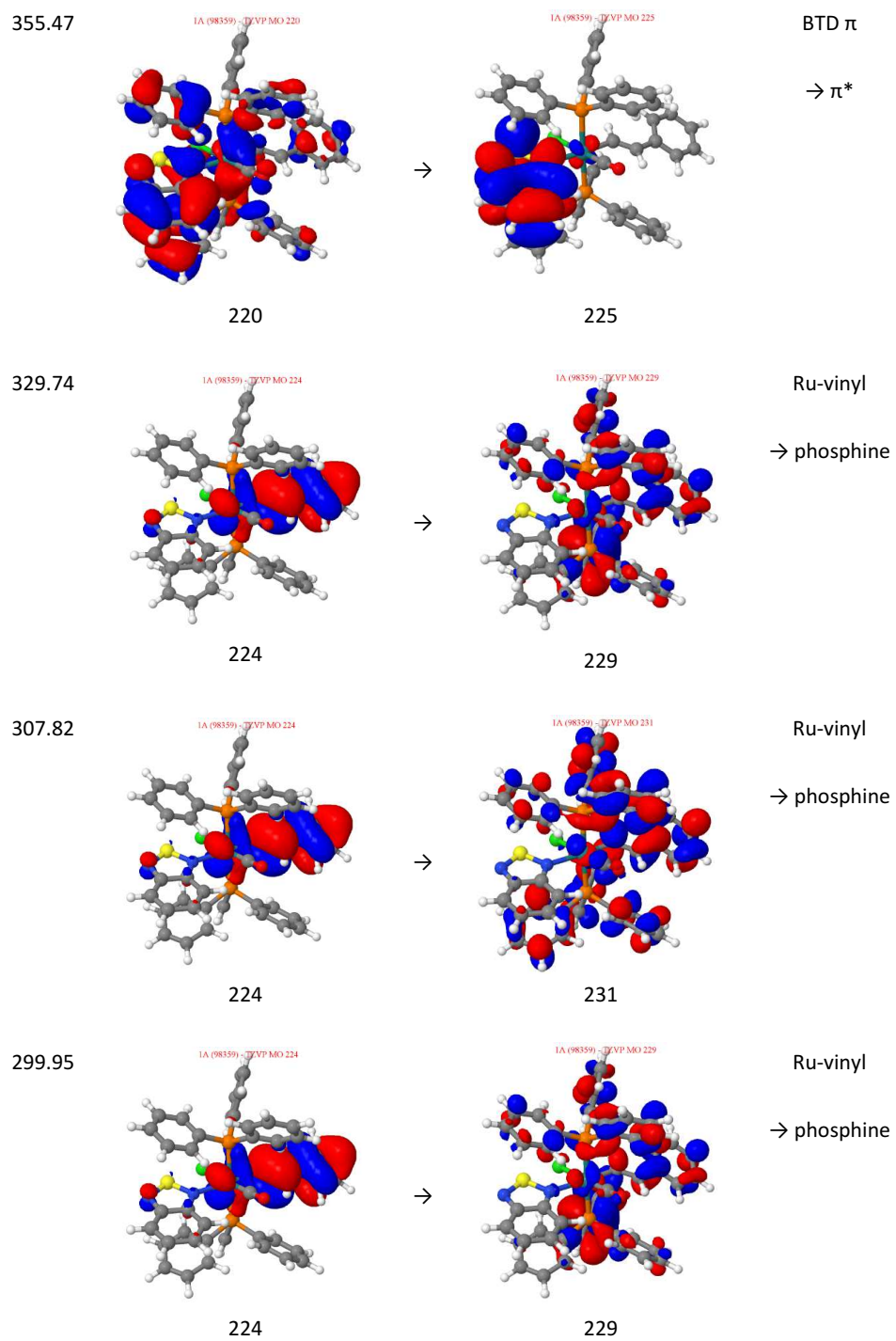


Table S5. Molecular orbitals for Compound 3.

λ (nm)	MO	Transition
575.57	<p>IA (98359) - TZVP MO 224</p> <p>224</p> <p>→</p> <p>225</p>	<p>Ru-vinyl → BTD</p>



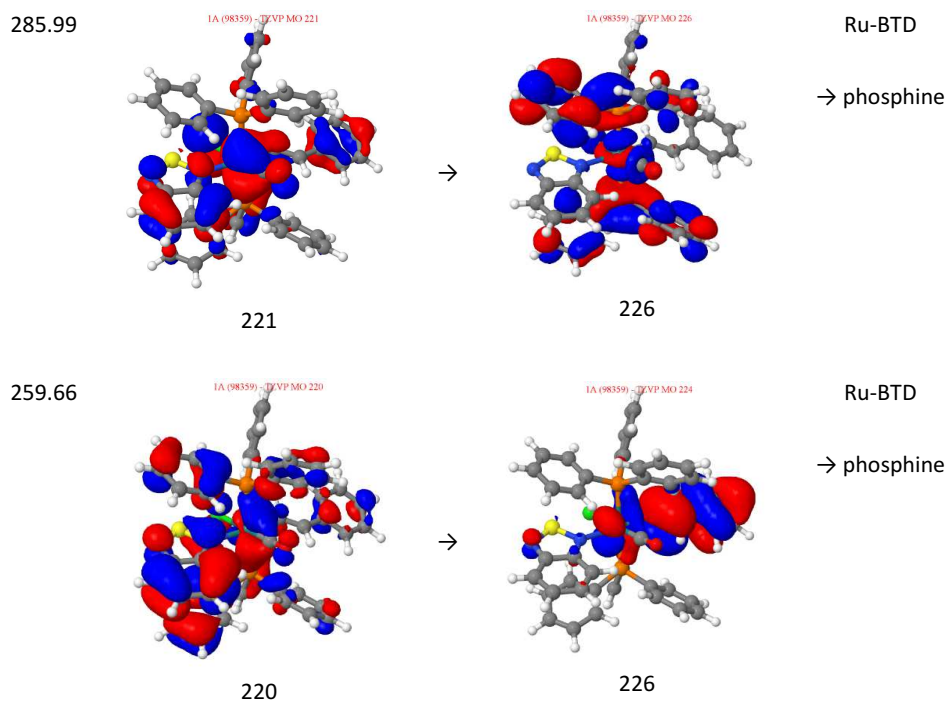
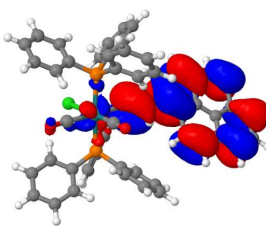
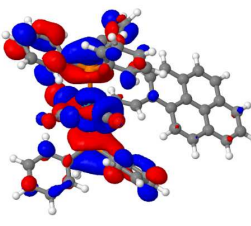


Table S6. Molecular orbitals for Compound 1·CO.

λ (nm)	MO	Transition
409.53	<p>2B (92190) - TZVP MO 228</p>  <p>228</p> <p>→</p> <p>2B (92190) - TZVP MO 230</p>  <p>230</p>	<p>Ligand</p> <p>→ metal P (LMCT)</p>

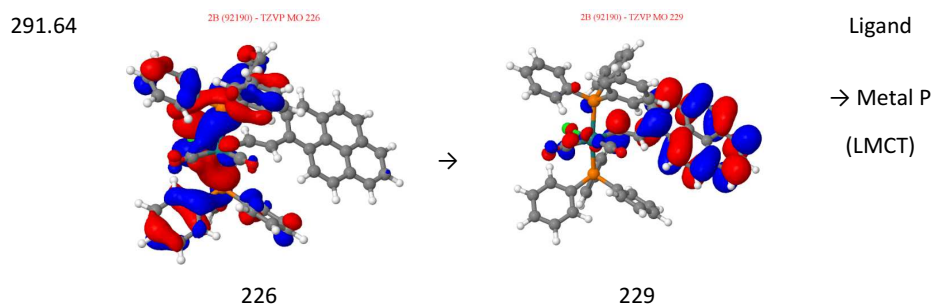
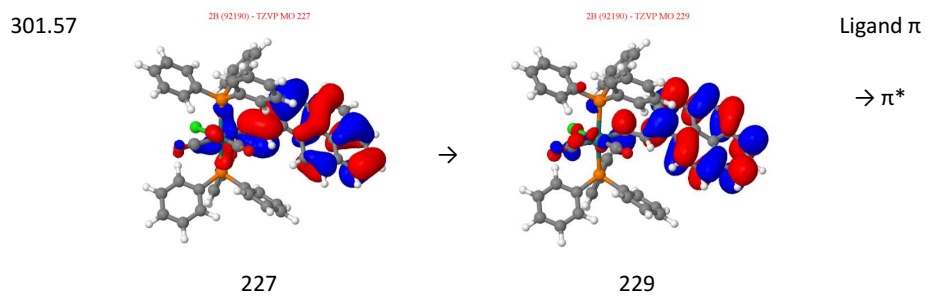
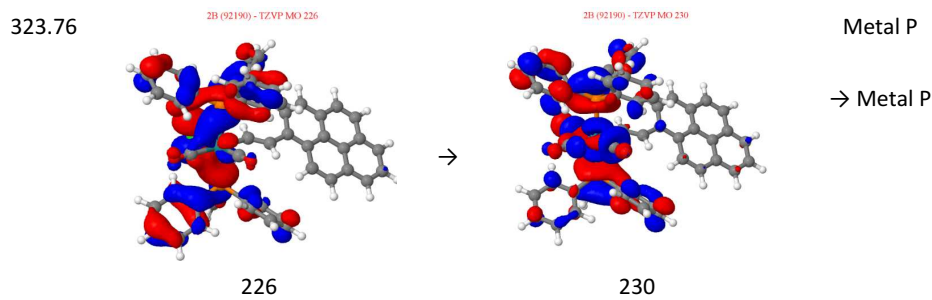
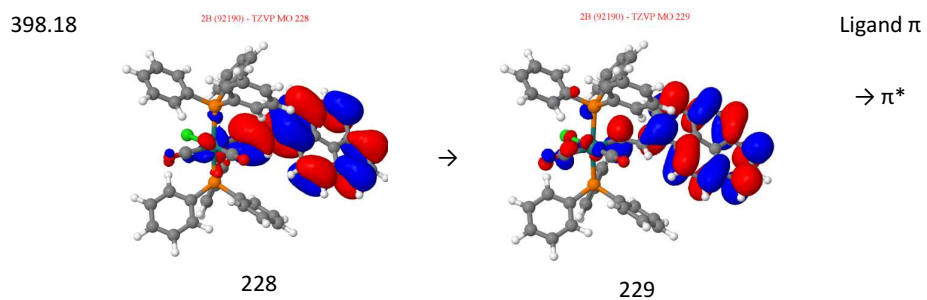
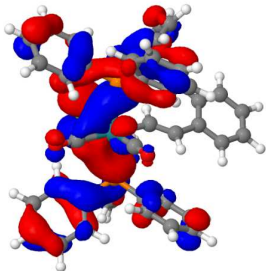
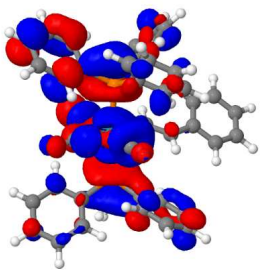
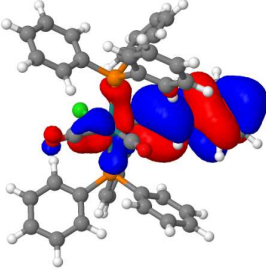
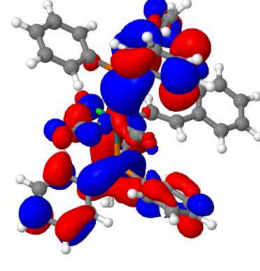
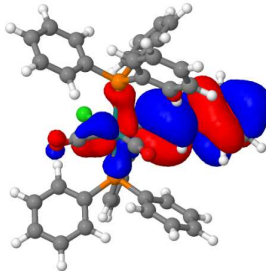
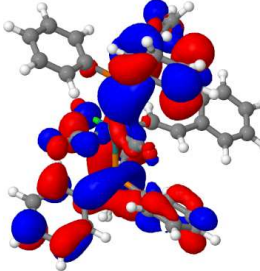
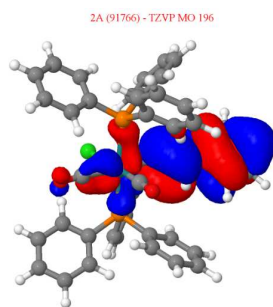


Table S7. Molecular orbitals for Compound 3-CO.

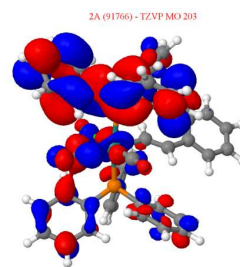
λ (nm)	MO	Transition	
322.38	<p>2A (91766) - TZVP MO 195</p>  <p>195</p>	<p>2A (91766) - TZVP MO 197</p>  <p>197</p>	<p>Metal P</p> <p>→ Metal P</p>
313.9	<p>2A (91766) - TZVP MO 196</p>  <p>196</p>	<p>2A (91766) - TZVP MO 199</p>  <p>199</p>	<p>Metal ligand</p> <p>→ Metal P</p>
310.6	<p>2A (91766) - TZVP MO 196</p>  <p>196</p>	<p>2A (91766) - TZVP MO 199</p>  <p>199</p>	<p>Metal ligand</p> <p>→ Metal P</p>

291.34



196

→

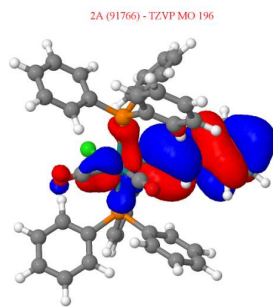


203

Metal ligand

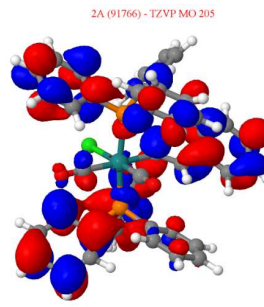
→ Metal P

278.46



196

→

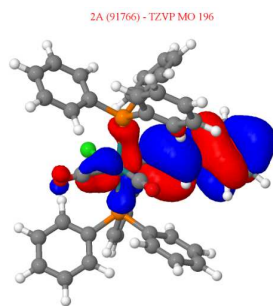


205

Metal ligand

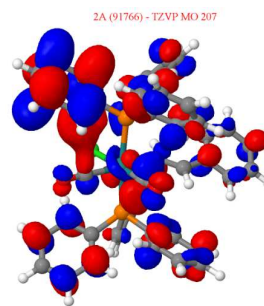
→ Metal P

267.77



196

→

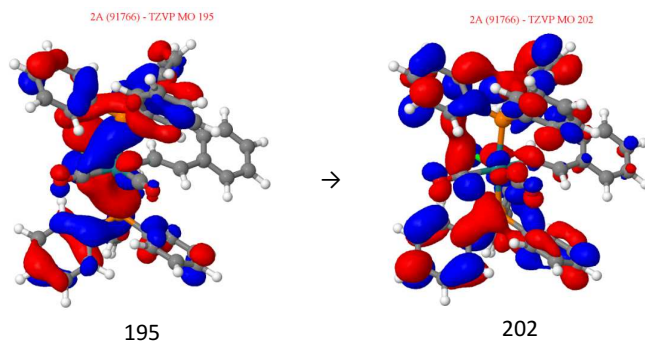


207

Metal ligand

→ Metal P

252.22



Metal ligand

→ Metal P

Calculated UV-Vis Spectra.

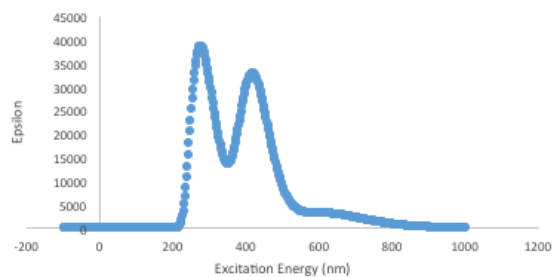


Figure S5. Calculated spectrum for compound 1.

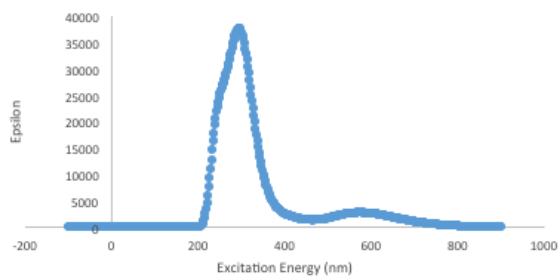


Figure S6. Calculated spectrum for compound 3.

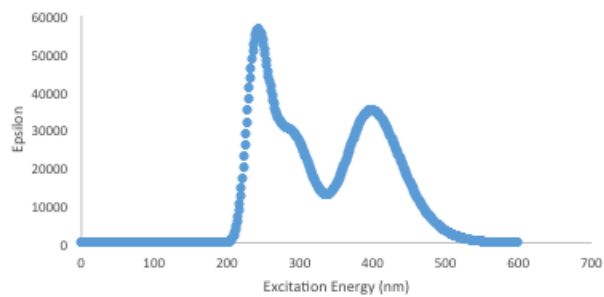


Figure S7. Calculated spectrum for compound 1·CO.

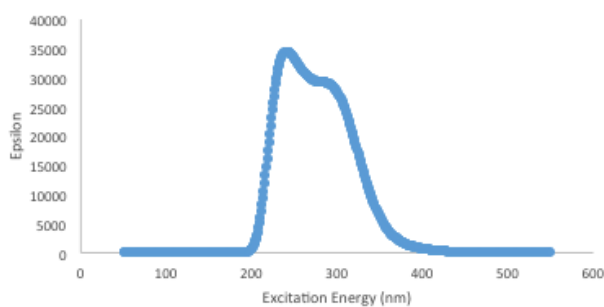


Figure S8. Calculated spectrum for compound 3·CO.

Comparisons of calculated spectra.

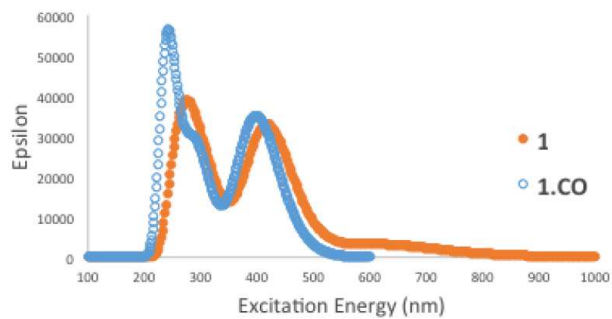


Figure S9. Comparison of calculated spectra for compounds 1 and 1·CO.

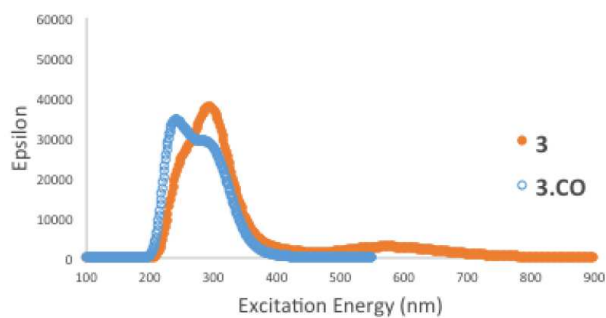


Figure S10. Comparison of calculated spectra for compounds **3** and **3.CO**.

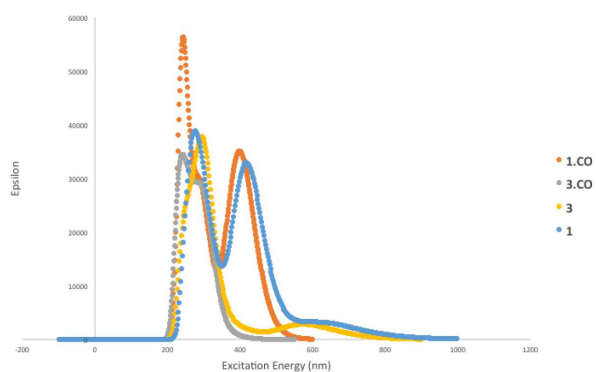


Figure S11. Comparison of calculated spectra for compounds **1**, **1.CO**, **3** and **3.CO**.

References

1. M. E. Moragues, A. Toscani, F. Sancenón, R. Martínez-Mañez, A. J. P. White, J. D. E. T. Wilton-Ely, *J. Am. Chem. Soc.*, **2014**, *136*, 11930-11933.
2. M. C. J. Harris, A. F. Hill, *Organometallics*, **1991**, *10*, 3903-3906.
3. A. F. Hill, J. D. E. T. Wilton-Ely, *J. Chem. Soc., Dalton Trans.*, **1998**, 3501-3510.
4. R. B. Bedford, A. F. Hill, C. Jones, A. J. P. White, D. J. Williams, J. D. E. T. Wilton-Ely, *Organometallics* **1998**, *17*, 4744-4753.
5. a) L. Vaska, *Z. Naturforsch.*, **1960**, *15B*, 56; b) L. Vaska, *J. Am. Chem. Soc.*, **1964**, *86*, 1943-1950; c) A. F. Hill, J. D. E. T. Wilton-Ely, *J. Chem. Soc., Dalton Trans.* **1999**, 3501-3510.
6. SHELXTL, Bruker AXS, Madison, WI; SHELX-97, G. M. Sheldrick, *Acta Cryst.*, **2008**, *A64*, 112-122.

6. Conclusions and perspectives

The detection of carbon monoxide in air is crucial for home and workplace safety due to its high toxicity and common presence in urban and indoor environments. Also, the recent rise of CO as therapeutic agent in biomedical research has required that methods followed to detect CO should involve not only chromogenic but also fluorogenic response. Taking into account these facts, and pursuing the development of sensory materials for the sensitive and selective optical detection of CO both in solution and in air, the following conclusions can be drawn from this thesis.

The first chapter of this PhD thesis has been devoted to the introduction of carbon monoxide and its different roles as pollutant and as therapeutic agent. Existing methods for CO detection and existing medical therapies involving CO used as regulator of neurotransmission, vascular tone, inflammation, cell proliferation, apoptosis, mitochondrial biogenesis and autophagy have been detailed.

In the second chapter the objectives to meet along the experimental chapters of this thesis have been raised.

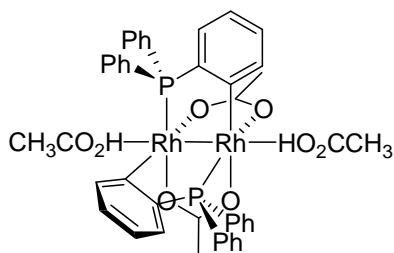
The third chapter reports a family of binuclear rhodium complexes and their use for the sensitive, selective and reversible chromogenic sensing of carbon monoxide in air. Moreover, after improving the handling of the chemical probe by changing the supporting material, the selected rhodium probes have been implemented in an opto-chemical device able to quantitatively sense carbon monoxide present in air.

Chapter four is related to the potential use of CO as therapeutic agent in biomedicine applications, and the use of selected cyclometalated binuclear rhodium complexes as CORMs has been evaluated. Dicarbonyl dirhodium complexes have been found to clearly inhibit nitrite levels in biological assays carried out in inflammation-stimulated mouse cells.

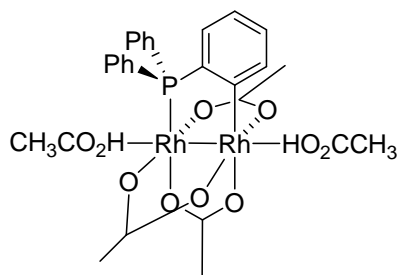
Finally, in the fifth chapter, a collection of vinyl ruthenium and osmium complexes has been prepared and their use for sensitive and selective chromo-fluorogenic sensing of carbon monoxide in air has been essayed.

Encouraged to keep the biological importance of CO in mind and considering the potential use of carbon monoxide for therapeutic applications, our current studies are focused on the development of water-soluble transition metal complexes able to detect and determine CO in biological and cellular media.

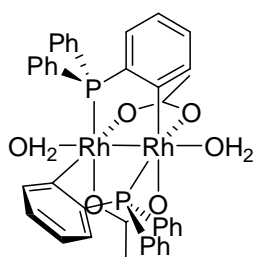
Appendix - Index of complexes

**A**

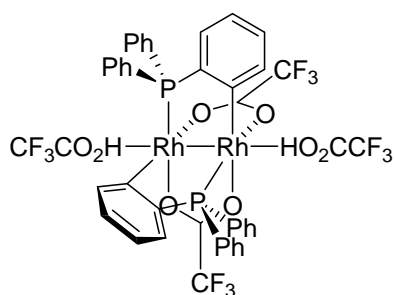
(1·(CH₃CO₂H)₂ in Angew. Chem. 2010;
 2·(CH₃CO₂H)₂ in JACS 2011;
 1 in Inorg. Chem. 2013)

**B**

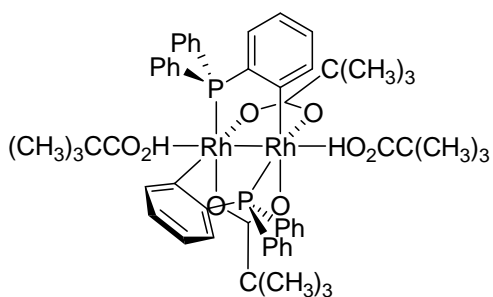
(1·(CH₃CO₂H)₂ in JACS 2011)

**C**

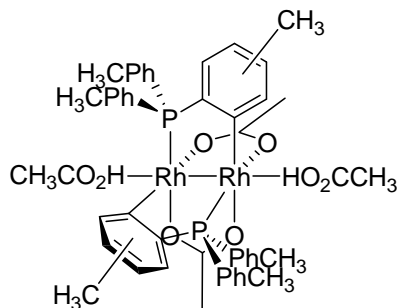
(2·(H₂O)₂ in JACS 2011)

**D**

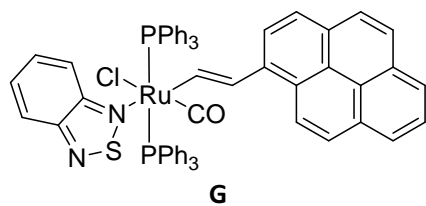
(3·(CF₃CO₂H)₂ in JACS 2011;
 1 in Sens. Act. B 2014)

**E**

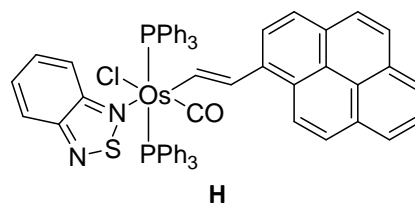
(4·((CH₃)₃CCO₂H)₂ in JACS 2011)

**F**

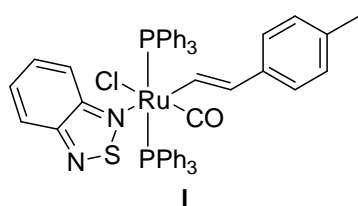
(5·(CH₃CO₂H)₂ in JACS 2011;
 2 in Inorg. Chem. 2013)



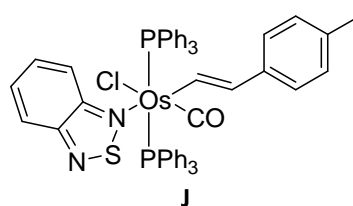
(1 in JACS 2014;
1 in Chem. Sci. 2014)



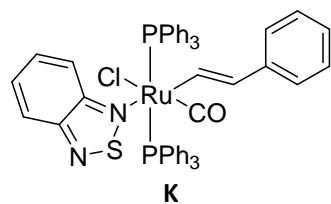
(2 in Chem. Sci. 2014)



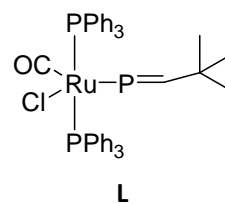
(3 in Chem. Sci. 2014)



(4 in Chem. Sci. 2014)



(5 in Chem. Sci. 2014)



(6 in Chem. Sci. 2014)

*Gracias al Ministerio de Ciencia e Innovación por concederme
una beca de Formación del Profesorado Universitario (FPU)*